UNIMORE
UNIVERSITÀ DEGLI STUDI DI MODENA E REGGIO EMILIA

UNIVERSITÀ DEGLI STUDI DI MODENA E REGGIO EMILIA

Dottorato di ricerca in Models and methods for material and environmental sciences

Ciclo XXXVIII

MULTI-GENE PHYLOGENY FOR A NEW APPROACH TO GASTROTRICH TAXONOMY

Candidato: Agata Cesaretti

Relatore (Tutor): Prof. M. Antonio Todaro

Coordinatore del Corso di Dottorato: Prof. Lugli Stefano

INDEX

ABSTRACT (IT)

Il phylum Gastrotricha comprende microscopici invertebrati marini e d'acqua dolce, prevalentemente bentonici, presenti in tutto il mondo. Le circa 900 specie note sono suddivise nei due ordini Chaetonotida e Macrodasyida, ciascuno con decine di generi e almeno una decina di famiglie. Tuttavia, l'uso di dati molecolari ha rivelato che molti gruppi non sono monofiletici, mettendo in dubbio la validità dei tratti morfologici usati nella classificazione tradizionale.

Più di recente, le moderne tecniche di microscopia e le analisi filogenetiche basate su dati molecolari hanno permesso descrizioni più accurate e classificazioni più solide. Tuttavia, l'approccio basato su un solo marcatore (18S rDNA) e un campionamento tassonomico limitato ha mostrato limiti nella risoluzione dei rapporti evolutivi profondi. Questo lavoro affronta tali problematiche mediante analisi filogenetiche multigeniche, un ampio campionamento tassonomico e l'impiego di tecnologie avanzate come Whole Genome Amplification (WGA), Next Generation Sequencing (NGS) e strumenti bioinformatici.

La tesi è strutturata come raccolta di articoli e si compone di quattro capitoli. I primi due sono dedicati al genere *Urodasys*, caratterizzato da una lunga coda e una notevole varietà di strutture riproduttive. Il primo capitolo descrive una nuova specie tramite microscopia DIC e CLSM, con un'analisi morfo-funzionale dell'apparato riproduttore, in particolare dell'organo copulatore e dello stiletto. Il secondo capitolo presenta un'analisi filogenetica multigenica (18S rDNA, 28S rDNA, COI mtDNA) su diverse specie, suggerendo che l'antenato comune possedesse gonadi pari e organi accessori, e che lo stiletto si sia evoluto all'interno dell'organo copulatore prima della perdita del testicolo sinistro.

Il terzo capitolo analizza le relazioni filogenetiche dei Macrodasyida su base multigenica e un ampio campionamento tassonomico, in particolare delle famiglie Cephalodasyidae e Macrodasyidae, rivelandone la polifilia. Viene proposta una nuova classificazione con l'introduzione di due famiglie (Mesodasyidae n.fam. e Urodasyidae n.fam.) e un nuovo genere (*Paraurodasys* n.gen.). Inoltre, *Dolichodasys* e *Paradasys* vengono assegnati ai Redudasyidae, mentre *Cephalodasys mahoae* è trasferito al genere *Paradasys*.

Il quarto capitolo esplora il genoma mitocondriale di 20 specie rappresentative della diversità ecologica e riproduttiva del phylum. L'analisi comparativa mostra forti differenze tra Macrodasyida e Chaetonotida: i membri del gruppo Oiorpata (Chaetonotida) presentano una struttura genomica conservata, indicativa di stasi evolutiva, mentre i Macrodasyida mostrano variabilità nella disposizione genica, polarità dei filamenti e presenza di ripetizioni. Queste differenze sembrano riflettere le strategie riproduttive (partenogenesi vs ermafroditismo) e gli habitat (acqua dolce vs marino), ma è più probabile che derivino da fenomeni di drift genico. L'analisi filogenetica dei geni mitocondriali codificanti supporta la nuova classificazione proposta per i Macrodasyida sulla base

dei geni nucleari e COI, e suggerisce una possibile origine marina del gruppo Oiorpata; purtroppo, origine e alleanze filogenetiche di *Neodasys* restano punti irrisolti.

In sintesi, l'approccio molecolare multigenico e l'ampliamento del campionamento tassonomico hanno migliorato il supporto statistico delle analisi filogenetiche, offrendo nuove prospettive sull'evoluzione, la tassonomia e la diversità genetica dei gastrotrichi.

Lo stesso approccio potrebbe essere applicato per la risoluzione di problematiche non affrontate in questo progetto. In tale prospettiva, la principale criticità consisterà nel reperimento di un numero sufficiente di specie target, spesso rare o endemiche di aree geografiche remote e di difficile accesso.

ABSTRACT (ENG)

The phylum Gastrotricha comprises microscopic marine and freshwater invertebrates, predominantly benthic, found worldwide. The approximately 900 known species are divided into the two orders Chaetonotida and Macrodasyida, each with many genera and at least ten families. However, the use of molecular data has revealed that many groups are not monophyletic, questioning the validity of the morphological traits used in traditional classification.

More recently, modern microscopy techniques and molecular-based phylogenetic analyses have enabled more accurate descriptions and more robust classifications. Nonetheless, the single-marker approach (18S rDNA) and limited taxonomic sampling have shown limitations in resolving deep evolutionary relationships. This research addresses these challenges through multigene phylogenetic analyses, extensive taxonomic sampling, and the application of advanced technologies, including Whole Genome Amplification (WGA), Next Generation Sequencing (NGS), and bioinformatics tools.

The thesis is structured as a collection of articles and consists of four chapters. The first two are dedicated to the genus *Urodasys*, characterized by a long tail and a remarkable variety of reproductive structures. The first chapter describes a new species using DIC and CLSM microscopy, with a morpho-functional analysis of the reproductive system, particularly the copulatory organ and the stylet. The second chapter presents a multigene phylogenetic analysis (18S rDNA, 28S rDNA, COI mtDNA) of several species, suggesting that the common ancestor of these species had paired gonads and accessory organs, and that the stylet evolved within the copulatory organ before the loss of the left testis.

The third chapter analyses the phylogenetic relationships of the order Macrodasyida on a multigene basis and a broad taxonomic sampling, particularly of the families Cephalodasyidae and Macrodasyidae, revealing their polyphyly. A new classification is proposed, introducing two

families (Mesodasyidae n.fam. and Urodasyidae n.fam.) and a new genus (*Paraurodasys* n.gen.). Furthermore, *Dolichodasys* and *Paradasys* are assigned to the Redudasyidae, while *Cephalodasys mahoae* is transferred to the genus *Paradasys*.

The fourth chapter explores the mitochondrial genome of 20 species representative of the ecological and reproductive diversity of the phylum. Comparative analysis identifies significant differences between between Macrodasyida and Chaetonotida: members of the Oiorpata group (Chaetonotida) exhibit a conserved genomic structure, indicative of evolutionary stasis, while Macrodasyida exhibit variability in gene arrangement, strand polarity, and the presence of repeats. These differences appear to reflect reproductive strategies (parthenogenesis vs. hermaphroditism) and habitats (freshwater vs. marine), but are more likely to result from gene drift. Phylogenetic analysis of mitochondrial protein coding genes supports the proposed new classification for Macrodasyida based on nuclear and COI genes, and suggests a possible marine origin for the Oiorpata. Unfortunately, the origin and phylogenetic alliances of *Neodasys* remain unresolved.

In summary, the multigenic molecular approach and expanded taxonomic sampling have improved the statistical support of phylogenetic analyses, offering new insights into the evolution, taxonomy, and genetic diversity of gastrotrichs.

The same approach could be applied to resolve issues not addressed in this project. From this perspective, the main challenge will be finding a sufficient number of target species, which are often rare or endemic to remote and difficult-to-access geographical areas.

1. INTRODUCTION

1.1. An overview of Gastrotricha

Gastrotrichs are microscopic (70 μm – 3.8 mm in length), aquatic, free-living invertebrates found in both marine and freshwater ecosystems, with a cosmopolitan distribution. In unpolluted beach environments, they can represent the third or even second most abundant group of the Meiofauna. The term "Meiofauna" describes the microscopic motile fauna, of size comprised between 38 μm and 1 mm, that is found in aquatic and limnoterrestrial habitats (Higgins and Thiel, 1988; Giere, 2009). Although meiofaunal organisms are largely invisible to the naked eye, they are among the most diverse in the animal kingdom, including representatives from 24 different metazoan phyla, out of the known 30-35 (Rundell and Leander, 2010; Semprucci and Sandulli, 2020).

The many species of the phylum Gastrotricha are vermiform, dorsally vaulted and ventrally flattened, with dense ventral locomotory ciliation that gives the phylum its name (from the Greek: gastro = belly, trichos = hair). The cilia are completely enclosed within a flexible cuticle that covers the entire body: this feature is the main autapomorphic trait of the group. The cuticle is transparent and multilayered. It can be smooth or form surface ornamentations, such as scales or spines of various shapes. These structures serve as species-specific distinguishing features and can result in spectacular combinations (Rieger and Rieger, 1977; Kieneke and Schmidt-Rhaesa, 2014).

In addition to the cilia and musculature (Leasi et al., 2006, Leasi and Todaro, 2008), in their locomotion gastrotrichs use adhesive tubes located on the body surface. These tubes are connected to a dual-gland adhesive system, in which one gland secretes an adhesive substance and the other releases a solvent. The sequential adhesion to and detachment from the substrate enables movement within the interstitial space.

To date, the phylum comprises over 900 described species, classified into two orders: Macrodasyida (385 species) and Chaetonotida (520 species) (Saponi et al., 2024; Minowa et al., 2025a; Gastrotricha World Portal, www.gastrotricha.unimore.it; WoRMS, 2025).

Macrodasyidan gastrotrichs are predominantly marine, with the notable exceptions of the genera *Redudasys* Kisielewski, 1987 and *Marinellina* Ruttner-Kolisko, 1955 (Todaro et al., 2012). Their body shape varies significantly across genera but is generally elongated and is often described as "strap-shaped" or "tongue-shaped" (Ruppert, 1991; Kieneke and Schmidt-Rhaesa, 2014; Todaro et al., 2019a). They are exclusively benthic and generally possess numerous adhesive tubes distributed all along the body, likely as an adaptation to interstitial life.

Chaetonotidan gastrotrichs occur in both marine and freshwater environments and can be benthic or, rarely, planktonic. They are generally smaller than the species of the order Macrodasyida (70 – 300 μm). Most chaetonotidan gastrotrichs have a tenpin-shaped body, ending posteriorly in the furca, a structure formed by two symmetrical body extensions. On the distal end of the furcal branches there are two (rarely four, as in *Diuronotus* and in *Xenotrichula quadritubulata*) adhesive tubes, which are often the only ones present in the whole animal (Todaro et al., 2019a).

Gastrotrichs feed on detritus, small protozoans, unicellular algae and bacteria, and are preyed upon by bigger animals such as turbellarians, amoebas and ciliates (Giere, 2009; Todaro and Luporini, 2022). The mouth is terminal, often surrounded by a ring of cuticular teeth-like processes. The food is ingested through the powerful sucking action of the mioepithelial pharynx, whose walls are wrapped by a muscular double helix and are internally lined with cuticle (Hochberg and Litvaitis, 2001, 2003; Bekkouche and Worsaae, 2016). Most macrodasyidan gastrotrichs also possess paired pharyngeal pores connecting with the external body surface, to expel the excess water ingested while feeding. Nutrient digestion and absorption take place in the midgut. The intestine is simple and linear, opening in a ventral anus in most species.

Both circulation and gas exchange occur through diffusion, due to the small size of these animals. Though gastrotrichs are most common superficial sediment of clean waters, some species have been found living in anoxic sediment at greater depths. It is currently unknown if their adaptations to such environments only include tolerance of low oxygen levels, or if they possess anaerobic metabolic pathways (Powell et al., 1983; Boaden, 1985; Todaro et al., 2000). However, these living conditions seem linked to an absence of mitochondria in the sperm cells in at least two species (Balsamo et al., 2007).

Excretion happens through protonephridia, which are located on each side of the body, along the intestine. The protonephridia open into nephridiopores on the body surface of the animal.

The nervous system is composed by a symmetrical, bi-lobed cerebral ganglion, located dorsal to the anterior pharynx. From each lobe depart one or multiple longitudinal nervous cords, presenting several ganglia along their length. These cords run from the brain to the posterior end of the body (e.g., Todaro et al., 2015). Most sensory structures are mechanical and tactile sensors (ie., sensory cilia), and are most abundant on the head, often arranged in groups or symmetrical tufts. Chemoreceptor structures, called piston pits, graviceptors and eye spots are also found in certain species (Ruppert, 1991; Marotta et al., 2008; Kieneke and Schmidt-Rhaesa, 2014).

The anatomy of the reproductive system exhibits a remarkable variety. Freshwater gastrotrichs are generally parthenogenetic, likely as an adaptation to the unstable conditions of freshwater environments, while most marine species are hermaphroditic (Todaro et al., 2012;

Kieneke and Schmidt-Rhaesa, 2014; Kolicka et al., 2020). The male reproductive system comprises one or two testes that lead into sperm ducts (vas deferens), which typically end on the body's ventral surface, forming either a single median gonopore or paired gonopores. Many macrodasyidan species present an accessory copulatory organ, called caudal organ, which has the function of transferring sperms to the partner during the copula (Guidi et al., 2022). The caudal organ is directly connected to the vas deferens only in rare cases (genera *Acanthodasys* Remane, 1927; *Diplodasys* Remane 1927, *Mesodasys* Remane, 1951 and *Hummondasys* Todaro, Leasi & Hochberg, 2014). In all remaining species, the organ is charged with autosperms through an external pore on the body surface. This process was observed and described in detail in species of genus *Macrodasys* Remane, 1924 (Ruppert, 1978; Guidi et al., 2022). Several species also present a frontal organ, which receives the allosperms from the partner during the copula and transfers them to the eggs waiting in the ovary. Ovaries can be either single or paired. In both parthenogenetic and hermaphroditic species, egg deposition happens through rupture of the body wall; the animal survives this process, and lays multiple times during its life cycle (Balsamo and Todaro 1987, 1988). The eggs are laid singly and stick to the substrate through an adhesive substance that covers the shell. Parthenogenetic, freshwater gastrotrichs are capable of producing resting eggs, with a thicker shell, which develop after a period of dormancy (Rieger and Rieger, 1980; Araujo et al., 2023; Minowa et al., 2025b). The phylum also includes a single ovoviviparous species, *Urodasys viviparus* Wilke, 1954.

The development is direct, with no larval stages or cuticle molting. Juvenile gastrotrichs closely resemble their parents, aside from their smaller size, a larger head relative to the body and a greater pharynx/gut length ratio. The number of adhesive tubes can also differ, with juveniles generally having fewer than the adults. These juveniles reach sexual maturation just a few days after hatching. The entire gastrotrich life cycle is similarly fast and has been observed to span less than thirty days in two chaetonotidan species (Balsamo and Todaro, 1987, 1988). Some macrodasyidan gastrotrichs are assumed to live for several months (Artois et al., 2011), but the exact longevity and life history traits have never been determined in wild populations (Hummon and Hummon, 1992; Kieneke and Schmidt-Rhaesa, 2014).

1.2. Exploring the phylogeny of phylum Gastrotricha

The study of phylogeny aims to reconstruct the evolutionary history of organisms, both living and extinct. Through the recovery of branches and nodes that link modern species to their common ancestors, phylogenetic trees uncover the relationships between all extant forms of life and the evolutionary trends that shaped them. After establishing their connections, the branches of the

tree can be then described and classified through taxonomy. Understanding these relationships enables the hierarchical organization of species into monophyletic groups, Linnaean taxonomic categories (e.g., from domain to species), and beyond. Systematics and taxonomy thus serve as a foundational framework to comprehend the biology of a species.

Gastrotrichs were first described as a group by Metschnikoff (1865). The number of known species has steadily increased over the past century and recent decades, with new descriptions being published every year. Nevertheless, the phylum is still relatively understudied. Many aspects of gastrotrich biology are currently poorly understood and have been investigated only in a limited number of species. Due to their small size, details of the internal anatomy of these animals have become visible only through the modern advancements of microscopy technologies, and were previously hidden from past investigators.

A significant challenge in studying gastrotrichs lies in their fragility. Specimens are typically examined while alive, as no fixation technique maintains their diagnostic features for more than a few days (Todaro et al., 2019a). Once mounted on slides, fresh specimens can deteriorate within minutes. In most cases, no physical holotype exists. Consequently, species descriptions have often been accompanied by illustrations of holotypes, which were initially hand-drawn by the authors.

Because of these constraints, available morphological data heavily depend on the original observer's visual and artistic skills as well as on the technology available at the time, particularly for species described before the 21st century. Moreover, it is not possible to obtain new data from deposited holotypes. Every new morphological investigation requires fresh, living individuals: a significant obstacle, especially to the study of rare species. Nowadays, the absence of physical type material endures, but the artworks, mostly digital, are supplemented with high-resolution microphotography and video footage, as voucher.

The traditional classification of the gastrotrichs based on the general morphology, with the cuticular ornamentations being of particular relevance, has been subject to extensive debate and frequent revisions, fueled by a steady influx of new data (Balsamo et al., 2010).

Gastrotrichs were originally considered to be part of the Aschelminthes/Pseudocelomates, closely related to either Rotifera (Hyman, 1951), Gnathostomulida (Rieger and Mainiz, 1977; Boaden, 1985; Sterrer et al., 1985), or Nematoda (Remane, 1936; Teuchert, 1968, 1977; Ruppert, 1982; Boaden, 1985). The ultrastructural studies by Ruppert (1991) then pointed out that gastrotrichs are acelomate, and thus could not be part of the group. The phylum Aschelminthes was later identified as polyphyletic through an analysis of the sequence of the 18S rRNA gene, leading to the rejection of the group's validity (Winnepenninckx et al., 1995). Subsequently, cladistics studies on morphological traits (e.g, structure of the cuticle, position of the mouth, shape of the brain) proposed Gastrotricha as the sister taxon of Ecdysozoa (Schmidt-Rhaesa et al., 1998;

Nielsen, 2001; Zrzavý, 2003). Meanwhile, Cavalier-Smith (1998) suggested their inclusion in the Platyzoa group, along with Platyhelminthes, Rotifera, Acanthocephala and Gnathostomulida. However, with the introduction of molecular data to the study of phylogenetics, this scenario and the monophyly of Platyzoa were questioned by various authors (Zrzavý, 2003; Dunn et al., 2008; Giribet, 2008). Later phylogenetic analyses confirmed that the group was likely a systematic artifact (Struck et al., 2014; Laumer et al., 2015). In the meantime, the first molecular study to involve a high number of gastrotrich species had proposed the phylum as a member of Lophotrochozoa (Todaro et al., 2006), though it was not yet possible to identify its sister taxon.

Currently, Gastrotricha is recognized as a member of the Protostomia Spiralia (formerly Lophotrocozoa) forming the Rouphozoa clade together with the Platyhelminthes. In turn Rouphozoa is recognized as the sister group of Lophotrocozoa, in its current and correct meaning. This phylogenetic collocation is supported by transcriptomic data (Struck et al., 2014; Egger et al., 2015; Laumer et al., 2015, 2019) and highlights the importance of understanding this group for the study of protostome evolution (Fig. 1).

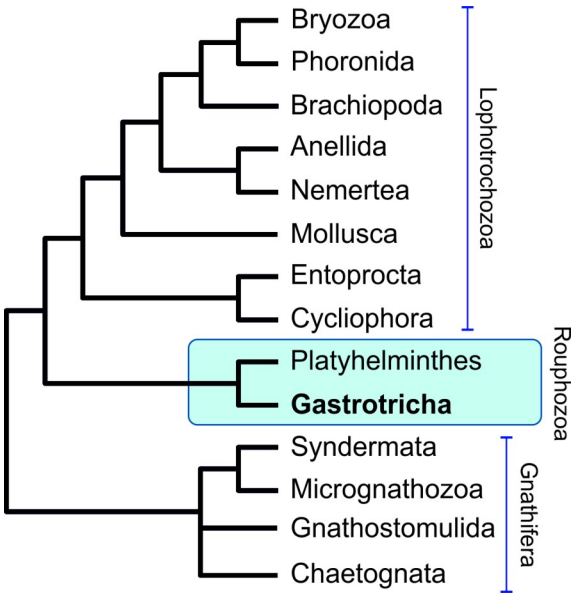

Fig. 1. Cladogram depicting the current phylogenetic collocation and relationships of the phylum Gastrotricha in the clade Spiralia. Redrawn from Laumer et al. (2019).

While the phylum Gastrotricha now appears to have reached a stable phylogenetic placement among the Metazoa, its internal evolutionary history remains in a state of flux, as the constant discovery of new species brings new information every year. Furthermore, the increasing use of molecular data in phylogenetic studies has uncovered the non-monophyly of several genera and families, underscoring the lack of homology in the morphological traits traditionally used for classification (e.g., Todaro et al., 2012, 2019b; Kånneby et al., 2013; Garraffoni et al., 2017; Rataj

Križanová and Vďačný, 2023; Gammuto et al., 2024; Saponi et al., 2024; see also Guidi et al., 2014).

Early ultrastructural studies have revealed fascinating distinctions between different groups of Gastrotricha. Notably, species within the order Macrodasyida are uniquely characterized by the presence of pharyngeal pores and of a pharyngeal lumen that resembles an inverted Y when viewed in cross-section. In stark contrast, Chaetonotidan species display a Y-shaped cross-section of their pharyngeal lumen but lack these distinctive pores. Despite these intriguing differences, the true nature and characteristics of the last common ancestor of this phylum remain shrouded in mystery (Ruppert, 1991; Kieneke and Schmidt-Rhaesa, 2014). Additionally, genus *Neodasys* Remane, 1929 represents a peculiar case not easily solved by this classification. All known *Neodasys* species present a pharyngeal lumen with a Y-shaped cross-section, and on this basis the genus is classified in the order Chaetonotida. However, these animals more closely resemble macrodasyidan gastrotrichs in their external morphology, as they also have a distinctly elongated body and multiple lateral adhesive tubes. For these reasons, this genus is the only member of the chaetonotidan suborder Multitubulatina d'Hont, 1971. All remaining chaetonotidan taxa are grouped in the suborder Paucitubulatina d'Hont, 1971. However, more recent observations on the muscular apparatus and the organization of the reproductive organs show evidence that this genus may actually belong to the order Macrodasyida (Hochberg, 2005; Bekkouche and Worsaae, 2016). The position of *Neodasys* within Gastrotricha has been the subject of much speculation over the years, and is debated to this day (Todaro et al., 2003, 2006; Kieneke et al., 2008; Kieneke and Schmidt-Rhaesa, 2014).

Even among the remaining taxa there is still much uncertainty, especially regarding the identity of the most basal lineages. In the order Chaetonotida, the families Xenotrichulidae Remane, 1927 and Muselliferidae Leasi & Todaro, 2008 have both been considered basal, a conclusion supported by data on the pattern of body musculature and of sperm ultrastructure (Kieneke et al., 2008; Balsamo et al., 2010). It is unclear whether they are sister taxa or if one of the two families is more derived, although recent molecular data suggests Muselliferidae as the sister taxon of all remaining Paucitubulatina (Kolicka et al., 2020).

Within Macrodasyida, the matter is even more complex. Through time, there have been many candidates for the earliest branch of this order: the family Dactylopodolidae Strand, 1929 has been proposed by multiple authors (Ruppert, 1982, 1991; Travis, 1983; Hochberg and Litvaitis, 2000; Todaro et al., 2003; Zrzavý, 2003), sharing the position with genera *Xenodasys* Swedmark, 1967 and *Acanthodasys* Remane, 1927 (Todaro et al., 2003), or with *Paradasys* Remane 1934, *Cephalodasys* Remane, 1926, *Urodasys* Remane, 1926, and *Neodasys* (Todaro et al., 2006). Genera *Xenodasys* and *Cephalodasys* have also been resolved as the earliest branch without

Dactylopodolidae (Marotta and al., 2005; Petrov et al., 2007; Kieneke et al., 2008), based on sperm morphology and on analysis conducted on the sequence of the 18S rDNA gene.

1.3. Molecular methodologies in the study of gastrotrichs

The rise of molecular genetics has had a profound impact on the studies on the evolutionary history of the phylum, bringing new ways to examine old questions. Following the first phylogenetic study including gastrotrich DNA sequences, conducted by Winnipenninckx et al. (1995), the integration of morphological observations with molecular data has been steadily growing, both in species description and evolutionary work. Compared to morphological data, molecular information has the clear advantage of being less subject to the personal interpretation of individual researchers. More importantly, DNA sequences possess a much higher amount of possible character states, as the divergence between different taxa can be measured through the variations of each nucleotide in the examined region. A single gene includes hundreds of nucleotide bases, resulting in hundreds of character states. Since the beginning of the 2000s, several phylogenetic analyses of Gastrotricha have been conducted on molecular data, with early studies focusing on the 18S rDNA gene sequence (Todaro et al. 2003, 2006; Zrzavy et al., 2003; Manylov et al., 2004; Paps and Riutort, 2012).

Ribosomal genes represent an ideal target for phylogenetic studies. The genes that constitute the so-called nuclear ribosomal operon (i.e., 18S rDNA, 28S rDNA, 5.8S rDNA, and the internal transcribed spacers ITS1 and ITS2) are essential housekeeping genes, responsible for the synthesis of rRNA and thus of ribosomes. As such, they are found in all eukaryotic organisms. Moreover, they are consistently present in multiple copies within the nuclear genome of each cell, making them suitable targets for PCR amplification even in small-sized organisms. The 18S rDNA gene in particular displays a high degree of conservation, facilitating the design of generalist primers compatible with multiple phyla. Its slow mutation rate permits the detection of relatedness among distant species, while still being sufficiently diversified to serve as a reliable barcoding target (Hillis and Dixon, 1991). This set of characteristics has long established the 18S gene as the principal marker used in studies on gastrotrich evolution, and it has proved highly effective in identifying taxa at the genus level. However, this marker alone may be inadequate for resolving deep phylogenetic relationships within the phylum. Studies relying exclusively on the 18S gene in most cases generated trees whose statistical support was insufficient to clarify relationships among many genera and families, especially those that were poorly sampled in the analysis (Todaro et al., 2015; Kieneke and Todaro, 2021).

The 28S rDNA gene is less commonly used, as it lacks a strong phylogenetic signal when used alone. However, when used in combination with the 18S gene it has been shown to improve the robustness of the resulting phylogenetic trees, with many nodes receiving higher statistical support than with either gene alone (e.g. in Gammuto et al., 2024).

The subunit 1 of the cytochrome c oxidase gene, commonly abbreviated as COI, is another widely used molecular marker in both phylogenetic studies and species delimitation. This gene is located within the mitochondrial genome. Differently from nuclear DNA, mtDNA is present in multiple copies in every cell. This redundancy reduces the impact of detrimental mutations, allowing for a higher mutation rate in the mitogenome than in the nuclear genome, despite the functional importance of the genes it includes (Gissi et al., 2008). Because of this high variability, the COI gene is the primary barcoding marker employed in biodiversity research on bacteria and metazoans alike. The results have shown that, with few exceptions, the COI gene consistently distinguishes closely related species, and often different populations within the same species (Kånneby et al., 2012; Kieneke et al., 2012; Rataj Križanová and Vďačný, 2023). In fact, this marker is most suited to detect recent divergence and performs badly when used alone to infer phylogenetic relationships, as the faster evolutionary rate of mtDNA tends to eliminate ancestral polymorphisms in its sequence (Toews and Brelsford, 2012).

Commercially available 'universal' primers are capable of amplifying and sequencing the initial portion of the COI gene located at the 5’ end, known as the 'Folmer fragment', across most known taxa. However, the use of these primers is not without limitations. The COI gene is also present in bacterial DNA, and many universal primers can and will amplify its sequence regardless of the kingdom it belongs to. This problem can be readily circumvented in large animals, where tissue material may be sampled and treated according to specific needs. But, when working with meiofauna, it is necessary to process whole specimens to obtain sufficient quantities of genetic material for analysis. Consequently, contamination from bacteria present in the digestive tracts and on the surface of the animals becomes difficult to avoid and can compromise the accuracy of the results.

To overcome the limitations of single-gene analyses, a widely adopted approach is the concatenation of multiple sequences to create 'hybrid genes', with the most frequently used combination being 18S, 28S and COI genes. The use of multiple genes substantially increases the characters-to-taxa ratio, enhancing the statistical support of phylogenetic analyses, and has led to numerous discoveries in evolutionary histories that would otherwise remain obscure (Giribet et al., 2004; Todaro et al., 2011, 2012; Kolicka et al., 2020; Rataj Križanová and Vďačný, 2023). Employing both nuclear and mitochondrial genes increases the resolution of the analyses, as the same specimen is represented through two independent sources of information with different

evolutionary rates (Toews and Brelsford, 2012; Fontaneto et al., 2015). Additionally, this approach eliminates (or at least reduces) the risk of obtaining phylogenetic trees that reflect only the evolutionary history of the single genes, instead of the real history of the taxon.

However, using multiple molecular markers poses new practical challenges when applied to meiofaunal species. As these organisms are largely understudied, commercial Sanger sequencing primers do not always bind properly, requiring repeated optimization steps to identify the most effective primer combinations (Fontaneto et al., 2015). Another very significant obstacle lies in the small amount of genetic material that can be extracted from meiofaunal specimens using standard protocols. The need for multiple rounds of amplification and sequencing carries the risk of completely depleting the DNA sample, which is particularly problematic when working with rare species. Since PCR and Sanger sequencing can typically generate a maximum of 1000 bp per reaction, obtaining the full sequence of longer genes, such as the 28S gene (approximately 3500 bp), requires the use of multiple primers and amplification steps (see for example the methodology used by Kolicka et al., 2020).

To solve these limitations, recent studies on meiofauna, and other small organisms, molecular genetics have implemented a Whole Genome Amplification (WGA) step in their pipelines (Serra et al., 2020; Lee et al., 2023). WGA relies on a high-output Taq polymerase, used in combination with a mixture of multiple high-coverage primers. The WGA amplification reaction unfolds over several hours, and in this time the polymerase generates numerous copies of the entire genetic input. Commercial WGA kits include an initial step of cell lysis and DNA extraction from the starting biological sample, which may range from a single cell to entire microscopic specimens. The final product yields approximately 40 µl of highly concentrated DNA. This material can be diluted at a 1:100 ratio and still be viable for PCR amplification, enabling a considerably higher number of reactions than traditional DNA extraction products. However, the primary advantage of WGA is that the amount of amplified DNA it produces allows for sequencing via Next Generation Sequencing (NGS) technologies, which are capable of sequencing entire genomes. Traditional DNA extraction from meiofauna rarely yields sufficient quantities to construct libraries for these techniques, which require at least 25 µl of genetic material (Lin et al., 2021; Lee et al., 2023). The application of a WGA step effectively resolves this bottleneck, making it possible to generate gene libraries from a single specimen or from previously extracted DNA. Thus, the need to design gene-specific sequencing primers is entirely bypassed. Thanks to advances in this methodology, de novo sequence acquisition can now be achieved in a relatively short time and with considerably less effort. However, bioinformatics skills and significant computing power are required.

While generally reliable, WGA presents some downsides too. It is very vulnerable to sample contamination, as the universal primers it employs do not discriminate and will amplify any genetic

material they come in contact with. To minimize this risk, the preparation for the reaction must be conducted in a sterile environment e.g., under a UV sterilized hood.

Furthermore, by using whole animals, the process inevitably amplifies the genetic material of any symbionts and germs present in the intestinal tract or attached externally. This can negatively impact both the amplification process and the quality of the amplified product from the tested subject. The problem is particularly relevant when working with smaller specimens, where the quantities of DNA belonging to the subject and bacterial DNA can be dangerously close.

1.4. Next Generation Sequencing: Illumina and Nanopore approaches

Next-generation sequencing includes several different approaches. For my projects, I selected two established and widely used sequencing technologies: the Illumina and Oxford Nanopore platforms. Each of these technologies has its own advantages and disadvantages. Both are well-suited for de novo sequencing of single genes as well as entire genomic regions, and they have been previously utilized in studies involving small organisms (Montoliu-Nerin et al., 2020; Serra et al., 2020; Lee et al., 2023).

The “Illumina” approach is also called SBS, Sequencing By Synthesis. This methodology was developed in the 2000s and saw its first major application in the sequencing of the first complete human genome (Bentley et al., 2008). In SBS, the starting double-strand DNA is randomly fragmented into short molecules. In these fragments, each strand is ligated with a pair of adapter oligonucleotides on both ends, in a forked configuration. These adapters anneal to complementary oligonucleotides bound to the sequencing flow-cell, resulting in an array of single-strand DNA molecules. The single strands are amplified using the bound adapter as a primer; the original strand is denaturated, leaving behind the new single-strand molecule. The adaptor sequence at the free end of each copied strand is then annealed to a new surface-bound complementary oligonucleotide, forming a bridge and generating a new site for the synthesis of a second strand (Alekseyev et al., 2018). This repeated duplication creates clusters of identical strands bound to the same area of the flow-cell, a step that is known as “clustering” and results in a high density of identical amplified DNA. This material is then amplified once more, incorporating dNTPs with fluorescent tags in the new strands. The clusters are excited by a light source after the addition of each nucleotide, and the tags emit a luminous signal that is read by the sequencing machine. This step is what gives the name “Illumina” to this technology. The signal wavelength is characteristic for each of the four nucleotidic bases, and determines the base-call. The final sequencing output is thus determined by the signal detected from the whole cluster, in which all strands are sequenced simultaneously, site by site. The result is a final library of short reads (up to 600 bps) that must then

be assembled together by finding the points of overlap to build longer, contiguous sequences (Alekseyev et al., 2018; Lin et al., 2021).

The NanoPore sequencing technology is, by contrast, capable of producing reads ranging from 1kbp to several millions of base pairs in length. It involves no synthesis of new DNA strands, relying instead on a series of nanoscopic pores to directly sequence the DNA input. These nanopores are located on membranes located inside a cell filled with electrolytic fluid and presenting an anode and a catode on opposite ends. The ionic current between the poles causes the negatively-charged nucleic acid molecules to drift away from the negative electrode, towards the anode, and through the nanopore. The passage of each nucleic acid base through this structure causes a disruption in the ionic current, resulting in a measurable signal which differs base by base. The signal, once amplified, is used to reconstruct both the sequence of the nucleotides and the total length of the DNA strand (Lin et al., 2021).

This method is considerably cheaper than SBS, and the sequencing of a complete genome can be completed overnight (Alekseyev et al., 2018; Lin et al., 2021). For a time, there was however a trade-off in reads quality. The NanoPore methodology could guarantee an accuracy from 87% to a maximum of 98%, against the consistent 99% accuracy of Illumina reads (Lin et al., 2021). Currently, the improvement of the technology has considerably narrowed this gap, to the point that the latest generation of NanoPore sequencers are approaching the reliability of the Illumina method (Bogaerts et al., 2024). The opportunity to rapidly obtain a high number of de novo gene sequences opens a world of new possibilities, especially for understudied groups like Gastrotricha.

1.5. Mitochondrial DNA as a resource for phylogeny

The mitochondrial genome is a source of precious evolutionary information and it is gaining popularity in phylogenetic studies. Aside from containing the popular COI gene, its small size and presence in multiple copies in any eukaryotic cell facilitate its use in molecular biology. It also presents a high level of plasticity while maintaining a number of conserved regions, which allow the development of universal barcodes (Hebert et al., 2003) to examine the differences among related species. While the mitogenome is generally conserved in deuterostomes, and especially in vertebrates, its structure is variable in protostomes (Gissi et al., 2008).

The traditional model of the metazoan mitogenome is a circular chromosome, approximately 14-20 kb in length, containing 13 protein-coding genes, 2 ribosomal RNA genes, and 22 tRNA genes (Boore, 1999; Saccone et al., 1999; Gissi et al., 2008). The protein-coding genes include the three subunits of the cytochrome c oxidase complex (COI, COII, COIII), the cytochrome B gene, the seven subunits of the NADH dehydrogenase complex (NAD1, NAD2, NAD3, NAD4, NAD4L,

NAD5, NAD6) and the two subunits of the ATP synthase complex (ATP6, ATP8) (Fig. 2). The sequencing of the mitogenome of hundreds of species has shown that its structure can present different variations from what was considered to be a highly conserved structure. These changes can involve the number of genes present in the mitogenome and their order, as well as variations in the structure of the mtDNA molecule itself (linear vs circular) (Smith, 2016; Lavrov and Pett, 2016; Shtolz and Mishmar, 2023; Struck et al., 2023). In several metazoan groups, some protein-coding genes were evolutionarily transferred from the mitochondrial genome to the nuclear genome, despite their functional relevance. Significant amounts of sequence variation and structural differences can also be observed between congeneric species, and even in taxa that are morphologically almost indistinguishable (Gissi et al., 2008; Shtolz and Mishmar, 2023; Struck et al. 2023). The sum of these characteristics make mitochondrial genomes a great source of evolutionary insight, and they have been employed in several lines of research, including phylogenetics (Golombek et al., 2015), phylogeography (Morin et al., 2010), population genetics (Lake et al., 2024), and genome evolution studies (Butenko et al., 2024).

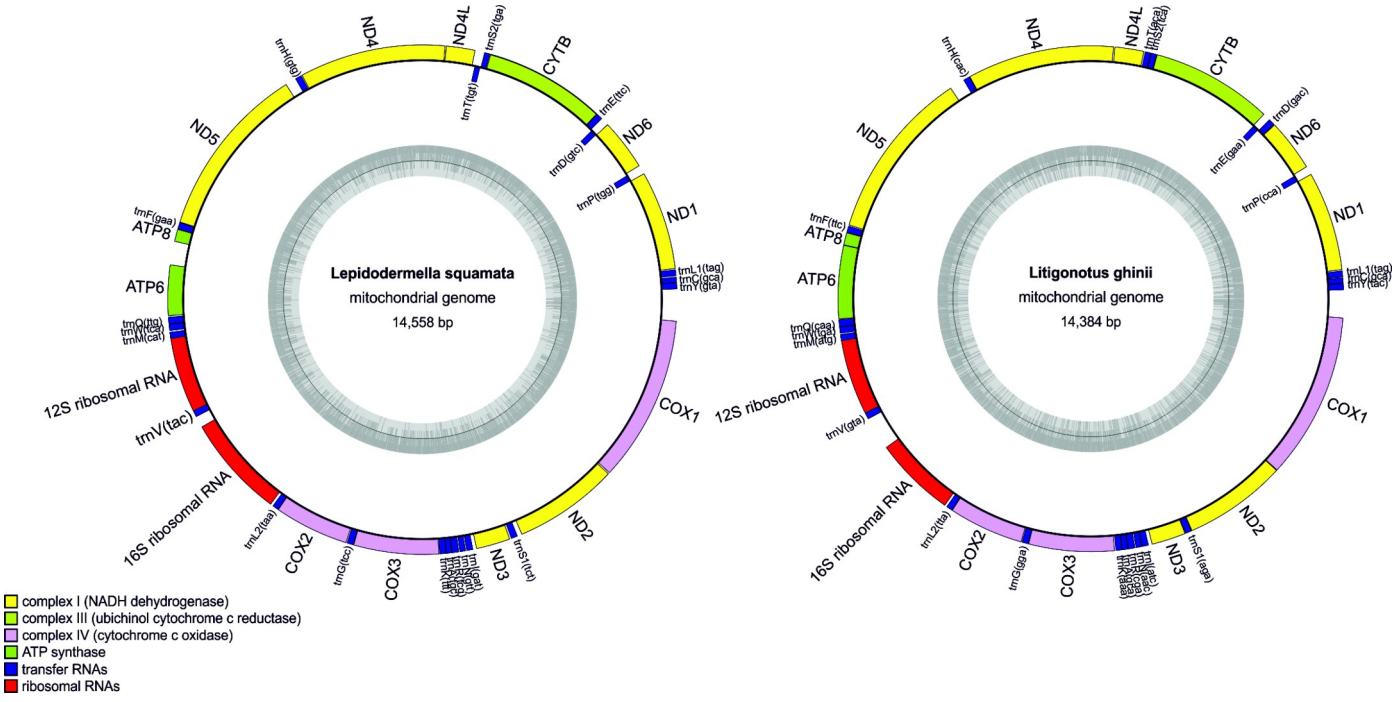

Fig. 2. Mitochondrial gene maps of *Lepidodermella squamata* and *Litigonotus ghinii*, showing the high degree of similarity between these species. The grey inner circles indicate the GC content of the corresponding region.

2. AIMS OF THE THESIS

This PhD project aims to investigate the biodiversity and internal phylogeny of phylum Gastrotricha using concatenated sequences of widely used molecular markers (18S, 28S, COI), obtained by implementing modern DNA amplification and sequencing technologies throughout a WGA + NGS bioinformatic pipeline. Additionally, the project aims to provide additional complete gastrotrich mitochondrial genomes to deepen our understanding of this understudied phylum, and to conduct a new phylogenetic analysis including all protein-coding mitochondrial genes. The use of these sequences is expected to further clarify the phylogenetic relationships left unresolved by the use of three markers.

Starting from these objectives, the project followed three main lines of research.

2.1. Anatomy and evolution of the genus *Urodasys*

The genus *Urodasys* (Macrodasyida) includes 17 species, easily recognizable due to the presence of a peculiar contractile tail that can be three times as long as the body. Besides the extravagant long tail, the genus *Urodasys* fascinates gastrotrichologists and researchers working on reproductive biology, as its members present a particularly complex variety of reproductive organs and strategies. While all species feature paired ovaries, the male reproductive systems vary, with some species having paired testes, others a single testis, and two species lacking male gonads altogether. The presence of accessory reproductive organs also varies, with 12 species possessing a caudal organ that features a unique stylet for sperm transfer (Atherton and Hochberg, 2014; Todaro et al., 2019c). While most *Urodasys* species reproduce via biparental reproduction and oviparity, *U. viviparus* is notable for being parthenogenetic and ovoviviparous, which may explain its cosmopolitan distribution. At the time of my enrollment in the PhD course, the origin and evolution of the astonishing complexity and variety of the reproductive system in *Urodasys* were still largely unclear. Moreover, the sclerotized stylet was thought to have a copulatory function, but the mechanism through which the autosperms are loaded in the structure were unknown (Atherton and Hochberg, 2014).

The first part of the research on *Urodasys* involved the description of a new species and a detailed examination of its reproductive anatomy. This was done using both DIC microscopy and CLSM, offering new insights into the structure and function of the caudal organ and its associated stylet. Furthermore, the use of specimens of the new species allowed us to obtain molecular data for the second part of the research (see below), and their description certified the information on its

reproductive system. The study was conducted in collaboration with professor Francesca Leasi, of the University of Tennesse at Chattanooga (Chapter 1).

The second part investigated the phylogenetic alliances within the group, using an ample taxonomic sampling and a multi-gene approach to further test the evolution of the reproductive systems and modalities of its members. Expanding the genetic sampling across the known reproductive system combinations is expected to yield a more robust understanding of the evolution of this genus (Chapter 2).

The molecular phylogeny of *Urodasys* represented a good starting point for the whole PhD project, as it employed a lower number of specimens in a smaller, highly diverse, taxonomic group. This research not only contributes to the understanding of the evolution of the reproductive traits in an iconic gastrotrich group, but also led to the development and refinement of the WGA + NGS molecular methodology and bioinformatics pipeline. These techniques were subsequently applied throughout the rest of the thesis.

2.2. Multi-gene phylogenetic analysis of the order Macrodasyida

Moving on from the analysis of a single genus, the same methodology was then applied to the study of the phylogeny of the order Macrodasyida.

The project started with a focus on the family Cephalodasyidae Hummon and Todaro, 2010. Traditional taxonomy, based on morphological characteristics, groups in the family Cephalodasyidae five genera: *Cephalodasys*, *Dolichodasys* Gagne, 1977, *Mesodasys*, *Paradasys* and *Pleurodasys* Remane, 1927 (Hummon and Todaro, 2010). However, the family is likely non monophyletic as the current cephalodasyid genera only share either plesiomorphic (for example, a vermiform to strap-shaped body and pharyngeal pores located near the junction of the pharynx and intestine), or negative traits (such as the absence of cuticular scales or spines). The different organization of the reproductive systems in the five genera suggest that the family is non-monophyletic, but do not indicate alternative groupings (Kieneke and Schmidt-Rhaesa, 2014). More recently, molecular phylogenetic studies based on the 18S gene have also indicated that the family is likely polyphyletic, with the five genera appearing variably distributed across the macrodasyidan phylogenetic tree (Todaro et al., 2015; Kieneke and Todaro, 2021). However, support at the relevant nodes in these tree was generally low, leaving doubts about the alliances of the different cephalodasyid genera.

The family Macrodasyidae Remane, 1924 is another group whose monophyly has been questioned by molecular analyses. It includes the four genera *Kryptodasys* Todaro, Dal Zotto, Kånneby & Hochberg, 2019, *Macrodasys*, *Thaidasys* Todaro, Dal Zotto & Leasi, 2015, and

Urodasys. However, the species of the genus *Urodasys* do not cluster with the rest of the family in previous analyses based mainly on the 18S gene alone. Their real phylogenetic position could not be determined in those occasions, due to poor statistical support at the nodes (Todaro et al., 2015; Kieneke and Todaro, 2021).

There was reason to believe that the unstable alliances of the members of these families within the order Macrodasyida, as shown by past molecular studies, was due to poor taxonomic and molecular sampling (Kieneke and Todaro, 2021). In this project I focused on enhancing the analysis by sequencing three genes (18S, 28S, COI) from a significant number of additional species, primarily those belonging to under-sampled genera (i.e. 5 *Cephalodasys* species, 2 *Dolichodasys* species, 2 *Paradasys* species, and the first *Dendrodasys* sequences ever obtained). Additionally, for the first time in the study of the order, the analysis included a significant number of *Urodasys* species representing the genus's main lineages, thanks to the work previously conducted in this thesis (Chapter 3).

2.3. The structure of the gastrotrich mitochondrial genome

When my PhD began, there was only one published gastrotrich mitochondrial genome, belonging to *Lepidodermella squamata* (Dujardin, 1841). This parthenogenetic chaetonotidan species is a widely studied organism and one of the few gastrotrich species that has been successfully cultured (Balsamo and Todaro, 1988; Golombek et al., 2015). Notably, it is the only gastrotrich species available for purchase, as it is listed in the catalogue of the American company Carolina Biological Supply. For this reason, *L. squamata* is recognized as the model species for gastrotrich research (Fromm et al., 2019; Araujo et al., 2023).

The mitogenome of *L. squamata* presents the commonly found 13 protein-coding genes and 22 tRNA genes (Golombek et al., 2015). A second mitogenome, belonging to *Litigonotus ghinii* Gammuto, Serra, Petroni & Todaro, 2024, was sequenced very recently (Gammuto et al., 2024) and shows a striking similarity to the one of *L. squamata* (Fig. 2). This result is not surprising, as both species belong to the family Chaetonotidae and are freshwater and parthenogenetic. Research conducted in other phyla indicates that the biological and ecological diversity of gastrotrichs is likely mirrored in the structure of their mitochondrial genomes. Consequently, it would be of great interest to sequence and analyse additional chaetonotidans, as well as macrodasyidan gastrotrichs including marine and hermaphroditic species. This will help enhance our understanding of the structure and characteristics of the mitochondrial genome within this phylum.

The third line of research in my PhD project aimed to investigate the molecular architecture of mitochondrial genomes in gastrotrichs. The sequenced specimens belong to different lineages

representative of the ample taxonomic spectrum of the phylum, in an effort to identify any potential relationship between mitogenome features and the different ecological and biological traits of these animals. Additionally, the study conducted a comprehensive phylogenetic analysis based on the newly obtained sequences of protein-coding mitochondrial genes.

This project was performed in collaboration with researchers from the universities of Pisa and Bologna, and from the Naturalis Biodiversity Center in Leiden (Netherlands), where I spent my research period abroad during the winter of 2024 (Chapter 4).

CHAPTER 1

CONFOCAL LASER SCANNING MICROSCOPY APPLIED TO A NEW SPECIES HELPS UNDERSTAND THE FUNCTIONING OF THE REPRODUCTIVE APPARATUS IN STYLET-BEARING *URODASYS* (GASTROTRICHA: MACRODASYIDA)

(published in *Water* 15, 1106. https://doi.org/10.3390/w15061106)

water

MDPI

Article

Confocal Laser Scanning Microscopy Applied to a New Species Helps Understand the Functioning of the Reproductive Apparatus in Stylet-Bearing *Urodasys* (Gastrotricha: Macrodasyida) †

Agata Cesaretti [1], Francesca Leasi [2] and M. Antonio Todaro [1,3,*]

[1] Department of Life Sciences, University of Modena and Reggio Emilia, 41125 Modena, Italy
[2] Department of Biology, Geology and Environmental Science, University of Tennessee at Chattanooga, Chattanooga, TN 37403, USA
[3] National Biodiversity Future Center (NBFC), 90133 Palermo, Italy
* Correspondence: antonio.todaro@unimore.it
† urn:lsid:zoobank.org:pub:BEB0E157-DE10-44D9-8E62-9E7B64928123; urn:lsid:zoobank.org:act:F6DE1286-082E-441B-8608-34F7CBDCF47A.

Abstract: Gastrotrichs are highly diverse and abundant in all aquatic ecosystems; however, they are often overlooked. During a biodiversity survey in Sardinia (Italy), a new species of gastrotrich herein described was discovered. Specimens of *Urodasys bifidostylis* sp. nov. were found in sandy sediments from two submarine caves. Using an integrative approach of traditional light (DIC) and high-resolution (CLSM) microscopies, we herein reveal, for the first time, the fine structure and function of the reproductive organ in an *Urodasys* representative. This is particularly relevant considering the complex reproductive organs and strategies of this group. Results allow comparisons between the reproductive apparatus and sperm transfer modalities in *Urodasys* and the closely related genus *Macrodasys*. One similarity is that both groups transfer male gametes in packets, suggesting the production of spermatophores to be a common phenomenon in Gastrotricha. Unique to *Urodasys* is the ability of multiple and consecutive copulations and sperm transfers and, differently than *Macrodasys*, the transfer of sperms unlikely occurs simultaneously between the two hermaphroditic partners. These findings provide new insights into the reproductive strategies of *Urodasys* and are expected to advance future studies on the evolution of reproductive strategies and the rise of interspecific reproductive barriers in interstitial meiofauna.

Keywords: biodiversity; CLSM; meiofauna; reproduction; spermatophores; taxonomy

Citation: Cesaretti, A.; Leasi, F.; Todaro, M.A. Confocal Laser Scanning Microscopy Applied to a New Species Helps Understand the Functioning of the Reproductive Apparatus in Stylet-Bearing *Urodasys* (Gastrotricha: Macrodasyida). *Water* **2023**, *15*, 1106. https://doi.org/10.3390/w15061106

Academic Editor: Roberta Pedrazzani

Received: 3 February 2023
Revised: 2 March 2023
Accepted: 11 March 2023
Published: 14 March 2023

1. Introduction

The phylum Gastrotricha is composed of small-sized (0.08–3.5 mm in length) meiobenthic, worm-like invertebrates, commonly found in both marine and freshwater environments. The clade is highly diversified, and, to date, it includes more than 860 species in 60 genera, 18 families and 2 orders: Macrodasyida and Chaetonotida [1,2]. The phylum is cosmopolitan, and its representatives are numerically abundant in all the aquatic systems, especially in the marine interstitial environments where they typically rank among the top three meiobenthic taxa [3,4].

Despite their abundance and variety, gastrotrichs are still understudied, and many questions regarding the structure and functions of their internal organs are yet to find satisfactory answers. Traditional light microscopy, while informative on general external morphology, is unable to uncover many internal characteristics in animals of such small size as gastrotrichs; for this reason, the application of high-resolution microscopy techniques is becoming more commonplace in the study of this phylum in line with the more modern integrated approaches in the field of biodiversity research [5].

One of these techniques is confocal laser scanning microscopy (CLSM), which, in combination with appropriate fluorochromes, allows for the reconstruction of three-dimensional structures by capturing multiple two-dimensional images on a vertical *z*-axis at different depths [6]. For example, CLSM combined with fluorescent phalloidin has unveiled the full muscular organisation of numerous microinvertebrates [7–9], particularly gastrotrichs [10–13]. Based on these studies, the general muscle arrangement appears to be relatively conserved among Gastrotricha at a higher taxonomic ranking, while the diversification of the selected muscular characteristics seems connected to the reproductive and ecological strategies of the diverse taxa [14,15]; for these reasons, the muscular system also bears potential phylogenetic significance as well as insights on the ecological adaptations [11]. This work focuses on the iconic genus *Urodasys* (Macrodasyida), whose representatives are easily identifiable by the presence of a long contractile tail. Among Gastrotricha, the genus *Urodasys* is of particular interest regarding their reproduction, as its members present a particularly complex variety of reproductive organs and strategies, whose origin and evolution are still unclear. Based on the reproductive characteristics, species of the genus can be allocated into three main groups: (i) hermaphroditic species lacking a copulatory sclerotised stylet; (ii) hermaphroditic species possessing a copulatory sclerotised stylet; (iii) *Urodasys viviparus*, a parthenogenetic, ovoviviparous species lacking testicles and accessory reproductive structures altogether [16,17].

The sclerotised stylet is an accessory structure of the male reproductive apparatus, and its shape also represents an essential feature for identifying the species, as it presents an astounding variety of species-specific forms (e.g., [18,19]). The stylet is part of the caudal organ, which as a whole collects autosperm and transfers them to the partner during copulation. The allosperm are received and stored in the frontal organ, which is structurally simpler and often described as "sack-like" [20,21].

The caudal organ is primarily muscular, but its complex structure and function are not fully understood. In this work, we describe a new stylet-bearing species of *Urodasys* examined through more traditional light microscopy (e.g., DIC) and high-resolution confocal microscopy (CLSM), with the primarily goal to shed light on the fine structure and function this complex reproductive apparatus.

2. Materials and Methods

2.1. Sampling and Sample Processing

Specimens of the new species were found in sandy sediments collected from two submarine caves near Capo Caccia (Sardinia, Italy) during a meiofauna biodiversity survey focused on the Italian marine protected areas in 2005 [22,23]. Being microscopic and not pathogenic invertebrates, the collection, handling and use of meiofaunal organisms and particularly Gastrotricha is not regulated/prohibited; moreover, their collection does not damage the environment. Sampling was performed by scuba divers who filled up, by hand, two 500 mL plastic jars by scraping the top 5 cm sediment layer from each cave. Further information on sampling sites and characteristics of the microhabitats is provided below (see type material). After collection, samples were transported to the field laboratory in Fertilia near Alghero (Sassari) and processed within one week. Fauna were extracted daily by the narcotisation–decantation technique, using a 7% $MgCl_2$ solution, and by pouring aliquots of the supernatant straight into a 5/3 cm diameter Petri dish.

2.2. Microscopical Study

2.2.1. Differential Interference Contrast (DIC)

Animals were searched for using a Wild M3 stereomicroscope, and when located, single, narcotised gastrotrichs were transferred by a micropipette to a glass slide and studied alive under a Leitz Dialux 20 microscope, fitted for Nomarski observation (DIC, differential interference contrasts optics) and a Nikon 995 digital camera for vouchering.

2.2.2. Confocal Laser Scanning Microscopy (CLSM)

Two identified specimens were fixed at 4 °C for 1 h in 4% paraformaldehyde in 0.1 M phosphate-buffered saline solution and stored in PBS for later use. At the Modena laboratory, the fixed specimens were repeatedly rinsed with freshly made 0.1 M PBS solution, permeabilised for 1 h in a 0.2% Triton X-100 solution, stained for 1.5 h with TRITC-phalloidin (Sigma, Schnelldorf, Germany), washed again in PBS and embedded Citifluor (Plano, Wetzlar, Germany) on microscope slides, and surveyed using a Leica DM IRE 2 Confocal Laser Scanning Microscope (see [11]). Image stacks of optical sections were projected in one maximum-projection (MPJ) image or visualised as a simulated fluorescence projection (SFPJ) for a three-dimensional appearance.

2.3. General Conventions

The convention used in the description of the new species, the logic for the derivation of its ecological characteristics and the procedure to obtain the granulometric parameters of the sediment are the same as in Todaro et al. [24].

3. Results

Taxonomic Account

Order Macrodasyida Remane, 1925 [25] [Rao and Clausen, 1970] [26]
Family Macrodasyidae Remane, 1924 [27]
Genus *Urodasy*s Remane, 1926 [28]
Urodasys bifidostylis sp. nov. (Figures 1–4)

Diagnosis: Body worm-like, up to 493 µm in total length (LT), vaulted dorsally, flattened ventrally and with numerous epidermal glands along the sides; cuticle smooth; body width mostly uniform but presenting an evident constriction in the posterior third of the trunk region; head blunt, narrowing towards the mouth, with sparse sensorial cilia but deprived of pestle organs or eyespots; other sensory hairs organised in columns on the lateral and dorsolateral sides of the body; locomotory ciliature in form of a continuous field under the cephalic and pharyngeal region, then forming two paired bands spanning to the end of the body. TbA, five to six per side, arranged in a lateral (four to five tubes) and a medial column (one tube); TbVL, seven per side, broadly even spaced from the pharyngeal pores to the end of the body region; TbL, two per side, one along the pharyngeal region and one in the posterior trunk region; TbDL, three per side, one anterior to the trunk constriction and two past it. TbD and TbV apparently absent. Mouth narrow and terminal; buccal cavity weakly cuticolarised; pharynx up to 202 µm in length; pharyngeal pores, sub-basal, with ventrolateral openings; pharyngo-intestinal junction (PhIJ) at about U45; intestine simple and apparently blind; testis single, on the right side; male pore ventral; mature sperm, filiform (48 µm in length), showing a slightly spiralled anterior portion; female gonads paired, oocytes maturing in a caudocephalic direction; largest egg dorsal to the mid-intestine; frontal organ dorsal to the intestine, centred at U74; sac-like, with slightly muscularised wall (56 µm in length and 16–18 µm in width), external pore dorsal; caudal organ in the posterior body region; strongly muscularised and furnished of a sclerotised stylet; stylet compose of narrow funnel-shaped anterior portion and a characteristic distally-forked posterior portion; one end is corkscrew-shaped while the other is in the form of a short hook.

Etymology:*Bifidostylis* (from the Latin *bifidus* = bifurcated) referring to the bifurcated terminal portion of the sclerotised stylet in the caudal organ.

Examined material: The description of *Urodasys bifidostylis* sp. nov. is derived from five adult specimens, three observed alive, under DIC optics, and two studied with confocal microscopy. The microscopically examined specimens were destroyed during observation. The holotype, LT 493 µm, is the adult shown in Figure 2 (International Code of Zoological Nomenclature, Articles 73.1.1, 73.1.4 see also recommendation 73G–J of Declaration 45—Addition of Recommendations to Article 73, 19) [29,30].

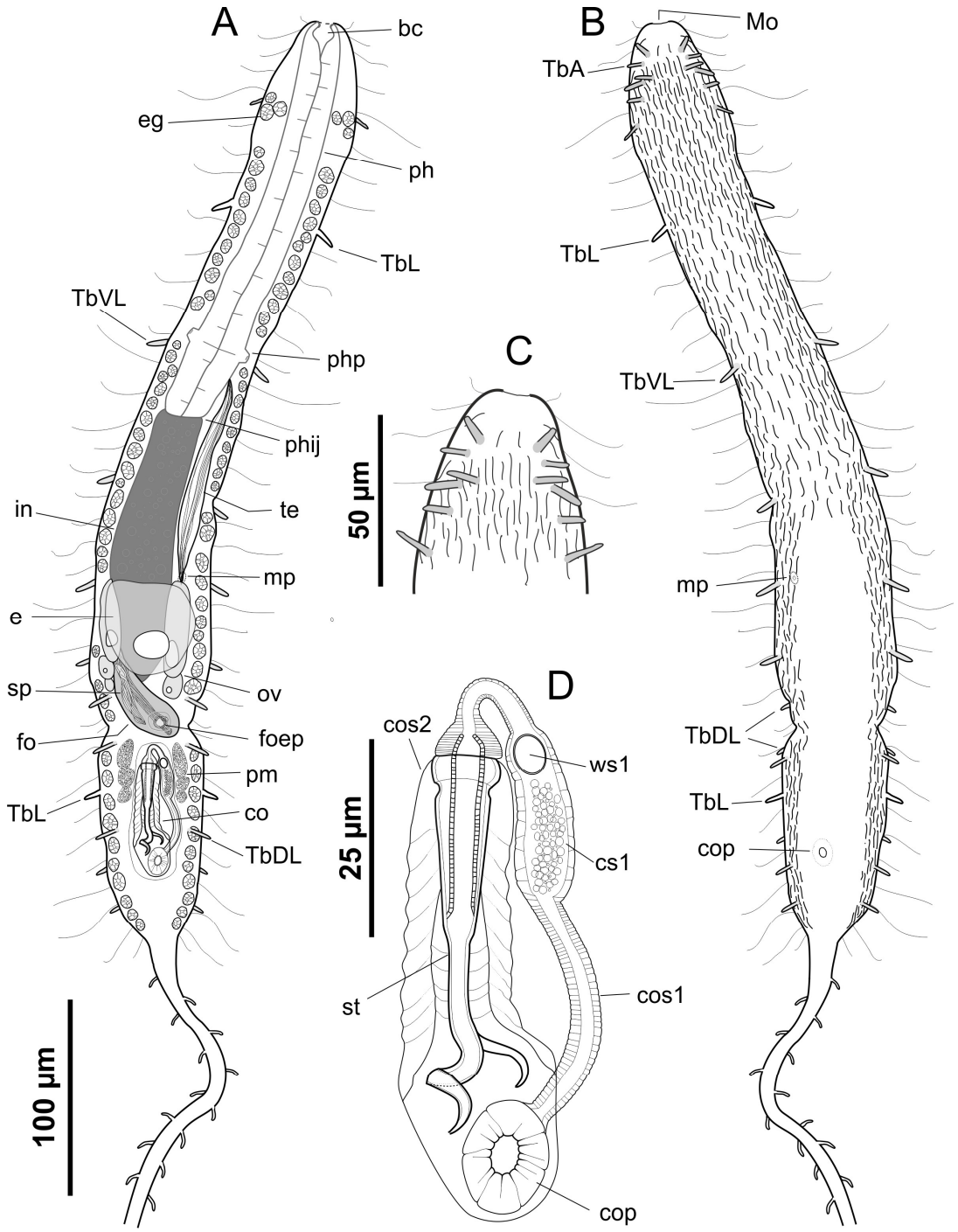

Figure 1. Line art illustration of *Urodasys bifidostylis* sp. nov. (**A**) *Habitus*, showing the internal anatomy seen from a dorsal view; (**B**) *habitus*, ventral view; (**C**) detail of the anterior end, ventral view, showing the anterior adhesive tubes; (**D**) detail of the caudal organs, ventral view, showing the internal organisation in two connected muscular structures. bc—buccal cavity, co—caudal organ, cop—caudal organ pore, cos1—muscular structure 1 of the caudal organ, cos2—muscular structure 2 of the caudal organ, cs1—chamber of structure 1, e—egg, eg—epidermal gland, fo—frontal organ, foep—external pore of the frontal organ, mo—mouth, mp—male pore, ov—ovary, ph—pharynx, phij—pharyngo-intestinal junction, pm—prostatic glandular material, sp—allosperm packets inside the frontal organ (=spermatophore), st—stylet, te—testis, ws1—window of structure 1, TbA—anterior adhesive tubes, TbDL—dorsolateral adhesive tubes, TbL—lateral adhesive tubes, TbVL—ventrolateral adhesive tubes.

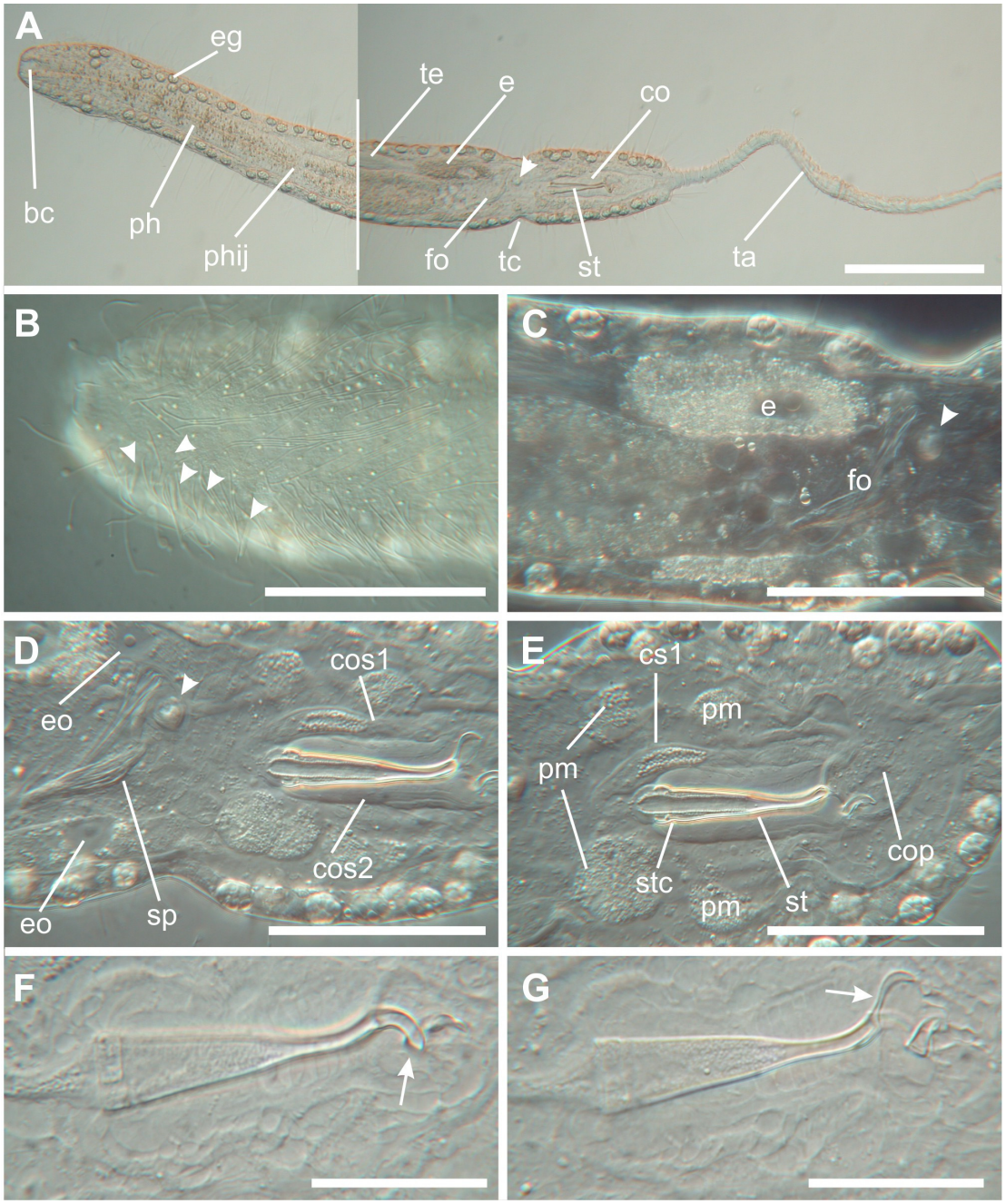

Figure 2. Photomicrographs of *Urodasys bifidostylis* sp. nov. holotype (Nomarski optics). (**A**) *Habitus*, showing the internal anatomy seen from a dorsal view; the arrowhead indicates the external pore of the frontal organ. (**B**) Details of the anterior end, ventral view, showing the anterior adhesive tubes (arrowheads). (**C**) Details past the mid-trunk region showing the internal organs. (**D**,**E**) Details of the posterior trunk region, showing the internal organs; the arrowhead indicates the external pores of the frontal organ, inside which two packets of allosperm are seen. (**F**,**G**) Details of the copulatory stylet seen at different focal planes, showing the forked posterior end; the arrow indicates the corkscrew-shaped injecting portion while the arrowhead indicated the secondary hooked extremity. bc—buccal cavity, co—caudal organ, cop—caudal organ pore, cos1—muscular structure 1 of the caudal organ, cos2—muscular structure of the caudal organ, cs1—chamber of structure 1, e—egg, eg—epidermal gland, eo—early oocyte, fo—frontal organ, ph—pharynx, phij—pharyngo-intestinal junction, pm—prostatic glandular material, sp—allosperm packet inside the frontal organ (=spermatophore), st—stylet, stc—stylet constriction, ta—tail, tc—trunk constriction, te—testis. Scale bars: (**A**) = 100; (**B**–**E**) = 50 μm; (**F**,**G**) = 25 μm.

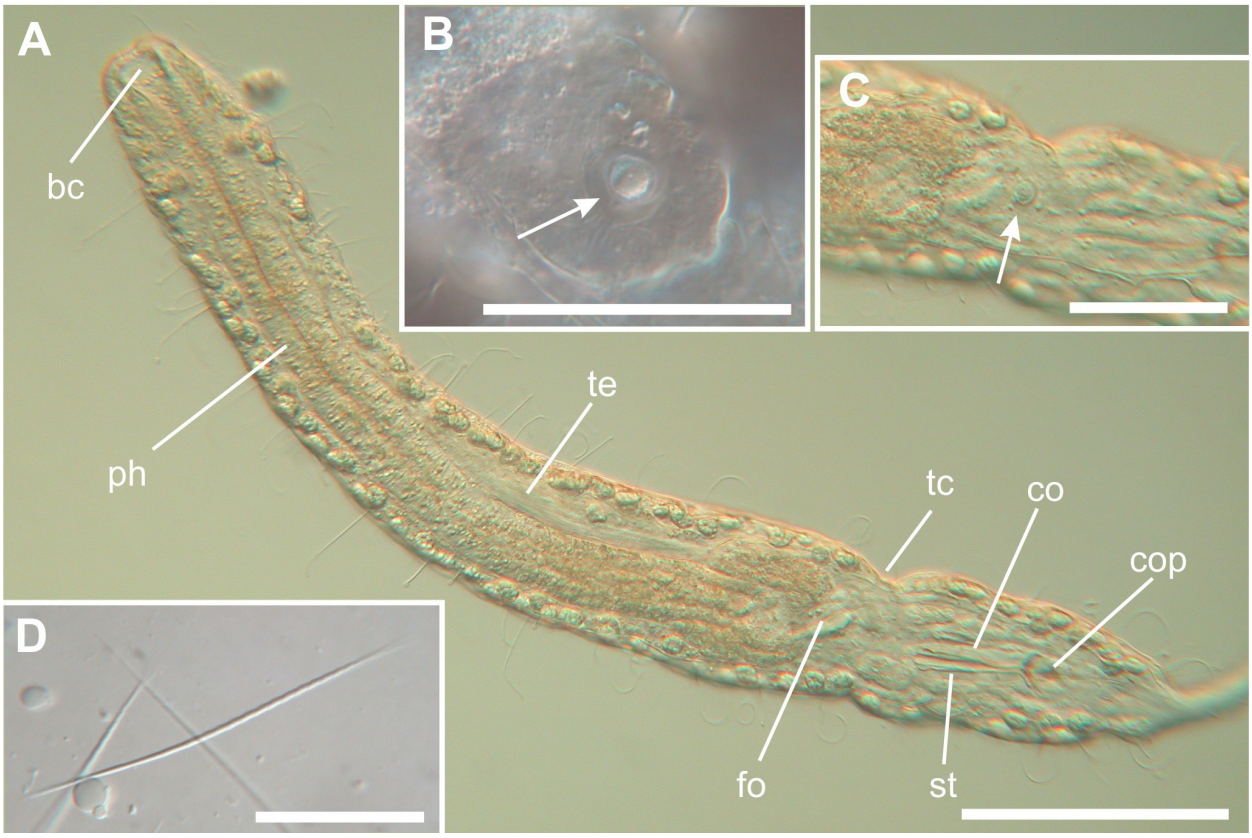

Figure 3. Photomicrographs of *Urodasys bifidostylis* sp. nov. (Nomarski optics). (**A**) *Habitus* of an adult specimen, with detail of the internal anatomy as seen from the ventral side. Inserts (**B**,**C**) details from the dorsal side showing the external pore of the frontal organ. Insert (**D**) testicular spermatozoa. bc—buccal cavity, co—caudal organ, cop—caudal organ pore, fo—frontal organ, ph—pharynx, st—stylet, tc—trunk constriction, te—testis. Scale bars: (**A**) = 100; (**B**,**C**) = 50 µm; (**D**) = 20 µm.

Distribution and ecology: Sardinia (Italy)—Type locality: Grotta il Porticato (submarine cave il Porticato, latitude 40°34′17.3″ N; longitude 08°09′39.6″ E); common in frequency and numerous in abundance at 20 m depth in coarse (Medium grain size = 0.51 phi = 0.7 mm) moderately sorted (sorting value = 0.84) sand. Other locations: Nereo's cave (latitude 40°33′70.5″ N, longitude 08°09′62.9″ E); common in frequency of occurrence and scarce in abundance in medium (medium grain size = 1.28 phi = 0.41 mm), moderately sorted (sorting value = 0.88) sand collected at a depth of 30.7 m. Two additional specimens of this species were found in 2010 at a nearby location (Costa Paradiso, 41°3′8.84″ N, 8°56′15.71″ E, see Curini et al. [23], Urodasys sp.3 it, Table 6S). These two specimens were stored in alcohol and are kept in the senior author's collection for future DNA analysis. At the three sites reported above, values of water temperature and salinity at the time of samplings were invariably 13 °C and 38‰, respectively. So far, the new species has been found always together with the recently described *Kryptodasys curinii* Todaro et al., 2019 [24].

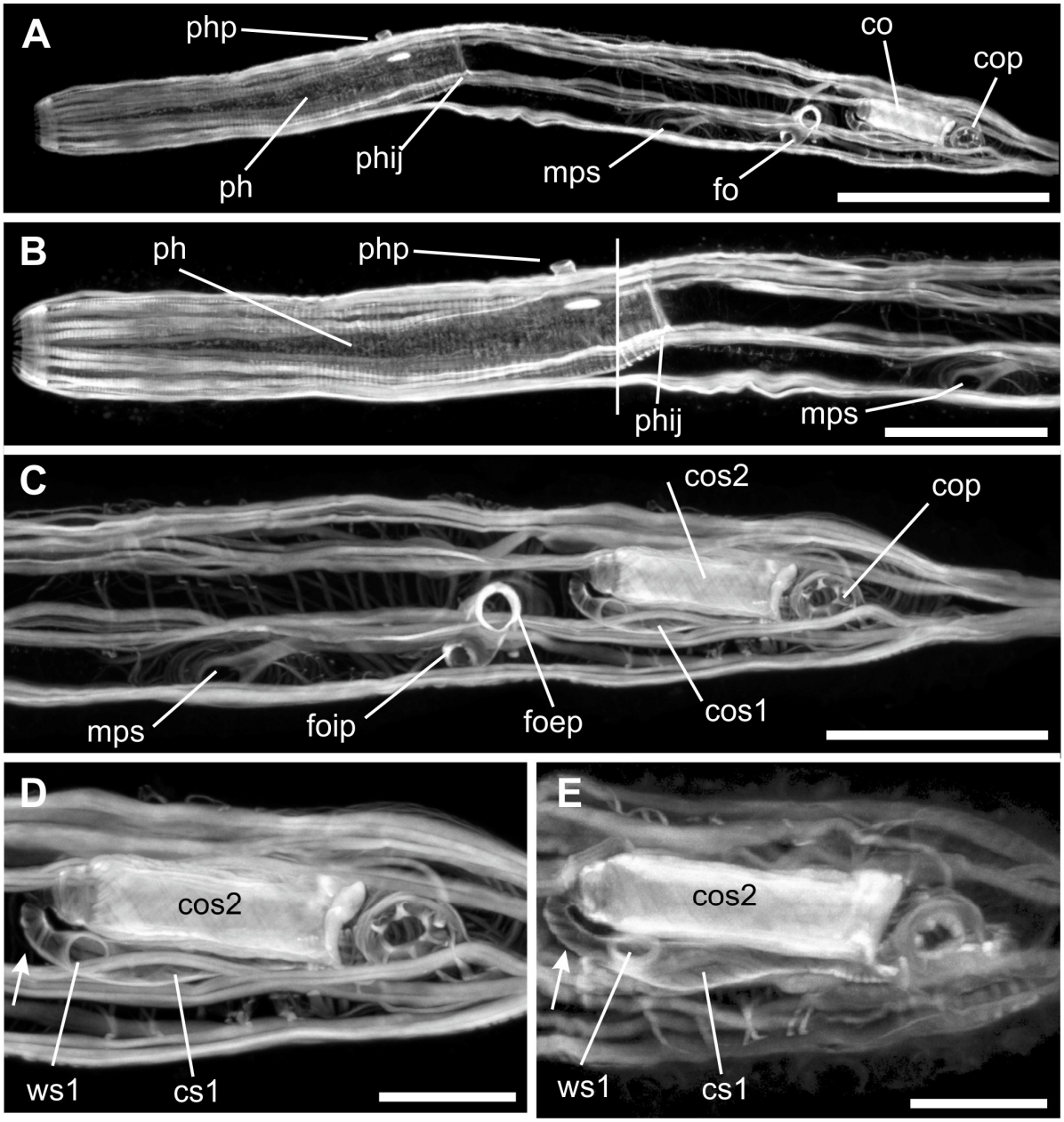

Figure 4. Photomicrographs of *Urodasys bifidostylis* sp. nov. (muscular system visualised with CLSM). (**A**) Whole adult specimen. (**B**) Close-up of the pharyngeal and mid trunk region. (**C**) Close-up of the mid- and posterior trunk region. (**D**) Details of the caudal organ, arrow indicates the connection between structure 1 and 2. (**E**) Details of the caudal organ of a different specimen; details of the caudal organ, arrow indicates the connection between structure 1 and 2. co—caudal organ, cop—caudal organ pore, cos1—caudal organ structure 1, cos2—caudal organ structure 2, cs1—chamber of structure 1, fo—frontal organ, mps—male pore sphincter, ph—pharynx, phij—pharyngo-intestinal junction, php—pharyngeal pore, ws1—window of structure 1. Scale bars: (**A**) = 100; (**B**,**C**) = 50 µm; (**D**,**E**) = 20 µm.

Description: based mostly on the full adult specimen (holotype) of total body length 493 µm (tail not included), shown in (Figures 1 and 2). Body worm-like, elongated and quite narrow, vaulted dorsally, ventrally flattened with numerous epidermal glands, single testis along the right side, and an evident sclerotised stylet. The cuticle is smooth and does not present ornamentations, such as scales and/or spines. Body width mostly uniform in the pharynx region, increasing slightly in the gut region and presenting an evident

constriction in the posterior third of the trunk region, at U77; the width then increases again and finally tapers to the elongated tail, which appears cut off (Figure 2A). Head blunt, narrowing towards the mouth, with sparse sensorial cilia but deprived of eyespots and pestle organs. Body widths as follows: head, min 27 µm at U0, max 50 µm at U10; pharynx region min 47 µm at U22, max 51 µm at U45; trunk, max 61 µm at U67, constriction 42 µm at U77, min 31 µm at the base of tail (U99).

Epidermal glands: numerous (about 45–48 on each side), round to oval in shape (diameter about 7–8 µm), distributed in a single row per side from U10 to U100 with noticeable 2–3 glands clusters on the sides of the head at U10 (Figures 1A and 2A). A rounded structure, similar to the epidermal glandes is present more medially in the anterior trunk region at U53.

Ciliation: sensory hairs up to about 15–16 µm in length present sparsely in the head region, others up to 37 µm in length organised in columns on the lateral and dorsolateral sides of the body (Figure 1A,B). Locomotory ciliature forms a continuous field from the cephalic region to the beginning of the gut region (U2–U51), then forms two paired bands continuing to the end of the body (Figures 1B and 2B).

Adhesive tubes: TbA, 10 in total, from U3 to U9, 7–10 µm long and arranged in 4 columns, 2 lateral with 4 tubes each and 2 more medial of 2 tubes each (Figures 1C and 2B); TbV, not present; TbVL, 7 per side, 10–12 µm long, broadly even spacing from the pharyngeal pores to the end of the body region; TbL, 2 per side, 9–10 µm long, 1 along the pharyngeal region (at U22) and 1 in the posterior trunk region (at U84); TbDL, 3 per side, 9–10 µm long, 1 anterior to the trunk constriction and 2 past it (U74-U85) (Figure 1A,B). TbD apparently absent. Moreover, numerous adhesive tubes (5–6 µm long) are inserted asymmetrically on the whole length of the tail.

Digestive tract: mouth terminal, narrow, 8 µm in diameter, presenting a weakly cuticolarised buccal cavity (10–11 µm wide, 16 µm long) (Figures 1A and 2A). The pharynx is 200 µm long measured from the posterior edge of the buccal cavity, showing a more or less uniform width (about 25 µm); pharyngeal pores, sub-basal, at U37, with ventrolateral openings (Figures 1A and 4A,B). Pharyngo-intestinal junction at about U45 (Figures 1A and 4A,B). The intestine spans to U73; it is simple and apparently blind; broadest in its middle region, much narrower to the rear; anus apparently absent (Figure 1A).

Reproductive tract: hermaphroditic; single testis on the right side of the body, extending from the posterior pharyngeal region (U40) to about mid-trunk (U69) (Figures 1A, 2A and 3A). The posterior-most end of the testis lies along the ovary and appears to empty externally via an independent pore controlled by a muscular sphincter as revealed by confocal microscopy (Figure 4A–C). Mature sperm are filiform cells (48 µm), showing a slightly spiralised anterior portion (Figure 3D). Female gonads paired, oocytes maturing in a caudocephalic direction from U62 to U74 (Figure 2A,D,E); largest egg dorsal to the intestine, centred at about U67. Frontal organ, extending dorsoventrally, centred at U74; sac-like, with slightly muscularised walls, measuring 56 µm in length and 16–18 µm in width. In the holotypic specimen, the organ contained two distinct elongated masses of spermatozoa (Figure 2C). The frontal organ did not show a clear anatomical–functional compartmentalisation; however, an evident external pore was present on the dorsal side near the trunk constriction (Figures 2A and 3B,C). Confocal microscopy revealed the external pore to possess a strong muscular sphincter; a weaker muscular sphincter is also present toward the ventral side of the frontal organ surrounding what is interpreted as the internal pore (Figure 4A,C).

The caudal organ is located in the posterior body region from just past the trunk constriction to U93. It appears as a roughly cylindrical capsule (68 µm long, 19–20 µm wide) that encloses two muscular structures which are connected frontally and share a common pore distally (Figures 1A,D, 2A,D,E and 4A,C–E). The common pore empties externally on the ventral surface of the animal at U92 (Figure 3A). More specifically, one of the muscular structures (called structure 2) is located on the left side of the caudal organ, it is strongly muscularised, of more or less similar diameter throughout its extension (14–16 µm); most importantly, it encloses a characteristic sclerotised stylet (Figures 2A,D–G, 3A and 4A,C–E).

The sclerotic stylet is 48 µm long; it consists of a narrow, proximal portion, which is shaped like a slender funnel (24 µm in length and max width 9 µm) bearing a noticeable constriction at 3 µm from the rim (Figures 1A,D and 2A,D,E). The distal portion (24 µm in length), is mostly straight and cylindrical in shape (about 3 µm in diameter), then is sharply bent at the distal end, where it twists towards the dorsal side resulting in a short corkscrew-shaped tip (distance from base to tip 10–11 µm; Figures 1D and 2F,G); at the base of the corkscrew-shaped tip, a second hooked extremity originates ventrally from the right side. The second tip appears smaller and with a distally blind canal (Figure 2G); consequently, an accessory function may be envisioned for it.

The other structure (called structure 1) in the caudal organ is less muscularised and it is composed of at least three distinct parts (Figures 1D, 2D,E and 4D,E). The proximal portion resembles a funnel whose conical mouth is in connection with the frontal portion of the stylet-containing structure, while the neck is sharply curved backwards and empties in the intermediate portion (Figures 2D,E and 4D,E); this next portion is wider, originating a sort of oblong chamber in which a number of secretory globulets may be seen (Figure 2D,E). Confocal microscopy reveals that the proximal portion of the chamber's wall presents a pore on the medial side (Figure 4D,E); the third portion is tubular in shape and connects posteriorly the chamber to the ventral pore shared by the two muscular structures (Figure 4D,E).

Anterior and lateral on both sides to the caudal organ (from U79 to U86) are two elongated and irregular masses of secretory glandular material (Figures 1A and 2D,E); a connection between the two masses is not clearly visible, but quite likely. The material found in these masses appears identical to the refringent droplets contained in the chamber of the right structure of the caudal organ (Figure 2D,E).

Morphological variability: Most of the diagnostic characteristics reported for the holotype were present in the other studied specimens (e.g., presence of the trunk constriction, the peculiar, posteriorly bifid stylet, etc) (Figure 2A). Some variability concerned (i), the total body length, which ranged from 445 to 493 µm (mean = 470 µm ± 16.30 SD, n = 3); (ii) the number of TbA ranged from 10 to 12; (iii) the number and distribution of the adhesive tubes along the pharynx and trunk regions, which ranged from 7 pairs to 12 pairs; and (iv) the span of the testis/deferent, as in a single specimen, it appeared to extend more posteriorly at the level of the frontal organ. The tail appeared visibly cut off in most specimens except in one individual where it appeared to be complete and reached four times the length of the body (about 1800 µm in length).

4. Discussion

4.1. Taxonomic Affinities

The genus *Urodasy*s includes a total of 11 nominal, stylet-bearing species (*U. acanthostylis* Fregni, Tongiorgi and Faienza 1998 [19]; *U. bucinastylis* Fregni, Faienza, Grimaldi, Tongiorgi and Balsamo 1999 [31]; *U. calicostylis* Schöpfer-Sterrer 1974 [18]; *U. completus* Todaro, Cesaretti and Dal Zotto 2019 [17]; *U. cornustylis* Schöpfer-Sterrer 1974 [18]; *U. nodostylis* Schöpfer-Sterrer 1974 [18]; *U. poculostylis* Atherton, 2014 [32]; *U. remostylis* Schöpfer-Sterrer 1974 [18]; *U. spirostylis* Schöpfer-Sterrer 1974 [18]; *U. toxostylus* Hummon 2011 [33]; *U. uncinostylis* Fregni, Tongiorgi and Faienza 1998) [19]. One of these, *U. completus,* is clearly distinct from the others as it possesses paired testes, instead of the single testis as in the other species [17]. *U. bifidostylis* sp. nov. presents a single testis and is therefore likely to be phylogenetically closer to the latter species [16,17]. In stylet-bearing species, the shape of this organ is of taxonomic relevance as it is species-specific. Based on the appearance of the anterior portion, shaped as a narrow funnel bearing a constriction near the apex, the stylet of *U. bifidostylis* sp. nov. is most similar to the stylet possessed by *U. nodostylis*, known from Bermuda [Schöpfer-Sterrer 1974] [18] and *U. toxostylus,* described from the Red Sea [Hummon, 2011] [33], though the distal portion of the organ is clearly different in the three taxa. In *U. bifidostylis* sp. nov., the distal portion is straight, needle-like, with a bifurcated posterior end, in *U. toxostylus* it is curved and simple (with no additional appendixes in

the terminal portion), while in *U. nodostylis* it is straight, with a shovel-like posterior end, flanked by two cuticular processes. Other characters that set *U. bifidostylis* sp. nov. apart from *U. toxostylus* and *U. nodostylis* include (i) presence of a trunk constriction (a feature unique among *Urodasys* species); (ii) lack of pestle organs; (iii) the distribution and number of the adhesive tubes (*U. bifidostylis* sp. nov.: 6 TbA, 5–7 TbVL, 1–2 TbL, 2–3 TbDL per side; *U. nodostylis*: 8 TbA, 7 TbVL, 10 TbDL per side; *U. toxostylis*: 7 TbA, 4 TbVL, 4 TbL, 5 TbD per side); and iv) a higher number of epidermal glands (>40 in the new species < 30 in *U. nodostylis* and < 20 in *U. toxostylis*). Moreover, the spermatozoa of the new species look different from those of *U. nodostylis* (the spermatozoa of *U. toxostylus* have not yet been described). In *U. bifidostylis* sp. nov. spermatozoa are 48 µm long, filiform cells, gradually tapering at both ends, and with a slightly spiralled anterior portion; by contrast, in *U. nodostylis*, spermatozoa are 35 µm long, consisting of a noticeable spiralled head and a posterior smooth tail, which according to Schöpfer-Sterrer [18] "*twists back on itself like a whip on its handle*."

4.2. Reproductive System Functioning

In most Gastrotricha Macrodasyida, fertilisation is internal and crossed, and involves two accessory reproductive organs, which, based on their mutual position along the animal's trunk, are defined as the caudal organ and the frontal organ. The transfer of sperm from one partner to another takes place through the caudal organ, which therefore assumes the function of a copulatory organ. Since the vas deferens are generally not in functional continuity with the caudal organ, the latter must first load itself with autosperm before transferring them into the partner's frontal organ. Therefore, it is a type of indirect fertilisation, and the frontal organ is female in function (e.g., [34]). To load the caudal organ with autosperm, the animal folds its caudal part ventrally until the opening of the copulatory organ encounters the male pore; a luminal continuity between the vas deferens and the caudal organ itself is therefore established and the passage of spermatozoa between the two structures may take place. Probably, the spermatozoa are pulled into the caudal organ thanks to the suction action exerted by a part of its muscular component.

The description of such a reproductive behaviour is based on detailed observations carried out on species of the genus *Macrodasys* [34,35], and it is supposed to occur also in most other macrodasyidans, including the stylet-bearing *Urodasys* species (e.g., [20,21]).

In this framework, the stylet, present in many species of *Urodasys*, would facilitate sperm transfer. However, the details of how this may happen still need to be clarified. In this regard, there are two hypotheses: (i) the stylet fills first with sperm and then is inserted as a whole in the frontal organ of the partner, or (ii) the stylet works like a hypodermic needle and simply serves to inject with greater efficacy the sperm in the frontal organ of the partner (see e.g., [17,20]). In the first case, the stylet of *Urodasys* species would have the same function as the copulatory tube that forms in the caudal organ of members of the genus *Macrodasys.* Therefore, it would be homologous to it and, like the copulatory tube of *Macrodasys*, it would have to be reconstructed after each copula [17]. However, our observations support the second hypothesis. A specimen we observed had two elongated masses of spermatozoa inside the frontal organ, but no structure attributable to more or less large portions of a sclerotised stylet. The two healthy-looking masses of spermatozoa were arranged one above the other, and the ventral one was placed towards the outer side of the animal; in contrast, the dorsal one appeared in a more medial position, i.e., closer to the entrance pore. This observation suggests that (i) the spermatozoa are injected in groups and (ii) the two packets of sperm had been inoculated recently and at successive times, even if close to each other. We would like to emphasise that the size of the stylet, particularly the funnel-shaped portion, is compatible with the size of the sperm packets (i.e., it could contain the sperm packets). If these hypotheses are correct, as our observation would suggest, the stylet will function as a simple hypodermic needle, helpful in transferring sperm during several copulas (i.e., its reconstruction after each copula is not needed). Consequently, its functional similarity with the copulatory tube present in *Macrodasys*

seems not supported by our study. However, how do autosperm get to the stylet and pack before being passed to the partner? The confocal images we obtained on two specimens shed light on these details. The photomicrographs clearly show that the caudal organ includes two distinct muscular structures, which appear to be in luminal continuity and associate two specific and sequential functions (Figures 2D,E and 4C–E). If the structure that contains the stylet (structure 2) is functional for the discharge of the sperm, the other (structure 1) inevitably serves for the collection of the autosperm and, therefore, for their compacting into packets. Once formed, sperm packets are then sent/passed to the stylet (in structure 2). The formation of sperm packets requires the presence of glandular secretions. In the case of our specimens, droplets of glandular secretions were abundant near the caudal organ and to a lesser extent inside it, and more precisely in the chamber of the muscular structure functional to sperm intake (structure 1). In some instances, droplets were also visible adjacent to the inner wall of the stylet (structure 2; Figure 2D,E). The different quantities of secretory material, higher outside and lower inside the caudal organ, suggests that (i) secretion is produced by a glandular tissue external to the organ and (ii), when necessary, a certain quantity is transferred inside the caudal organ to allow for sperm packing. The presence of a window along the muscular sheath of structure 1 (Figure 4D,E) suggests that the "prostatic" material enters the caudal organ through this route, although a duct is not visible in any of our images (likely, its walls lack muscular fibres). As hypothesised for the spermatozoa, the prostatic secretion would be pulled into the caudal organ by the suction action generated by the contraction of the muscles of structure 1. The assembly/formation of the packets of spermatozoa would take place in the chamber identified in structure 1 (Figures 2E and 4D,E), which is the most compatible, in terms of size, to contain both the glandular secretion and the sperm themselves. The packets of sperm would then be conveyed one by one to the stylet and then progressively injected into the frontal organ of the partner.

The two continuous functional structures of the caudal organ in *U. bifidostylis* sp. nov. allow for the unidirectional path of the spermatozoa inside it and the sequential transfer of sperm to one or multiple partners. As such, the reproductive behaviour of the stylet-bearing *Urodasys* and those described for *Macrodasys* are fundamentally different. In fact, *Macrodasys* representatives are equipped with a caudal organ blind-ended, and inoculation of several packets of sperm by a single partner is not possible (at least in the short run) given the time needed to reconstruct the copulatory tube [34]. Another difference between species of the two taxa is also related to where the entry of the allosperm takes place. The entrance pore of the frontal organ is located on the dorsal side in *Urodasys*, while in *Macrodasys* it is ventral. This could also have effects on the mating system adopted by the members of the two groups. The simultaneous exchange of spermatozoa between two copulating individuals observed by Ruppert [35] for *Macrodasys* would be mechanically unlikely in *Urodasys*, since it would require the reciprocal insertion of the ventral stylet on the dorsal side of the partner. In *Urodasys*, the insemination could still be reciprocal between the same two partners but at different times.

5. Conclusions

Our study has highlighted several differences between *Urodasys* and *Macrodasys* regarding the reproductive apparatus and sperm transfer modalities. However, an important similarity between the reproductive strategies of *Urodasys* and *Macrodasys* is that in both cases, male gametes are transferred in packets, not as single, loose spermatozoa. According to Mann [36], "*spermatophores are male reproductive structures that package sperm cells to aid in their transmission to females during mating in a variety of invertebrate animals*." If this definition applies to Gastrotricha, in cases of *Urodasys* and *Macrodasys*, and in all other taxa in which the spermatozoa are transferred in tight bundles, the term spermatophore should identify the sperm packets. Consequently, within Gastrotricha, the production of spermatophores is a generalised phenomenon that occurs in most species (except e.g., *Mesodasys*), especially

those in which the copulatory organ is not in a luminal continuity with the vas deferens (cfr [16,37]).

Author Contributions: All authors conceived the ideas; M.A.T. performed DIC Survey, F.L. acquired CLSM images. All authors contributed to data interpretation; the final version was written by all authors. All authors have read and agreed to the published version of the manuscript.

Funding: This research was partially supported by a grant 'Far attrezzature 2021' to M.A.T. from the University of Modena e Reggio Emilia, Italy; the 2005 sampling was made possible thanks to a grant to M.A.T. from the Italian Ministry of Research (MIUR Prin-2004 "Contributo della meiofauna alla biodiversità marina italiana").

Data Availability Statement: The data presented in this study are available only in the present study.

Acknowledgments: The authors would like to thank Marco Curini-Galletti for arranging the survey in Sardinia and for collecting the sandy samples.

Conflicts of Interest: The authors declare no conflict of interest.

References

1. Todaro, M.A.; Sibaja-Cordero, J.A.; Segura-Bermúdez, O.A.; Coto-Delgado, G.; Goebel-Otárola, N.; Barquero, J.D.; Mariana Cullell-Delgado, M.; Dal Zotto, M. An introduction to the study of Gastrotricha, with a taxonomic key to families and genera of the group. *Diversity* **2019**, *11*, 117. [CrossRef]
2. Kieneke, A.; Todaro, M.A. Discovery of two 'chimeric' Gastrotricha and their systematic placement based on an integrative approach. *Zool. J. Linn. Soc.* **2021**, *192*, 710–735. [CrossRef]
3. Balsamo, M.; Artois, T.; Smith, J.P.S.; Todaro, M.A.; Guidi, L.; Leander, B.S.; Van Steenkiste, N.W.L. The curious and neglected soft-bodied meiofauna: Rouphozoa (Gastrotricha and Platyhelminthes). *Hydrobiologia* **2020**, *847*, 2613–2644. [CrossRef] [PubMed]
4. Todaro, M.A.; Luporini, P. Not too big for its mouth: Direct evidence of a macrodasyidan gastrotrich preyed in nature by a dileptid ciliate. *Eur. Zool. J.* **2022**, *89*, 785–790. [CrossRef]
5. Dayrat, B. Towards integrative taxonomy. *Biol. J. Linn. Soc.* **2005**, *85*, 407–417. [CrossRef]
6. Paddock, S.W. (Ed.) *Confocal Microscopy: Methods and Protocols*; Humana Press: Totowa, NJ, USA, 1999; pp. 1–446.
7. Leasi, F.; Neves, R.C.; Worsaae, K.; Sørensen, M.V. Musculature of *Seison nebaliae* Grube, 1861 and *Paraseison annulatus* (Claus, 1876) revealed with CLSM: A comparative study of the gnathiferan key taxon. *Zoomorphology* **2012**, *131*, 185–195. [CrossRef]
8. Neves, R.C.; Bailly, X.; Leasi, F.; Reichert, H.; Sørensen, M.V.; Kristensen, R.M. A complete three-dimensional reconstruction of the myoanatomy of Loricifera: Comparative morphology of an adult and a Higgins larva stage. *Front. Zool.* **2013**, *10*, 1–21. [CrossRef]
9. Altenburger, A. The neuromuscular system of *Pycnophyes kielensis* (Kinorhyncha: Allomalorhagida) investigated by confocal laser scanning microscopy. *EvoDevo* **2016**, *7*, 25. [CrossRef]
10. Leasi, F.; Rothe, B.H.; Schmidt-Rhaesa, A.; Todaro, M.A. The musculature of three species of gastrotrichs surveyed with confocal laser scanning microscopy (CLSM). *Acta Zool.* **2006**, *87*, 171–180. [CrossRef]
11. Leasi, F.; Todaro, M.A. The muscular system of *Musellifer delamarei* (Renaud-Mornant, 1968) and other chaetonotidans with implications for the phylogeny and systematization of the Paucitubulatina (Gastrotricha). *Biol. J. Linn. Soc.* **2008**, *94*, 379–398. [CrossRef]
12. Leasi, F.; Todaro, M.A. Meiofaunal cryptic species revealed by confocal microscopy: The case of Xenotrichula intermedia (Gastrotricha). *Mar. Biol.* **2009**, *156*, 1335–1346. [CrossRef]
13. Todaro, M.A.; Dal Zotto, M.; Leasi, F. An integrated morphological and molecular approach to the description and systematisation of a novel genus and species of Macrodasyida (Gastrotricha). *PLoS ONE* **2015**, *10*, e0130278. [CrossRef] [PubMed]
14. Hochberg, R. Musculature of the primitive gastrotrich *Neodasys* (Chaetonotida): Functional adaptations to the interstitial environment and phylogenetic significance. *Mar. Biol.* **2005**, *146*, 315–323. [CrossRef]
15. Kieneke, A.; Arbizu, P.M.; Riemann, O. Body musculature of *Stylochaeta scirtetica* Brunson, 1950 and *Dasydytes* (Setodytes) *tongiorgii* (Balsamo, 1982) (Gastrotricha: Dasydytidae): A functional approach. *Zool. Anz.* **2008**, *247*, 147–158. [CrossRef]
16. Atherton, S.; Hochberg, R. The evolution of the reproductive system of *Urodasys* (Gastrotricha: Macrodasyida). *Invert. Biol.* **2014**, *133*, 314–323. [CrossRef]
17. Todaro, M.A.; Cesaretti, A.; Dal Zotto, M. Marine gastrotrichs from Lanzarote, with a description of a phylogenetically relevant species of *Urodasys* (Gastrotricha, Macrodasyida). *Mar. Biodivers.* **2019**, *49*, 2109–2123. [CrossRef]
18. Schoepfer-Sterrer, C. Five new species of *Urodasys* and remarks on the terminology of the genital organs in Macrodasyidae (Gastrotricha). *Cah. Biol. Mar.* **1974**, *15*, 229–254.
19. Fregni, E.; Tongiorgi, P.; Faienza, M.G. Two new species of *Urodasys* (Gastrotricha, Macrodasyidae) with cuticular stylet. *Ital. J. Zool.* **1998**, *65*, 377–380. [CrossRef]
20. Ruppert, E.E. Gastrotricha. In *Microscopic Anatomy of Invertebrates*; Harrison, F.W., Ruppert, R.R., Eds.; Wiley-Liss: New York, NY, USA, 1991; Volume 4, pp. 41–109.

21. Kieneke, A.; Schmidt-Rhaesa, A. Gastrotricha. In *Handbook of Zoology*; Schmidt-Rhaesa, A., Ed.; De Gruyter: Berlin, Germany, 2015; pp. 1–134.
22. Dal Zotto, M.; Tongiorgi, P.; Todaro, M.A. I Gastrotrichi dell'area marina protetta di Capo caccio-Isola Piana (Sardegna). In Proceedings of the 68° Congress of the Unione Zoologica Italiana, Lecce, Italy, 24–27 September 2007.
23. Curini-Galletti, M.; Artois, T.; Delogu, V.; De Smet, W.H.; Fontaneto, D.; Jondelius, U.; Leasi, F.; Martinez, A.; Meyer-Wachsmuth, I.; Nilsson, K.S.; et al. Patterns of diversity in soft-bodied Meiofauna: Dispersal ability and Body size matter. *PLoS ONE* **2012**, *7*, e33801. [CrossRef] [PubMed]
24. Todaro, M.A.; Dal Zotto, M.; Kånneby, T.; Hochberg, R. Integrated data analysis allows the establishment of a new, cosmopolitan genus of marine Macrodasyida (Gastrotricha). *Sci. Rep.* **2019**, *9*, 7989. [CrossRef]
25. Remane, A. Neue aberrante Gastrotrichen II: *Turbanella cornuta* nov.spec. und *T. hyalina* M. Schultze, 1853. *Zool. Anz.* **1925**, *64*, 309–314.
26. Rao, G.C.; Clausen, C. *Planodasys marginalis* gen. et sp. nov. and Planodasyidae fam. nov. (Gastrotricha Macrodasyoidea). *Sarsia* **1970**, *42*, 73–82. [CrossRef]
27. Remane, A. Neue aberrante Gastrotrichen. I. *Macrodasys buddenbrocki* nov. gen. nov. spec. *Zool. Anz.* **1924**, *61*, 289–297.
28. Remane, A. Morphologie und Verwandtschaftbeziehungen der aberranten Gastrotrichen I. *Z. Morph. Oekol. Tiere* **1926**, *5*, 625–754.
29. ICZN. *International Code of Zoological Nomenclature*, 4th ed.; The International Trust for Zoological Nomenclature: London, UK, 1999.
30. ICZN Declaration 45—Addition of Recommendations to Article 73 and of the term "specimen, preserved" to the Glossary. *Bull. Zool. Nomencl.* **2017**, *73*, 2–4.
31. Fregni, E.; Faienza, M.G.; Grimaldi-De Zio, S.; Tongiorgi, P.; Balsamo, M. Marine gastrotrichs from the Tremiti Archipelago in the southern Adriatic Sea, with the description of two new species of *Urodasys*. *It. J. Zool.* **1999**, *66*, 183–194. [CrossRef]
32. Atherton, S. *Urodasys poculostylis* sp. nov., a new stylet-bearing gastrotrich (Macrodasyida) from Capron Shoal, Florida. *Mar. Biol. Res.* **2014**, *5*, 530–536. [CrossRef]
33. Hummon, W.D. Marine Gastrotricha of the Near East: 1. Fourteen new species of Macrodasyida and a redescription of *Dactylopodola agadasys* Hochberg, 2003. *Zookeys* **2011**, *94*, 1–59. [CrossRef] [PubMed]
34. Guidi, L.; Balsamo, M.; Grassi, L.; Semprucci, F.; Todaro, M.A. New data on reproductive system and spermatozoa confirm *Macrodasys* as a model in comparative reproductive analysis in Macrodasyida (Gastrotricha). *Water* **2022**, *14*, 3085. [CrossRef]
35. Ruppert, E.E. The reproductive system of gastrotrichs. II. Insemination in Macrodasys: A unique mode of sperm transfer in Metazoa. *Zoomorphologie* **1978**, *89*, 201–228.
36. Mann, T. *Spermatophores: Development, Structure, Biochemical Attributes and Role in the Transfer of Spermatozoa*; Springer: Heidelberg, Germany, 1984; pp. 1–217.
37. Kieneke, A.; Arbizu, P.M.; Ahlrichs, W.H. Anatomy and ultrastructure of the reproductive organs in *Dactylopodola typhle* (Gastrotricha: Macrodasyida) and their possible functions in sperm transfer. *Invertebr. Biol.* **2008**, *127*, 12–32. [CrossRef]

CHAPTER 2

GAINING AND LOSING ON THE WAY: THE EVOLUTIONARY SCENARIO OF REPRODUCTIVE DIVERSIFICATION IN GENUS *URODASYS* (MACRODASYIDA: GASTROTRICHA) INFERRED BY MULTI-GENE PHYLOGENY

(published in the *Zoological Journal of the Linnean Society* 202(4), zlae148.
https://doi.org/10.1093/zoolinnean/zlae148)

Zoological Journal of the Linnean Society, 2024, **202**, zlae148
https://doi.org/10.1093/zoolinnean/zlae148
Advance access publication 7 December 2024
Original Article

OXFORD

Original Article

Gaining and losing on the way: the evolutionary scenario of reproductive diversification in genus *Urodasys* (Macrodasyida: Gastrotricha) inferred by multi-gene phylogeny

Agata Cesaretti[1,*], Anush Kosakyan[1,2], Francesco Saponi[1,2,3], M. Antonio Todaro[1,2]

[1]Department of Life Sciences, University of Modena and Reggio Emilia, via G. Campi, 213/D, 41125 Modena, Italy
[2]National Biodiversity Future Center (NBFC), Piazza Marina 61, 90133 Palermo, Italy
[3]Department of Earth and Marine Sciences, University of Palermo, Via Archirafi, 22, 90123 Palermo, Italy

[*]Corresponding author. Department of Life Sciences, University of Modena and Reggio Emilia, via G. Campi, 213/D, 41125 Modena, Italy. E-mail: agata.cesaretti@unimore.it

ABSTRACT

The microscopic members of the genus *Urodasys* are easily recognizable due to their exceptionally long tail. There are 17 described species within this iconic genus, each distinguished by various sexual organ arrangements and reproduction modalities, including the sole known ovoviviparous gastrotrich species. The remarkable variety in reproductive characteristics has captured the interest of researchers aiming to illuminate its origin and evolution. The recent discovery of a species bearing a novel set of reproductive structures has challenged early hypotheses. However, all the evolutionary scenarios put forward need to be more convincing. To gain deeper insight into the evolutionary history of these iconic animals, we obtained the nucleotide sequence of two nuclear genes and one mitochondrial gene from species' representatives of the four known possible combinations of the reproductive apparatus and reproduction modalities. The multi-gene data matrix was analysed phylogenetically using three approaches. The analyses yielded phylogenetic trees with invariant topology. In all cases, the specimens appear organized in four robustly supported clades and subclades that reflect their reproductive system organization. Our results suggest that the sclerotized stylet evolved inside the copulatory organ before the loss of the left testis and offers a new scenario for the evolutionary history of genus *Urodasys*.

Keywords: benthos; cladistics; cytochrome *c* oxidase; evolution; meiofauna; molecular data; ovoviviparity; parthenogenesis; rDNA; reproduction

INTRODUCTION

Gastrotricha are a phylum of microscopic, benthic invertebrates, ranging in size from 80 μm to 3.5 mm that are found in freshwater and marine environments worldwide. The name 'Gastrotricha' comes from the Greek words for 'hairy bellies' (γαστήρ, gastḗr, 'belly', and θρίξ, thríx, 'hair'), describing the distinct ventral ciliation that allows these animals to glide on, and inside, the sediment. There are over 890 species in this group, and they play a significant role in the foodwebs of aquatic systems (Kieneke and Schmidt-Rhaesa 2014, Todaro and Luporini 2022). Despite their great biodiversity and ecological importance, information about these soft-bodied animals is still relatively limited (Balsamo *et al.* 2020, Curini-Galletti *et al.* 2020). The systematics and classification of Gastrotricha are constantly evolving due to the ongoing discovery of species bearing novel morphologic characteristics and the increasing use of molecular data in phylogeny reconstruction (e.g. Kånneby *et al.* 2012, Todaro *et al.* 2014, 2015, 2019a, Kånneby and Todaro 2015, Garraffoni *et al.* 2017, Kieneke and Todaro 2021). For instance, the application of molecular phylogenetic analysis has unveiled a distinct position along the Gastrotricha tree of life of several taxa previously associated with traditional groups, which are diagnosed mainly on morphological traits (Todaro *et al.* 2012a, Gammuto *et al.* 2024, Rataj Križanová and Vďačný 2024). These results raise doubts about the value of some morphological characteristics for systematics. Gastrotrich morphology is both highly diversified and challenging to interpret in a phylogenetic context, and superficial similarities often mask deeper differences (Gammuto

Received 31 July 2024; revised 11 October 2024; accepted 22 October 2024

et al. 2024, Rataj Križanová and Vďačný 2024). Efforts to define monophyletic groupings based on robust phylogenies have been turning to more integrative methods (see: Todaro *et al.* 2011, 2014, 2019a, Kånneby *et al.* 2012, 2013, Garraffoni *et al.* 2019, Kolicka *et al.* 2020, Kieneke and Todaro 2021, Rataj Križanová and Vďačný 2022, 2024).

The morphological peculiarities of these microscopic animals and the variety of biological and ecological adaptations they can present are vast topics for research. Much more remains to be uncovered and understood, especially regarding their reproductive biology.

Reproduction in this phylum shows a surprising array of structures and strategies, with the most incredible diversity arguably found in the order Macrodasyida Remane, 1925. Macrodasyidan gastrotrichs are typically hermaphrodites with paired gonads and internal cross-fertilization. Usually, two accessory sexual organs, called frontal and caudal organs because of their relative position in the trunk, aid in sperm transfer. The caudal organ serves as a copulatory organ; it takes up the autosperm and transfers them to the partner. The frontal organ receives and stores the partner's sperm and conveys them to the ova for fertilization. It is interesting that, in many gastrotrichs with accessory sexual organs, the testes and the caudal organs are not connected internally, and the deferentia convey sperms to the outside through male pores. As a result, the animal must first fill its caudal organ with autosperm before mating (Ruppert 1991, Kieneke and Schmidt-Rhaesa 2014, Guidi *et al.* 2022). However, among macrodasyidan gastrotrichs, there are significant variations in the organization of the reproductive system that include differences in the number and position of ovaries, testes, and the accessory reproductive organs. Understanding these variations is crucial for classifying these organisms and for gaining insights into their evolutionary relationships (Guidi *et al.* 2009, 2011, 2014, 2021, 2022, Todaro *et al.* 2012b).

Species of the genus *Urodasys* Remane, 1926 illustrate the ample variety of reproductive system organizations and reproduction modalities within the order Macrodasyida. The members of this genus are easily recognizable due to their remarkably long, contractile tails, which distinguish them from other species (Fig. 1), although the adaptive value of such a long tail is still unknown. Their spermatozoa are also unique as they lack mitochondria (Balsamo *et al.* 2007). It has been hypothesized that the absence of mitochondria may be related to the dysoxic sediment in which the species live (Todaro *et al.* 2000, Balsamo *et al.* 2007).

Currently, there are 17 described species within this genus, all of which have paired ovaries but differ in other reproductive traits (Supporting Information, Table S1). The male reproductive system varies among species, with some having paired testes (Wilke 1954, Fregni *et al.* 1999) (Figs 2A, B, 3A–F), others having a single testis (Figs 2C, 4A–D), and two species (*U. bucinastylis* Fregni *et al.*, 1999, and *U. viviparus* Wilke, 1954) lacking male gonads altogether (Figs 2D, 2E, 4E). The presence of accessory reproductive organs also varies among the species. The caudal organ has been reported for 12 species. Uniquely among Gastrotricha, the caudal organ is equipped with a species-specific sclerotized stylet (Figs 2B–D, 3F, 4D), which plays a role in facilitating sperm transfer (e.g. Schoepfer-Sterrer 1974, Ruppert 1991). Recent studies have clarified that, during copulation, the stylet transfers densely packed sperm cells and these spermatophores are assembled inside the caudal organ (Todaro *et al.* 2017, Cesaretti *et al.* 2023). The frontal organ (Fig. 4B) has been reported only for a few species. The production of offspring also varies within the genus, highlighting once again the diversity of the reproductive process. In general, offspring in *Urodasys* are produced through biparental reproduction and oviparity, except *U. viviparus*, which reproduces through parthenogenesis and ovoviviparity (Hummon and Hummon 1983; see also: Kieneke and Schmidt-Rhaesa 2014) potentially contributing to the putative cosmopolitan distribution of this species (Artois *et al.* 2011). *Urodasys bucinastylis* possesses a caudal organ with a stylet but lacks testes; consequently, it is considered an obligate parthenogenetic species (Fregni *et al.* 1999).

Figure 1. Light micrograph of *Urodasys viviparus*, whole specimen in dorsal view showing the long contractile tail typical of the genus *Urodasys*. Scale bar = 100 μm. Abbreviations: em, embryo; mo, mature ovum. Differential interference contrast microscopy (Nomarski).

The origin and evolution of the exceptionally complex variety of sexual organs and the different reproductive strategies of the *Urodasys* species are still unclear.

Fregni *et al.* (1999) were the first to propose an ingroup evolutionary scenario based on reproductive traits. They suggested that the ancestor was a simultaneous hermaphroditic species with paired ovaries and testes, a frontal organ, and a caudal organ with a sclerotic stylet. According to these authors, the three reproductive groups known at that time would have derived from this plesiomorphic condition through mechanisms of progressive reduction along two evolutionary lines. Species of one lineage would have lost the accessory sexual organs while retaining

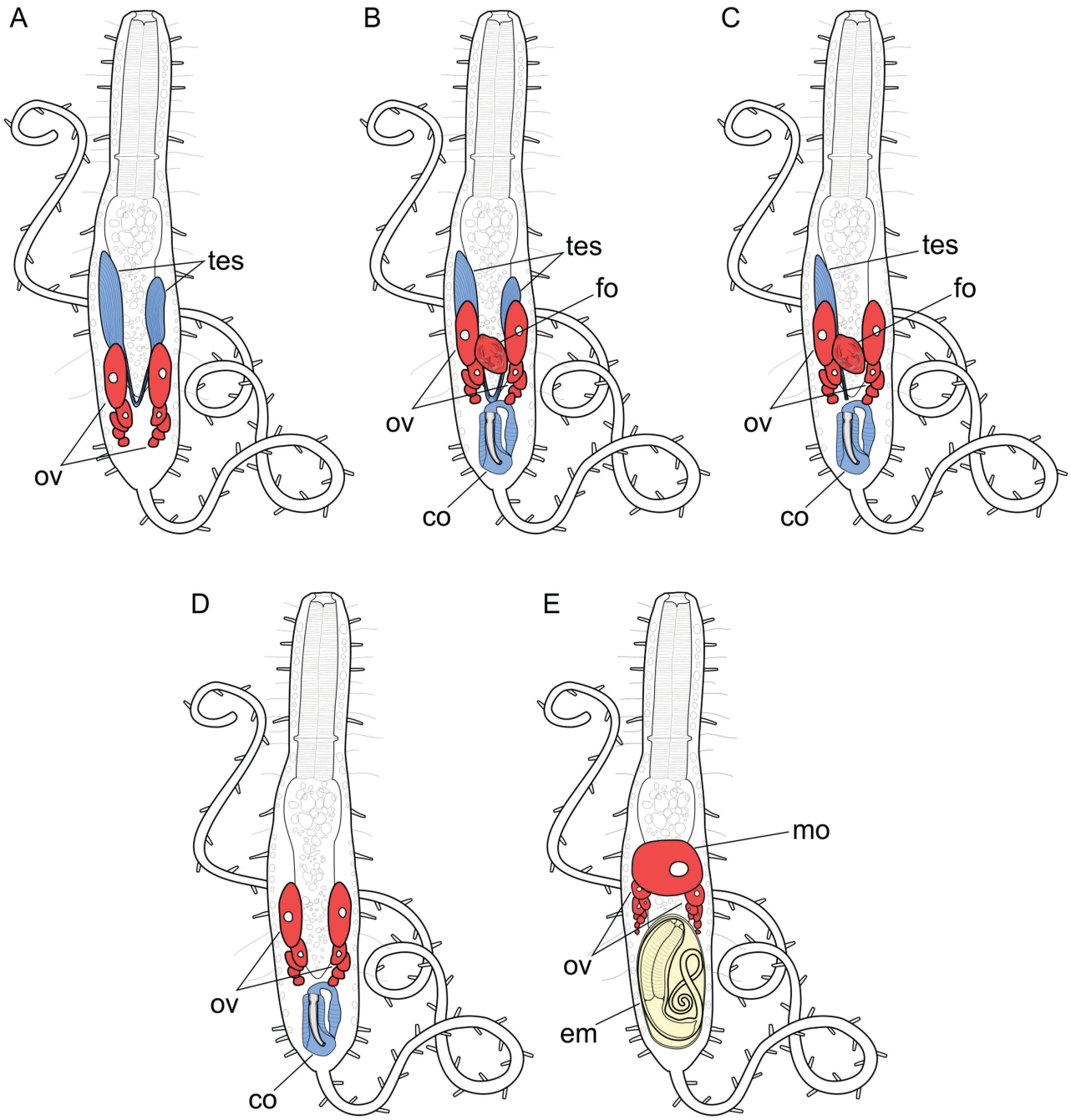

Figure 2. Schematic representation of reproductive structures and their combinations found in species of the genus *Urodasys*. A, hermaphroditic oviparous species with paired ovaries, paired testes, lacking frontal and caudal organs. B, hermaphroditic oviparous species with paired ovaries, paired testes, frontal and caudal organs. C, hermaphroditic oviparous species with paired ovaries, a single testis, frontal and caudal organs. D, parthenogenetic oviparous species with paired ovaries, lacking testes and the frontal organ, but with the caudal organ. E, parthenogenetic ovoviviparous species with paired ovaries, lacking testes and both frontal and caudal organs. Abbreviations: co, caudal organ; em, embryo; fo, frontal organ; mo, mature ovum; ov, ovaries; tes, testes.

paired ovaries and testes. Members of the second lineage would have retained the caudal and frontal organs but would have faced a progressive reduction of the male gonads. Species possessing the copulatory stylet, a single testis, or no testes would have descended from this second lineage. The study was unable to determine whether the parthenogenetic *U. viviparus* originated from one lineage or the other (Fregni *et al.* 1999).

Fifteen years later, Atherton and Hochberg (2014) tried to clarify the evolutionary transformations in the reproductive system of *Urodasys* by conducting the first phylogenetic analysis based on molecular traits (18S rDNA gene). Their results confirmed the two evolutionary lineages hypothesized by Fregni *et al.* (1999) and positioned *U. viviparus* as a sister-group to the stylet-bearing species. In contrast with the early investigators (Fregni *et al.* 1999), Atherton and Hochberg (2014) hypothesized a late origin of the copulatory stylet (it evolved after the loss of the right testis), and that the plesiomorphic condition included a simpler, stylet-less caudal organ (see: Atherton and

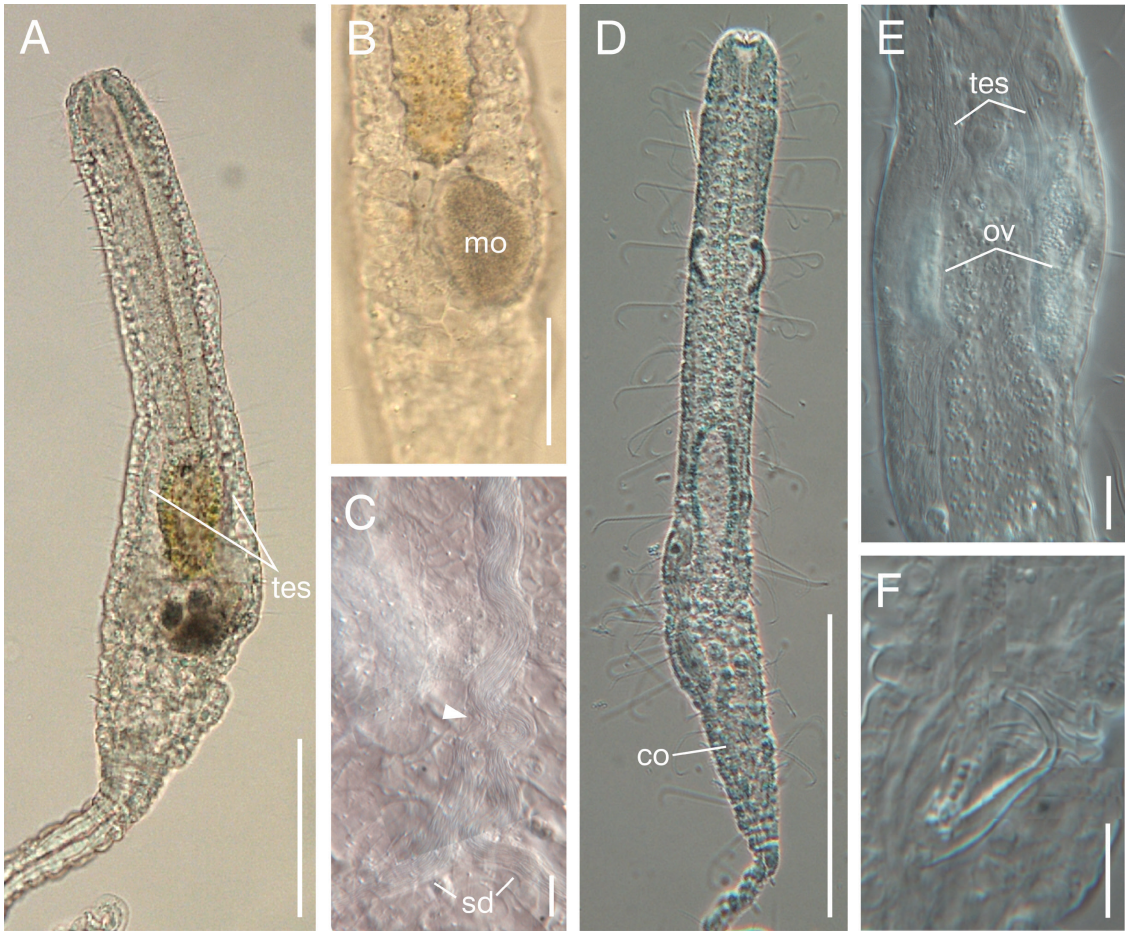

Figure 3. Light micrographs of reproductive apparatus in two *Urodasys* species with paired testes used in this study. A, *Urodasys mirabilis*, whole specimen in dorsal view with details of the paired testes; B, trunk anatomy showing a mature egg; C, details of the paired sperm ducts and the point where they meet (arrowhead); D, *Urodasys completus*, whole specimen in dorsal view showing the position of the caudal organ; E, trunk anatomy showing the paired testes and paired ovaries; F, details of the stylet inside the caudal organ. Scale bars: A, D = 100 µm; B = 50 µm; C, E, F = 10 µm. Abbreviations: co, caudal organ; mo, mature ovum; ov, ovaries; tes, testes; sd, sperm ducts. A, D, bright field microscopy; B, C, E, F, differential interference contrast microscopy (Nomarski). D, E, F, modified from Todaro *et al.* (2017).

Hochberg 2014: Fig. 4). However, the use of relatively short sequences (*c.* 800 bp) and the moderate support for the subclade composed of *U. viviparus* and stylet-bearing species, leave room for a deeper investigation.

In 2017, a new species with an unknown reproductive system layout was discovered: *Urodasys completus* Todaro *et al.* (2017). This species (Fig. 3D, E) has a sclerotic stylet but, unlike other stylet-bearing species, it has paired testes. In a broader context, the reproductive apparatus of *U. completus* aligns with the plesiomorphic condition proposed by Fregni *et al.* (1999). However, a cladistic analysis, based on seven traits related to the composition and layout of reproductive apparatus organs and the reproductive condition, revealed that the 17 species in the study grouped into two main clades based on the presence or absence of a sclerotic stylet. *Urodasys viviparus* clusters with hermaphroditic species that lack accessory sexual organs, while *U. completus* represents an early divergent clade along the evolutionary line of stylet-bearing species (Todaro *et al.* 2017). The moderate support at the nodes and the numerous polytomies indicate a need for a more thorough investigation.

In this study, we investigate the phylogeny of *Urodasys* using a multi-gene approach to test previous hypotheses on the evolution of the reproductive system and reproduction modality in the genus. We expect that expanding the genetic sampling substantially and including species representatives from all four main described combinations of reproductive system organization and reproduction modalities will lead to a more robust hypothesis on the evolution of this iconic group of micrometazoans.

MATERIALS AND METHODS

Species' selection

Specimens of *Urodasys* involved in this study were retrieved from the Gastrotricha BioBank available in the MeioLab at the University of Modena and Reggio Emilia (Table 1; Figs 3, 4). They were obtained by one of the authors (M.A.T.) during past Gastrotricha and meiofauna faunistic surveys (e.g. Curini-Galletti *et al.* 2012, Todaro *et al.* 2017). At the time, the specimens were extracted from the sandy samples using a 7% $MgCl_2$ narcotizing solution following the protocols of Todaro *et al.* (2019b). Species' identification was carried out under a

Figure 4. Light micrographs of reproductive apparatus in *Urodasys bifidostylis* and in *Urodasys viviparus*, two species used in this study. A, *Urodasys bifidostylis*, whole specimen in dorsal view detailing the position of the caudal organ; B, details of the frontal organ, with spermatophores; C, trunk anatomy showing the single testis, paired ovaries and the relative position of the caudal organ; D, details of the stylet inside the caudal organ. E, *Urodasys viviparus*, whole specimen in dorsal view with a mature egg and a developing embryo. Scale bars: A, E = 100 µm; B, C, D = 50 µm. Abbreviations: co, caudal organ; em, developing embryo; mo, mature ovum; ov, ovaries; sp, sperms; tes, testes. Differential interference contrast microscopy (Nomarski). A, D, modified from Cesaretti *et al.* (2023).

Normarski microscope and high-resolution photomicrographs were taken for vouchers (see Figs 3, 4). The identified species were preserved in 95% ethanol at –20°C inside 2-mL criovials. The specimen from Curaçao was collected in 2012 and it has been identified as *U. mirabilis* Remane, 1926 based on the general morphology and in agreement with the similar specimens found in the nearby island of Tobago by Atherton and Hochberg (2014). A preliminary maximum likelihood (ML) phylogenetic analysis, based on the 18S rDNA gene sequences from these specimens complemented with the sequences from Atherton and Hochberg (2014), confirmed the current specimens as fitting representatives of the recognized reproductive groups of *Urodasys* species (Supporting Information, Table S3, Fig. S1). In all phylogenetic analyses, two undescribed species of the genus *Macrodasys* Remane, 1924 were selected as the outgroup. Both *Urodasys* and *Macrodasys* belong to the Linnaean family Macrodasyidae, and, within this family, members of *Macrodasys* have a reproductive apparatus layout most similar to the basal condition hypothesized for *Urodasys* (e.g. Guidi *et al.* 2021). Additionally, *Macrodasys* was selected as the outgroup in the works by Atherton and Hochberg (2014) and Todaro *et al.* (2017).

DNA extraction, amplification, and sequencing

The study was conducted on seven specimens belonging to six different *Urodasys* species. The ethanol-preserved specimens were washed in clean absolute ethanol, singly transferred into sterile 0.5-mL tubes using a glass micro-pipette, and left overnight at 25.5°C in a cleaned ISCO micra 18 incubator to eliminate any residual ethanol through evaporation. Subsequently, 4 µL of Phosphate-buffered saline solution (PBS) were added to each sample. The samples were then processed for DNA extraction and whole genome amplification (WGA) using the REPLI-g Single Cell Kit (QIAGEN®) following the manufacturer's instructions. The resulting amplified DNA product was validated through polymerase chain reaction (PCR) amplification of the 18S rDNA gene and Sanger sequencing. All PCRs

Table 1. Specimens used in this study, with sampling locations, GenBank accession codes and references.

Species	Sampling location with coordinates	GenBank Accession (18S, 28S, *COI*)	Reference
Urodasys acanthostylis	Puerto del Carmen, Lanzarote (Canary Islands, Spain) 28°55′08.5″N; 13°40′06.6″W	PQ415490, PQ429034, PQ462511	Present study
Urodasys apuliensis	Budelli (Italy) 41°16′43.9″N; 09°21′28.7″E	PQ415491, PQ429035, PQ462513	Present study
Urodasys bifidostylis	Costa Paradiso (Italy) 41°03′08.8″N; 08°56′15.7″E	PQ415492, PQ429036, PQ462512	Present study
Urodasys completus 1	Puerto del Carmen, Lanzarote (Canary Islands, Spain) 28°55′08.5″N; 13°40′06.6″W	PQ415493, PQ429037, PQ462510	Present study
Urodasys completus 2	Puerto del Carmen Lanzarote (Canary Islands, Spain) 28°55′08.5″N; 13°40′06.6″W	PQ415494, PQ429038, PQ462516	Present study
Urodasys mirabilis	Beach of the Marine Biological Station (CARMABI) (Curaçao) 12°07′19.8″N; 68°58′09.4″W	PQ415495, PQ429039, PQ462514	Present study
Urodasys viviparus	Abruzzo (Italy) 42°40′44.1″N; 14°01′05.4″E	PQ415496, PQ429040, PQ462515	Present study
Macrodasys sp1	Torre Civette (Italy) 42°50′42.0″N; 10°46′31.0″E	JF357654, JF357702, JF432040	Todaro *et al.* (2011)
Macrodasys sp2	Bohuslän area (Sweden) 58°52′05.04″N; 11°04′57.9″E	JF357670, JF357714, JF432052	Todaro *et al.* (2011)

were carried out in a T-Personal thermal cycler (Biometra, Goettingen, Germany). High-fidelity Takara Ex Taq PCR reagents were employed (Takara Bio Inc., Otsu, Japan) according to the manufacturer's instructions. Each reaction used 2 µL of amplified DNA diluted 1:100 in water, 29.38 µL of water, 4 µL of reaction buffer, 4 µL of dNTPs in solution, 0.4 µL of paired primers, and 0.22 µL of Takara Taq-polymerase. Primer combinations and thermal cycler programs used for validation are presented in the Supporting Information, Table S2. The resulting products were purified with the Monarch PCR & DNA Cleanup Kit (New England BioLabs Inc., Ipswich, MA, USA) and subsequently sent for Sanger sequencing to a sequencing company (Macrogen Europe Laboratory in Milan, Italy) using the sequencing primers indicated in the Supporting Information, Table S2. Reads resulting from the Sanger sequencing of PCR products were assembled using the STADEN package v.2.0 (Staden 1996). The obtained sequences were examined with the GenBank online BLAST tool (https://blast.ncbi.nlm.nih.gov/Blast.cgi) and used in the preliminary phylogenetic analysis reported above (see Species' selection). The validated DNA samples from WGA were then sent to Macrogen Europe (https://www.macrogen-europe.com/) and processed with a TrueSeq DNA PCR Free Library kit and *de novo* whole genome sequencing (WGS) at NovaSeq 6000 Illumina Platform to generate a total of 40 million reads (paired-ends 2 × 150 bp).

Data assembly and gene mining

The obtained WGS data was analysed through a bioinformatic pipeline, optimized from Kumar *et al.* 2013 (see: Serra *et al.* 2020, Gammuto *et al.* 2024, Saponi *et al.*2024). The quality of the reads was evaluated through the FASTQC software (http://www.bioinformatics.babraham.ac.uk/projects/fastqc/) (Andrews 2010). The reads were then trimmed for quality and adapters with TRIMMOMATIC 0.39 (Bolger *et al.* 2014) setting the minimum length to 140 bp; the other parameters were kept as default. Reads with quality scores inferior to 30 were discarded. The remaining paired reads were assembled through the SPAdes v.3.6.0 software (Bankevich *et al.* 2012) to obtain a collection of longer contigs. The assembled contigs matching ribosomal and mitochondrial genes were identified through blastn and tblastn analysis. As queries, we used published gastrotrich sequences obtained from the NCBI database, and, for the ribosomal genes, data produced in the lab through Sanger sequencing in the validation step.

The softwares StructRNAfinder (https://structrnafinder.integrativebioinformatics.me/) (Arias-Carrasco *et al.* 2018) and MITOs (http://mitos.bioinf.uni-leipzig.de/help.py) (Bernt *et al.* 2013) were used to examine the nodes of interest isolated from the data assembly and to confirm the location of the identified genes. We used BioEdit v.7.2.5 Freeware (Hall 1999) when needed to manually align, examine, and assemble the extracted sequences, and to compare the sequences obtained through WGS sequencing with the ones obtained through Sanger sequencing. This was done in order to verify the reliability of the methodology and the accuracy of the results. Sequences of the two *Macrodasys* species were obtained from GenBank (Table 1).

Gene alignment and phylogenetic analysis

The sequences of each gene were aligned separately. The alignments were carried out using the MUSCLE (multiple sequences comparison by log expectation) algorithm (Edgar 2004) as implemented in the MEGA X software package (Kumar *et al.*

2018). The mitochondrial protein-coding cytochrome *c* oxidase subunit I (*COI*) sequences were aligned using the invertebrate mitochondrial genetic code. Before codon alignment, the *COI* sequences were individually examined for their correct reading frame using GENEIOUS PRIME software (v.2019.2.3) (https://www.geneious.com/).

We obtained an 18S rDNA dataset with 1993 positions, a 28S rDNA dataset with 3759 positions, and a *COI* dataset with 1557 positions. All three alignments were concatenated into a single final matrix, resulting in 7252 sites. Phylogenetic analyses on the dataset were conducted using three different approaches: maximum parsimony (MP), ML, and Bayesian inference (BI). For ML and BI, we applied the GTR+G+I (general time reversible) evolutionary model for nuclear substitution as it was favoured by the Aikake Information Criterion corrected (AICc) and the Bayesian Information Criterion (BIC) criteria in MEGA X (Model Finder tool). MP and ML analyses were conducted on MEGA X using 1000 bootstrap replicates and other parameters set as default. The BI analyses were performed using the program MrBayes v.3.2.7 (Ronquist *et al.* 2012). The BI tree search on the final concatenated dataset ran with two parallel runs, on eight independent Markov chains performed in 2 000 000 generations, sampling the trees every 100 generations and with a relative burn-in fraction of 25%. Convergence of the Markov chain Monte Carlo (MCMC) analyses was confirmed with the in-built diagnostics of the program: the average standard deviation of split frequencies was 0.000047, the potential scale reduction factor (PSRF) converged to 1.00 for all parameters, the effective sample sizes (EES) of all parameters were >200 (i.e. min. ESS = 768.1206, av. ESS = 933.7091). The resulting tree was visualized using FigTree v.1.4.4 (http://tree.bio.ed.ac.uk/software/figtree/).

All the trees were computed as unrooted and then rooted using as the outgroup the two *Macrodasys* species. To facilitate reading, the final trees were edited using CorelDraw X7 (Corel Corporation, Ottawa, Canada).

RESULTS

Molecular phylogeny

The analysis of the multi-gene data matrix leads to a clear evolutionary scenario. The phylogenetic trees obtained from the MP, ML, and BI analyses all display the same structure, with nodes receiving high to full statistical support (PP = 0.99 to PP = 1.00, BS = 98 to BS = 100). The invariant topology shows the *Urodasys* species distributed into four clades/subclades, each reflecting the different reproductive system organizations of the species involved in the analyses (Fig. 5; Supporting Information, Fig. S2). More specifically, clade A groups the species with paired gonads and no accessory organs (i.e. *U. apuliensis* Fregni *et al.* 1999 and *U. mirabilis*), while clade B encompasses the remaining species. In turn, clade B contains three subclades (B1, B2, and B3), which provide insights into the evolutionary transformations that occurred. In particular, subclade B1, which includes specimens with, among other characteristics, paired testes and a sclerotic stylet (*U. completus*), is seen as an early divergent line from the main branch and is in a sister-group relationship with a monophyletic group consisting of two more derived subclades (B2 and B3). Subclade B2 consists of species bearing a single testis and the sclerotic stylet (*U. acanthostylis* Fregni *et al.*, 1998 and *U. bifidostylis* Cesaretti *et al.*, 2023), while subclade B3 comprises the parthenogenetic *U. viviparus*.

DISCUSSION

The sheer variety of reproductive organs and strategies found in the species of the genus *Urodasys* is fascinating. It even includes a rare example of parthenogenesis coupled with ovoviviparity, which is unusual among metazoans (Kamimura *et al.* 2016). The molecular phylogeny produced in this study is highly congruent with hypotheses about reproductive character evolution in *Urodasys*. The hierarchical distribution of the clades allows for tracing the evolutionary changes that have occurred in the layout of the reproductive apparatus of the species involved in the analyses. While the constraint of using six out of the 17 known species of genus *Urodasys* may appear as a limitation for this study, this framework helps in inferring patterns of ancestry on a larger scale.

Our analysis of the evolutionary relationships shows that the species can be divided into two main groups. The first group includes *U. apuliensis* and *U. mirabilis*, which have paired gonads and no accessory organs. The second group consists of several subgroups. *Urodasys completus*, with paired testes and a sclerotic stylet, diverges early from the main branch and is in a sister-group relationship with two more derived subclades: one consisting of species bearing a single testis and the sclerotic stylet (*U. acanthostylis* and *U. bifidostylis*) and the other of parthenogenetic species (*U. viviparus*) (Fig. 5).

Based on these results, the evolutionary changes in the reproductive system of *Urodasys* species involve loss and gain. We can hypothesize that paired ovaries, paired testes, and frontal and caudal organs were features of the reproductive system of the stem species. From this ground pattern, evolution proceeded along two lines. In one line, species lost the accessory sexual organs while retaining paired gonads, and in the other line the copulatory organ (caudal organ) gained a sclerotic stylet. In turn, the line encompassing the stylet-bearing species experienced a progressive reduction of the male structures, starting from the gonads (most species present a single testis) and eventually extending to the sexual accessory organs. In this framework, *U. bucinastylis* bears relevance as it possesses a sclerotic stylet but not the testes, suggesting a decoupling between parthenogenesis (*U. bucinastylis* and *U. viviparus*) and ovoviviparity (*U. viviparus*) (Fig. 6). It is possible that one or two testes may form temporarily, as observed in freshwater chaetonotidans (Weiss 2001), although we believe this is highly unlikely.

It is unclear if the condition of *U. bucinastylis* is more widespread because there is another species, *U. toxostylus* Hummon, 2011, described without testes but bearing the stylet. However, the author considered it as probably hermaphroditic (Hummon 2011). In the broader framework, the peculiar organization of the reproductive system in certain *Urodasys* species can be observed in various distantly related gastrotrich taxa. For example, *Urodasys* species without a copulatory organ have a similar condition to members of the family Turbanellidae Remane, 1926 (Balsamo *et al.* 2002). Meanwhile, species with a copulatory organ but lacking testes (*U. bucinastylis*) match the condition of

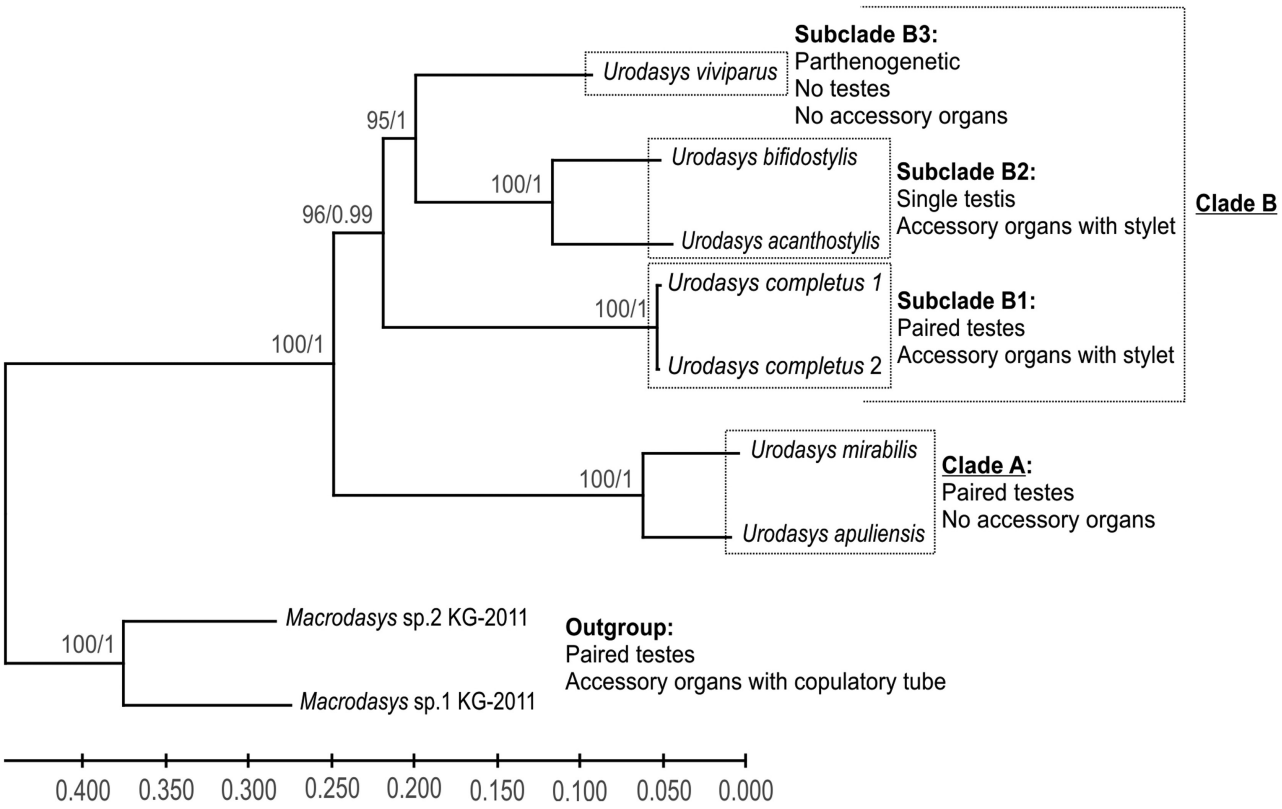

Figure 5. Phylogenetic relationships of the genus *Urodasys* inferred from Bayesian inference (BI) and maximum likelihood (ML) analysis of a concatenated dataset of 18S rDNA, 28S rDNA, and *COI* sequences. Numbers at nodes represent bootstrap (1000 replicates) and posterior probability values, respectively. The outgroup is represented by two species of *Macrodasys*.

the macrodasyid *Thaidasys tongiorgii* Todaro *et al.*, 2015 (Todaro *et al.* 2015). The reasons for the development and persistence of these similarities (analogies) still need to be explored.

Our results differ from the hypothesis of Todaro *et al.* (2017), based on morphological data. In their study, *Urodasy viviparus* was grouped with the hermaphroditic species that lack accessory sexual organs. Our findings also contrast with the hypotheses proposed by Fregni *et al.* (1999) and Atherton and Hochberg (2014). This is not surprising considering *U. completus* was described well after the publication of these works.

The consistent topology and strong support at nodes obtained from three different phylogenetic approaches instil confidence in our results. This reaffirms that molecular data can be valuable in establishing phylogenetic relationships that may be challenging to determine solely based on morphological data, as long as there is thorough taxonomic and genetic sampling.

CONCLUSION

Our results point to a trend of progressive reduction in the evolution of the reproductive system of genus *Urodasys*. In this scenario some species have lost the accessory organs and retained the paired testes, while others have retained the accessory organs but lost the right testis instead. This could be explained by an increased efficiency in sperm exchange through the acquisition of a copulatory stylet. Because of it, these species could reduce their energy expenses in sperm production and save precious resources by losing a testis. Matters concerning *U. viviparus* are more complex. While we can conclude that the evolution of parthenogenesis was the end result of a progressive reduction, ovoviviparity is a complete novelty in this phylum and deserves further investigation. Future studies on this species should focus on its functional traits and on a better understanding of its life cycle (Kamimura *et al.* 2016, Xu *et al.* 2022). Likewise, conducting additional research on *U. bucinastylis* and *U. toxostylus* could yield new and more reliable information regarding their reproductive status.

The genus *Urodasys* is unique among Gastrotricha also because of its long tail, which makes these meiobenthic animals easily identifiable, even for non-specialists. This genus has a worldwide distribution and currently consists of 17 described species, with several more known but not yet formally described (e.g. Schoepfer-Sterrer 1974, Valbonesi and Luporini 1984). Most of these species live in sandy areas, preferring finer sediment rich in detritus and low oxygen conditions (Todaro *et al.* 2000). They may be found in both littoral and sublittoral zones, with higher records from the latter. Some species have a wider geographic range than others, which seems to be related to their reproduction. Generally, species with a sclerotic stylet have a more limited distribution compared to those without it. Among the latter species, the parthenogenetic *Urodasys viviparus* is found worldwide, while the hermaphroditic species (e.g. *U. anorektoxys* Todaro *et al.*, 2000, *U. apuliensis*, and *U. elongatus* Renaud-Mornant, 1969) have a more limited distribution (Schoepfer-Sterrer 1974, Fregni *et al.* 1999, Atherton and Hochberg 2014, Todaro *et al.* 2017). As for other phyla, Gastrotricha species' identification is also primarily based on morphological traits. Consequently, the potential widespread distribution of certain species may result from

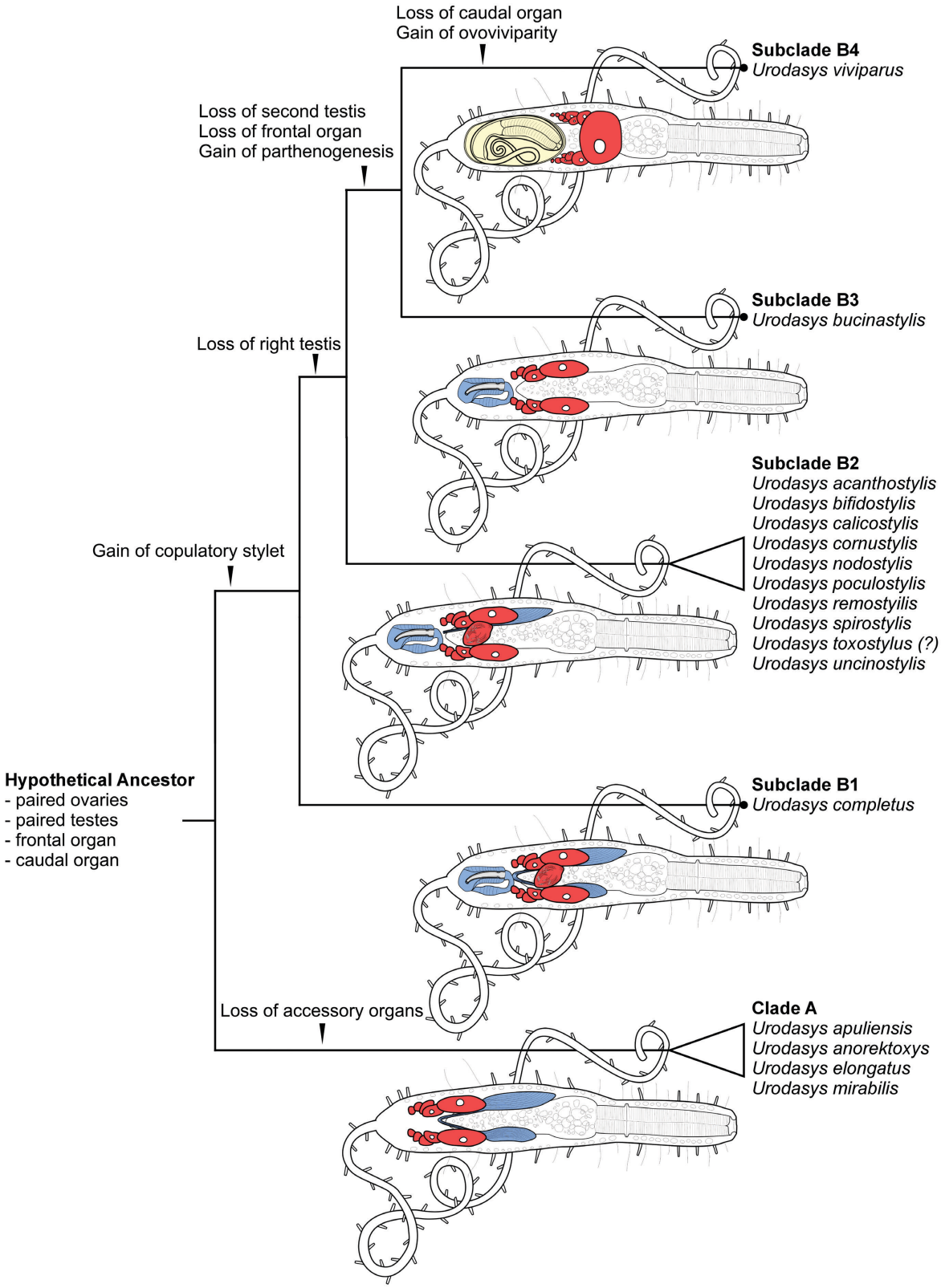

Figure 6. Reconstruction of the evolution of the reproductive system in the species of genus *Urodasys*. The hypothetical ancestor possessed paired testes, paired ovaries, and both frontal and caudal organ. Species in clade A lost both accessory organs, while clade B maintained them, evolving a copulatory stylet inside the caudal organ and reaching the reproductive anatomy found in subclade B1 (*U. completus*). Subclade B2 groups the species with a single testis and the copulatory stylet, which evolved by losing the right testis. *Urodasys bucinastylis* (subclade B3) then lost the remaining testis and the frontal organ, likely becoming parthenogenetic and retaining only the caudal organ. Finally, *U. viviparus* (subclade B4) lost the caudal organ and gained ovoviviparity.

misidentifications, which are more likely to occur in species lacking hard structures (e.g. stylet) or an inside embryo, that are easier to observe. Cryptic and pseudocryptic species can be distinguished using molecular data (e.g. Todaro *et al.* 1996, Magpali *et al.* 2021). The 21 new nucleotide sequences from three genes and six species found in various regions around the world, which we have provided, could also be beneficial for future studies exploring the geographic distribution of *Urodasys* species.

SUPPLEMENTARY DATA

Supplementary data are available at *Zoological Journal of the Linnean Society* online.

ACKNOWLEDGEMENTS

A.C. is deeply grateful to L. Gammuto, V. Serra, and G. Petroni (University of Pisa, Italy) for introducing her to the WGA pipeline and for their help with the bioinformatic tools.

FUNDING

This project is partially funded under the National Recovery and Resilience Plan (NRRP), Mission 4 Component 2 Investment 1.4—Call for tender No. 3138 of 16 December 2021, rectified by Decree n. 3175 of 18 December 2021 of the Italian Ministry of University and Research funded by the European Union—NextGenerationEU. Project Code CN_00000033, Concession Decree No. 1034 of 17 June 2022 adopted by the Italian Ministry of University and Research, CUP E93C22001090001, Project title "National Biodiversity Future Center—NBFC".

CONFLICT OF INTEREST

The authors declare that they have no conflicts of interest in relation to this work.

DATA AVAILABILITY

The data underlying this article are available in the GenBank Nucleotide Database (https://www.ncbi.nlm.nih.gov/nucleotide/), accession numbers PQ415490–PQ415496, PQ429034–PQ429040, PQ462510–PQ462516. Results of all analyses are available in the article and in its online supplementary material.

REFERENCES

Andrews S. *FastQC: a Quality Control Tool for High Throughput Sequence Data*. Online, 2010. http://www.bioinformatics.babraham.ac.uk/projects/fastqc/ (29 July 2024, date last accessed).

Arias-Carrasco R, Vásquez-Morán Y, Nakaya HI *et al.* StructRNAfinder: an automated pipeline and web server for RNA families prediction. *BMC Bioinformatics* 2018;**19**:55. https://doi.org/10.1186/s12859-018-2052-2

Artois T, Fontaneto D, Hummon WD *et al.* Ubiquity of microscopic animals? Evidence from the morphological approach in species identification. In: Fontaneto D (ed.), *Biogeography of Microscopic Organisms: Is Everything Small Everywhere?* Cambridge: Cambridge University Press, 2011, 244–83.

Atherton S, Hochberg R. The evolution of the reproductive system of *Urodasys* (Gastrotricha: Macrodasyida). *Invertebrate Biology* 2014;**133**:314–23. https://doi.org/10.1111/ivb.12068

Balsamo M, Ferraguti M, Guidi L *et al.* Reproductive system and spermatozoa of *Paraturbanella teissieri* (Gastrotricha, Macrodasyida): implications for sperm transfer modality in Turbanellidae. *Zoomorphology* 2002;**121**:235–41. https://doi.org/10.1007/s00435-002-0061-0

Balsamo M, Guidi L, Pierboni L *et al.* Living without mitochondria: spermatozoa and spermatogenesis in two species of *Urodasys* (Gastrotricha, Macrodasyida) from dysoxic sediments. *Invertebrate Biology* 2007;**126**:1–9. https://doi.org/10.1111/j.1744-7410.2007.00071.x

Balsamo M, Artois T, Smith JPS *et al.* The curious and neglected soft-bodied meiofauna: Rouphozoa (Gastrotricha and Platyhelminthes). *Hydrobiologia* 2020;**847**:2613–44. https://doi.org/10.1007/s10750-020-04287-x

Bankevich A, Nurk S, Antipov D *et al.* SPAdes: a new genome assembly algorithm and its applications to single-cell sequencing. *Journal of Computational Biology* 2012;**19**:455–77. https://doi.org/10.1089/cmb.2012.0021

Bernt M, Donath A, Jühling F *et al.* MITOS: improved de novo metazoan mitochondrial genome annotation. *Molecular Phylogenetics and Evolution* 2013;**69**:313–9. https://doi.org/10.1016/j.ympev.2012.08.023

Bolger AM, Lohse M, Usadel BT. a flexible trimmer for Illumina sequence data. *Bioinformatics* 2014;**30**:2114–20. https://doi.org/10.1093/bioinformatics/btu170

Cesaretti A, Leasi F, Todaro MA. Confocal laser scanning microscopy applied to a new species helps understand the functioning of the reproductive apparatus in stylet-bearing *Urodasys* (Gastrotricha: Macrodasyida). *Water* 2023;**15**:1106. https://doi.org/10.3390/w15061106

Curini-Galletti M, Artois T, Delogu V *et al.* Patterns of diversity in soft-bodied meiofauna: dispersal ability and body size matter. *PLoS One* 2012;**7**:e33801. https://doi.org/10.1371/journal.pone.0033801

Curini-Galletti M, Artois T, Di Domenico M *et al.* Contribution of soft-bodied meiofaunal taxa to Italian marine biodiversity. *European Zoological Journal* 2020;**87**:369–84. https://doi.org/10.1080/24750263.2020.1786607

Edgar RC. MUSCLE: a multiple sequence alignment method with reduced time and space complexity. *BMC Bioinformatics* 2004;**5**:113. https://doi.org/10.1186/1471-2105-5-113

Fregni E, Faienza M, Grimaldi S *et al.* Marine gastrotrichs from the Tremiti archipelago in the southern Adriatic Sea, with the description of two new species of *Urodasys*. *Italian Journal of Zoology* 1999;**66**:183–94. https://doi.org/10.1080/11250009909356254

Gammuto L, Serra V, Petroni G *et al.* Molecular phylogenetic position and description of a new genus and species of freshwater Chaetonotidae (Gastrotricha: Chaetonotida: Paucitubulatina), and the annotation of its mitochondrial genome. *Invertebrate Systematics* 2024;**38**:IS23059. https://doi.org/10.1071/IS23059

Garraffoni ARS, Araujo TQ, Lourenco AP *et al.* A new genus and new species of freshwater Chaetonotidae (Gastrotricha: Chaetonotida) from Brazil with phylogenetic position inferred from nuclear and mitochondrial DNA sequences. *Systematics and Bodiversity* 2017;**15**:49–62. https://doi.org/10.1080/14772000.2016.1214189

Garraffoni ARS, Araujo TQ, Lourenco AP *et al.* Integrative taxonomy of a new *Redudasys* species (Gastrotricha: Macrodasyida) sheds light on the invasion of fresh water habitats by macrodasyids. *Scientific Reports* 2019;**9**:2067. https://doi.org/10.1038/s41598-018-38033-0

Guidi L, Ferraguti M, Todaro MA *et al.* Unusual spermatozoa and reproductive modalities of *Xenodasys eknomios* (Gastrotricha: Xenodasyidae). *Italian Journal of Zoology* 2009;**76**:165–72. https://doi.org/10.1080/11250000802527634

Guidi L, Todaro MA, Ferraguti M *et al.* Reproductive system of the genus *Crasiella* (Gastrotricha, Macrodasyida). *Helgoland Marine Research* 2011;**65**:175–85. https://doi.org/10.1007/s10152-010-0213-4

Guidi L, Todaro MA, Ferraguti M *et al.* Reproductive system and spermatozoa ultrastructure support the phylogenetic proximity of *Megadasys* and *Crasiella* (Gastrotricha, Macrodasyida). *Contributions to Zoology* 2014;**83**:119–31. https://doi.org/10.1163/18759866-08302003

Guidi L, Balsamo M, Ferraguti M *et al.* Reproductive organs and spermatogenesis of the peculiar spermatozoa of the genus *Kryptodasys* (Gastrotricha, Macrodasyida), with an appraisal of the occurrence and origin of the tail-less spermatozoa in Gastrotricha. *Journal of*

Zoological Systematics and Evolutionary Research 2021;**59**:1673–88. https://doi.org/10.1111/jzs.12556

Guidi L, Balsamo M, Grassi L *et al*. New data on reproductive system and spermatozoa confirm Macrodasys as a model in comparative reproductive analysis in Macrodasyida (Gastrotricha). *Water* 2022;**14**:3085. https://doi.org/10.3390/w14193085

Hall TB. a user-friendly biological sequence alignment editor and analysis program for Windows 95/98/NT. *Nucleic Acids Symposium Series* 1999;**41**:95–8. https://doi.org/10.1021/bk-1999-0734.ch008

Hummon WD. Marine Gastrotricha of the Near East: fourteen new species of Macrodasyida and a redescription of *Dactylopodola agadasys* Hochberg, 2003. *Zookeys* 2011;**94**:1–59. https://doi.org/10.3897/zookeys.94.794

Hummon WD, Hummon MR. Gastrotricha. In: Adiyodi KG, Adiyodi RG (eds), *Reproductive Biology of Invertebrates. Vol. I. Oogenesis, Oviposition, and Oosorption*. London: Wiley, 1983, 201–6.

Kamimura Y, Tee H-S, Lee C-Y. Ovoviviparity and genital evolution: a lesson from an earwig species with coercive traumatic mating and accidental breakage of elongated intromittent organs. *Biological Journal of the Linnean Society* 2016;**118**:443–56. https://doi.org/10.1111/bij.12755

Kånneby T, Todaro MA. The phylogenetic position of Neogosseidae (Gastrotricha: Chaetonotida) and the origin of planktonic Gastrotricha. *Organisms Diversity & Evolution* 2015;**15**:459–69. https://doi.org/10.1007/s13127-015-0223-9

Kånneby T, Todaro MA, Jondelius U. A Phylogenetic approach to species delimitation in freshwater Gastrotricha from Sweden. *Hydrobiologia* 2012;**683**:185–202. https://doi.org/10.1007/s10750-011-0956-1

Kånneby T, Todaro MA, Jondelius U. Phylogeny of Chaetonotidae and other Paucitubulatina (Gastrotricha: Chaetonotida) and the colonization of aquatic ecosystems. *Zoologica Scripta* 2013;**42**:88–105. https://doi.org/10.1111/j.1463-6409.2012.00558.x

Kieneke A, Schmidt-Rhaesa A. Gastrotricha. In: Schmidt-Rhaesa A (ed.), *Handbook of Zoology. Gastrotricha, Cycloneuralia and Gnathifera. Vol. 3: Gastrotricha and Gnathifera*. Berlin: De Gruyter, 2014, 1–134.

Kieneke A, Todaro MA. Discovery of two 'chimeric' Gastrotricha and their systematic placement based on an integrative approach. *Zoological Journal of the Linnean Society* 2021;**192**:710–35. https://doi.org/10.1093/zoolinnean/zlaa117

Kolicka M, Dabert M, Olszanowski Z *et al*. Sweet or salty? The origin of freshwater Gastrotrichs (Gastrotricha, Chaetonotida) revealed by molecular phylogenetic analysis. *Cladistics* 2020;**36**:458–80. https://doi.org/10.1111/cla.12424

Kumar S, Jones M, Koutsovoulos G *et al*. Blobology: exploring raw genome data for contaminants, symbionts and parasites using taxon-annotated GC-coverage plots. *Frontiers in Genetics* 2013;**4**:237. https://doi.org/10.3389/fgene.2013.00237

Kumar S, Stecher G, Li M *et al*. MEGA X: Molecular Evolutionary Genetics Analysis across computing platforms. Curated by Fabia Ursula Battistuzzi. *Molecular Biology and Evolution* 2018;**35**:1547–9. https://doi.org/10.1093/molbev/msy096

Magpali L, Machado DR, Araujo TQ *et al*. Long distance dispersal and pseudo-cryptic species in Gastrotricha: first description of a new species (Chaetonotida, Chaetonotidae, *Polymerurus*) from an oceanic island with volcanic rocks. *European Journal of Taxonomy* 2021;**746**:62–93. https://doi.org/10.5852/ejt.2021.746.1319

Rataj Križanová F, Vďačný P. A huge undescribed diversity of the subgenus *Hystricochaetonotus* (Gastrotricha, Chaetonotidae, *Chaetonotus*) in Central Europe. *European Journal of Taxonomy* 2022;**840**:1–93. https://doi.org/10.5852/ejt.2022.840.1941

Rataj Križanová F, Vďačný P. A *Heterolepidoderma* and *Halichaetoderma* gen. nov. (Gastrotricha: Chaetonotidae) riddle: integrative taxonomy and phylogeny of six new freshwater species from Central Europe. *Zoological Journal of the Linnean Society* 2024;**200**:283–335. https://doi.org/10.1093/zoolinnean/zlad079

Ronquist F, Teslenko M, van der Mark P *et al*. MrBayes 3.2: efficient Bayesian phylogenetic inference and model choice across a large model space. *Systematic Biology* 2012;**61**:539–42. https://doi.org/10.1093/sysbio/sys029

Ruppert EE. Gastrotricha. In: Harrison FW, Ruppert RR (eds), *Microscopic Anatomy of Invertebrates. Vol 4: Aschelmintes*. NY: Wiley-Liss, 1991, 41–109.

Saponi F, Kosakyan A, Cesaretti A *et al*. A contribution to the taxonomy and phylogeny of the genus *Chaetonotus* (Gastrotricha, Paucitubulatina, Chaetonotidae), with description of a new species from Italian inland waters. *The European Zoological Journal* 2024;**91**:1078–92. https://doi.org/10.1080/24750263.2024.2397473

Schoepfer-Sterrer C. Five new species of *Urodasys* and remarks on the terminology of the genital organs in Macrodasyidae (Gastrotricha). *Cahiers de Biologie Marine* 1974;**15**:229–54.

Serra V, Gammuto L, Nitla V *et al*. Morphology, ultrastructure, genomics, and phylogeny of *Euplotes vanleeuwenhoeki* sp. nov. and its ultra-reduced endosymbiont '*Candidatus Pinguicoccus supinus*' sp. nov. *Scientific Reports* 2020;**10**:20311. https://doi.org/10.1038/s41598-020-76348-z

Staden R. The Staden sequence analysis package. *Molecular Biotechnology* 1996;**5**:233–41. https://doi.org/10.1007/BF02900361

Todaro MA, Luporini P. Not too big for its mouth: direct evidence of a Macrodasyidan Gastrotrich preyed in nature by a Dileptid Ciliate. *The European Zoological Journal* 2022;**89**:785–90. https://doi.org/10.1080/24750263.2022.2095048

Todaro MA, Fleeger JW, Hu YP *et al*. Are meiofauna species cosmopolitan? Morphological and molecular analysis of *Xenotrichula intermedia* (Gastrotricha: Chaetonotida). *Marine Biology* 1996;**125**:735–42. https://doi.org/10.1007/bf00349256

Todaro MA, Bernhard JM, Hummon WD. A new species of *Urodasys* (Gastrotricha, Macrodasyida) from dysoxic sediments of the Santa Barbara Basin (California, U.S.A.). *Bulletin of Marine Science* 2000;**66**:467–76.

Todaro MA, Kånneby T, Dal Zotto M *et al*. Phylogeny of Thaumastodermatidae (Gastrotricha: Macrodasyida) inferred from nuclear and mitochondrial sequence data. Curated by Art Poon. *PLoS One* 2011;**6**:e17892. https://doi.org/10.1371/journal.pone.0017892

Todaro MA, Dal Zotto M, Jondelius U *et al*. Gastrotricha: a marine sister for a freshwater puzzle. Curated by Bernd Schierwater. *PLoS One* 2012a;**7**:e31740. https://doi.org/10.1371/journal.pone.0031740

Todaro MA, Guidi L, Ferraguti M *et al*. A fresh look at *Dinodasys mirabilis* (Gastrotricha, Macrodasyida), with focus on the reproductive apparatus and sperm ultrastructure. *Zoomorphology* 2012b;**131**:115–25. https://doi.org/10.1007/s00435-012-0147-2

Todaro MA, Leasi F, Hochberg R. A new species, genus and family of marine Gastrotricha from Jamaica, with a phylogenetic analysis of Macrodasyida based on molecular data. *Systematics and Biodiversity* 2014;**12**:473–88. https://doi.org/10.1080/14772000.2014.942718

Todaro MA, Dal Zotto M, Leasi F. An integrated morphological and molecular approach to the description and systematisation of a novel genus and species of Macrodasyida (Gastrotricha). Curated by Michael L Fine. *PLoS One* 2015;**10**:e0130278. https://doi.org/10.1371/journal.pone.0130278

Todaro MA, Cesaretti A, Dal Zotto M. Marine gastrotrichs from Lanzarote, with a description of a phylogenetically relevant species of *Urodasys* (Gastrotricha, Macrodasyida). *Marine Biodiversity* 2017;**49**:2109–23. https://doi.org/10.1007/s12526-017-0747-7

Todaro MA, Dal Zotto M, Kånneby T *et al*. Integrated data analysis allows the establishment of a new, cosmopolitan genus of marine Macrodasyida (Gastrotricha). *Scientific Reports* 2019a;**9**:7989. https://doi.org/10.1038/s41598-019-43977-y

Todaro MA, Sibaja-Cordero JA, Oscar A *et al*. An introduction to the study of Gastrotricha, with a taxonomic key to families and genera of the group. *Diversity* 2019b;**11**:117. https://doi.org/10.3390/d11070117

Valbonesi A, Luporini P. Researches on the coast of Somalia. Gastrotricha Macrodasyidea. *Italian Journal of Zoology Supplement* 1984;**1**:1–34. https://doi.org/10.1080/00269786.1984.11758576

Weiss MJ. Widespread hermaphroditism in freshwater gastrotrichs. *Invertebrate Biology* 2001;**120**:308–41. https://doi.org/10.1111/j.1744-7410.2001.tb00040.x

Wilke U. Mediterrane Gastrotrichen. *Zoologische Jahrbücher. Abteilung für Systematik, Ökologie und Geographie der Tiere* 1954;**82**:497–550.

Xu S, Huynh TV, Snyman M. The transcriptomic signature of obligate parthenogenesis. *Heredity* 2022;**128**:132–8. https://doi.org/10.1038/s41437-022-00498-1

CHAPTER 3

IMPROVED TAXONOMIC AND GENE SAMPLING ADVANCE THE KNOWLEDGE OF DEEP RELATIONSHIPS WITHIN MACRODASYIDA (GASTROTRICHA)

(published in *Cladistics* 42(1), 25–45. https://doi.org/10.1111/cla.70013)

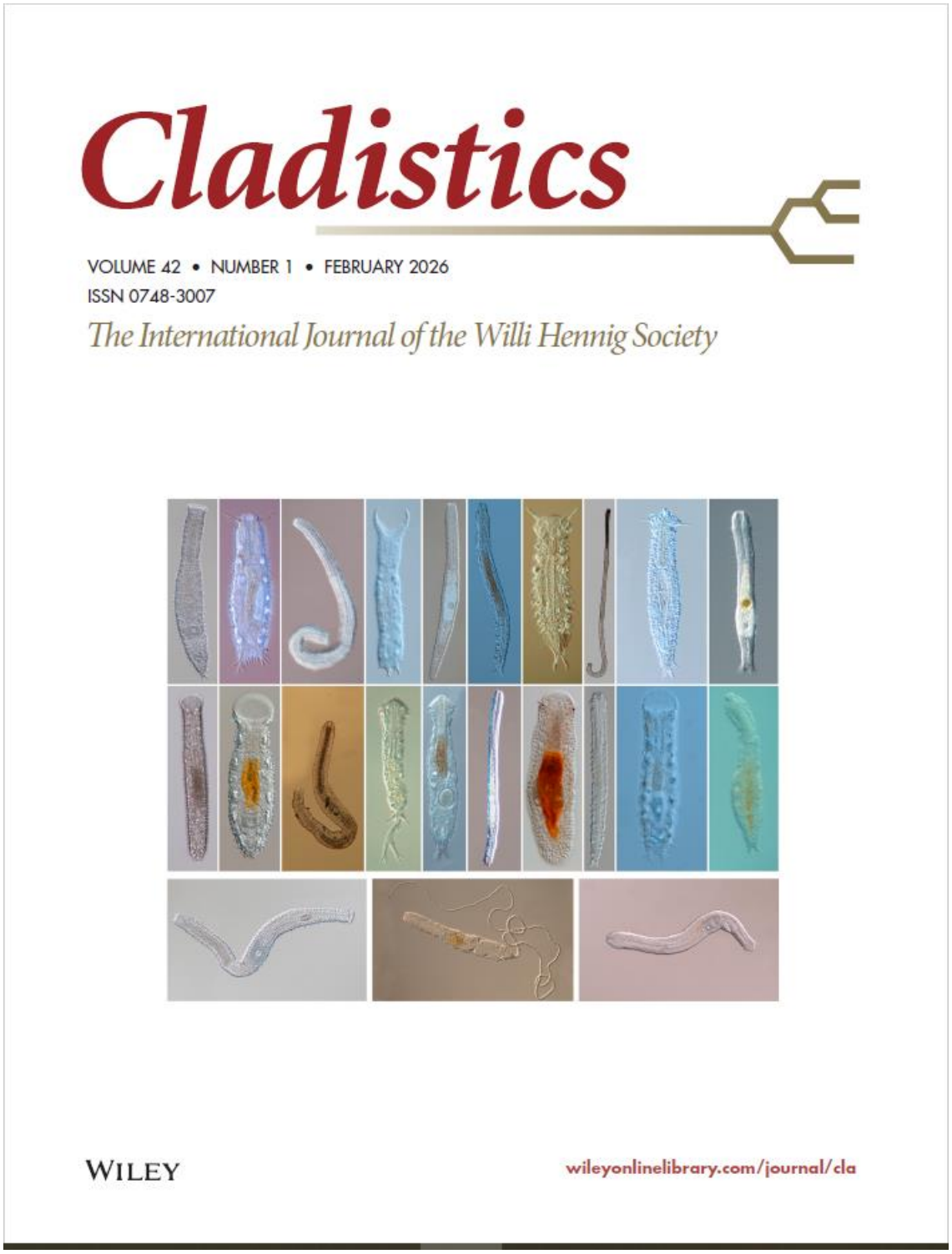

WILEY

Cladistics

Cladistics 42 (2026) 25–45

doi: 10.1111/cla.70013

Improved taxonomic and gene sampling advance the knowledge of deep relationships within Macrodasyida (Gastrotricha)

Agata Cesaretti[a,*], Anush Kosakyan[a,b], Francesco Saponi[a,b,c] and M. Antonio Todaro[a,b]

[a]*Department of Life Sciences, University of Modena and Reggio Emilia, Modena, Italy;* [b]*National Biodiversity Future Center (NBFC), Palermo, Italy;* [c]*Department of Earth and Marine Sciences, University of Palermo, Palermo, Italy*

Received 13 June 2025; Revised 7 September 2025; Accepted 6 October 2025

Abstract

Advances in Macrodasyida (Gastrotricha) phylogenetics, fuelled by new species discoveries and molecular data, are reshaping taxonomic classifications. Molecular analyses suggest polyphyly in Cephalodasyidae and Macrodasyidae, yet insufficient sampling continues to obscure precise relationships. Our study seeks to enhance the resolution of Macrodasyida's internal phylogeny through expanded taxonomic and molecular sampling. We obtained 63 new sequences from 21 Macrodasyidan species, integrating them with published data. Our dataset includes representatives from nine Macrodasyida families and 21 genera, alongside two chaetonotidans. We analysed the concatenated sequences of three genes (*18S*, *28S* rRNA, *COI* mtDNA) from 51 terminals using Maximum Parsimony, Maximum Likelihood and Bayesian Inference. Our findings confirm the polyphyly of Cephalodasyidae. *Dolichodasys* and *Paradasys* cluster with Redudasyidae, while *Cephalodasys* and *Mesodasys* form unrelated lineages. *Cephalodasys mahoae* is nested within *Paradasys* rather than *Cephalodasys*, suggesting an original misidentification. The phylogenetic placement of *Pleurodasys* remains uncertain. Macrodasyidae is non-monophyletic, with *Urodasys* forming an independent lineage. The first molecular data ever obtained for *Dendrodasys* hint that the family Dactylopodolidae is likely polyphyletic as well. We propose an updated classification of Macrodasyida, introducing Mesodasyidae fam. nov., Urodasyidae fam. nov. and *Parurodasys* gen. nov. Furthermore, we reassign *Dolichodasys* and *Paradasys* to Redudasyidae and *Cephalodasys mahoe* to *Paradasys*.

Introduction

The phylum Gastrotricha includes microscopic, free-living, mostly benthic invertebrates inhabiting aquatic ecosystems worldwide (Kieneke and Schmidt-Rhaesa, 2014; Todaro et al., 2019c; Garraffoni et al., 2021). The approximately 900 formally described species are distributed into two orders: Chaetonotida (520 spp.) and Macrodasyida (380 spp.) (Saponi and Todaro, 2024; Souid et al., 2025). The taxonomy and classification of these metazoans are in a state of constant evolution, driven by the ongoing discovery of new species bearing unusual morphological traits and the increasing incorporation of molecular data into phylogenetic studies (Todaro et al., 2015, 2019b; Garraffoni and Balsamo, 2017; Kieneke and Todaro, 2021). For example, molecular phylogenetic analyses have revealed that certain taxa previously linked to traditional groups, which were primarily identified based on morphological features, occupy distinct positions on the Gastrotricha tree of life (Todaro et al., 2012, 2019b; Gammuto et al., 2024; Rataj Križanová and Vd'ačný, 2024; Minowa et al., 2025). This finding raises questions about the reliability of certain morphological characteristics in systematics. The morphology of Gastrotricha is not only highly diverse but also complex, making phylogenetic interpretation challenging; superficial similarities can often conceal significant underlying differences (Todaro et al., 2019b;

*Corresponding author:
E-mail address: agata.cesaretti@unimore.it

Gammuto et al., 2024). Consequently, the phylum Gastrotricha includes some examples (see below) of what taxonomists call "systematic wastebaskets", taxa that group species on the basis of characters that are not homologous and often on negative traits (Plotnick and Wagner, 2006; Rataj Križanová and Vďačný, 2022). The classification using plesiomorphic and negative characters results in heterogeneous and poorly defined groups, connected by superficial and often subjective similarities, without any solid evolutionary hypotheses (Plotnick and Wagner, 2006). One of the most extreme and well-known cases of "systematic wastebaskets" is the taxonomically obsolete kingdom Protista, which was originally used to group all single-celled eukaryotes that could not be clearly classified as animals, plants, or fungi (Whittaker, 1969). Concerning Gastrotricha, the evolutionary interpretation of the morphological characters is currently challenging due to confusion surrounding the ancestral character states at the base of different lineages. Gastrotrichs are small organisms, measuring between 80 μm and 3.8 mm in length, exhibiting a significant range of morphological diversity (Minowa et al., 2025; Souid et al., 2025), which may be even greater due to the common occurrence of unrecognized homoplasies (Rataj Križanová and Vďačný, 2022). Studying gastrotrichs can be quite difficult: they are entirely covered by a delicate cuticle, which is fragile. As a result, they are assigned to the soft-bodied meiofauna in ecological and biogeographical studies (Artois et al., 2011; Balsamo et al., 2020; Curini-Galletti et al., 2020). Taxonomic surveys and identification of gastrotrichs must be conducted on living specimens, as fixation processes alter their diagnostic features (Todaro et al., 2019c). This requirement makes it essential for morphological surveys to be quick and heavily reliant on the quality of the equipment used and the skills of the researchers. Additionally, re-evaluating the original material that underpins current classifications with modern techniques is practically unfeasible. Most of the type material (holotypes) is nearly non-existent, and descriptions prior to 1954, when the first gastrotrich photographic material was published by Wilke (1954), are complemented solely with drawings of varying quality. To address these limitations, researchers are increasingly using integrative methods to establish monophyletic groupings supported by strong phylogenetic evidence. Morphological surveys, conducted using high-resolution microscopy techniques, such as DIC, SEM, and CLSM, are supported by detailed photomicrographs and video footages (e.g., Munter and Kieneke, 2017; Schuster et al., 2017; Campos et al., 2020; Kieneke and Todaro, 2021; Magpali et al., 2021; Cesaretti et al., 2023; Araújo, 2024). Additionally, molecular data have become crucial in enhancing traditional morphological analyses to clarify taxonomic groupings (e.g., Cesaretti et al., 2024; Saponi et al., 2024). However, many taxa remain underrepresented in molecular studies, which creates uncertainties about their origins and phylogenetic relationships. In the order Macrodasyida, the family Cephalodasyidae Hummon and Todaro, 2010 presents a puzzling example of a potential unnatural grouping. This family currently comprises five genera: *Cephalodasys* Remane, 1926 (15 species), *Dolichodasys* Gagne, 1977 (3 species), *Mesodasys* Remane, 1951 (8 species), *Paradasys* Remane, 1934 (6 species), and *Pleurodasys* Remane, 1927 (2 species) (Fig. 1).

Previously, these five genera, along with *Lepidodasys* Remane, 1926 and *Megadasys* Schmidt, 1974, were classified under the family Lepidodasyidae. However, significant morphological differences between *Lepidodasys* and the other genera, such as the presence of robust, keeled scales on the cuticle, a pharynx without pharyngeal pores, and unique characteristics in the ultrastructure of spermatozoa led Hummon and Todaro (2010) to propose a much-needed systematic revision of the group. They determined that *Lepidodasys* should remain in the family Lepidodasyidae as its type genus, while the other genera were grouped into the newly established family Cephalodasyidae. A follow-up study examining reproductive traits and using early phylogenetic reconstruction with molecular markers suggested transferring *Megadasys* to the family Planodasyidae (Guidi et al., 2014).

Despite the removal of *Megadasys*, the five remaining genera of cephalodasyids still only share traits that are either plesiomorphic (for example, a vermiform to strap-shaped body and pharyngeal pores located near the junction of the pharynx and intestine) or negative traits (such as the absence of cuticular scales or spines) (Kieneke and Schmidt-Rhaesa, 2014). Furthermore, studies using *18S* rDNA sequences suggest that this family may be polyphyletic (Todaro et al., 2012; Yamauchi and Kajihara, 2018; Kieneke and Todaro, 2021). However, the precise phylogenetic relationships of its genera remain unclear, hindering a more comprehensive revision of the taxon.

Similarly, there are indications that the family Macrodasyidae Remane, 1924 may not be monophyletic. This taxon currently comprises four genera: the well-known *Macrodasys* Remane, 1924 and *Urodasys* Remane, 1926, along with the more recent additions of *Kryptodasys* Todaro, Dal Zotto, Kånneby and Hochberg, 2019, and *Thaidasys* Todaro, Dal Zotto and Leasi, 2015 (Fig. 2). The inclusion of the latter two genera in this family is based on a systematic approach that integrates both morphological and molecular data (Todaro et al., 2015, 2019b). In contrast, molecular phylogenetic analyses conducted thus far do not appear to support the inclusion of *Urodasys* within this family, despite significant morphological

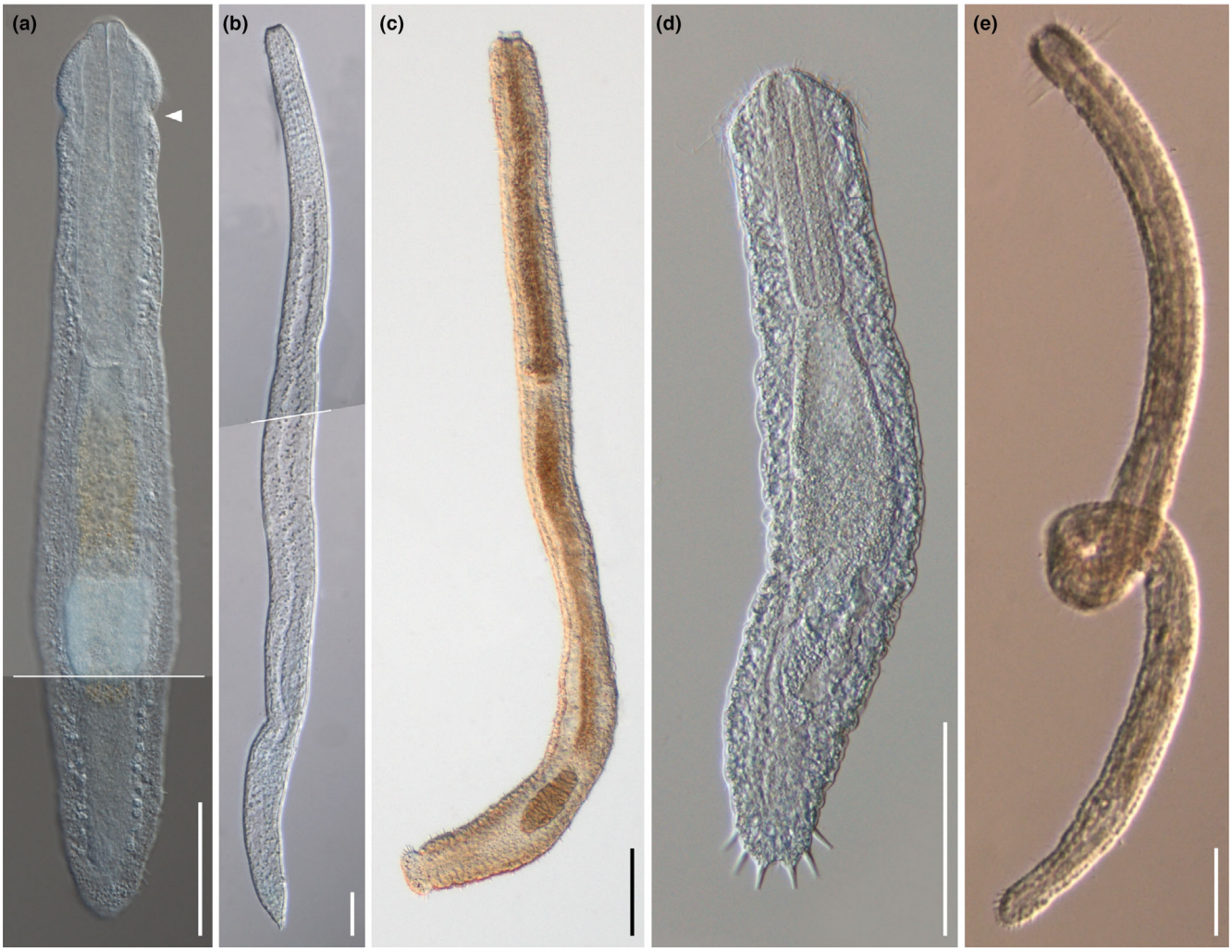

Fig. 1. Some of the Cephalodasyidae specimens used in the study, showing the general morphology of each genus in the family. (a) *Cephalodasys maximus* Remane, 1929, photo composition, showing the anterior constriction typical of the genus (arrowhead); (b) *Dolichodasys* sp. 2, photo composition; (c) *Mesodasys laticaudatus* Remane, 1951; (d) *Paradasys* sp. 1; (e) *Pleurodasys incomptus* Todaro, Dal Zotto, Bownes and Perissinotto, 2017. Differential interference contrast microscopy (Nomarski), scale bar = 100 μm.

homologies that have been hypothesized to exist between *Urodasys* and *Macrodasys* (Ruppert, 1991). Furthermore, molecular phylogenetic studies have not clarified the evolutionary position of *Urodasys* within the Macrodasyida lineage (Todaro et al., 2019b; Kieneke and Todaro, 2021).

Given the challenges in interpreting morphological characteristics within a phylogenetic framework, thorough molecular investigations may help to clarify the issues mentioned above. To date, molecular research has primarily focused on a limited number of species from both Cephalodasyidae and Macrodasyidae and has often relied on sequences from just one gene. Expanding both the variety of taxa studied and the number of genes sampled is expected to resolve many of the existing uncertainties. In this study, we present new molecular data for 22 species of Macrodasyida, including 14 species from the family Cephalodasyidae. Additionally, we carried out phylogenetic analyses that incorporated sequences from five species of *Urodasys*, which were acquired only recently (Cesaretti et al., 2024). These species have not yet been part of any comprehensive phylogenetic studies focused on clarifying the internal relationships within the order Macrodasyida.

Materials and methods

Taxonomic and gene sampling

To explore the relationships within the Macrodasyida, which encompasses 10 families and 37 genera, we aimed to involve as many families and genera as possible in our analysis. For reliable and

Fig. 2. Representatives of the Macrodasyidae genera. (a) *Kryptodasys carlosrochai* Todaro, Dal Zotto, Kånneby, Hochberg, 2019; (b) *Macrodasys* sp.; (c) *Thaidasys tongiorgii* Todaro, Dal Zotto and Leasi, 2015; (d) *Urodasys completus* Todaro, Cesaretti and Dal Zotto, 2017. Differential interference contrast microscopy (Nomarski), scale bars = 100 μm. (a) Modified from Todaro et al. (2019b).

robust results, we based the phylogenetic analysis on the combined sequences of three molecular markers: the nuclear *18S* and *28S* rRNA genes and the mitochondrial *COI* gene. To increase/balance taxonomic representation, we focus our efforts on obtaining new molecular data from members of Cephalodasyidae (13 spp.) and other families underrepresented in previous studies or for which available molecular data are limited to a single gene such as Dactylopodololidae (1 sp.), Lepidodasyidae (3 spp.), Macrodasyidae (1 sp.), Planodasyidae, Redudasyidae (1 sp.), and Xenodasyidae (1 sp.). Unfortunately, attempts to obtain sequences from the monotypic Hummondasyidae were unsuccessful. For this study, we generated 66 new sequences from 21 species and 22 terminals. A complete list of specimens sequenced for this study is provided in Table 1. The specimens analysed in this study were collected during various faunistic surveys conducted by one of the authors (MAT). Shortly after collection, the gastrotrichs were extracted from the sandy substrate using a 7% $MgCl_2$ solution; they were identified to the lowest possible taxonomic level under Nomarski optics, then fixed in 95% ethanol and stored at −20°C for further analysis. No special permissions or permits were required for collecting these organisms, as gastrotrichs are microscopic and non-pathogenic. The field study did not involve any endangered species, and the sampling took place in publicly accessible areas. Sampled locations included the coastal areas of Costa Rica, Greece, Italy, Madagascar, South Africa, St John Island, Sweden, and Thailand (see Table 1). Additionally, we complemented our new sequences with data from 25 species sourced from GenBank (Table S1). We prioritized including species that would help establish a comprehensive taxonomic framework or whose phylogenetic relationships remain unclear, particularly those from the families Macrodasyidae and Redudasyidae. Notably, we included a significant number of *Urodasys* species (5 spp.), representing the genus's main lineages (Cesaretti et al., 2024). Sequences from these species were recently obtained in our laboratory and have never been included in comprehensive phylogenetic analyses of Macrodasyida. Intentionally, we opted to include only a limited number of species from families such as Turbanellidae and Thaumastodermatidae because their monophyletic nature is well established (e.g., Todaro et al., 2011, 2014; Kieneke and Todaro, 2021). This decision also helps to reduce the time required for our analyses. The complete dataset comprises 51 species representing nine families and 21 genera of Macrodasyida, along with two families and two genera of Chaetonotida (see Table 1, Table S1).

Table 1
Specimens sequenced in this study, with respective sampling areas and vouchers

Taxon	Sampling area	Voucher
Cephalodasyidae		
Cephalodasys maximus 1 Remane, 1926	Hållö Island, Sweden 58°20′27″ N; 11°12′42″ E	T2B7
Cephalodasys maximus 2	Hållö Island, Sweden 58°20′27″ N; 11°12′42″ E	W3B
Cephalodasys sp. 1	St John Island, USA 18°21′50″ N; 64°43′47″ W	W39
Cephalodasys sp. 2	St John Island, USA 18°21′50″ N; 64°43′47″ W	W3
Cephalodasys sp. 3	Ambanja district, Madagascar 13°36′52″ S; 47°53′20″ E	W10
Cephalodasys sp. 4	Kos Island, Greece 36°54′23″ N; 27°17′06″ E	W26
Dolichodasys sp. 1	Sicily, Italy 37°25′58″ N; 13°14′29″ E	T116A
Dolichodasys sp. 2	Umhlanga, RSA 29°43′37″ S; 31°05′24″ E	W42
Mesodasys laticaudatus 1 Remane, 1951	Calabria, Italy 38°54′28″ N; 16°48′43″ E	W20
Mesodasys littoralis 1 Remane, 1951	Sicily, Italy 36°47′18″ N; 14°29′34″ E	T111C
Mesodasys sp. 1	Ambanja district, Madagascar 13°36′52″ S; 47°53′20″ E	W24
Paradasys sp. 1	Marche, Italy 43°29′41″ N; 13°37′38″ E	M71
Paradasys sp. 2	Sardinia, Italy 41°03′9″ N; 8°56′16″ E	MS5
Pleurodasys incomptus Todaro, Dal Zotto, Bownes and Perissinotto, 2017	Umhlanga, RSA 29°43′37″ S; 31°05′24″ E	W23
Dactylopodolidae		
Dendrodasys sp. 1	Ambanja district, Madagascar 13°36′52″ S; 47°53′20″ E	W36
Lepidodasyidae		
Lepidodasys martini Remane, 1926	Hållö Island, Sweden 58°20′27″ N; 11°12′42″ E	W56
Lepidodasys unicarenatus Balsamo, Fregni and Tongiorgi, 1994	Tuscany, Italy 42°34′32″ N; 10°52′57″ E	W55
Lepidodasys sp. 1	Sicily, Italy 37°34′37″ N; 12°53′43″ E	T118C
Macrodasyidae		
Thaidasys tongiorgii Todaro, Dal Zotto and Leasi, 2015	Phuket Island, Thailand 07°48′12″ N; 98°17′55″ E	W2
Planodasyidae		
Crasiella sp. 1	Nicoya Penisula, Costa Rica 09°59′38″ N; 85°42′07″ W	W60
Redudasyidae		
Anandrodasys agadasys (Hochberg, 2003)	St John Island, USA 18°21′50″ N; 64°43′47″ W	S40
Xenodasyidae		
Xenodasys riedli (Schoepfer-Sterrer, 1969)	St John Island, USA 18°21′50″ N; 64°43′47″ W	S42

DNA extraction, amplification, and sequencing

Single ethanol-fixed specimens were rinsed in clean absolute ethanol and transferred into a sterile 0.5 mL microtube using a clean, dedicated glass micropipette. The tubes with the specimens were left overnight at 25°C in a cleaned ISCO micra 18 incubator to eliminate any residual ethanol through evaporation. DNA extraction and whole-genome amplification (WGA) were carried out using the REPLI-g Single Cell Kit (QIAGEN®) according to the manufacturer's protocol. The presence of gastrotrich genetic material in the amplified DNA product was ascertained through a validation step involving PCR (polymerase chain reaction) amplification and Sanger sequencing of the *18S* rRNA gene of these animals. Details regarding the validation steps are available in File S1 and Table S2. All the WGA DNA products that passed the validation step were sent to the Macrogen Europe laboratories (https://www.macrogen-europe.

com/), where they were processed with a TrueSeq DNA PCR Free Library kit and *de novo* whole-genome sequencing (WGS) on the NovaSeq 6000 Illumina Platform, generating a total of 40 million reads (paired-ends 2 × 150 bp).

Data assembly and gene extraction

The Illumina reads resulting from the sequencing of the WGA products were analysed through a bioinformatic pipeline, optimized from Kumar et al. (2013) (see also Serra et al., 2020; Cesaretti et al., 2024; Gammuto et al., 2024; Saponi et al., 2024). After being evaluated for quality using the Fastqc software (http://www.bioinformatics.babraham.ac.uk/projects/fastqc/) (Andrews, 2010; Kumar et al., 2018), the reads were trimmed using the Trimmomatic 0.39 software (Bolger et al., 2014), keeping parameters as default and with a minimum quality score of 30. The processed paired reads were then assembled using the SPAdes v3.6.0 software (Bankevich et al., 2012). Using the Blastn and tBlastn tools, we identified and isolated the nodes that target the ribosomal and mitochondrial regions for each sequenced specimen. The queries for the Blastn and Tblastn searches were both published gastrotrich sequences, publicly available on the NCBI GenBank database, and sequences obtained in our lab during the previous PCR validation step through Sanger sequencing. These same *18S* rRNA gene sequences were utilized as a reference to confirm the accuracy and reliability of the WGS sequencing results. This verification was performed by aligning the sequences using the BioEdit v7.2.5 Freeware software (Hall, 1999).

StructRNAfinder (https://structrnafinder.integrativebioinformatics.me/) (Arias-Carrasco et al., 2018) and MITOS2 (Bernt et al., 2013), available on the Galaxy Europe Web Portal (https://usegalaxy.eu) (The Galaxy Community, 2024), were used to examine the nodes of interest isolated from the genomic assembly and to confirm the location of the identified genes (*18S*, *28S* and *COI*). The newly obtained COI sequences were individually analysed using the Geneious Prime software (v. 2019.2.3) (https://www.geneious.com/) to identify the correct reading frame. All the new sequences published in the present work were obtained through the WGA-WGS pipeline.

Phylogenetic analysis

Each gene dataset was aligned separately through the MUSCLE (multiple sequences comparison by Log expectation) algorithm (Edgar, 2004) implemented in the MEGA X software package (Kumar et al., 2018). The mitochondrial protein-coding COI sequences were aligned as codons using the invertebrate mitochondrial genetic code. The alignments were then trimmed to the length of the majority of the sequences. The trimmed and aligned datasets resulted in 2019 (*18S* rDNA), 6988 (*28S* rDNA) and 1596 (*COI*) nucleotide sites, and the final concatenated matrix resulted in 10 603 sites. Phylogenetic analyses were conducted using the maximum likelihood (ML), Bayesian inference (BI) and Maximum Parsimony (MP) approaches. Two chaetonotidan species, *Diuronotus aspetos* Todaro, Balsamo and Kristensen, 2005 (Muselliferidae) and *Xenotrichula intermedia* Remane, 1934 (Xenotrichulidae) were chosen as the outgroup.

The ML analysis was conducted using the IQ-TREE v.1.6.10 software (Nguyen et al., 2015; Yudina et al., 2021). The best-fit models according to BIC (Bayesian information criterion) were determined separately for each partition by this same software: TIM3e+I+G4 for *18S* sequences, TIM3+F+I+G4 for *28S* sequences, and TVM+F+G4 for *COI* sequences. The analysis used the edge-unlinked partition option, and was conducted using 1000 replicates of complete non-parametric bootstrap (Guindon et al., 2010). The BI analyses were conducted in the programme MrBayes v.3.2.7 (Ronquist et al., 2012). As the evolutionary models suggested by IQ-TREE were not available in MrBayes, we replaced them with the GTR+Γ+G4 (general time reversible) model, which is widely recognized as the best alternative in such cases (see for example, Yudina et al., 2021). This model was applied to all three partitions. The BI tree search for the final concatenated dataset ran with two parallel runs, using eight independent Markov chains over 6 000 000 generations. Tree sampling occurred every 100 generations, with a burn-in fraction set at 25%. Convergence of the Markov chain Monte Carlo (MCMC) analyses was validated using the programmes built-in diagnostics: the average standard deviation of split frequencies approached zero, the potential scale reduction factor (PSRF) converged to 1.00 for all parameters, and the effective sample sizes (ESS) for all parameters exceeded 200 (with a minimum ESS of 8345.943 and an average ESS of 8967.733). The MP analysis was conducted on MEGA X using 1000 bootstrap replicates and with the other parameters set as default.

All the trees were computed as unrooted and then rooted in FigTree v.1.4.3 (http://tree.bio.ed.ac.uk/software/figtree/) using *X. intermedia* and *D. aspetos* as the outgroup. Finally, the trees were edited with the CorelDraw X7 software (Corel Corporation, Ottawa, ON, Canada) to improve readability.

Results

Sequencing

We obtained a total of 66 new gene sequences belonging to 21 Macrodasyidan species (22 terminals), across seven families and 12 genera: Cephalodasyidae (13 species), Dactylopodolidae Strand, 1929 (1 sp.), Lepidodasyidae (3 spp.), Macrodasyidae (1 sp.), Planodasyidae Rao and Clausen, 1970 (1 sp.), Redudasyidae (1 sp.), and Xenodasyidae Todaro, Guidi, Leasi and Tongiorgi, 2006 (1 sp.).

The length of the obtained sequences varies from 1731 to 1948 bp for the *18S* rRNA gene, from 2611 to 4267 bp for the *28S* rRNA gene and from 633 to 1584 bp for the *COI* mtDNA gene. These differences are mostly imputable to limitations of the sequencing process, which produces reads of varying quality. Therefore, it was not always possible to assemble the reads containing the entire gene sequence.

Phylogenetic analysis

Our phylogenetic analyses of the concatenated dataset produced trees with mostly congruent topologies. The results from both maximum likelihood (ML) and Bayesian inference (BI) analyses were consistent with each other and revealed several well-supported main clades (Figs 3 and 4). In contrast, the Maximum Parsimony (MP) tree is less resolved at higher taxonomic levels, exhibiting lower support values at most deeper nodes. However, its general topology aligns with the other methods by resolving the analysed Macrodasyida species distributed in three main clusters (I, II, and III, Figs 3–5). In detail, genera that included two or more

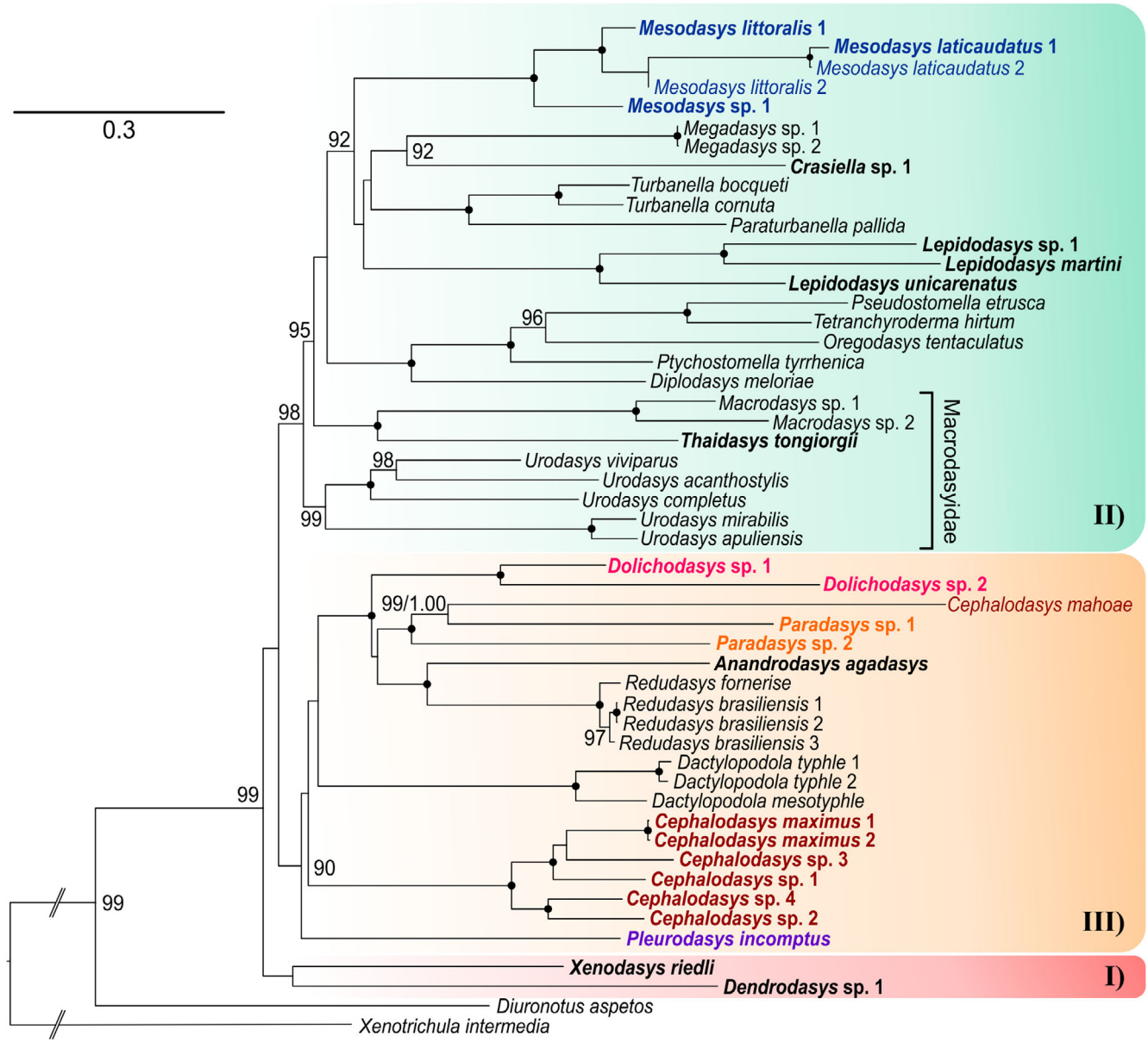

Fig. 3. Phylogenetic relationships of the order Macrodasyida inferred from maximum likelihood (ML) analysis of concatenated *18S*, *28S* rDNA, and *COI* mtDNA sequences. The analyses include 51 terminals, of which 49 belong to the order Macrodasyida. Two Chaetonotida, *Xenotrichula intermedia* (Xenotrichulidae) and *Diuronotus aspectos* (Muselliferidae), are used as the outgroup. In bold, taxa sequenced in this study; in colour, the Cephalodasyidae coded by genus. Numbers at nodes represent bootstrap support (1000 replicates). A black dot at the node indicates full bootstrap support for the branch. Bootstrap values <90 are not reported.

species were resolved as monophyletic by all analyses. The exception was *Cephalodasys*, specifically due to *C. mahoae*, which consistently clusters with *Paradasys* (Figs 3–5). Among the families represented by terminals of two or more genera, only Redudasyidae, Thaumastodermatidae, and Turbanellidae were resolved as monophyletic across all analyses. Planodasyidae was recognized as a clade by both the ML and BI analyses (Figs 3 and 4), receiving high to full support. However, the MP analysis indicated Planodasyidae as paraphyletic due to the nested position of *Lepidodasys*, with relatively low support at the nodes (Fig. 5).

The current families Cephalodasyidae, Dactylopodolidae, and Macrodasyidae were consistently found to be non-monophyletic in all tree analyses (Figs 3–5). Specifically, Dactylopodolidae appears polyphyletic, with the early branching of *Dendrodasys* sp. along the Macrodasyida evolutionary tree. All analyses demonstrated that *Dendrodasys* sp. is associated with *Xenodasys riedli* instead of *Dactylopodola* (Cluster I);

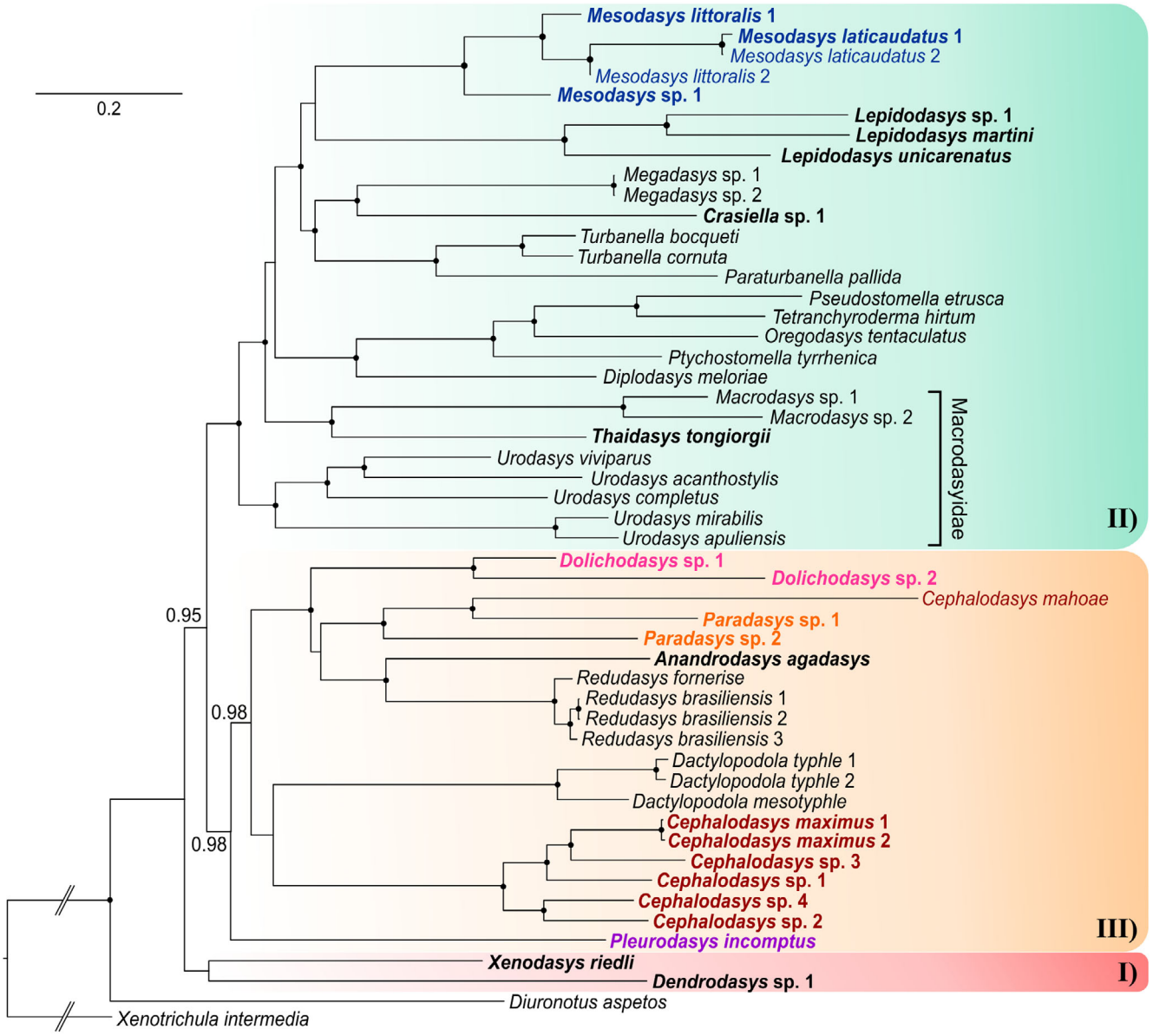

Fig. 4. Phylogenetic relationships of the order Macrodasyida inferred from Bayesian inference (BI) analysis of concatenated *18S*, *28S* rDNA, and *COI* mtDNA sequences. The analyses include 51 terminals, of which 49 belong to the order Macrodasyida. Two Chaetonotida, *Xenotrichula intermedia* (Xenotrichulidae) and *Diuronotus aspetos* (Muselliferidae), are used as the outgroup. In bold, taxa sequenced in this study; in colour, the Cephalodasyidae coded by genus. Numbers at nodes represent posterior probability support. A black dot at the node indicates full posterior probability support for the branch. Posterior probability values <0.95 are not reported.

however, this grouping did not receive high support in any of the analyses (Figs 3–5).

Our results indicate that Macrodasyidae is indeed polyphyletic, with the early offshoot of *Urodasys* serving as the sister taxon to a large clade that includes other Macrodasyidae (i.e., *Macrodasys* and *Thaidasys*), as well as members from four other families (Lepidodasyidae, Planodasyidae, Thaumastodermatidae, and Turbanellidae), and terminals from the genus *Mesodasys* (LPTTM group). The alliance of *Urodasys* alongside the LPTTM taxa (Cluster II) received high to full statistical support from both the ML and BI analyses but showed relatively weak support (59% bootstrap) from the MP analysis. The internal topology of the genus *Urodasys* reveals that hermaphroditic species lacking accessory sexual organs, namely, *U. apuliensis* and *U. mirabilis*, form a separate branch, which is strongly supported in all analyses (Figs 3–5). In contrast, the parthenogenetic species *U. viviparus* is positioned within the branch that includes

hermaphroditic species equipped with a sclerotized stylet, specifically *U. acanthostylis* and *U. completus*.

As initially suspected, the family Cephalodasyidae appears to be polyphyletic based on our analyses. Members of its currently affiliated genera are scattered along the Macrodasyida phylogenetic tree (Figs 3–5). The well-sampled genera *Cephalodasys* (excluding *C. mahoae*) and *Mesodasys* emerge as distinct and phylogenetically distant lineages; however, there is no consensus across the three analyses regarding which taxon may be their closest relatives. Notwithstanding, *Cephalodasys* appears to be phylogenetically closer than *Mesodasys* to most members of Cephalodasyidae (Cluster III, Figs 3–5). The Maximum Parsimony (MP) analysis shows the strongest support for a grouping that includes *Cephalodasys* and *Dactylopodola* (73%; Fig. 5). A similar close relationship between *Cephalodasys* and *Dactylopodola* is observed in the tree from Bayesian inference, although this finding has low support (Fig. 4). Conversely, the maximum likelihood (ML) analysis suggests that *Cephalodasys* is the sister taxon to a larger group that comprises *Dactylopodola*, Redudasyidae, and two genera of Cephalodasyidae: *Dolichodasys* and *Paradasys* along with *Cephalodasys mahoae* (DRDP group). Both ML and Bayesian inference approaches support the hypothesis that the cephalodasyid *Pleurodasys incomptus* is the sister taxon to the DRDP taxa.

Our analyses reveal a clear distinction for *Mesodasys* among the cephalodasyids, positioning it in a prominently derived position within Cluster II (refer to Figs 3–5). Both ML and BI analyses consistently show that *Mesodasys* shares a closer phylogenetic connection with Lepidodasyidae, Turbanellidae, and Planodayidae than with Thaumastodermatidae, Macrodasyidae, and *Urodasys*. The ML findings strongly support (92% bootstrap support) *Mesodasys* as the sister taxon to these closely related families, while the BI analysis intriguingly suggests a potential clustering between *Mesodasys* and *Lepidodasys* (0.87 PP support). This compelling evidence underscores the unique evolutionary significance of *Mesodasys* within the Macrodasyidan lineage.

Discussion

Our research has substantially expanded the available molecular data, particularly for members of the family Cephalodasyidae. Before our work, public repositories included the *18S*, *28S*, and *COI* gene sequences from vouchered specimens of only three species: *C. mahoae* (Yamauchi and Kajihara, 2018), *Mesodasys laticaudatus*, and *Mesodasys littoralis* (Remane, 1951), as detailed in Table S1. Notably, we acquired sequences for three genetic markers for species within the genera *Dolichodasys*, *Paradasys*, and *Pleurodasys*, for which only the *18S rDNA* sequence was previously accessible. This also applies to species in the genera *Thaidasys* (fam. Macrodasyidae), *Crasiella* (fam. Planodasyidae), *Anandrodasys* (fam. Redudasyidae), and *Xenodasys* (fam. Xenodasyidae). Additionally, we substantially increased the molecular information available for the family Lepidodasyidae by providing a complete set of sequences for three species of *Lepidodasys*. Finally, this study presents the first nucleotide sequences obtained for the previously elusive genus *Dendrodasys* Wilke, 1954 (fam. Dactylopodolidae). Our study sheds new light on the origin and evolutionary relationships of Macrodasyida, revealing important insights that challenge previous understandings. We conducted three cladistic analyses using maximum likelihood (ML), Bayesian inference, and Maximum Parsimony (MP) approaches, which yielded topologies that are highly congruent with one another. Most of the common groups received strong support, evidenced by bootstrap values and Bayesian posterior probabilities exceeding 75% and 0.98, respectively (Figs 3–5). Among the robustly supported monophyletic groups, we identify the remarkably uniform families Turbanellidae and Thaumastodermatidae, alongside most genera that align seamlessly with evolutionary hypotheses derived from morphological studies (e.g., Hochberg and Litvaitis, 2001; Kieneke et al., 2008a). However, one intriguing exception emerges: *Cephalodasys*. Notably, the Japanese species, *C. mahoae*, clusters with members of the genus *Paradasys*, revealing a critical discrepancy as it does not nest with its congeneric relatives. This unexpected finding suggests a likely misidentification, urging a re-evaluation of previously held classifications.

Reassignment of Cephalodasys mahoae *Yamauchi and Kajihara, 2018 to the genus* Paradasys *Remane, 1924*

During the formal description of *C. mahoae*, the authors Yamauchi and Kajihara (2018) expressed some uncertainty regarding its classification due to the striking similarity of the Japanese species to *Paradasys subterraneus* Remane, 1934. However, they ultimately based their classification decision on the results of their phylogenetic analysis, based on molecular data, which showed the new species allied with *Cephalodasys* sp. from the White Sea (Petrov et al., 2007). Additionally, *C. mahoae* features ventrolateral adhesive tubes, a characteristic previously undocumented in *Paradasys* (Hummon, 1974, 2008), but common in *Cephalodasys* (Araújo, 2024).

We would like to highlight that among Macrodasyida there are other genera that include species both presenting and lacking ventrolateral adhesive tubes (e.g., *Paraturbanella*), which casts doubts on the

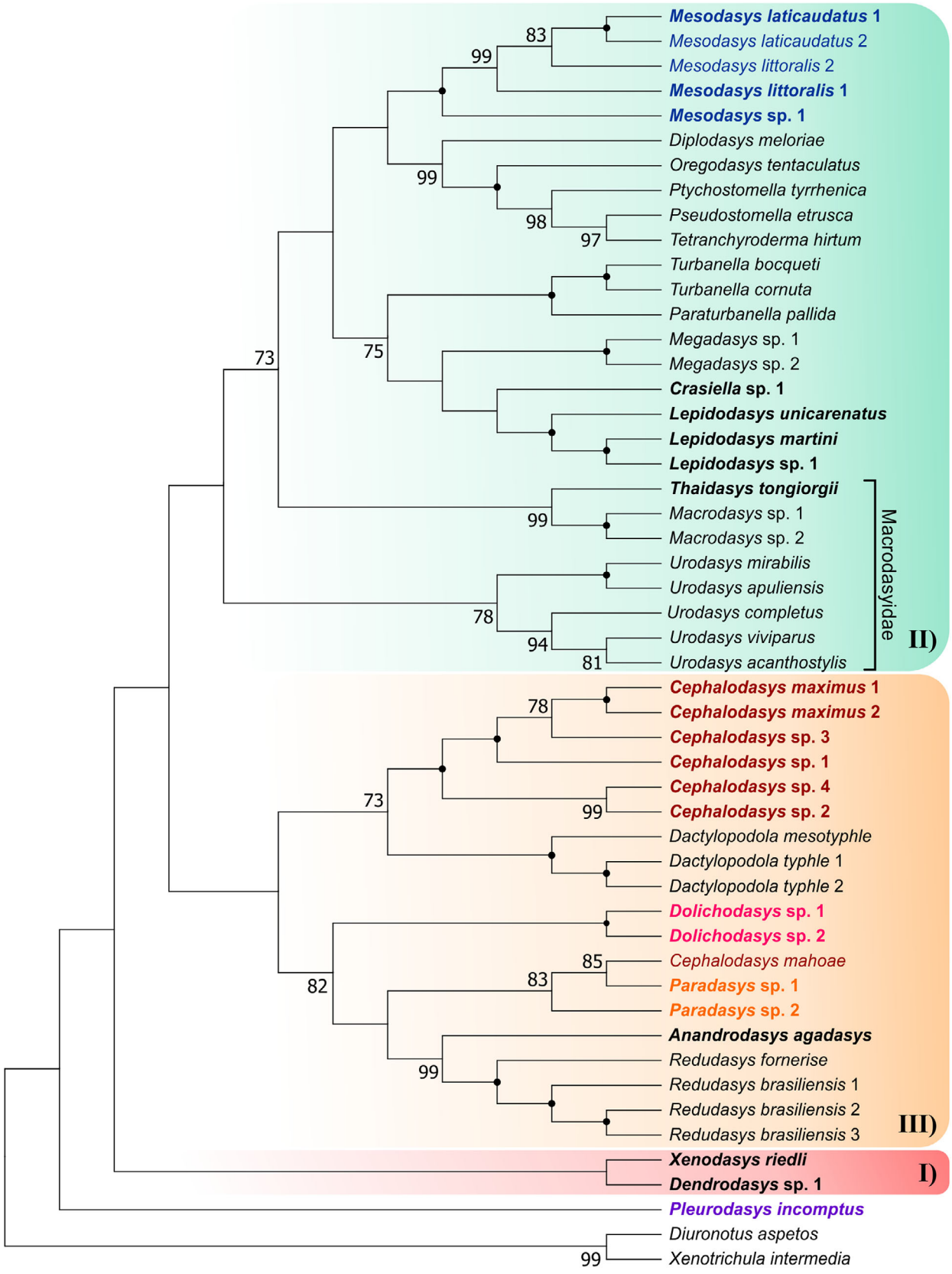

Fig. 5. Phylogenetic relationships of the order Macrodasyida inferred from Maximum Parsimony (MP) analysis of concatenated *18S*, *28S* rDNA, and *COI* mtDNA sequences. The analyses include 51 terminals, of which 49 belong to the order Macrodasyida. *Xenotrichula intermedia* (Xenotrichulidae) and *Diuronotus aspetos* (Muselliferidae) are used as the outgroup. The most parsimonious tree resulted with length = 33 390 is shown. The consistency index was (0.287742), the retention index was (0.437808), and the composite index was 0.142973 (0.125975) for all sites and parsimony-informative sites (in parentheses). In bold, taxa sequenced in this study; in colour, the Cephalodasyidae coded by genus. Bootstrap support for the clades is indicated in each node. A black dot at the node indicates full bootstrap support. Bootstrap values <70 are not reported. Macrodasyidan species appear distributed in three clusters (I, II, and III), except for *Pleurodasys incomptus*; see text for details.

usefulness of this trait for an above-species classification. The ventrolateral adhesive tubes of *C. mahoae* are very short, almost resembling small papillae, and papillae-like adhesive tubes are reported in *Dolichodasys*, whose members cluster in our analyses with *Paradasys* (Figs 3–5) indicating a potential plesiomorphy. Regarding the outcome of the phylogenetic analysis conducted by Yamauchi and Kajihara (2018), we note that in their tree, another species of *Cephalodasys, C. turbanelloides*, is positioned far from the cluster that includes *Cephalodasys* sp. and *C. mahoae*. This suggests that contamination or misidentification may affect at least some of these sequences. Problems with these sequences were noted also by Paps and Riutort (2012). Despite the original decision, the classification of *C. mahoae* has remained contentious because several characteristics distinguish it from other *Cephalodasys* species. Most notably, *C. mahoae* features a broadly triangular anterior region, with lateral lobes, instead of the round shape defined by a constriction typical of the genus *Cephalodasys*. Furthermore, the oocyte development in the Japanese species follows a caudocephalic pattern, similar to *Paradasys hexadactylus* Karling, 1954, *P. littoralis* Rao and Ganapati, 1968, and *P. subterraneus* Remane, 1934. By contrast, *Cephalodasys* species exhibit frontocaudal maturation of oocytes (Fig. 6). Based on our molecular analyses and the morphological traits mentioned, we propose formally transferring *C. mahoae* to the genus *Paradasys*. Below, we present a revision of the diagnostic characters for *Paradasys*, now including the presence of lateral adhesive tubes.

Monophyly of Thaumastodermatidae, Turbanellidae, Redudasyidae, and Planodasyidae

The families Thaumastodermatidae and Turbanellidae were consistently found to be monophyletic across all tree analyses (Figs 3–5). This finding aligns with traditional classifications based on morphological characteristics, which have also received support from early molecular phylogenetic studies (e.g., Kieneke et al., 2008a; Todaro et al., 2011; Kieneke and Todaro, 2021). Our study also provides full support for the current family Redudasyidae, established more recently on molecular data, as well as on the re-evaluation of the morphological characteristics of its members (*Redudasys* and *Anandrodasys*; Todaro et al., 2012). These results, combined with the monophyly of all analysed genera, strengthen our findings and suggest that other phylogenetic hypotheses, when statistically supported, are highly likely to be accurate.

Planodasyidae was recognized as monophyletic by both the ML and BI analyses (Figs 3 and 4), receiving high to full support. However, the MP analysis indicated that Planodasyidae may be paraphyletic due to the position of *Lepidodasys*. Nevertheless, the relatively low support at the *Crasiella* + *Lepidodasys* node (Fig. 5) does not rule out Planodasyidae as a monophyletic group. The reproductive system and the ultrastructure of spermatozoa provide evidence for a close phylogenetic relationship between *Megadasys* and *Crasiella* (Guidi et al., 2014) reinforcing the classification of Planodasyidae as a natural group, as resolved by previous phylogenetic analyses based on molecular information (e.g., Todaro et al., 2012). We consider Planodasyidae to be monophyletic and attribute the MP result to the limited number of terminals included in our analysis, as well as to the high levels of divergence in our molecular dataset, an aspect which is known to negatively affect the results of this approach (Bergsten, 2005). Future studies that include additional species, particularly within the genus *Crasiella*, should further support this hypothesis.

Phylogenetic status of Dactylopodolidae

Our study consistently found that the current families Cephalodasyidae, Dactylopodolidae, and Macrodasyidae are artificial, meaning they are non-monophyletic (see Figs 3–5). Specifically, Dactylopodolidae appears to be polyphyletic, with *Dendrodasys* sp. branching early along the Macrodasyida evolutionary tree and *Dactylopodola* included in the more derived Cluster III. Currently, Dactylopodolidae includes three genera: the traditional *Dactylopodola* (type genus) and *Dendrodasys*, along with the monotypic genus *Dendropodola*, which was added later by Hummon et al. (1993). Cladistic analyses based on morphology have found this family to be monophyletic, with *Dactylopodola* frequently resolved as the earliest macrodasyidan branch (Hochberg and Litvaitis, 2001; Kieneke et al., 2008b). However, these morphological hypotheses have never been tested by molecular studies, as previous research

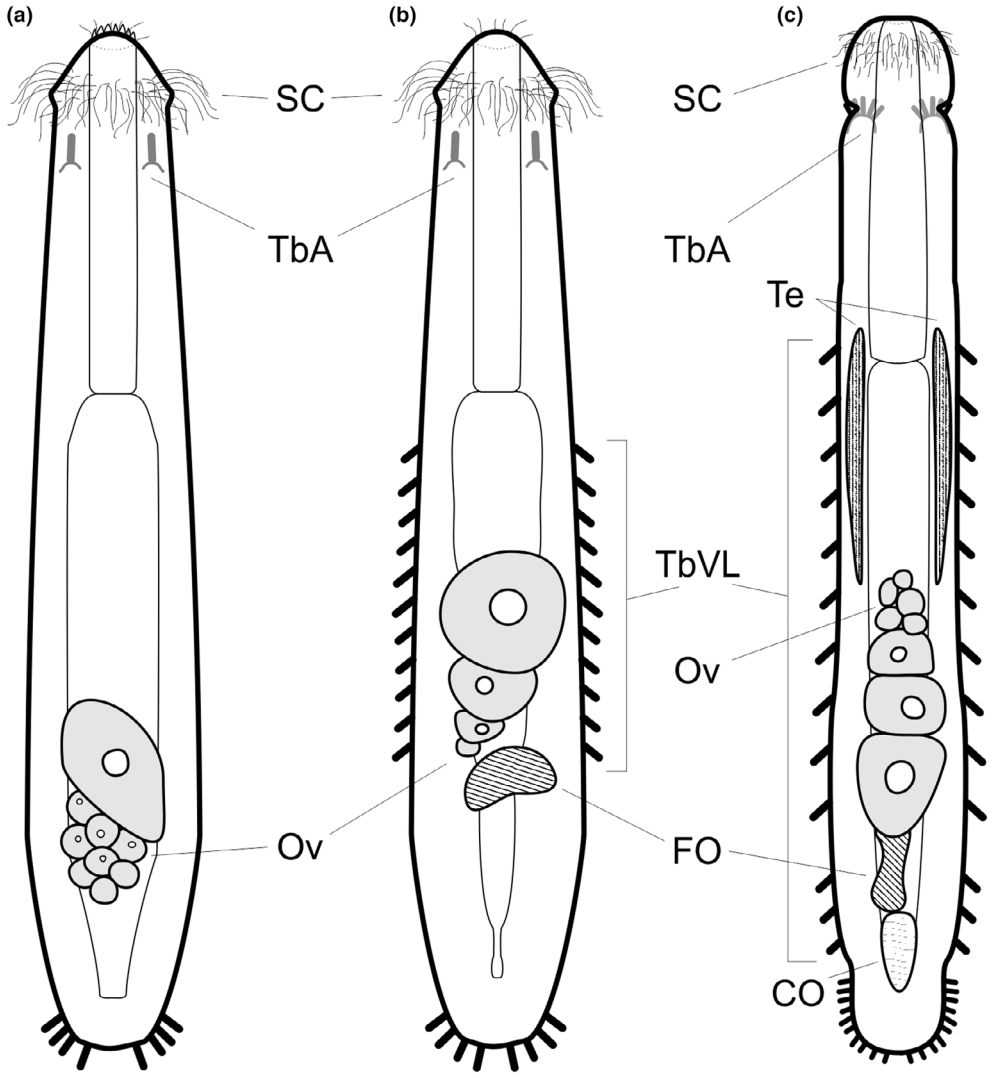

Fig. 6. Line drawings comparing some anatomical traits of *Paradasys subterraneus* (a), *Cephalodasys mahoae* (b), and *Cephalodasys maximus* (c), combined dorsal and internal view. Anterior adhesive tubules shown in transparency. Note the direction of oocyte maturation in the ovary, which is caudocephalic in a, b, and frontocaudal in c. CO, caudal organ; FO, frontal organ; Ov, ovaries with developing oocytes; SC, sensory cilia; TbA, anterior adhesive tubes; TbVL, ventrolateral adhesive tubes; Te, testes. (a) Redrawn from Remane (1934); (b) Redrawn from Yamauchi and Kajihara (2018); (c) Redrawn from Remane (1926).

has examined only *Dactylopodola* species. In our opinion, the available morphological information is insufficient to support Dactylopodolidae as an unquestionable monophylum. The cosmopolitan genus *Dactylopodola* includes 12 recognized species. The general morphology and ultrastructure of some of its members are relatively well understood, although traits of the reproductive apparatus and reproductive modality remain contentious (see Ruppert, 1991 vs. Kieneke et al., 2008b). *Dendrodasys* currently consists of six species that are only known at the level of gross anatomy. The general morphology of *Dendrodasys*, characterized by a distinct head, a caudal peduncle, and cross-striated muscles suggests it is closer to *Dactylopodola* (Kieneke and Schmidt-Rhaesa, 2014). However, differences in their reproductive systems and the distinct appearance of spermatozoa at the light microscopy level raise doubts about the close phylogenetic relationship between these two genera (see Hummon et al., 1998; Kieneke et al., 2008b; Hummon, 2011). *Dendropodola* is poorly known; its only representative, *D. transitionalis* Hummon, Todaro and Tongiorgi, 1993, has been found only once and was described based on a single subadult specimen that exhibited a general appearance intermediate between *Dactylopodola* and *Dendrodasys* (Hummon et al., 1993). All the above underscores the need for a more thorough examination of the phylogenetic status of Dactylopodolidae. In the absence of

consistent, strong support for separating *Dendrodasys* from *Dactylopodola*, we prefer to provisionally maintain the current classification unchanged.

Polyphyly of Macrodasyidae, reassignment of Urodasys *Remane, 1926 to Urodasyidae fam. nov. and establishment of* Paraurodasys *gen. nov.*

Our findings suggest that the Macrodasyidae family is polyphyletic. The early branch of *Urodasys* is positioned as the sister taxon to a significant clade that encompasses other Macrodasyidae (OM) members (specifically *Macrodasys* sp.1 and sp.2, and *Thaidasys*), along with representatives from four additional families: Lepidodasyidae, Planodasyidae, Thaumastodermatidae, and Turbanellidae, as well as species from the genus *Mesodasys* (LPTTM group). The relationship between *Urodasys* and the clade formed by OM + LPTTM taxa (in Cluster II) received robust statistical support from both the ML (98%) and BI (100%) analyses, along with nearly 60% support from the MP approach (see Figs 3–5). Given the very high statistical support for the OM clade and the strong evidence for its sister–taxon relationship with the LPTTM taxa, the hypothesis that *Urodasys* represents a phyletic lineage independent from the other members of Macrodasyidae (and any other Macrodasyida) is highly plausible.

From a morphological perspective, members of *Urodasys* are characterized by several autapomorphic traits, including an extremely long tail, a blind intestine, and spermatozoa that lack mitochondria (Balsamo et al., 2007; Kieneke and Schmidt-Rhaesa, 2014). These distinctive traits, along with the well-supported molecular phylogenetic placement of *Urodasys* representatives in our analyses, justify the establishment of a new family. Therefore, we reclassify *Urodasys* from Macrodasyidae to the newly established family Urodasyidae fam. nov. Below, we provide a diagnosis for this new family as well as a revised diagnosis of Macrodasyidae.

The genus *Urodasys* is notable for its remarkable diversity in reproductive structures and strategies among its members. Currently, 17 species have been described, which exhibit five distinct combinations of reproductive methods and structures. This variety includes the only known parthenogenetic and ovoviviparous gastrotrich, several species that possess a copulatory organ equipped with a sclerotized stylet, and other species that have sperm but lack a copulatory organ (Atherton and Hochberg, 2014; Todaro et al., 2019a; Cesaretti et al., 2024). A recent phylogenetic analysis, based on molecular markers, suggested that *Urodasys* species may be divided into two subclades: one consisting of hermaphroditic species that lack a copulatory organ, and the other including species that have a copulatory organ with a sclerotized stylet, as well as species that reproduce via parthenogenesis (Cesaretti et al., 2024). A similar scenario had been reached previously by work conducted on morphological data (Todaro et al., 2019a). In the current study, we analysed a subset of the data from Cesaretti et alii in a more comprehensive taxonomic framework and using a different outgroup. Our results corroborate previous findings, indicating that hermaphroditic species lacking a copulatory organ, specifically *U. apulensis* and *U. mirabilis*, form a distinct clade. In contrast, species that possess a copulatory organ with a sclerotized stylet, namely, *U. acanthostylis* and *U. completus*, as well as the parthenogenetic species *U. viviparus*, belong to a separate clade (Figs 3–5). To better reflect the differing evolutionary patterns in the reproductive systems of these organisms within a Linnaean classification framework, we suggest to separate the current *Urodasys* species into two distinct genera. We propose the establishment of a new genus, *Paraurodasys* gen. nov., to group the species with a sclerotized stylet and those that reproduce by parthenogenesis, while the type species *U. mirabilis* and others that share similar lay-out of the reproductive system are to be maintained in *Urodasys*. Below, we provide a diagnosis for the new genus along with an amended diagnosis for *Urodasys*. *P. viviparus* is chosen as the type species for *Paraurodasys* gen. nov. in accordance with the principle of priority (article 23 of the International Code of Zoological Nomenclature).

Polyphyly of Cephalodasyidae, with reassignment of Mesodasys *to Mesodasyidae fam. nov. and reassignment of* Dolichodasys *Gagne, 1977 and* Paradasys *Remane, 1934 to the family Redudasyidae*

As suggested by previous phylogenetic analyses, the Cephalodasyidae family appears to be polyphyletic in our study as well. The genera currently affiliated with this family are scattered throughout the Macrodasyida phylogenetic tree (see Figs 3–5). In the Results, we previously discussed *Mesodasys*, which seems to be the most phylogenetically distant taxon among the current members of Cephalodasyidae, indicated by its placement in Cluster II (Figs 3–5). In all our analyses, the clade formed by *Mesodasys* species consistently appears distinct from the other members of the LPTTM cluster, although there is no consensus on what its sister taxon might be. Regardless, our findings do not support the inclusion of *Mesodasys* in any of the currently recognized families represented in the cluster. Moreover, the general morphological characteristics of the *Mesodasys* species, along with the structure of their reproductive system, where the vas deferens are directly connected to the copulatory organ, coupled with the unique feature of hypodermic

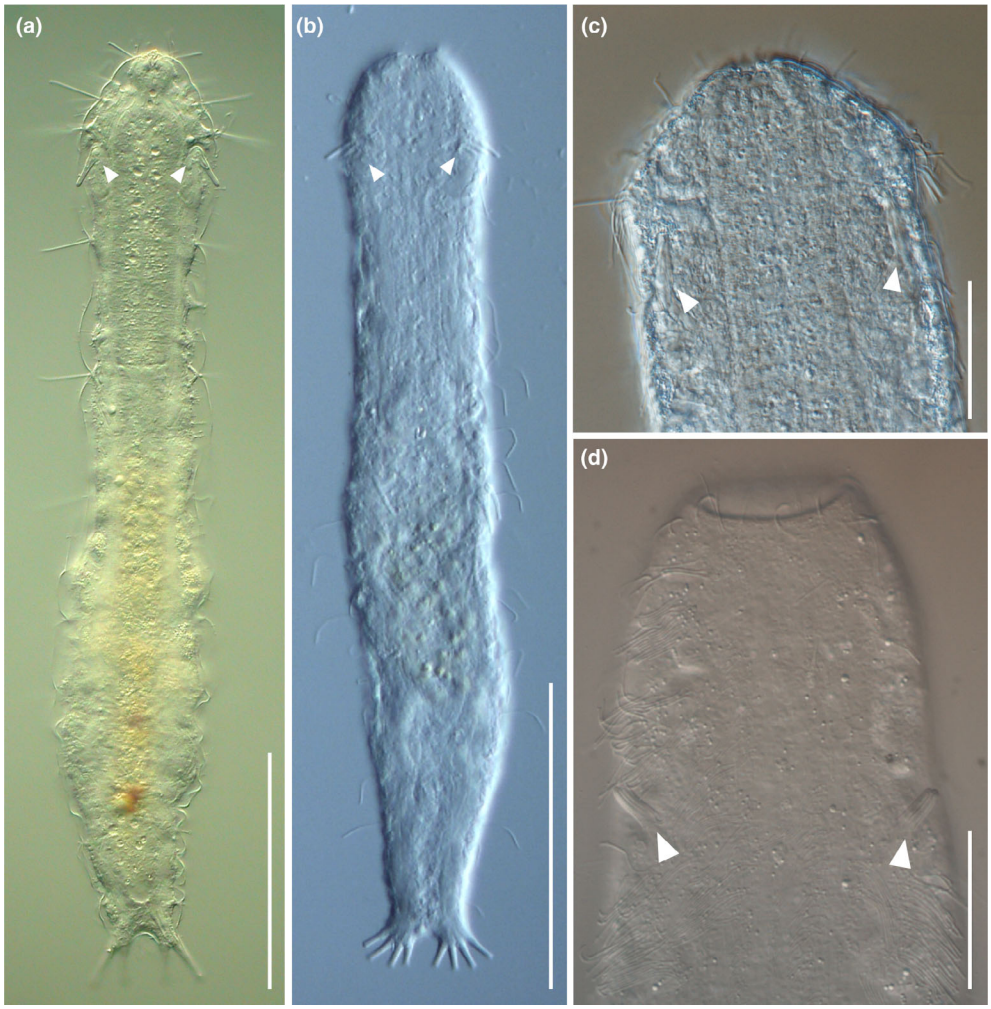

Fig. 7. Light micrographs of representatives of the genera in the emended family Redudasyidae, ventral view showing the anterior adhesive tubes (arrowheads). (a) *Redudasys fornerise*; (b) *Anandrodasys agadasys*. (c) *Paradasys* sp. 1, anterior region; (d) *Dolichodasys* sp. 2, anterior region. Differential interference contrast microscopy (Nomarski), scale bar a, b = 100 μm; c, d = 30 μm.

insemination (known to occur in some species, possibly applicable to all) (e.g., Ruppert, 1991; Ferraguti and Balsamo, 1995; Fregni et al., 1999), suggest that these traits are unlikely to be among the synapomorphic characteristics that differentiate members of the distinct families Lepidodasyidae, Planodasyidae, Thaumastodermatidae, and Turbanellidae (Guidi et al., 2004; Hummon and Todaro, 2010; Todaro et al., 2011; Campos et al., 2025). Given these reasons, we propose assigning the genus *Mesodasys* to a newly established monogeneric family, Mesodasyidae fam. nov. Below, we provide a detailed diagnosis for this family.

In contrast to *Mesodasys*, the other cephalodasyid genera are all resolved in cluster III (see Figs 3–5). The genera *Dolichodasys* and *Paradasys* appear to be closely related, while *Cephalodasys* and *Pleurodasys* are identified as distinct lineages. Specifically, *Dolichodasys* is positioned as a sister group to a branch formed by *Paradasys* (which encompasses *C. mahoae*) and the family Redudasyidae (comprising *Redudasys* and *Anandrodasys*). While the relationship *Dolichodasys* + *Paradasys* + Redudasyidae is consistently and highly supported across all three analyses (refer to Figs 3–5), the close phylogenetic alliance of *Paradasys* with Redudasyidae received weak statistical support.

We may note a trend in *Dolichodasys*, *Paradasys*, and Redudasyidae gastrotrichs towards the reduction of certain traits shared with other taxa in cluster III. For example, all gastrotrichs in cluster III bear the anterior adhesive tubes arranged in two bilateral groups. In species, such as *Dolichodasys*, *Paradasys*, and Redudasyidae, these tubes are limited to one or, at most, three per side (Fig. 7). This trend of reduction also applies to the ventrolateral tubes, which are either

absent in members of *Redudasys* and most *Paradasys* or very short, resembling a papilla-like structure in *Dolichodasys* and *C. mahoae* (= *P. mahoae*, as discussed in the present study). An exception to this trend is *Anandrodasys agadasys*, which possesses ventrolateral adhesive tubes, albeit reduced to 3–4 per side (e.g., Kieneke et al., 2013). An evolutionary trend towards reduction is also evident in the male reproductive system. The full suite of male features, including testes, sperm, and a copulatory/caudal organ, is only observed in *Dolichodasys* (Ruppert and Shaw, 1978), while the other taxa lack male features entirely. The possible exception is *C. mahoae* (= *P. mahoae*), which has been reported to contain spermatozoa in the frontal organ (Yamauchi and Kajihara, 2018). However, the nature of the sperm in this Japanese species, as seen under light microscopy, requires confirmation through ultrastructural studies, especially since their thread-like appearance differs from the pod-like shape of the tailless spermatozoa observed in *Dolichodasys* (Guidi et al., 2017). The results of our phylogenetic analyses, along with the morphological evidence presented above, indicate that *Dolichodasys* and *Paradasys* should no longer be classified as part of the family Cephalodasyidae. Instead, we suggest that they be included in the family Redudasyidae, which may be accomplished by slightly expanding the morphological criteria for this taxon. Consequently, we propose this reclassification and provide an updated diagnosis of the Redudasyidae in the section below.

In our analyses, the well-sampled genus *Cephalodasys* (excluding *C. mahoae*) is recognized as a distinct lineage. Although it is phylogenetically closer to most members of the current family Cephalodasyidae than to *Mesodasys* (see Cluster III, Figs 3–5), there is no consensus among the three analyses regarding which taxon is the closest relative of *Cephalodasys*. The Maximum Parsimony analysis provides the highest support, among all analyses conducted, for a grouping that includes *Cephalodasys* and *Dactylopodola*, though the support value remains moderate (73%; see Fig. 5). A close relationship between *Cephalodasys* and *Dactylopodola* is also observed in the Bayesian inference tree, although this finding has low support (Fig. 4). From a morphological standpoint, *Cephalodasys* and *Dactylopodola* appear quite different. For instance, species of *Cephalodasys* are larger and worm-like, while those of *Dactylopodola* are smaller and tenpin-shaped. The posterior end of *Cephalodasys* members is unilobed, while that of *Dactylopodola* is bilobed. Other differences exist in the organization of the reproductive system and the ultrastructure of the spermatozoon (Kieneke and Schmidt-Rhaesa, 2014). Given the lack of consensus in our phylogenetic investigation and the morphological differences, we can conclude that *Cephalodasys* and *Dactylopodola* represent two distinct evolutionary lineages, justifying their classification in two separate families within the Linnaean context.

Concerning *Pleurodasys*, the last genus currently linked to the Cephalodasyidae, our analyses reveal that the species involved in the investigation (*P. incomptus*) represents an early evolutionary branch within the order Macrodasyida. In the ML and BI trees, it is positioned as a sister taxon to the other species in cluster III. In the MP tree, it even ranks as the sister taxon of all remaining Macrodasyida (Figs 3–5). However, none of the relevant nodes received sufficient statistical support to confidently endorse one hypothesis over another. Considering the morphological similarities shared with *Cephalodasys*, such as the distinctly separated anterior region of the head from the rest of the body, the number and arrangement of the anterior adhesive tubules, and the unilobed posterior extremity, it seems reasonable to provisionally retain *Pleurodasys* within the Cephalodasyidae. Below, we propose an amended diagnosis for the Cephalodasyidae family that incorporates traits from the genera *Cephalodasys* and *Pleurodasys*.

Conclusions

Following the reclassification of *Paradasys mahoae* comb. nov., the transfer of *Dolichodasys* and *Paradasys* to Redudasyidae and of *Mesodasys* to Mesodasyidae fam. nov., the family Cephalodasyidae now includes two genera and 16 nominal species; the family Macrodasyidae, after the transfer of *Urodasys* to Urodasyidae fam. nov., now includes three genera and 40 nominal species. Consequently, the updated order Macrodasyida includes 12 families and 38 genera.

Our results once again demonstrate that the phylogeny of Macrodasyidan gastrotrichs often deviates from the conclusions suggested so far by morphological data alone. In addition to confirming the polyphyly of the Cephalodasyidae and Macrodasyidae and finding new relationships for their former members, the multigene analysis provided new insights on the deeper phylogeny of the order Macrodasyida.

This study highlights the importance of integrating molecular data, especially through multigene sequencing when feasible, into species descriptions to enhance our understanding of their evolutionary histories. Focused efforts should be made to better describe and sequence those taxa whose position is still questionable, such as *C. miniceraus* Hummon, 1974 and *C. hadrosomus* Hummon, Todaro and Tongiorgi, 1993 in genus *Cephalodasys* (Araújo, 2024) and *P. lineatus* Rao, 1980 in genus *Paradasys*, to verify and eventually update their classification. This would both strengthen the diagnosis of each taxon, hopefully reducing the number of "systematic wastebaskets" in the phylum,

and enhance the taxonomic sampling in future molecular studies on the evolution of gastrotrichs.

Including additional species from the genera *Dendrodasys* and *Pleurodasys* in the analysis could provide better insights into the phylogenetic status of the Dactylopolidae and enhance our understanding of the origin and early evolution of Macrodasyidan Gastrotricha. Several previous reconstructions of the stem species of Gastrotricha have been based on the assumption that either the genus *Dactylopodola* or *Cephalodasys* is the sister taxon to the rest of the order Macrodasyida (Kieneke and Schmidt-Rhaesa, 2014). However, molecular data now challenge this assumption. Including a complete set of three genes from *Hummondasys jamaicensis* (Hummondasyidae) in the analysis could help clarify the origin and cause of the rare male reproductive system configuration in this species, characterized by the confluence of the vas deferens in the caudal organ. A similar configuration is also found in *Mesodasys* and in Thaumastodermatinae. However, it remains unresolved whether this similarity is due to convergent evolution, parallel evolution, or evolutionary reversals.

While the findings outlined in this article do not resolve all outstanding questions, they illuminate several critical gaps in our understanding of Macrodasyida evolution. More importantly, they lay a solid groundwork for future research endeavours. To advance our knowledge, it is essential that upcoming studies enhance molecular and taxonomic sampling in phylogenetic analyses. Additionally, there is a pressing need to delve deeper into the fascinating traits of these organisms, particularly their reproductive biology and ecological roles. Despite their diminutive size, these remarkable creatures demonstrate astonishing diversity, offering a wealth of unexplored avenues for investigation. Embracing these opportunities could significantly enrich our understanding of this unique group.

Diagnoses

Order Macrodasyida Remane, 1925 [Rao and Clausen, 1970]

Family Cephalodasyidae Hummon and Todaro, 2010

Emended diagnosis: Elongate Macrodasyidans up to 1800 μm in total length. Body strap-shaped, flattened ventrally and vaulted dorsally; head rounded, marked by a posterior constriction; head sensorial structures in the form of circumcephalic cilia; posterior end rounded, broadly expanded or tapering into a medial process. Cuticular covering smooth, without scales or spines; epidermal glands often present. Anterior adhesive tubes (TbA) in two groups, inserting on fleshy "hands"; dorsolateral, lateral, and ventrolateral adhesive tubes (TbDL/TbL/TbVL) arranged in columns along the body; posterior adhesive tubes (TbP) arranged marginally around the posterior end. Ventral ciliation split into two paired longitudinal bands along the body, reuniting caudally. Mouth, terminal or slightly subterminal, narrow; buccal cavity broadly cylindrical, lightly cuticularized. Sphincter muscle developed around the mouth opening; well-developed striated radial pharyngeal musculature. Circular muscles present in lateral regions of the body. Y-cells absent. Pharynx bearing pores at the base, opening ventrolaterally; broad anterior intestine, narrowing caudally; anus ventral. Hermaphroditic; ovary single, central, oocytes maturing posterior to anterior (*Pleurodasys*) or anterior to posterior (*Cephalodasys*). Testes paired, male gametes mature posterior to anterior. Frontal organ usually present; caudal organ occasionally present in *Cephalodasys*, absent in *Pleurodasys*. Interstitial, marine. Included genera: *Cephalodasys* Remane, 1926 (type genus); *Pleurodasys* Remane, 1927.

Family Macrodasyidae Remane, 1924

Emended diagnosis: Elongate macrodasyidans up to 1000 μm in total length. Body strap-shaped, elongated; head bluntly rounded or ovoid, sometimes marked by a posterior constriction (*Kryptodasys*, *Thaidasys*); head sensorial structures in the form of circumcephalic cilia and pestle organs, or leaf-like organs (*Thaidasys*); posterior end ovoidal or tapering, sometimes in the form of a short tail (*Macrodasys*). Cuticular covering smooth, without scales or spines; epidermal glands either inconspicuous or visible (*Thaidasys*). TbA 2–7 per side, inserted directly on the body surface in diagonal columns or short arcs; TbD/TbDL sometimes present; TbL/TbVL arranged in columns along the body; TbP arranged marginally around the posterior end or along the tail. Ventral ciliation either split into two paired longitudinal bands along the body (*Thaidasys*), or forming a single field that can split into two paired longitudinal bands along the caudal region. Mouth, terminal, medium size; buccal cavity lightly cuticularized, shallow. Pharynx bearing pores significantly anterior to the pharyngo-intestinal junction, opening ventrolaterally; intestine straight, sometimes broader in the middle section (*Kryptodasys*); anus ventral. Hermaphroditic; ovary single, oocytes maturing posterior to anterior. Testes paired, elongated, starting near the pharyngo-intestinal junction, or absent (*Thaidasys*). Frontal organ, present or absent (*Thaidasys*); caudal organ is present as a muscular organ containing a copulatory tube or a canal. Interstitial, marine. Included genera: *Macrodasys* Remane, 1924 (type genus); *Kryptodasys* Todaro, Dal Zotto, Kånneby and Hochberg, 2019; *Thaidasys* Todaro, Dal Zotto and Leasi, 2015.

Family Mesodasyidae fam. nov.

LSID: urn:lsid:zoobank.org:act:53A43C3C-92C2-446D-8CD9-BECC3F9172B6

Diagnosis: Macrodasyidans up to 2000 μm in total length. Body strap-shaped, elongated; head bluntly rounded or truncated, unmarked from the body; head sensorial structures in the form of circumcephalic cilia; posterior end rounded, tapering, or ending in a rounded caudal lobe. Cuticular covering smooth, without scales or spines; numerous epidermal glands are visible for the whole length of the body, in lateral columns. TbA numerous, inserted directly on the body surface in transverse rows, diagonal columns, or a single uninterrupted arc following the anterior profile; TbD numerous when present; TbL numerous; TbVL numerous when present; TbP numerous, inserted on the caudal margin of the body or on a caudal plate. Ventral ciliation split into two paired longitudinal bands running for the whole length of the body, either reuniting in the cephalic and caudal regions or forming a continuous field covering the pharyngeal region (*M. adenotubulatus*, *M. ischiensis*). Mouth, terminal, opening medium to large; buccal cavity lightly cuticularized, presenting an external hyaline protrusion in *M. ischiensis*. Pharynx bearing pores at the base, opening ventrolaterally; broad anterior intestine, narrowing caudally; anus ventral. Hermaphroditic; ovaries paired; oocytes mature in the caudocephalic direction. Testes elongated, paired, starting near the pharynx-intestine junction; posteriorly directed vas deferens, discharging directly into the caudal organ. Frontal organ absent; fertilization likely happens through hypodermic impregnation. Interstitial, marine. Included genus: *Mesodasys* Remane, 1951 (type genus).

Family Redudasyidae Todaro, Dal Zotto, Jondelius, Hochberg, Hummon, Kanneby and Rocha, 2012

Emended diagnosis: Macrodasyidans up to about 1000 μm in total length, occasionally reaching up to 2700 μm (*Dolichodasys*). Body strap-shaped; head rounded or bluntly triangular; head sensorial structures in the form of several circumcephalic cilia; posterior end rounded, truncated, or two-lobed, without peduncles. Cuticular covering smooth, without scales or spines. TbA, 1–3 per side: either 1–2 tubes per side, occasionally fused, inserted on short lobes, protruding to the head (*Dolichodasys*, *Paradasys*), or 2–3 tubes of unequal length per side, fused, borne from a common base and emerging from a ventrolateral furrow (*Redudasys*), or inserted in parallel (*Anandrodasys*), protruding obliquely to the rear; TbD absent; TbL/TbVL absent or present, sometimes in the form of short adhesive papillae (*Dolichodasys, P. mahoae*); TbP, present, distributed symmetrically along the caudal margin, or along the caudal lobes; Ventral ciliation split into two paired longitudinal bands along the body, reuniting in an unpaired patch or row caudal to the anus (*Paradasys*, *Redudasys*), or forming a unified field, posterior to the mouth, split in the trunk region into four longitudinal bands, with the two medial bands running along the pharyngeal region and the two lateral bands extending to the caudal region (*Anandrodasys*, *Dolichodasys*). Mouth, terminal or slightly subterminal, narrow; buccal cavity, shallow, lightly cuticularized, sometimes presenting external denticles (*Paradasys*). Pharynx bearing pores at base, opening ventrolaterally. Intestine straight; anus ventral. Ovaries in the hindgut region, paired or central unpaired, with oocytes maturing anteriorly or posteriorly (*Dolichodasys*); male gonad absent in *Anandrodasys*, *Redudasys*, *and* most *Paradasys* species; paired testes in *Dolichodasys*. Frontal organ present in *Dolichodasys*, and occasionally in *Paradasys*, absent in *Anandrodasys* and *Redudasys*; caudal organ present in *Dolichodasys*, absent in *Anandrodasys*, *Paradasys*, and *Redudasys*. Interstitial, marine, or freshwater. Included genera: *Redudasys* Kisielewski, 1987 (type genus); *Anandrodasys* Todaro, Dal Zotto, Jondelius, Hochberg, Hummon, Kånneby and Rocha, 2012; *Dolichodasys* Gagne, 1977; *Paradasys* Remane, 1934.

Genus *Paradasys* Remane, 1934

Emended diagnosis: Macrodasyidans up to 1000 μm in total length. Body strap-shaped; head weakly marked, bluntly trapezoidal, often bearing shallow lateral lobes; head sensorial structures in the form of circumcephalic cilia; posterior end truncated or two-lobed (*P. bilobocaudatus, P. pacificus*), without peduncles. Cuticular covering smooth, without scales or spines, often presenting a granular appearance. TbA 1–2 per side, inserted directly on the ventral body surface or on short lobes; TbD, TbDL, and TbL absent; TbVL absent or short, along the anterior trunk region (*P. mahoae*); TbP from 6 to many, located symmetrically on lateral and posterior borders of the posterior end, separated into groups on either side of the midline, or on lobes. Ventral ciliation split into two paired longitudinal bands along the body, reuniting in an unpaired patch or row caudal to the anus. Mouth, terminal or slightly subterminal, narrow; buccal cavity broadly cylindrical, cuticularized, sometimes presenting external denticles. Pharynx bearing pores at the base, opening ventrolaterally; broad anterior intestine, narrowing caudally; anus ventral. Parthenogenetic or hermaphroditic; ovary single or paired (*P. pacificus*) in the hindgut region; oocytes mature anteriorly. Testes absent in most species; paired testes in *P. lineatus* and *P. littoralis*. Frontal organ, when present, in a caudal position to the oocytes. Interstitial, marine. Included species: *P. subterraneus* Remane, 1934 (type species); *P. bilobocaudus* Hummon, 2008; *P. hexadactylus* Karling, 1954; *P. lineatus* Rao, 1980; *P. littoralis* Rao and Ganapati, 1968; *P. mahoae* (Yamauchi and Kajihara, 2018), comb. nov.; *P. pacificus* Schmidt, 1974.

Family Urodasyidae fam. nov.

LSID: urn:lsid:zoobank.org:act:42199BA2-50BD-4266-BC52-D17775FC177E

Diagnosis: Elongate Macrodasyidans, body strap-shaped, vaulted dorsally and flattened ventrally; head bluntly rounded or oval, weakly marked or not marked from the body; head sensorial structures in the form of circumcephalic cilia, occasionally along with paired piston pits (*Paraurodasys*); the posterior margin ends in a long, filiform, contractile tail, up to three times the length of the body. Cuticular covering smooth, without scales or spines; numerous epidermal glands visible on the whole length of the body, in lateral columns. TbA inserted directly on body surface, in paired diagonal columns or small clusters, sometimes absent (*U. anorektoxys*); TbD/TbDL often present; TbL occurring both in the pharyngeal and trunk region; TbV/TbVL occasionally present; TbP numerous, inserted on the whole length of the tail. Ventral ciliation forms a united field in the pharyngeal region, either continuing uninterrupted for the length of the body (*Urodasys*) or splitting into two paired bands in the trunk region. Mouth, terminal, narrow; buccal cavity shallow, lightly cuticularized. Pharynx bearing pores in the last third, opening ventrolaterally; intestine simple and blind. Hermaphroditic or parthenogenetic; ovaries paired; oocytes mature in the caudocephalic direction; ovoviviparity present in *P. viviparus*. Testes, paired, unpaired, or absent; when present, either elongated, starting near the pharynx-intestine junction, or short, starting near the caudal region of the intestine; posteriorly directed vas deferens, discharging into a ventral pore. Frontal and caudal organs, present or absent. Interstitial, marine.

Interstitial, marine. Included genera: *Urodasys* Remane, 1926 (type genus); *Paraurodasys*, gen. nov.

Genus Paraurodasys gen. nov.

LSID: urn:lsid:zoobank.org:act:ADBCEEB7-CCFC-49BD-BCD0-088AAF00E3CE

Etymology: *Paraurodasys* from the union of "para", meaning "near to", plus *Urodasys*, as this new genus is the sister taxon of the established genus *Urodasys* and they share the iconic long tail.

Diagnosis: Macrodasyidans up to about 650 μm in total body length, tail excluded. Body strap-shaped, vaulted dorsally and flattened ventrally; head bluntly rounded or oval, weakly marked or not marked from the body; head sensorial structures in the form of circumcephalic cilia and occasionally paired piston pits; lateral trunk margins can present indentations (*P. bifidostylis, P. poculostylis*); posterior margin ends in a long, filiform, contractile tail, up to three times the length of the body. Cuticular covering smooth, without scales or spines; numerous epidermal glands visible on the whole length of the body, in lateral columns. TbA 3–10 per side, inserted directly on the body surface, in paired diagonal columns or small clusters; TbD/TbDL often present; TbL numerous, occurring both in the pharyngeal and trunk regions; TbV/TbVL occasionally present; TbP numerous, inserted on the whole length of the tail. Ventral ciliation forms a united field in the pharyngeal region, splitting into two paired bands in the trunk region. Mouth, terminal, narrow; buccal cavity shallow, lightly cuticularized. Pharynx bearing pores in the last third, opening ventrolaterally; intestine simple and blind. Hermaphroditic or parthenogenetic (*P. bucinastylis*, *P. viviparus*); ovaries paired; oocytes mature in a caudocephalic direction; ovoviviparity present in *U. viviparus*. Testes paired (*P. completus*) or unpaired, occasionally absent (*P. bucinastylis*, *P. viviparus*); when present, elongated, starting near the pharynx-intestine junction; posteriorly directed vas deferens, discharging into a ventral pore. Frontal organ, present or absent; when present, posterior to the intestine, muscularized, sac-like; one external pore, opening dorsally. Caudal organ, when present, a muscular organ containing a sclerotized copulatory stylet with species-specific conformation, and presenting one external pore, opening ventrally; absent in *P. viviparus*. Interstitial, marine. Included species: *Paraurodasys viviparus* (Wilke, 1954) comb. nov. (type species); *P. acanthostylis* (Fregni, Tongiorgi and Faienza, 1998) comb. nov.; *P. bifidostylis* (Cesaretti et al., 2023) comb. nov.; *P. bucinastylis* (Fregni, Faienza, Grimaldi, Tongiorgi and Balsamo, 1999) comb. nov.; *P. calicostylis* (Schoepfer-Sterrer, 1974) comb. nov.; *P. completus* (Todaro, Cesaretti and Dal Zotto, 2017) comb. nov.; *P. cornustylis* (Schoepfer-Sterrer, 1974) comb. nov.; *P. nodostylis* (Schoepfer-Sterrer, 1974) comb. nov.; *P. poculostylis* (Atherton, 2014) comb. nov.; *P. remostylis* (Schoepfer-Sterrer, 1974) comb. nov.; *P. spirostylis* (Schoepfer-Sterrer, 1974) comb. nov.; *P. toxostylus* (Hummon, 2011) comb. nov.; *P. uncinostylis* (Fregni, Tongiorgi and Faienza, 1998) comb. nov.

Genus *Urodasys* Remane, 1926

Emended diagnosis: Macrodasyidans up to about 1100 μm in total body length, tail excluded. Body strap-shaped, vaulted dorsally and flattened ventrally; head bluntly rounded or oval, weakly marked or not marked from the body; head sensorial structures in form of circumcephalic cilia; posterior margin ends in a long, filiform, contractile tail, up to three times the length of the body. Cuticular covering smooth, without scales or spines; numerous epidermal glands visible on the whole length of the body, in lateral columns. TbA 4–10 per side, inserted directly on body surface, in paired diagonal columns or small clusters, sometimes absent (*U. anorektoxys*); TbD/TbDL present; TbL numerous, occurring both in the pharyngeal and trunk region; TbV/TbVL occasionally present; TbP numerous, inserted on the whole length of the tail. Ventral ciliation forms a united field in the

pharyngeal region, either continuing uninterrupted for the length of the body (*U. anorektoxys*, *U. mirabilis*) or splitting into two paired bands in the trunk region. Mouth, terminal, narrow; buccal cavity shallow, lightly cuticularized. Pharynx bearing pores in the last third, opening ventrolaterally; intestine simple and blind. Hermaphroditic; ovaries paired; oocytes mature in caudocephalic direction. Testes: paired, with the left testes often larger than the other; posteriorly directed vas deferens, discharging into a ventral pore. Frontal and caudal organs absent. Interstitial, marine. Included species: *Urodasys mirabilis* Remane, 1926 (type species); *U. anorektoxys* Todaro, Bernhard and Hummon, 2000; *U. apuliensis* Fregni, Faienza, Grimaldi, Tongiorgi and Balsamo, 1999; *U. elongatus* Renaud-Mornant, 1969.

Acknowledgements

This project is partially funded under the National Recovery and Resilience Plan (NRRP), Mission 4 Component 2 Investment 1.4—Call for tender No. 3138 of 16 December 2021, rectified by Decree n. 3175 of 18 December 2021 of the Italian Ministry of University and Research funded by the European Union—NextGenerationEU. Project Code CN_00000033, Concession Decree No. 1034 of 17 June 2022 adopted by the Italian Ministry of University and Research, CUP E93C22001090001, Project title "National Biodiversity Future Center—NBFC". Finally, we would like to thank the reviewers for their valuable comments on an early draft of the manuscript. Open access publishing facilitated by Universita degli Studi di Modena e Reggio Emilia, as part of the Wiley - CRUI-CARE agreement.

Conflict of interest

The authors declare no conflict of interest.

Data availability statement

The data that support the findings of this study are openly available on Figshare under the DOI 10.6084/m9.figshare.30580799, and will be available in GenBank at https://www.ncbi.nlm.nih.gov/genbank/ after publication.

References

Andrews, S., 2010. FastQC: a quality control tool for high throughput sequence data. http://www.bioinformatics.babraham.ac.uk/projects/fastqc/. Accessed 29 July 2024.

Araújo, T.Q., 2024. A description of a new species of *Cephalodasys* (Macrodasyida: Gastrotricha) from Florida, USA using an integrative morphological approach. Zootaxa 5463, 581–597. https://doi.org/10.11646/zootaxa.5463.4.8.

Arias-Carrasco, R., Vásquez-Morán, Y., Nakaya, H.I. and Maracaja Coutinho, V., 2018. StructRNAfinder: an automated pipeline and web server for RNA families prediction. BMC Bioinform. 19, 55. https://doi.org/10.1186/s12859-018-2052-2.

Artois, T., Fontaneto, D., Hummon, W.D., Mcinnes, S.J., Todaro, M.A., Sorensen, M.V. and Zullini, A., 2011. Ubiquity of microscopic animals? Evidence from the morphological approach in species identification. In: Fontaneto, D. (Ed.), Biogeography of Microscopic Organisms: Is Everything Small Everywhere? Cambridge University Press, Cambridge, pp. 244–283.

Atherton, S. and Hochberg, R., 2014. The evolution of the reproductive system of *Urodasys* (Gastrotricha: Macrodasyida). Invertebr. Biol. 133, 314–323. https://doi.org/10.1111/ivb.12068.

Balsamo, M., Artois, T., Smith, J.P.S., Todaro, M.A., Guidi, L., Leander, B.S. and Van Steenkiste, N.W.L., 2020. The curious and neglected soft-bodied meiofauna: Rouphozoa (Gastrotricha and Platyhelminthes). Hydrobiologia 847, 2613–2644. https://doi.org/10.1007/s10750-020-04287-x.

Balsamo, M., Guidi, L., Pierboni, L., Marotta, R., Todaro, M.A. and Ferraguti, M., 2007. Living without mitochondria: spermatozoa and spermatogenesis in two species of *Urodasys* (Gastrotricha, Macrodasyida) from dysoxic sediments. Invertebr. Biol. 126, 1–9. https://doi.org/10.1111/j.1744-7410.2007.00071.x.

Bankevich, A., Nurk, S., Antipov, D., Gurevich, A.A., Dvorkin, M., Kulikov, A.S., Lesin, V.M., Nikolenko, S.I., Pham, S., Prjibelski, A.D., Pyshkin, A.V., Sirotkin, A.V., Vyahhi, N., Tesler, G., Alekseyev, M.A. and Pevzner, P.A., 2012. SPAdes: a new genome assembly algorithm and its applications to single-cell sequencing. J. Comput. Biol. 19, 455–477. https://doi.org/10.1089/cmb.2012.0021.

Bergsten, J., 2005. A review of long-branch attraction. Cladistics 21, 163–193. https://doi.org/10.1111/j.1096-0031.2005.00059.x.

Bernt, M., Donath, A., Jühling, F., Externbrink, F., Florentz, C., Fritzsch, G., Pütz, J., Middendorf, M. and Stadler, P.F., 2013. MITOS: improved *de novo* metazoan mitochondrial genome annotation. Mol. Phylogenet. Evol. 69, 313–319. https://doi.org/10.1016/j.ympev.2012.08.023.

Bolger, A.M., Lohse, M. and Usadel, B.T., 2014. A flexible trimmer for Illumina sequence data. Bioinformatics 30, 2114–2120. https://doi.org/10.1093/bioinformatics/btu170.

Campos, A., Thiago Quintão Araùjo, T.Q., Todaro, M.A. and Garraffoni, A.R.S., 2025. Description of a new species of *Paraturbanella*, new record of *Paraturbanella tricaudata* and new insights on reproductive traits in Turbanellidae (Gastrotricha: Macrodasyida). Zool. Anz. 317, 46–59. https://doi.org/10.1016/j.jcz.2025.05.010.

Campos, A., Todaro, M.A. and Garraffoni, A.R.S., 2020. A new species of *Paraturbanella* Remane, 1927 (Gastrotricha, Macrodasyida) from the Brazilian Coast, and the molecular phylogeny of Turbanellidae Remane, 1926. Diversity 12, 42. https://doi.org/10.3390/d12020042.

Cesaretti, A., Kosakyan, A., Saponi, F. and Todaro, M.A., 2024. Gaining and losing on the way: the evolutionary scenario of reproductive diversification in genus *Urodasys* (Macrodasyida: Gastrotricha) inferred by multi-gene phylogeny. Zool. J. Linnean Soc. 202, zlae148. https://doi.org/10.1093/zoolinnean/zlae148.

Cesaretti, A., Leasi, F. and Todaro, M.A., 2023. Confocal laser scanning microscopy applied to a new species helps understand the functioning of the reproductive apparatus in stylet-bearing *Urodasys* (Gastrotricha: Macrodasyida). Water 15, 1106. https://doi.org/10.3390/w15061106.

Curini-Galletti, M., Artois, T., Di Domenico, M., Fontaneto, D., Jondelius, U., Jörger, K.M., Leasi, F., Martínez, A., Norenburg, J.L., Sterrer, W. and Todaro, M.A., 2020. Contribution of soft-bodied meiofaunal taxa to Italian marine biodiversity. Eur.

Zool. J. 87, 369–384. https://doi.org/10.1080/24750263.2020.1786607.
Edgar, R.C., 2004. MUSCLE: a multiple sequence alignment method with reduced time and space complexity. BMC Bioinform. 5, 113. https://doi.org/10.1186/1471-2105-5-113.
Ferraguti, M. and Balsamo, M., 1995. Comparative spermatology of Gastrotricha. In: Jamieson, B.G.M., Ausio, J. and Justine, J.L. (Eds.), Advances of Spermatozoal Phylogeny and Taxonomy, Vol. 166. Muséum National d'Histoire Naturelle, Paris, pp. 105–117.
Fregni, E., Balsamo, M. and Ferraguti, M., 1999. Morphology of the reproductive system and spermatozoa of *Mesodasys adenotubulatus* (Gastrotricha: Macrodasyida). Mar. Biol. 135, 515–520. https://doi.org/10.1007/s002270050652.
Gammuto, L., Serra, V., Petroni, G. and Todaro, M.A., 2024. Molecular phylogenetic position and description of a new genus and species of freshwater Chaetonotidae (Gastrotricha: Chaetonotida: Paucitubulatina), and the annotation of its mitochondrial genome. Invertebr. Syst. 38, 1–16. https://doi.org/10.1071/IS23059.
Garraffoni, A.R.S. and Balsamo, M., 2017. Is the ubiquitous distribution real for marine gastrotrichs? Detection of areas of endemism using Parsimony Analysis of Endemicity (PAE). Proc. Biol. Soc. Wash. 130, 198–211. https://doi.org/10.2988/17-00011.
Garraffoni, A.R.S., Sørensen, M.V., Worsaee, K., Di Domenico, M., Sales, L.P., Santos, J. and Lourenço, A., 2021. Geographical sampling bias on the assessment of endemism areas for marine meiobenthic fauna. Cladistics 37, 571–585. https://doi.org/10.1111/cla.12453
Guidi, L., Pierboni, L., Ferraguti, M., Todaro, M.A. and Balsamo, M., 2004. Spermatology of the genus *Lepidodasys* Remane, 1926 (Gastrotricha, Macrodasyida): towards a revision of the family Lepidodasyidae Remane, 1927. Acta Zool. 85, 211–221. https://doi.org/10.1111/j.0001-7272.2004.00172.x.
Guidi, L., Todaro, M.A., Cesaroni, L. and Balsamo, M., 2017. The unusual spermatozoa of *Dolichodasys* sp. (Gastrotricha, Macrodasyida). Proc. Biol. Soc. Wash. 130, 187–197. https://doi.org/10.2988/17-00009.
Guidi, L., Todaro, M.A., Ferraguti, M. and Balsamo, M., 2014. Reproductive system and spermatozoa ultrastructure support the phylogenetic proximity of *Megadasys* and *Crasiella* (Gastrotricha, Macrodasyida). Contrib. Zool. 83, 119–131. https://doi.org/10.1163/18759866-08302003.
Guindon, S., Dufayard, J.F., Lefort, V., Anisimova, M., Hordijk, W. and Gascuel, O., 2010. New algorithms and methods to estimate maximum-likelihood phylogenies: assessing the performance of PhyML 3.0. Syst. Biol. 59, 307–321. https://doi.org/10.1093/sysbio/syq010.
Hall, T.B., 1999. A user-friendly biological sequence alignment editor and analysis program for Windows 95/98/NT. Nucleic Acids Symp. Ser. 41, 95–98. https://doi.org/10.1021/bk-1999-0734.ch008.
Hochberg, R. and Litvaitis, M.K., 2001. Macrodasyida (Gastrotricha): a cladistic analysis of morphology. Invertebr. Biol. 120, 124–135. https://doi.org/10.1111/j.1744-7410.2001.tb00116.x.
Hummon, W., 2011. Marine Gastrotricha of the near east: 1. Fourteen new species of Macrodasyida and a redescription of *Dactylopodola agadasys* Hochberg, 2003. ZooKeys 94, 1–59. https://doi.org/10.3897/zookeys.94.794.
Hummon, W.D., 1974. Some taxonomic revisions and nomenclatural notes concerning marine and brackish-water Gastrotricha. Trans. Am. Microsc. Soc. 93, 194. https://doi.org/10.2307/3225287.
Hummon, W.D., 2008. Gastrotricha of the North Atlantic Ocean: 1. Twenty four new and two redescribed species of Macrodasyida. Meiofauna Mar. 16, 117–174.
Hummon, W.D. and Todaro, M.A., 2010. Analytic taxonomy and notes on marine, brackish-water and estuarine Gastrotricha. Zootaxa 2392, 1–32. https://doi.org/10.11646/zootaxa.2392.1.1.
Hummon, W.D., Todaro, M.A. and Tongiorgi, P., 1993. Italian marine Gastrotricha: II. One new genus and ten new species of Macrodasyida. Boll. Zool. 60, 109–127. https://doi.org/10.1080/11250009309355798.
Hummon, W.D., Todaro, M.A., Tongiorgi, P. and Balsamo, M., 1998. Italian marine Gastrotricha: V. Four new and one redescribed species of Macrodasyida in the Dactylopodolidae and Thaumastodermatidae. Ital. J. Zool. 65, 109–119. https://doi.org/10.1080/11250009809386731.
Kieneke, A., Arbizu, P.M. and Ahlrichs, W.H., 2008. Anatomy and ultrastructure of the reproductive organs in *Dactylopodola typhle* (Gastrotricha: Macrodasyida) and their possible functions in sperm transfer. Invertebr. Biol. 127, 12–32. https://doi.org/10.1111/j.1744-7410.2007.00111.x.
Kieneke, A., Riemann, O. and Ahlrichs, W.H., 2008a. Novel implications for the basal internal relationships of Gastrotricha revealed by an analysis of morphological characters. Zool. Scr. 37, 429–460. https://doi.org/10.1111/j.1463-6409.2008.00334.x.
Kieneke, A., Rothe, B.H. and Schmidt-Rhaesa, A., 2013. Record and description of *Anandrodasys agadasys* (Gastrotricha: Redudasyidae) from Lee Stocking Island (Bahamas), with remarks on populations from different geographic areas. Meiofauna Mar. 20, 39–48.
Kieneke, A. and Schmidt-Rhaesa, A., 2014. Gastrotricha. In: Schmidt-Rhaesa, A. (Ed.), Handbook of Zoology. Gastrotricha, Cycloneuralia and Gnathifera. Vol. 3: Gastrotricha and Gnathifera. De Gruyter, Berlin, pp. 1–134.
Kieneke, A. and Todaro, M.A., 2021. Discovery of two "chimeric" Gastrotricha and their systematic placement based on an integrative approach. Zool. J. Linnean Soc. 192, 710–735. https://doi.org/10.1093/zoolinnean/zlaa117.
Kumar, S., Jones, M., Koutsovoulos, G., Clarke, M. and Blaxter, M., 2013. Blobology: exploring raw genome data for contaminants, symbionts, and parasites using taxon-annotated GC-coverage plots. Front. Genet. 4, 1–12. https://doi.org/10.3389/fgene.2013.00237.
Kumar, S., Stecher, G., Li, M., Knyaz, C. and Tamura, K., 2018. MEGA X: molecular evolutionary genetics analysis across computing platforms. Mol. Biol. Evol. 35, 1547–1549. https://doi.org/10.1093/molbev/msy096.
Magpali, L., Machado, D.R., Araújo, T.Q. and Garraffoni, A.R., 2021. Long distance dispersal and pseudo-cryptic species in Gastrotricha: first description of a new species (Chaetonotida, Chaetonotidae, *Polymerurus*) from an oceanic Island with volcanic rocks. Eur. J. Taxon. 746, 62–93.
Minowa, A.K., Kieneke, A., Campos, A., Balsamo, M., Plewka, M., Guidi, L., Araújo, T.Q. and Garraffoni, A.R.S., 2025. New branch on the tree of life of Gastrotricha: establishment of a new genus for limno-terrestrial species. Zool. J. Linnean Soc. 203, zlae166. https://doi.org/10.1093/zoolinnean/zlae166.
Munter, L. and Kieneke, A., 2017. Novel myo-anatomical insights to the *Xenotrichula intermedia* species complex (Gastrotricha: Paucitubulatina): implications for a pan-European species and reconsideration of muscle homology among Paucitubulatina. Proc. Biol. Soc. Wash. 130, 165–185. https://doi.org/10.2988/17-00013.
Nguyen, L.T., Schmidt, H.A., von Haeseler, A. and Minh, B.Q., 2015. IQ-TREE: a fast and effective stochastic algorithm for estimating maximum-likelihood phylogenies. Mol. Biol. Evol. 32, 268–274. https://doi.org/10.1093/molbev/msu300.
Paps, J. and Riutort, M., 2012. Molecular phylogeny of the phylum Gastrotricha: new data brings together molecules and morphology. Mol. Phylogenet. Evol. 63, 208–212. https://doi.org/10.1016/j.ympev.2011.12.010.
Petrov, N.B., Pegova, A.N., Manylov, O.G., Vladychenskaya, N.S., Mugue, N.S. and Aleshin, V.V., 2007. Molecular phylogeny of Gastrotricha on the basis of a comparison of the *18S* rRNA genes: rejection of the hypothesis of a relationship between Gastrotricha and Nematoda. Mol. Biol. 41, 445–452.
Plotnick, R.E. and Wagner, P.J., 2006. Round up the usual suspects: common genera in the fossil record and the nature of

wastebasket taxa. Paleobiology 32, 126–146. https://doi.org/10.1666/04056.1.
Rataj Križanová, F. and Vd'ačný, P., 2022. A huge undescribed diversity of the subgenus *Hystricochaetonotus* (Gastrotricha, Chaetonotidae, *Chaetonotus*) in Central Europe. Eur. J. Taxon. 840, 1–93. https://doi.org/10.5852/ejt.2022.840.1941.
Rataj Križanová, F. and Vd'ačný, P., 2024. A *Heterolepidoderma* and *Halichaetoderma* gen. nov. (Gastrotricha: Chaetonotidae) riddle: integrative taxonomy and phylogeny of six new freshwater species from central Europe. Zool. J. Linnean Soc. 200, 283–335. https://doi.org/10.1093/zoolinnean/zlad079.
Remane, A., 1926. Morphologie und Verwandtschaftsbeziehungen der aberranten Gastrotrichen. Z. Morph. Ökol. Tiere 5, 625–754.
Remane, A., 1934. Die Gastrotrichen des Kuestengrundwassers von Schilksee. Schr. Naturwiss. Ver. Schleswig-Holstein 20, 473–478.
Remane, A., 1951. *Mesodasys*, ein neues Genus der Gastrotricha Macrodasyoidea aus der Kieler Bucht. Kiel. Meeresforsch. 8, 102–105.
Ronquist, F., Teslenko, M., van der Mark, P., Ayres, D.L., Darling, A., Höhna, S., Larget, B., Liu, L., Suchard, M.A. and Huelsenbeck, J.P., 2012. MrBayes 3.2: efficient Bayesian phylogenetic inference and model choice across a large model space. Syst. Biol. 61, 539–542. https://doi.org/10.1093/sysbio/sys029.
Ruppert, E.E., 1991. Gastrotricha. In: Harrison, F.W. and Ruppert, R.R. (Eds.), Microscopic Anatomy of Invertebrates. Vol 4: Aschelmintes. Wiley-Liss, New York, pp. 41–109.
Ruppert, E.E. and Shaw, K., 1978. The reproductive system of gastrotrichs: introduction with morphological data for two new *Dolichodasys* species. Zool. Scr. 6, 185–195. https://doi.org/10.1111/j.1463-6409.1978.tb00769.x.
Saponi, F., Kosakyan, A., Cesaretti, A. and Todaro, M.A., 2024. A contribution to the taxonomy and phylogeny of the genus *Chaetonotus* (Gastrotricha, Paucitubulatina, Chaetonotidae), with the description of a new species from Italian inland waters. Eur. Zool. J. 91, 1078–1092. https://doi.org/10.1080/24750263.2024.2397473.
Saponi, F. and Todaro, M.A., 2024. Status of the Italian freshwater Gastrotricha biodiversity, with the creation of an interactive GIS-based web map. Diversity 16, 17. https://doi.org/10.3390/d16010017.
Schuster, J., Atherton, S., Todaro, M.A., Schmidt-Rhaesa, A. and Hochberg, R., 2017. Redescription of *Xenodasys riedli* (Gastrotricha: Macrodasyida) based on SEM analysis, with first report of population density data. Mar. Biodivers. 48, 259–271. https://doi.org/10.1007/s12526-017-0667-6.
Serra, V., Gammuto, L., Nitla, V., Castelli, M., Lanzoni, O., Sassera, D., Bandi, C., Sandeep, B.V., Verni, F., Modeo, L. and Petroni, G., 2020. Morphology, ultrastructure, genomics, and phylogeny of *Euplotes vanleeuwenhoeki* sp. nov. and its ultra-reduced endosymbiont "*Candidatus Pinguicoccus supinus*" sp. nov. Sci. Rep. 10, 20311. https://doi.org/10.1038/s41598-020-76348-z.
Souid, A., Gammoudi, M., Saponi, F., El Cafsi, M. and Todaro, M.A., 2025. First investigation of the marine gastrotrich fauna from the waters of North Tunisia, with the description of a new species of *Halichaetonotus* (Gastrotricha, Chaetonotida). Diversity 17, 17. https://doi.org/10.3390/d17010017.
The Galaxy Community, 2024. The Galaxy platform for accessible, reproducible, and collaborative data analyses: 2024 update. Nucleic Acids Res. 52, W83–W94. https://doi.org/10.1093/nar/gkae410.
Todaro, M.A., Cesaretti, A. and Dal Zotto, M., 2019a. Marine gastrotrichs from Lanzarote, with a description of a phylogenetically relevant species of *Urodasys* (Gastrotricha, Macrodasyida). Mar. Biodivers. 49, 2109–2123.
Todaro, M.A., Dal Zotto, M., Jondelius, U., Hochberg, R., Hummon, W.D., Kånneby, T. and Rocha, C.E.F., 2012. Gastrotricha: a marine sister for a freshwater puzzle. PLoS One 7, e31740. https://doi.org/10.1371/journal.pone.0031740.
Todaro, M.A., Dal Zotto, M., Kånneby, T. and Hochberg, R., 2019b. Integrated data analysis allows the establishment of a new, cosmopolitan genus of marine Macrodasyida (Gastrotricha). Sci. Rep. 9, 7989. https://doi.org/10.1038/s41598-019-43977-y.
Todaro, M.A., Dal Zotto, M. and Leasi, F., 2015. An integrated morphological and molecular approach to the description and systematisation of a novel genus and species of Macrodasyida (Gastrotricha). PLoS One 10, e0130278. https://doi.org/10.1371/journal.pone.0130278.
Todaro, M.A., Kånneby, T., Dal Zotto, M. and Jondelius, U., 2011. Phylogeny of Thaumastodermatidae (Gastrotricha: Macrodasyida) inferred from nuclear and mitochondrial sequence data. PLoS One 6, e17892. https://doi.org/10.1371/journal.pone.0017892.
Todaro, M.A., Leasi, F. and Hochberg, R., 2014. A new species, genus, and family of marine Gastrotricha from Jamaica, with a phylogenetic analysis of Macrodasyida based on molecular data. Syst. Biodivers. 12, 473–488. https://doi.org/10.1080/14772000.2014.942718.
Todaro, M.A., Sibaja-Cordero, J.A., Segura-Bermùdez, O.A., Coto-Delgado, G., Goebel-Otárola, N., Barquero, J.D., Cullell-Delgado, M. and Dal Zotto, M., 2019c. An introduction to the study of Gastrotricha, with a taxonomic key to families and genera of the group. Diversity 11, 117. https://doi.org/10.3390/d11070117.
Whittaker, R.H., 1969. New concepts of kingdoms or organisms. Evolutionary relations are better represented by new classifications than by the traditional two kingdoms. Science 163, 150–160.
Wilke, U., 1954. Mediterrane Gastrotrichen. Zool. Jahrb. Abt. Syst. Ökol. Geogr. Tiere 82, 497–550.
Yamauchi, S. and Kajihara, H., 2018. Marine Macrodasyida (Gastrotricha) from Hokkaido, northern Japan. Species Divers. 23, 183–192. https://doi.org/10.12782/specdiv.23.183.
Yudina, S.V., Schelkunov, M.I., Nauheimer, L., Crayn, D., Chantanaorrapint, S., Hroneš, M., Sochor, M., Dančák, M., Mar, S.S., Luu, H.T., Nuraliev, M.S. and Logacheva, M.D., 2021. Comparative analysis of plastid genomes in the non-photosynthetic genus *Thismia* reveals ongoing gene set reduction. Front. Plant Sci. 12, 602598. https://doi.org/10.3389/fpls.2021.602598.

Supporting Information

Additional supporting information may be found online in the Supporting Information section at the end of the article.

File S1. Protocol for the validation step.

Table S1. Sequences sourced from GenBank for this study, with sampling area, GenBank accession codes and references.

Table S2. 18S primers used in the validation step and their respective direction, sequence and usage.

Appendix S1. Summary of the nomenclatural acts.

CHAPTER 4

FROM RIGID ORDER TO RADICAL VARIATION: MITOGENOME EVOLUTION IN THE MAIN LINEAGES OF A LESSER KNOWN ANIMAL PHYLUM (GASTROTRICHA)

(manuscript in press in *Genome Biology and Evolution*. https://doi.org/10.1093/gbe/evag001)

From rigid order to radical variation: mitogenome evolution in the main lineages of a lesser-known animal phylum (Gastrotricha)

Anush Kosakyan[1,2*] ✝, Leandro Gammuto[3] ✝, Agata Cesaretti[1], Francesco Saponi[1,2,4], Valentina Serra[5], Giulio Petroni[5,6,7], Jan-Niklas Macher[8,9], Oscar Wallnoefer[10], Federico Plazzi[10], M. Antonio Todaro[1,2]

[1]Department of Life Sciences, University of Modena and Reggio Emilia, Modena, Italy
[2]National Biodiversity Future Center (NBFC), Palermo, Italy
[3]Department of Biology and Biotechnology "Lazzaro Spallazani", University of Pavia, Pavia, Italy
[4]Department of Earth and Marine Sciences, University of Palermo, Palermo, Italy
[5]Dipartimento of Biology, University of Pisa, Pisa, Italy
[6] Interdepartmental Center for Electron Microscopy (CIME), University of Pisa, Pisa, Italy
[7] Center for Instrument Sharing of the University of Pisa (CISUP), University of Pisa, Pisa, Italy
[8]Naturalis Biodiversity Center, Leiden, Netherlands
[9]Department of Environmental Biology, Institute of Environmental Sciences (CML), Leiden University, Leiden, The Netherlands
[10]Department of Biological, Geological and Environmental Sciences, University of Bologna, Bologna, Italy

*_Author for correspondence_: Anush Kosakyan, Department of Life Sciences, University of Modena and Reggio Emilia, Italy, Tel.: +39 0592055563, Fax: +39 0592055548, E-mail: anush.kosakyan@unimore.it

✝ these authors contributed equally to this work

Main text

ABSTRACT

Mitochondrial genomes offer valuable insights into biological and phylogenetic processes, yet the factors shaping their architecture across metazoan lineages remain poorly understood, largely due to limited taxonomic sampling. To address this gap, we analyzed mitochondrial genomes from 20 species spanning a broad taxonomic spectrum of the phylum Gastrotricha. Our findings, supported by phylogenetic analyses based on mitochondrial datasets, reveal two distinct evolutionary patterns: one lineage displays remarkable conservation in genome structure, while the other exhibits variability in gene content, arrangement, strand polarity, and repeat abundance. These contrasting patterns appear to be related to differences in reproductive strategies (hermaphroditism vs. parthenogenesis) and ecological habitats (marine vs. freshwater). While these associations are intriguing, further data are needed to understand the underlying processes.This study highlights the importance of broad phylum-scale mitogenomic sampling for uncovering genomic diversity and advancing our understanding of mitochondrial evolution across Metazoa.

Key words: Evolutionary adaptations, Gastrotricha, Mitochondrial genomes, mtDNA modifications, Mitochondrial phylogenetics.

SIGNIFICANCE STATEMENT

Mitochondrial genomes are widely used to study animal evolution, yet their structural diversity remains poorly understood due to limited sampling across many groups. One such group is Gastrotricha, a little-known phylum of aquatic invertebrates, for which mitochondrial data is very

limited (available only for two species out of 900 known species). This study generated and analyzed 21 mitogenomes, revealing lineage-specific patterns possibly linked to reproductive mode and habitat of these organisms. While these associations are preliminary and might be driven by phylogenetic non-independence, they offer intriguing insights into how ecological and life history traits may correlate with genome architecture. These findings underscore the importance of broader taxonomic sampling to uncover the mechanisms driving mitochondrial evolution in overlooked animal lineages.

INTRODUCTION

The metazoan mitochondrial genome was traditionally believed to be a circular chromosome, approximately 14-20 kb in length, containing 13 protein-coding genes, 2 ribosomal RNA genes, and 22 tRNA genes (Boore 1999; Saccone et al. 1999; Gissi et al. 2008). Over time, as mitochondrial genomes were sequenced for hundreds of metazoans, many species showed deviations from this conserved structure (Smith 2015; Lavrov and Pett 2016; Shtolz and Mishmar 2023; Struck et al. 2023). These deviations include variations in circular versus linear structure, gene order conservation, gene numbers, and, in some cases, the complete absence of mitochondria (Yahalomi et al. 2020). Information gathered from these mitochondrial genomes has significantly contributed to evolutionary and phylogenetic studies (Allio et al. 2017; Gibb et al. 2016; Dowling and Wolff 2023). The higher mutation rate of mitochondrial DNA compared to nuclear DNA, combined with conserved sites within genes like mtCOI that enable universal primer design, has facilitated the development of barcodes that further our understanding of species relationships (Hebert et al. 2003). Additionally, mitochondrial datasets have played an integral role in advancing phylogeographic studies (Morin et al. 2010), paleogenomics (Nesheva 2014; Posth et al. 2023),

population genetics (Lake et al. 2023), genome evolution studies (Butenko et al. 2024), and more. However, despite its extensive use, there are still many metazoan lineages with limited or no available mitochondrial genomic data. One such lineage is the phylum Gastrotricha Metschnikoff, 1865.

Gastrotrichs are microscopic, free-living aquatic animals that thrive in sediments at the bottom of marine and freshwater environments. Ranging in size from 80 µm to 3.8 mm, they play an important ecological role in aquatic systems as essential components of food webs (Todaro and Luporini 2022; Todaro et al. 2019, 2025; Souid et al. 2025). Currently, over 900 species of gastrotrichs are classified into two orders: Macrodasyida, which includes approximately 385 predominantly marine or estuarine species with only four exceptions, and Chaetonotida, which comprises about 520 mainly freshwater species (Saponi et al. 2024a,b, 2025; Gammuto et al. 2024; Minowa et al. 2025). It has been suggested that about one-fourth of Chaetonotida species have reinvaded marine environments during their evolution (Kolicka et al. 2020). Gastrotrichs exhibit diverse adaptations to marine and freshwater habitats and possess a fascinating array of reproductive strategies. Generally, chaetonotidan species are mostly found in freshwater and are parthenogenetic, while macrodasyidan species, are primarily marine and hermaphroditic, though exceptions exist in both groups (Kieneke and Schmidt-Rhaesa 2015; Cesaretti et al. 2024). For example, within the Macrodasyida order, the freshwater genus *Redudasys* (with 3 species), the marine genera *Anandrodasys* (1 species) and *Urodasys viviparus* reproduce through parthenogenesis. In contrast, in the Chaetonotida order, notable exceptions include species from the families Neodasyidae (4 species), Muselliferidae (8 species), and Xenotrichulidae (26 species), all of which are primarily marine and exhibit hermaphroditism (Todaro et al. 2019).

Despite their intriguing biology, the evolutionary history of gastrotrichs is not fully resolved, as it is primarily inferred from morphological data. Although molecular markers are available for a relatively high proportion of known species (approximately 21% as of NCBI 20.02.2025), these data are often limited to just a few genes, such as 18S rDNA, 28S rDNA, and mtCOI. Additionally, transcriptomic data is available for only seven species (Struck et al. 2014; Egger et al. 2015; Laumer et al. 2015), and complete mitochondrial genomes are available for only two species (Golombek et al. 2015; Gammuto et al. 2024), which presents a significant challenge to understanding the deep evolutionary history of the group. Recently, the first gastrotrich genome was published, once again confirming the phylogenetic position of Gastrotricha as a sister taxon to Platyhelminthes (Roberts et al. 2024).

The first phylogenetic studies of Gastrotricha based on molecular data began to emerge in the early 2000s, primarily using partial SSU rDNA gene sequences (Todaro et al. 2003, 2006; Zrzavy et al. 2003; Manilov et al. 2004; Paps and Riutort 2012). These reconstructions clearly divided the phylum into two well-supported clades: Macrodasyida and Chaetonotida. These groupings align well with the general morphology of the members of these orders, with macrodasyidans characterized by a vermiform body, multiple adhesive tubes, presence of pharyngeal pores and a pattern of an inverted Y of the cross-sectioned pharyngeal lumen, and chaetonotidans by a tenpin or bottle-shaped body, mainly a pair of adhesive tubes, a cross-sectioned Y-shaped pharyngeal lumen and lack of pharyngeal pores (Kieneke and Schmidt-Rhaesa 2019) (see details in Figures 1 and 2).

The status and phylogenetic positions of several taxa remained unresolved, calling for further research (Kieneke and Schmidt-Rhaesa 2019). Subsequent phylogenetic reconstructions that incorporated multiple genes, such as rDNA SSU, LSU, and mtCOI, have provided more robust insights. However, these studies have often focused on individual taxonomic groups at various

levels, from genus to order. Examples include *Heterolepidoderma* (Križanová and Vďačný 2024), *Urodasys* (Cesaretti et al. 2024), Chaetonotidae (Kanneby et al. 2013; Kolicka et al. 2020), and Macrodasyida (Todaro et al. 2012, Cesaretti et al. 2025). A recent study by Gammuto et al. (2024) contributes to this framework by providing insights into the phylogenetic relationships within the Oiorpata, a clade that encompasses both marine and freshwater Chaetonotida that primarily reproduce through parthenogenesis. Despite the numerous studies, many questions about the evolution and systematics of the involved taxa remain unanswered, which has led to ongoing debate and inquiry within the scientific community.

Mitochondrial genomes are typically rather conserved in many vertebrates and invertebrates; however, it was shown that various taxa (e.g., Cnidaria, Annelida, Porifera, Mollusca) exhibit structural rearrangements (Shtolz and Mishmar 2023; Struck et al. 2023). Therefore, not only mitochondrial gene sequences, but also aspects of mitochondrial genome architecture, such as gene order and structural features, can offer insights into lineage-specific evolutionary patterns (Dowling and Wolf 2023; Xiao et al. 2025).

Our study aims to investigate the molecular architecture of mitochondrial genomes in gastrotrichs across different lineages to identify potential evolutionary events linked to the biology and ecology of these minute organisms.

RESULTS

Phylogeny of gastrotrichs based on concatenated mitochondrial protein coding genes: We have successfully obtained and analyzed 21 gastrotrich mitochondrial genomes, of which nine belong to Chaetonotida and 12 to Macrodasyida (Table 1). Phylogenetic analyses based on ML and BI approaches generated similar results revealing two main groups including members of

Chaetonotida and Macrodasyida (Figure 3), concordant with the previous phylogenetic analyses based on rDNA SSU gene (Paps and Riutort 2012; Bekkouche and Worsaae 2016). Within Chaetonotida, the parthenogenetic species are grouped with 100% BB (bootstrap) and PP (posterior probabilities) support values, forming the Oiorpata subclade as it was suggested recently (Gammuto et al. 2024). Within Oiorpata, the marine species (*Aspidiphorus tentaculatus* and *Chaetonotus neptuni*) appear as early branching lineages within the group, suggesting a possible marine origin of the extant Oiorpata, although these nodes receive only 96% PP support. Two marine hermaphroditic taxa, *Xenotrichula* and *Neodasys*, appear as basal lineages to Oiorpata. While *Xenotrichula* is branching with the Oiorpata with 100% BB and PP support, the position of *Neodasys* still remains unresolved (Figure 3). The macrodasyidan clade in turn is monophyletic with 100% BB and PP support, where two well supported subclades can be observed: i) represented by two members of family Cephalodasyidae, namely *Paradasys* sp. and *Dolichodasys* sp., together with *Anandrodasys agadasys,* a representative of the Redudasyidae; ii) represented by all remaining taxa (i.e. *Turbanella, Paraturbanella, Megadasys, Urodasys,* and *Macrodasys*. Within this last subclade: a) all members belonging to genus *Urodasys* clustered together supporting the monophyly of the genus; b) two members from family Turbanellidae such as *Turbanella ambronensis* and *Paraturbanella pallida*, together with *Megadasys* sp. formed a well-supported subclade; c) the position of *Macrodasys meristocytalis* is weakly supported, with low BB and PP values preventing confident placement within the subclade. Additionally, we obtained a similar tree when analyzing the same dataset but excluding *atp6* and *atp8* (Suppl. Mat. 1), since these genes were not detected in several mitogenomes (see below). This confirms that omitting these genes neither alters the overall tree topology nor improves support for the putative nodes.

General structure of gastrotrich mitogenomes: The complete mitochondrial genomes of the studied gastrotrichs are single circular molecules ranging from 13 to 19 Kb in length (Table 1). They consist of 11-13 protein-coding genes, 17-22 tRNA genes, and two rRNA genes. The structural analyses revealed a clear distinction between members of the two orders in terms of mitogenome length, protein-coding gene number and order, GC content, the direction of encoded genes, tandem repeat numbers, and codon usage preferences. Additionally, we observed conserved mitogenome structures within the Oiorpata group (parthenogenetic chaetonotidans), whereas macrodasyidan species displayed considerable variability (Figure 4). Conserved structural patterns were noted to some extent in hermaphroditic marine chaetonotidans (e.g., the number of protein-coding genes is 12 vs. 13 in Oiorpata, *atp8* being the missing gene); however, the limited number of samples in this group precludes definitive conclusions. Our analyses showed that chaetonotidan mitogenomes are quite conserved in terms of mitogenome size (14,156-15,103 bp), with Oiorpata species ranging from 14,384-14,558 bp. In contrast, the mitogenome length is more variable in Macrodasyida, spanning from 13,340-19,008 bp (Table 1). This high range in the length of mtDNA is mainly due to two outliers, *U. apuliensis* and *U. mirabilis*, for which a possible gene duplication event was detected (see details below). Base composition analyses indicated that chaetonotidan mtDNA has higher GC content (37-42%, except for *Xenotrichula intermedia* at 31%) compared to macrodasyidan mtDNA (GC = 20-29%, except for *Turbanella ambronensis* at 46%) (Table 1, Suppl. Mat. 2). Tandem repeat analyses showed a similar pattern, with no or at most one tandem repeat found in chaetonotidans, while these repeats are more common in observed macrodasyidan species, ranging from 1 to 9 with variable copy numbers (Table 1, Suppl. Mat. 3). Statistical comparisons of GC content (Student's *t*-test) and tandem repeat abundance (Mann–Whitney *U* test) revealed significant differences in mitochondrial genome composition and architecture between the two orders (see Methods for details). GC content was significantly higher in

198 Chaetonotida compared to Macrodasyida (*t*-test, $p = 3.82 \times 10^{-5}$). Similarly, tandem repeat
199 content differed significantly between the groups (Mann–Whitney *U* test, $p = 3.87 \times 10^{-4}$).
200 Correlation analyses indicated a strong negative association between GC content and tandem
201 repeat abundance (Spearman's $r_s = -0.729$, $p = 3.94 \times 10^{-5}$). We did not observe gene duplication
202 events, with the exception in two representatives of early-branching lineages of *Urodasys* species:
203 *U. mirabilis* (with duplication of the *cox2* gene) and *U. apuliensis* (with duplication of the *nad4*
204 gene) (Figure 4). Re-sequencing the same specimens with Oxford nanopore technology confirmed
205 these duplications. Additionally, while one of the duplicated sequences in both species showed
206 higher variability, both the crystal structure and specific core regions remained highly conserved
207 across all sequences, supporting the existence of a true duplication rather than a bioinformatic
208 artifact.

209 **Protein Coding Gene Number, Order, and Transcriptional Direction:** We observed
210 complete synteny (same gene order) in parthenogenetic chaetonotidans (Oiorpata group) with 13
211 protein-coding genes (*cox1-3*, *cob*, *nad1-6, nad4l*, *atp6*, *atp8*) (Figure 4) and unidirectional
212 transcription, where all genes have the same direction ("+" strand as annotated by MITOS2, which
213 corresponds to the 5'→3' direction of the reference scaffold), except for *trnT*, *trnD*, and *trnP*
214 (Figure 5). The mitochondrial architecture differs slightly in exclusively marine and hermaphroditic
215 chaetonotidans (representatives of the families Neodasyidae and Xenotrichulidae), which have 12
216 protein-coding genes (*atp8* was not detected). The gene order in these species differs from other
217 chaetonotidans, but all genes are transcribed in the same direction. In contrast, macrodasyidans
218 have only 11 protein-coding genes, with *atp6* and *atp8* absent, and their gene order is highly
219 variable. The transcriptional direction of macrodasyidan mitochondrial genes also varies widely,
220 with no conserved patterns even at the genus level (e.g., no common pattern was observed in five
221 species of the genus *Urodasys* included in this study) (Table 2). We also observed a significant

222 negative correlation between GC content and transcriptional directionality (Spearman's r_s = –
223 0.749, $p = 1.94 \times 10^{-5}$), suggesting that mitogenomes with higher GC content tend to have more
224 unidirectional gene orientation.

225 Additional analyses were conducted to search for the *atp* genes. The *atp8* gene was not
226 recovered by MITOS2 in hermaphroditic marine chaetonotidan mtDNA, and the *atp6* and *atp8*
227 genes were not recovered in macrodasyidan mtDNA as well. We identified *atp6* candidates in all
228 studied macrodasydan nuclear contigs, with the exception of *U. bifidostylis* and *Dolychodasys* sp.
229 (Suppl. Mat 4), likely due to the lower quality of the assembly, in which the specific contig
230 containing *atp6* may have been lost. Notably, in *T. ambronensis*, *atp6* was found on two distinct
231 scaffolds. In all species, MITOS2 identified *atp6* as an isolated gene, without any neighboring
232 mitochondrial genes (that instead should be located in a unique contig). Exonerate also produced
233 similar and consistent results, further supporting the nuclear localization of *atp6*. The comparison
234 of putative *atp6* sequences against the non-redundant protein database (nr) using Blastx,
235 confirming their identity as *atp6*. Additionally, nuclear-localized candidate *atp6* sequences were
236 translated using the standard nuclear genetic code and analyzed for mitochondrial targeting
237 signals. Most sequences were compatible with the standard code and exhibited protein lengths
238 (~155 amino acids) comparable to those found in Chaetonotida, suggesting potential functionality.
239 However, in four species (*Urodasys mirabilis*, *U. viviparous*, *U. apuliensis*, and *Turbanella*
240 *ambronensis*), premature stop codons were detected under standard code translation, which may
241 reflect assembly artifacts, pseudogenization, or alternative coding interpretations. TargetP
242 (Emanuelsson et al. 2000) predicted putative mitochondrial targeting signals only in *U. mirabilis*, *T.*
243 *ambronensis*, and *Paraturbanella pallida* indicating a potential functional relocation of *atp6* in
244 these species, pending further validation. Conversely, *atp8* was not detected in any assembly,
245 likely due to its short length, making it difficult to identify.

Codon Usage Analysis: Codon usage analysis revealed conserved patterns for some amino acids across all studied gastrotrichs. For example, in the surveyed species Phenylalanine is most commonly encoded by UUU, Isoleucine by AUU, Valine by GUU, and Serine by UCU. Additionally, lineage-specific patterns were observed for other amino acids. For instance, in members of the Oiorpata group, the most commonly used codon is AUG for Methionine while all other examined gastrotrichs prefer AUA (except for macrodasyidan species *T. ambronensis* which prefers AUG, and has a higher CG content of 46%). Oiorpata members also have preference of CCU for Proline, ACU for Threonine, and AAA for Lysine (Table 2).

DISCUSSION

While mitochondrial structure and function vary across eukaryotes, mitogenome content tends to be conserved in major groups such as metazoans (Shtolz and Mishmar 2023). Yet, several lineages have undergone gene rearrangements, expansions, losses, or even genome fragmentation often associated with factors like extreme habitats, high metabolic rates, short generation times, or parasitic lifestyles (Yahalomi et al. 2020; Feng et al. 2022; Struck et al. 2023). Understanding these patterns provides a valuable framework for interpreting the mitogenomic diversity observed in Gastrotricha.

Gastrotrichs, a fascinating group of microscopic metazoans, have diversified in marine and freshwater habitats adopting various lifestyles and reproductive strategies, which seem related to variations in their mitochondrial genomes. Our phylogenetic analyses separated the studied gastrotrich species in two groups corresponding to the currently recognized two orders, reflecting well their morphology, reproductive biology and lifestyle. For instance, in the chaetonotidan group, the Oiorpata comprises parthenogenetic species, while the hermaphroditic species branch

as basal lineages to Oiorpata (Figure 3). Within Oiorpata, two marine species appear as early diverging clades, indicating a possible marine origin of the group, providing support to the evolutionary scenario hypothesized by previous phylogenetic analyses based on nuclear ribosomal genes and a denser taxonomic sampling (e.g., Kånneby et al. 2013; Bekkouche and Worsaae 2016; Saponi et al. 2024a; Minowa et al. 2025).

Kolicka et al. (2020) have challenged this scenario by proposing that the basal position of certain marine species along the Oiorpata evolutionary branch, as indicated by phylogenetic analyses based on nuclear genes (and mtCOI), might be an artefact resulting from a long branch attraction (LBA) effect (Bergsten 2005). The LBA may lead to these marine species appearing closer to other unrelated, early-diverging, long-branched chaetonotidan clades, such as the Xenotrichulidae and Muselliferidae (e.g., Kånneby et al. 2013; Bekkouche and Worsaae 2016). Indeed, in all previous phylogenetic studies involving marine species of the genus *Aspidiophorus* and the subgenus *Schizochaetonotus* (genus *Chaetonotus*), the length of their branches is significantly greater (i.e., about three times longer) than that of other Oiorpata, as noted by Kolicka et al. (2020). Their branch lengths are also somewhat comparable to the long branches of Xenotrichulidae. When *Aspidiophorus* and *Schizochaetonotus* species are excluded from the analyses, the phylogenetic scenario changes, revealing other taxa like *Bifidochaetonotus* as early divergent lineages within the Oiorpata (Kolicka et al. 2020). This new scenario suggests that the extant Oiorpata likely originated in freshwater environments, followed by a secondary invasion of the sea by all the marine species within this group.

Our phylogenetic analyses, similar to the studies mentioned earlier, show Xenotrichulidae as the sister group to Oiorpata, with the marine species *Aspidiophorus tentaculatus* and *Chaetonotus neptuni* (subgenus *Schizochaetonotus*) representing the earliest diverging lineages of the latter group. Moreover, in our analyses, we found that the branch lengths leading to *A.*

293 *tentaculatus* and *C. neptun*i are comparable to those of other Oiorpata species. This suggests that
294 their basal position is not a result of long-branch attraction, which challenges the hypothesis
295 proposed by Kolicka et al. (2020) while revitalizing the evolutionary scenario envisioned by earlier
296 studies that posited a marine origin for extant Oiorpata. Furthermore, in our study, the derived
297 position of *Chaetonotus apolemmus* suggests that a secondary invasion of the marine
298 environment has occurred, but this phenomenon applies only to some lineages, as previously
299 found by the seminal work of Kånneby et al. (2013). Our study also provides an indication of
300 *Neodasys* being a chaetonotidan branch, implied by the current classification, although with low
301 statistical support (Figure 3).
302 The classification of *Neodasys* has significantly evolved over time, highlighting the
303 challenges in achieving consistent hypotheses regarding phylogenetic relationships. Originally
304 established by Remane (1927) within the Macrodasyida, this intriguing genus faced a
305 transformative reclassification due to meticulous histological analyses of the pharynx in *Neodasys*
306 *chaetonotoideus*. These studies revealed a striking morphological feature: the pharyngeal lumen,
307 when viewed in cross-section, forms an inverted Y shape. This distinctive characteristic aligns with
308 the hallmark structure found in all Chaetonotida, ultimately justifying its important shift into this
309 category (Remane 1936). The distinct differences in body shape, reproductive biology, and
310 adhesive apparatus of *Neodasys* compared to other chaetonotidans led Hondt (1971) to establish
311 two suborders: Multitubulatina, which includes *Neodasys*, and Paucitubulatina, which
312 encompasses the other chaetonotidans. This classification emphasizes the clear disparities
313 between *Neodasys* and the rest of the chaetonotidans (Ruppert, 1991). Since then, *Neodasys*,
314 which currently comprises three described species (Saponi and Todaro 2024), has been included in
315 several phylogenetic reconstructions based on morphological or molecular datasets (Marotta et al.
316 2005; Todaro et al. 2003, 2006; Petrov et al. 2007; Kieneke et al. 2008; Paps & Riutort 2012);

however, it has never been convincingly assigned to either order. Like previous studies, our phylogenetic analyses based on 13 mitochondrial protein coding genes failed to consistently determine the position of *Neodasys*, highlighting the urgent need of analyses based on a broader sampling of species and genes.

Our results show that structures of the mtDNA in gastrotrichs are order specific; for example 12-13 PCGs in Chaetonotida vs. 11PCGs in Macrodasyida, high GC content in Chaetonotida vs. low GC content in Macrodasyida, 0-1 tandem repeats in Chetonotida vs. more than one repeats in Macrodasyida, almost or exclusively unidirectional mtDNA in Chaetonotida vs. non unidirectional mtDNA Macrodasyida. Notably, the gene synteny (the same gene order) is perfectly conserved among all investigated members of Oiorpata, even among those from different genera and families. Conversely, the situation is quite different in the order Macrodasyida, where there is no synteny (the gene order is not conserved) even among members of the same genus, as illustrated by *Urodasys*. These observed structural variations of the gastrotrich mitogenomes may be related to several factors, with mtDNA stability (e.g., less prone to mutations) being perhaps the most important. Chaetonotidan mtDNA appears to be more stable and less prone to mutations than macrodasyidan mtDNA, likely due to its higher GC content and, more notably, fewer tandem repeats (Yakovchuk et al. 2006; Chen and Skylaris 2025) (Table 1). It is possible that this stability facilitated the conservation of the gene order (Figure 4) and gene transcriptional directionality (Table 1, Figure 5) in chaetonotidans, preserving their mtDNA from rapid mutation as it was suggested in other organisms (Nguyen et al. 2020). In contrast, macrodasyidan mtDNA is prone to higher mutation rates, because it is characterized by lower GC content, a higher number of tandem repeats, variable gene order, and variable gene directionality. Indeed, it was shown that macrodayidans exhibit a generalized high mutation rate, as indicated by previous phylogenetic analyses based on nuclear and mitochondrial genes. These studies reveal

that members of this lineage have higher nucleotide and amino acid substitution rates and longer branch lengths, when compared to chaetonotidans (e.g., Bekkouche and Worsaae 2016). Increased nucleotide substitution rates may lead to increased gene rearrangement rates, as proposed in other metazoans (e.g., for insects as discussed in Shao et al. 2003, or for annelid worms as discussed in Struck et al. 2023). Codon Usage Bias (CUB) frequencies may influence mitogenome structural variation as well. For instance, CUB analysis revealed that CUB patterns may reflect mutational bias and natural selection, as suggested for reptiles (Montana-Lozano et al. 2023). Lastly, tRNA genes can also play a crucial role in mitochondrial genome rearrangements affecting its architecture (Prada and Boore 2019; Morena-Carmona et al. 2021). Indeed, we can notice that while the number of tRNAs is conserved in chaetonotidans (22), it is highly variable in macrodasyidans (17-22). We are not, however, excluding that some tRNA might not be detected with the algorithms integrated in MITOS2 or with manual alignment due to their extreme divergence in macrodasyidans.

Interestingly, *Turbanella ambronensis* appears to be an exception among studied macrodasyidans, exhibiting a relatively high GC content (46%) compared to other macrodasyidan species (20-31%). Notably, *T. ambronensis* also diverges in gene directionality: only six tRNAs are encoded on the on the reverse ("–") strand, while all other genes are located on the forward ("+") strand, which corresponds to the 5'→3' direction of the reference scaffold. In contrast, most macrodasyidan species show a more balanced distribution of genes across both strands. A similar trend emerges from codon usage bias (CUB) analysis: for instance, *T. ambronensis* shows a codon preference more closely aligned with chaetonotidans than with other macrodasyidans (Table 2). Indeed, all observed chaetonotidan species exhibit high GC content and predominantly, if not exclusively, unidirectional mitochondrial genomes.

These observations suggest a possible link between GC content and codon usage bias in mtDNA. Although gene directionality in *T. ambronensis* remains distinct from chaetonotidan species, which typically exhibit almost unidirectional mitochondrial genomes, it shows a partial resemblance to *Oiorpata,* where only three tRNAs are encoded on the ("–") strand. This contrasts with most macrodasyidan species, in which a substantial portion of protein-coding genes are located on the ("–") strand. These intermediate features in *T. ambronensis* may reflect lineage-specific variation or partial convergence in mitochondrial genome organization. Alternatively, it is possible that these features represent ancestral characteristics, retained in this species but independently lost or modified in other lineages due to relaxed selective pressure or lineage-specific adaptation. However, this remains a working hypothesis, and additional genomic data from *T. ambronensis* is needed to verify and clarify these patterns.

We also tried to explore potential connections between mitochondrial genome architecture and the lifestyle of the studied species, as inferred from their morphology and anatomy. Although we did not observe a direct correlation between mitogenome structure and marine versus freshwater habitats (e.g., both marine and freshwater species of *Oiorpata* exhibit conserved mitogenome features), certain anatomical and metabolic traits may still influence mitochondrial organization. For example, dorsoventral muscles are typically found in flat, hermaphroditic taxa inhabiting sandy marine environments (e.g., Xenotrichulidae), but are generally absent in flask-shaped, benthic freshwater taxa (e.g., Chaetonotidae). It has been proposed that these muscles originated in marine interstitial hermaphrodites and were progressively reduced or lost as species transitioned to epibenthic or periphytic lifestyles and parthenogenetic reproduction (Leasi et al. 2006; Leasi and Todaro 2008). These anatomical changes may reflect shifts in bioenergetic demands, potentially influencing mitogenome evolution. Supporting the link between mitogenome structure and anatomical traits of the organism, we observed gene duplications in two early-branching

388 species of *Urodasys*: *U. mirabilis* (cox2 duplication) and *U. apuliensis* (nad4 duplication). These
389 species also differ from other *Urodasys* taxa in reproductive morphology, notably lacking
390 accessory copulatory organs (Cesaretti et al. 2024), which may likewise point to distinct energetic
391 or developmental requirements. However, it is challenging to attribute the structural variability of
392 the macrodasyidans' mitogenome to specific factors. From a biological standpoint, a notable
393 difference between chaetonotidans from the Oiorpata group and macrodasyidans lies in their
394 reproductive methods: these chaetonotidans reproduce through apomictic parthenogenesis, while
395 macrodasyidans reproduce via cross-fertilization (Kieneke and Schmidt-Rhaesa 2019; Cesaretti et
396 al. 2024; Gammuto et al. 2024). While intriguing, any potential association between reproductive
397 mode and the absence or nuclear transfer of *atp6* and *atp8* genes remains speculative and
398 requires further investigation, particularly given that most metazoan mitochondrial genomes
399 retain these genes regardless of reproductive strategy.
400 In this highly uncertain framework, we outline three non-mutually exclusive scenarios
401 regarding the evolution of the mitochondrial genome in Gastrotricha. The most parsimonious
402 explanation is genetic drift, which likely underlies the independent retention, loss, or transfer of
403 ATP synthase genes across lineages. At the same time, we note two additional possibilities that
404 may warrant future investigation. (i) Within the mitogenome evolution module suggested by Kelly
405 (2021), the loss or transfer of mitochondrial genes to the nucleus could be associated with
406 bioenergetic demands in hermaphroditic macrodasyidans and marine hermaphroditic
407 chaetonotidans, although this remains highly tentative. (ii) The retention of ATP synthase-related
408 genes in parthenogenetic chaetonotidans could be consistent with lineage-specific regulatory
409 adaptations (e.g., mitochondrial stress responses or specialized transcriptional or translational
410 mechanisms during evolution Allen 2015; Casanova et al. 2023; Butenko et al. 2024), but this
411 hypothesis requires further genomic data to evaluate. Additionally, although we identified *atp6*

412 gene blast hits in the nuclear nodes of nearly all macrodasyidans and no hits for *atp8*, we cannot
413 rule out the possibility that these genes remain undetected in other nuclear datasets (Kohn et al.
414 2012). This limitation may stem from challenges in assembly and annotation in Gastrotricha, as
415 seen in related taxa such as Platyhelminthes (e.g., Shimada et al. 2023).
416 Practically nothing is known about the metabolic pathways of gastrotrichs, although a few
417 hypotheses have been suggested in the past, highlighting the possibility of anaerobiosis in some
418 species that occur deeper in the sediments (Boaden 1974, 1985; Todaro et al. 2000; Balsamo et al.
419 2007). While adaptation to anoxic conditions may contribute to accelerated mitochondrial
420 genome remodeling, the directionality and mechanisms of such changes remain complex and
421 potentially lineage-specific. Our results suggest that once an evolutionary path has been taken, it
422 is often difficult to revert back to a previous state. This is exemplified by the macrodasyidan
423 species *Urodasys viviparus* and *Anandrodasys agadasys*, which are parthenogenetic and still
424 maintain a reduced number of mitochondrial genes. Although a direct link between reproductive
425 mode and the retention of specific mitochondrial genes cannot be definitively established, the
426 persistence of this genomic pattern raises intriguing questions about the evolutionary inertia of
427 organelle architecture and the interplay between reproductive strategy, ecology, and
428 mitochondrial function.

429 **In conclusion**, our observations suggest the following tentative hypotheses:

430 1. Mitogenome conservation within Oiorpata and structural variability among Macrodasyida
431 may be influenced by genomic features such as lower GC content and elevated tandem
432 repeats, potentially contributing to reduced DNA stability in Macrodasyida.
433 2. Structural differences in mitochondrial genomes may coincide with lineage-specific aspects
434 of reproductive biology in gastrotrichs; however, these associations remain speculative and

require further investigation. For now, the genetic drift remains the most parsimonious explanation, especially given the limitations of phylogenetic non-independence.

3. Other factors that may play a role in shaping mitochondrial genome architecture may include lineage-specific codon usage patterns, tRNA rearrangements, elevated nucleotide substitution rates during evolution, and anatomical or metabolic adaptations associated with different lifestyles.

Together, these results highlight a striking separation in mitogenome evolution, from rigid order to radical variation across the two principal lineages of Gastrotricha. They underscore the importance of lineage-specific factors in shaping mitochondrial genome architecture and demonstrate how expanded taxonomic sampling can reveal unexpected complexity in genome evolution across Metazoa.

Additionally, beyond these biological insights, our study offers two practical contributions to the field: (i) the generation of 21 new mitochondrial genomes, which is important in advancing the field of mitochondrial genetics, and (ii) the successful demonstration of the WGA and Blobology pipeline (see details in Methods) as an effective approach for obtaining multiple sequences from single microeukaryotes in gastrotrich studies. This achievement is particularly valuable when working with rare and old specimens containing limited genomic material. Although the focus of this study was restricted to retrieving mitochondrial genomes, the pipeline holds great potential for broader applications. It can be utilized in future studies to recover hundreds of genes, enabling research in multigene phylogeny, functional genomics, and comparative genomics.

MATERIAL AND METHODS

Species selection

For comparison purposes, we chose 10 chaetonotidan and 12 macrodasyidan species with variable ecological adaptations (marine vs. freshwater) and reproductive modalities (hermaphroditic vs. parthenogenetic). Two of these species, both freshwater belonging to the order Chaetonotida, already have published mitochondrial genomes (Table 3). The other species were collected during several sampling campaigns (e.g., Curini-Galletti et al. 2012; Todaro et al. 2012, 2014, 2017, 2019). In brief, from freshwater samples, gastrotrichs were obtained by stirring the samples with a plastic pipette, and aliquots of the sediment-water mixture were decanted into 9 cm diameter plastic Petri dishes and analyzed under Wild-M8 stereo microscope. Individual gastrotrichs were picked with a glass micro-pipette and mounted on a slide in a drop of 1% $MgCl_2$ solution to be analyzed under compound light microscope. For marine samples, 1–2 spoons of the fauna-enriched top layer of sandy sample were placed into a small vessel with a 7% $MgCl_2$ added to cover the sand (as it is described in Todaro et al. 2019). The material is then swirled and allowed to sit for 5 minutes. After this the supernatant was decanted into Petri dishes, analyzed under stereo microscope and individual gastrotrichs were mounted on a slide for further analysis as it was done for freshwater species.

The morphological identification was conducted on living, relaxed specimens under a Nikon eclipse 90i or a Leitz Dialux 20 microscope equipped with differential interference contrast optics (DIC) and fitted with a Nikon DS-Fi3 camera operated by a NIS-Elements D software (v 4.60.00). After taking high-resolution photographs for vouchers (Figure 2), the specimens were retrieved from the slides, transferred to 0.5mL centrifuge tubes filled with 96% ethanol, and stored at -20 ° C for later DNA analysis.

481 **DNA extraction and amplification**

482 Ethanol-preserved specimens were washed in clean absolute ethanol, individually
483 transferred into sterile 0.5mL tubes using a glass micro-pipette and left overnight at 25 °C in a
484 cleaned ISCO micra 18 incubator to eliminate any residual ethanol through evaporation.
485 Subsequently, 4 µl of Phosphate-buffered saline solution (PBS) was added to each sample. The
486 samples were then processed for DNA extraction and Whole Genome Amplification (WGA) using
487 the REPLI-g Single Cell Kit (QIAGEN®) following the manufacturer's instructions (i.e., lysis and
488 denaturation at room temperature at 65°C for 10 minutes, amplification with incubation at 30°C
489 for 8 hours, and inactivation of DNA Polymerase at 60°C for 3 minutes). The resulting amplified
490 DNA product was validated for the presence of gastrotrich DNA footprint through Polymerase
491 Chain Reaction (PCR) amplification of the 18S rDNA gene and Sanger sequencing. For each 40 µl
492 PCR reaction volume 2ul of 1:100 diluted DNA template, 29.38 µL of water, 4 µL of reaction buffer,
493 4 µL of dNTPs in solution, 0.4 µL of paired primers, and 0.22 µL of Takara Taq-polymerasys was
494 used. The primer combinations and thermal cycler program used for validation PCR are available in
495 Suppl. Mat. 5. The PCR products were purified with the Monarch PCR & DNA Cleanup Kit (New
496 England BioLabs Inc., Ipswich, MA, USA) and subsequently sent for Sanger sequencing to the
497 Macrogen Europe Laboratory in Milan, Italy. Reads resulting from the Sanger sequencing were
498 assembled manually using BioEdit (Hall et al. 1999) into almost complete 18S rDNA sequences and
499 examined with GenBank online Blast tool (https://blast.ncbi.nlm.nih.gov/Blast.cgi). The validated
500 WGA DNA samples were then sent to Macrogen Europe (https://www.macrogen-europe.com/)
501 and processed with a TrueSeq DNA PCR Free Library kit and *de novo* whole genome sequencing
502 (WGS) at NovaSeq 6000 Illumina Platform to generate a total of 40 million reads (paired-ends
503 2 × 150 bp) for each sample.

504

505 **Mitochondrial genome assembly and annotation**

506 The obtained sequence data was analyzed through the Blobology pipeline followed by
507 Gammuto et al. (2024). In brief: the quality of the reads was evaluated through the FASTQC
508 software (Andrews et al. 2010). The reads were then trimmed for quality and adapters whenever
509 it was needed with TRIMMOMATIC 0.39 (Bolger et al. 2014) setting the minimum length to 140 bp
510 and leaving the other parameters as default. The remaining paired reads were assembled through
511 the SPAdes v.3.6.0 software (Bankevich et al. 2012) to obtain a preliminary assembly of the whole
512 genomic content of the sample (i.e., gastrotrich nuclear genome, gastrotrich mitochondrial
513 genome and eventually associated bacteria and ingested food). The assembled contigs matching
514 to mitochondrial genes were identified through tBlastn analysis using sequences of protein coding
515 genes of *Lepidodermella squamata* (GenBank acc. KP965862) and *Litigonotus ghinii* (GeneBank
516 acc. PP105008) mitochondrial genomes as queries. Where needed (i.e., in case the whole
517 mitochondrial genome was not assembled in a single circular contig), reads mapped to the so
518 identified contigs were extracted from the original set and separately assembled using SPAdes in
519 order to obtain the whole mitochondrial genome in a single contig. Ultimately, all mitogenomes
520 were assembled as single contigs, except for four species in which two overlapping nodes were
521 manually joined and confirmed to form circular genomes. Prediction and annotation of
522 mitochondrial genes were performed using MITOS2 (Bernt et al. 2013) integrated in the Galaxy
523 platform with the RefSeq63 Metazoan dataset and with the invertebrate mitochondrial genetic
524 code. Annotated gene boundaries were checked and fixed manually through alignments, Blastn,
525 Blastp and NCBI ORF finder when necessary. Additionally, tRNA genes were predicted using
526 *tRNAscan-SE* (Lowe and Chan 2016) with the invertebrate mitochondrial code, and results were
527 cross-validated through manual inspection and comparison with MITOS2 predictions.

To verify the accuracy of the assemblies for *Urodasys apuliensis* and *U. mirabilis*, as well as the annotation of their mtDNA (for which a potential gene duplication events were observed), their WGA templates were re-sequenced using Oxford Nanopore technology, and the results were compared. A second specimens of *X. intermedia* from a different population was investigated using the Oxford nanopore technology to look for possible differences due to technology and/or population genetics. For Oxford nanopore sequencing, first the amplified genomic DNA was cleaned with AMPure XP beads and then processed for endonuclease digestion using a T7 Endonuclease digestion kit (adapted from Lee et al. 2023). Next, the product was processed for native barcoding and adapter ligation using Native Barcoding Kit 24V14. The reads were assembled with Fly v.2.9.5 following the protocol of Lee et al. 2023. Gene duplication detected in *U. apuliensis* and *U. mirabilis* during the reads assembly was later confirmed by comparison of crystal structure (obtained with Alphafold3, Abramson et al. 2024) and specific core regions conserved across all sequences. In subsequent phylogenetic analyses, only the gene copy with the best alignment fit was used for these two species presenting duplications.

To confirm completeness and circularity of mtDNA in specimens where the start and end of the assembled sequences did not overlap (n=7 out of 21), we inferred completeness based on gene content and genome structure. As a proof of concept, we designed PCR primers targeting the two free extremities of two representative linear assemblies. Successful amplification across the predicted junction confirmed their circular topology (see details in Suppl. Mat. 6).

ATP gene search in macrodasyidan datasets

To investigate the presence/absence of *atp* genes in the order Macrodasyida we employed both a heuristic approach (Blast; Camacho et al. 2009) and an HMM-based method (Exonerate; Slater & Birney 2005). In both cases, *atp* sequences from Chaetonotida were used as queries

against Macrodasyda assemblies, and a completeness matrix (presence/absence) was generated (Suppl. Mat. 4). To test whether *atp* has translocated from the mitochondrion to the nucleus, we analyzed the scaffolds containing *atp* using MITOS2 (Bernt et al. 2013). As an additional validation, the putative *atp* sequences were compared against the non-redundant protein database (nr) using Blastx, confirming their identity as *atp*. Protein integrity analysis GetOrf (EMBOSS, Rice et al. 2000) was used to check the length of functional *atp* sequences. TargetP-2.0 (Emanuelsson et al. 2000) and MitoProt (Claros and Vincens 1996) web-based tools were used to assess the presence of mitochondrial targeting signals in *atp* sequences.

Phylogenetic analyses

Mitochondrial protein coding genes were used for the phylogenetic analysis. The mitochondrial amino acid sequences obtained from MITOS2 annotation output were aligned separately for each gene with MEGA X, using the integrated Muscle algorithm (Kumar et al. 2018). Next, all the alignments were concatenated into a final single matrix using MEGA X, resulting in 4150 aminoacid sites. Additionally, two free-living plathyhelminth species *Nematoplana* sp. (LC760198) and *Macrostomum lignano* (MF078637) were added to this analysis as an outgroup. Phylogenetic trees were built using Maximum Likelihood (ML) and Bayesian Inference (BI) approaches. ML analyses were performed in IQ-TREE v.1.6.10 (Nguyen et al. 2015) with the following settings and considerations: i) we used the best-fit partition models according to BIC (Bayesian information criterion) for 13 aminoacid dataset identified by IQ tree (see Suppl. Mat. 7), ii) edge-linked partition option, iii) 1000 ultrafast bootstrap pseudo-replicates with the SH-aLRT support activated to ensure additional confirmation for Ultrafast bootsrap values (i.e., to consider clade confident with the values SH-aLRT ≥80% and UFbootstrap ≥95%); and iv) the rest of the parameters were left as default. For the Bayesian analyses, the amino acid dataset was run in the

program MrBayes v.3.2.7 (Ronquist et al. 2012) with 200000 generations, with gamma distribution across invariable sites and fixed mtrev amino acid substitution model, with a sampling frequency of trees and parameters at 100, and with a relative burn-in fraction of 25%. Convergence of the MCMC analyses was confirmed with the in-built diagnostics of the program with the average standard deviation of split frequencies was 0.006792, the potential scale reduction factor converged to 1.00 for all parameters, the effective sample sizes (EES) of all parameters were >200 (i.e., min. ESS = 5.44E+08, av. ESS = 5.54E+08). The ML and BI trees were computed as unrooted and then were rooted in FigTree v.1.4.3 (http://tree.bio.ed.ac.uk/software/figtree/), with the flatworm species used as outgroup. Since both methods generated the same topology, ML tree is presented combining both Bootstrap (BB) and Posterior Probability (PP) support values obtained from both methods. The final tree was edited for better visualization using CorelDraw X7 (Corel Corporation, Ottawa, Canada). As the number of protein coding genes varied among the analysed species, we ran an additional phylogenetic analysis involving solely the genes present in all the investigated species, looking for possible effects of gene sampling (Suppl. Mat.1).

Mitochondrial genome structural analysis

Mitochondrial genome structure and specificity were analyzed by using several tools. The length of the mitochondrial genomes, number of the protein coding genes, their position, order (gene synteny), and transcriptional direction were observed from annotation reports generated by MITOS2 integrated in Galaxy platform (Arab et al. 2017, Donath et al 2019, The Galaxy Community 2024) and compared through species. Mitochondrial genome base count and GC content were calculated using BIC online calculator (https://www.biologicscorp.com/tools/GCContent/). Repeated elements were identified with Tandem Repeats Finder (Benson 1999) online tool (https://tandem.bu.edu/trf/home). Codon usage analysis was done using MEGA X software package (Kumar et al. 2018). The mitochondrial genome maps were created using circularMT

toolkit (Goodman and Carr 2024). To examine the relationship between mitochondrial genome features and phylogenetic groupings, we conducted a series of statistical tests in PAST version 5.2.1 (Hammer et al. 2001). Specifically, we assessed intergroup differences in GC content and repeat number and evaluated correlations among mitochondrial traits. A Student's *t*-test was performed to compare GC content between the two orders. To assess differences in tandem repeat content, we employed the non-parametric Mann-Whitney *U* test, as repeat counts did not conform to normality assumptions. We further explored the potential association between genome architecture and sequence composition by applying Spearman's rank correlation tests between (i) GC content and tandem repeat abundance, and (ii) GC content and transcriptional directionality (quantified as the proportion of genes encoded on the same strand).

REFERENCES

Abramson J, Adler J, Dunger J, Evans R, Green T, Pritzel A, Ronneberger O, Willmore L, Ballard AJ, Bambrick J, et al. 2024. Accurate structure prediction of biomolecular interactions with AlphaFold 3. Nature 630:493–500.

Al Arab M, Höner zu Siederdissen C, Tout K, Sahyoun AH, Stadler PF, Bernt M. 2017. Accurate annotation of protein-coding genes in mitochondrial genomes. Mol Phylogenet Evol 106:209–216.

Allen JF. 2015. Why chloroplasts and mitochondria retain their own genomes and genetic systems: colocation for redox regulation of gene expression. Proc Natl Acad Sci USA 112:10231–10238.

Allio R, Donega S, Galtier N, Nabholz B. 2017. Large variation in the ratio of mitochondrial to nuclear mutation rate across animals: implications for genetic diversity and the use of mitochondrial DNA as a molecular marker. Mol Biol Evol 34:2762–2772.

Andrews S. 2010. FastQC: a quality control tool for high throughput sequence data. Available from: http://www.bioinformatics.babraham.ac.uk/projects/fastqc/

Balsamo M, Guidi L, Pierboni L, Marotta R, Todaro MA, Ferraguti M. 2007. Living without mitochondria: spermatozoa and spermatogenesis in two species of Urodasys (Gastrotricha, Macrodasyida) from dysoxic sediments. Invertebr Biol 126:1–9.

Bankevich A, Nurk S, Antipov D, Gurevich AA, Dvorkin M, Kulikov AS, Lesin VM, Nikolenko SI, Pham S, Prjibelski AD, et al. 2012. SPAdes: a new genome assembly algorithm and its applications to single-cell sequencing. J Comput Biol 19:455–477.

Bekkouche N, Worsaae K. 2016. Neuromuscular study of early branching Diuronotus aspetos (Paucitubulatina) yields insights into the evolution of organs systems in Gastrotricha. Zool Lett 2:21.

Benson G. 1999. Tandem repeats finder: a program to analyze DNA sequences. Nucleic Acids Res 27:573–580.

Bergsten J. 2005. A review of long-branch attraction. Cladistics 21:163–193.

Bernt M, Merkle D, Middendorf M. 2008. An algorithm for inferring mitochondrial genome rearrangements in a phylogenetic tree. In: RECOMB-CG 2008. Lect Notes Bioinform 5267:143–157.

Bernt M, Donath A, Jühling F, Externbrink F, Florentz C, Fritzsch G, Pütz J, Middendorf M, Stadler PF. 2013. MITOS: improved de novo metazoan mitochondrial genome annotation. Mol Phylogenet Evol 69:313–319.

Boaden PJS. 1974. Three new thiobiotic Gastrotricha. Cah Biol Mar 15:367–378.

Boaden PJS. 1985. Why is a gastrotrich? In: Conway Morris S, George JD, Gibson R, Platt HM, editors. The origins and relationships of lower invertebrates. Syst Assoc Spec 28:248–260.

Bolger AM, Lohse M, Usadel B. 2014. Trimmomatic: a flexible trimmer for Illumina sequence data. Bioinformatics 30:2114–2120.

Boore JL. 1999. Animal mitochondrial genomes. Nucleic Acids Res 27:1767–1780.

Butenko A, Lukeš J, Speijer D, et al. 2024. Mitochondrial genomes revisited: why do different lineages retain different genes? BMC Biol 22:15.

Camacho C, Coulouris G, Avagyan V, Ma N, Papadopoulos J, Bealer K, Madden TL. 2009. BLAST+: architecture and applications. BMC Bioinformatics 10:421.

Casanova A, Wevers A, Navarro-Ledesma S, Pruimboom L. 2023. Mitochondria: it is all about energy. Front Physiol 14:1114231.

Cesaretti A, Kosakyan A, Saponi F, Todaro MA. 2024. Gaining and losing on the way: the evolutionary scenario of reproductive diversification in genus Urodasys (Macrodasyida: Gastrotricha) inferred by multi-gene phylogeny. Zool J Linn Soc 202:zlae148.

Cesaretti A, Kosakyan A, Saponi F, Todaro MA. 2025. Improved taxonomic and gene sampling advance the knowledge of deep relationships within Macrodasyida (Gastrotricha). Cladistics 41: 6. doi: 10.1111/cla.70013Chen H, Skylaris CK. 2021. Analysis of DNA interactions and GC content with energy decomposition in large-scale quantum mechanical calculations. Phys Chem Chem Phys 23:8891–8899.

Claros MG, Vincens P. 1996. Computational method to predict mitochondrially imported proteins and their targeting sequences. Eur J Biochem 241(3):779–786.

Curini-Galletti M, Artois T, Delogu V, De Smet WH, Fontaneto D, Jondelius U, Leasi F, Martinez A, Meyer-Wachsmuth I, Nilsson KS, et al. 2012. Patterns of diversity in soft-bodied meiofauna: dispersal ability and body size matters. PLoS One 7:e33801.

Dowling KD, Wolff JN. 2023. Evolutionary genetics of the mitochondrial genome: insights from Drosophila. Genetics 224:iyad036.

D'Hondt JL. 1971. Gastrotricha. Oceanogr Mar Biol Annu Rev 9:141–192.

Donath A, Jühling F, Al-Arab M, Bernhart SH, Reinhardt F, Stadler PF, Middendorf M, Bernt M. 2019. Improved annotation of protein-coding gene boundaries in metazoan mitochondrial genomes. Nucleic Acids Res 47:10543–10552.

Egger B, Lapraz F, Tomiczek B, Müller S, Dessimoz C, Girstmair J, Škunca N, Rawlinson KA, Cameron CB, Beli E, et al. 2015. A transcriptomic-phylogenomic analysis of the evolutionary relationships of flatworms. Curr Biol 25:1347–1353.

Emanuelsson O, Nielsen H, Brunak S, von Heijne G. 2000. Predicting subcellular localization of proteins based on their N-terminal amino acid sequence. J Mol Biol 300(4):1005–1016.

Feng S, Pozzi A, Stejskal V, et al. 2022. Fragmentation in mitochondrial genomes in relation to elevated sequence divergence and extreme rearrangements. BMC Biol 20:7.

Gammuto L, Cesaretti A, Sarno D, Fontaneto D, Todaro MA. 2024. Molecular phylogenetic position and description of a new genus and species of freshwater Chaetonotidae (Gastrotricha: Chaetonotida: Paucitubulatina), and the annotation of its mitochondrial genome. Invertebr Syst 38:IS23059.

Gibb GC, Condamine F, Kuch M, Enk J, Moraes-Barros N, et al. 2016. Shotgun mitogenomics provides a reference phylogenetic framework and timescale for living Xenarthrans. Mol Biol Evol 33:621–642.

Gissi C, Iannelli F, Pesole G. 2008. Evolution of the mitochondrial genome of Metazoa as exemplified by comparison of congeneric species. Heredity 101:301–320.

Goodman SJ, Carr IM. 2024. Drawing mitochondrial genomes with circularMT. Bioinformatics 40:btae450.

Golombek A, Tobergte S, Struck TH. 2015. Elucidating the phylogenetic position of Gnathostomulida and first mitochondrial genomes of Gnathostomulida, Gastrotricha and Polycladida (Platyhelminthes). Mol Phylogenet Evol 86:49–63.

Hall TA. 1999. BioEdit: a user-friendly biological sequence alignment editor and analysis program for Windows 95/98/NT. Nucleic Acids Symp Ser 41:95–98.

Hammer Ø, Harper DAT, Ryan PD. 2001. PAST: paleontological statistics software package for education and data analysis. Palaeontol Electron 4:9.

694 Hebert PDN, Ratnasingham S, deWaard JR. 2003. Barcoding animal life: cytochrome c oxidase
695 subunit 1 divergences among closely related species. Proc Biol Sci 270:S96–S99.

696 Kånneby T, Todaro MA, Jondelius U. 2013. Phylogeny of Chaetonotidae and other Paucitubulatina
697 (Gastrotricha: Chaetonotida) and the colonization of aquatic ecosystems. Zool Scr 42:88–105.

698 Kelly S. 2021. The economics of organellar gene loss and endosymbiotic gene transfer. Genome
699 Biol 22:345.

700 Kieneke A, Riemann O, Ahlrichs WH. 2008. Novel implications for the basal internal relationships
701 of Gastrotricha revealed by an analysis of morphological characters. Zool Scr 37:429–460.

702 Kieneke A, Schmidt-Rhaesa A. 2014. Gastrotricha. In: Schmidt-Rhaesa A, editor. Handbook of
703 Zoology. Gastrotricha, Cycloneuralia and Gnathifera. Vol. 3: Gastrotricha and Gnathifera. Berlin: De
704 Gruyter. p. 1–134.

705 Kohn AB, Citarella MR, Kocot KM, Bobkova YV, Halanych KM, Moroz LL. 2012. Rapid evolution of
706 the compact and unusual mitochondrial genome in the ctenophore, Pleurobrachia bachei. Mol
707 Phylogenet Evol 63:203–207.

708 Kolicka M, Dabert M, Olszanowski Z, Dabert J. 2020. Sweet or salty? The origin of freshwater
709 gastrotrichs (Gastrotricha, Chaetonotida) revealed by molecular phylogenetic analysis. Cladistics
710 36:458–480.

711 Križanová RF, Vďačný P. 2023. A Heterolepidoderma and Halichaetoderma gen. nov. (Gastrotricha:
712 Chaetonotidae) riddle: integrative taxonomy and phylogeny of six new freshwater species from
713 Central Europe. Zool J Linn Soc zlad079.

714 Kumar S, Stecher G, Li M, Knyaz C, Tamura K. 2018. MEGA X: molecular evolutionary genetics
715 analysis across computing platforms. Mol Biol Evol 35:1547–1549.

716 Lake NJ, Ma K, Liu W, et al. 2024. Quantifying constraint in the human mitochondrial genome.
717 Nature 635:390–397.

718 Laumer C, Bekkouche N, Kerbl A, Goetz F, Neves RC, Sørensen MV, Kristensen RM, Hejnol A, Dunn
719 CW, Giribet G, Worsaae K. 2015. Spiralian phylogeny informs the evolution of microscopic
720 lineages. Curr Biol 25:2000–2006.

721 Lavrov DV, Pett W. 2016. Animal mitochondrial DNA as we do not know it: mt-genome
722 organization and evolution in nonbilaterian lineages. Genome Biol Evol 8:2896–2913.

723 Leasi F, Rothe BH, Schmidt-Rhaesa A, Todaro MA. 2006. The musculature of three species of
724 gastrotrichs surveyed with confocal laser scanning microscopy (CLSM). Acta Zool 87:171–180.

725 Leasi F, Todaro MA. 2008. The muscular system of Musellifer delamarei (Renaud-Mornant, 1968)
726 and other chaetonotidans with implications for the phylogeny and systematization of the
727 Paucitubulatina (Gastrotricha). Biol J Linn Soc 94:379–398.

Lee YC, Ke HM, Liu YC, Lee HH, Wang MC, Tseng YC, Kikuchi T, Tsai IJ. 2023. Single-worm long-read sequencing reveals genome diversity in free-living nematodes. Nucleic Acids Res 51:8035–8047.

Lowe TM, Chan PP. 2016. tRNAscan-SE On-line: integrating search and context for analysis of transfer RNA genes. Nucleic Acids Res 8;44(W1):W54-7.

Manylov OG, Vladychenskaya NS, Milyutina IA, Kedrova OS, Korokhov NP, Dvoryanchikov GA, Aleshin VV, Petrov NB. 2004. Analysis of 18S rRNA gene sequences suggests significant molecular differences between Macrodasyida and Chaetonotida (Gastrotricha). Mol Phylogenet Evol 30:850–854.

Marotta R, Guidi L, Pierboni L, Ferraguti M, Todaro MA, Balsamo M. 2005. Sperm ultrastructure of Macrodasys caudatus (Gastrotricha: Macrodasyida) and a sperm-based phylogenetic analysis of Gastrotricha. Meiofauna Mar 14:9–21.

Minowa AK, Kieneke A, Campos A, Balsamo M, Plewka M, Guidi L, Araújo TQ, Garraffoni ARS. 2025. New branch on the tree of life of Gastrotricha: establishment of a new genus for limno-terrestrial species. Zool J Linn Soc 203:zlae166.

Montaña-Lozano P, Balaguera-Reina SA, Prada-Quiroga CF. 2023. Comparative analysis of codon usage of mitochondrial genomes provides evolutionary insights into reptiles. Gene 851:146999.

Morin PA, Archer FI, Foote AD, Vilstrup J, Allen EE, Wade P, Durban J, Parsons K, Pitman R, Li L, et al. 2010. Complete mitochondrial genome phylogeographic analysis of killer whales (Orcinus orca) indicates multiple species. Genome Res 20:908–916.

Moreno-Carmona M, Cameron SL, Prada Quiroga CF. 2021. How are the mitochondrial genomes reorganized in Hexapoda? Differential evolution and the first report of convergences within Hexapoda. Gene 791:145719.

Nesheva D. 2014. Aspects of ancient mitochondrial DNA analysis in different populations for understanding human evolution. Balkan J Med Genet 17:5–14.

Nguyen LT, Schmidt HA, von Haeseler A, Minh BQ. 2015. IQ-TREE: a fast and effective stochastic algorithm for estimating maximum-likelihood phylogenies. Mol Biol Evol 32:268–274.

Nguyen DT, Wu B, Xiao S, Hao W. 2020. Evolution of a record-setting AT-rich genome: indel mutation, recombination, and substitution bias. Genome Biol Evol 12:2344–2354.

Paps J, Riutort M. 2012. Molecular phylogeny of Acoelomorpha: evolutionary implications and methodological considerations. Mol Phylogenet Evol 63:208–212.

Petrov NB, Pegova AN, Manylov OG, Vladychenskaya NS, Mugue NS, Aleshin VV. 2007. Molecular phylogeny of Gastrotricha on the basis of a comparison of the 18S rRNA genes: rejection of the hypothesis of a relationship between Gastrotricha and Nematoda. Mol Biol 41:445–452.

Posth C, Yu H, Ghalichi A, et al. 2023. Palaeogenomics of Upper Palaeolithic to Neolithic European hunter-gatherers. Nature 615:117–126.

763 Prada CF, Boore JL. 2019. Gene annotation errors are common in the mammalian mitochondrial
764 genomes database. BMC Genomics 20:73.

765 Rice P, Longden I, Bleasby A. 2000. EMBOSS: the European Molecular Biology Open Software Suite.
766 Trends Genet 16:276–277.

767 Remane A. 1927. Gastrotricha. In: Grimpe G, editor. Die Tierwelt der Nord- und Ostsee. Leipzig:
768 Akademische Verlagsgesellschaft. p. 1–56. [In German]

769 Remane A. 1936. Gastrotricha. In: Bronns HG, editor. Klassen Ordnungen des Tierreichs, Band 4,
770 Abteilung II, Buch I, Teil 2, Liefrungen 1–2. Berlin: Akademie Verlagsgesellschaft. p. 1–242. [In
771 German]

772 Roberts NG, Gilmore MJ, Struck TH, Kocot KM. 2024. Multiple displacement amplification
773 facilitates SMRT sequencing of microscopic animals and the genome of the gastrotrich
774 *Lepidodermella squamata* (Dujardin 1841). Genome Biol Evol 16:evae254.

775 Ronquist F, Teslenko M, van der Mark P, Ayres DL, Darling A, Höhna S, Larget B, Liu L, Suchard MA,
776 Huelsenbeck JP. 2012. MrBayes 3.2: efficient Bayesian phylogenetic inference and model choice
777 across a large model space. Syst Biol 61:539–542.

778 Ruppert EE. 1991. Gastrotricha. In: Harrison FW, Ruppert EE, editors. Microscopic anatomy of
779 invertebrates. New York: Wiley & Sons. p. 41–109.

780 Saccone C, De Giorgi C, Gissi C, Pesole G, Reyes A. 1999. Evolutionary genomics in Metazoa: the
781 mitochondrial DNA as a model system. Gene 238:195–209.

782 Saponi F, Todaro MA. 2024a. Status of the Italian freshwater Gastrotricha biodiversity, with the
783 creation of an interactive GIS-based web map. Diversity 16:17.

784 Saponi F, Rebecchi C, Cesaretti A, Souid A, Todaro MA. 2024b. Nuovi dati sui gastrotrichi marini
785 della Sicilia = New data on marine gastrotrichs from Sicily. Biol Mar Medit 28:133–136.

786 Saponi F, Kosakyan A, Cesaretti A, Serra V, Todaro MA. 2025. Phylogenetic position of *Setopus*
787 (Gastrotricha, Paucitubulatina) among planktonic Gastrotricha, with the description of a new
788 species. Zool. Anz. DOI: 10.2139/ssrn.5737735 (in press)

789 Shao R, Dowton M, Murrell A, Barker SC. 2003. Rates of gene rearrangement and nucleotide
790 substitution are correlated in the mitochondrial genomes of insects. Mol Biol Evol 20:1612–1619.

791 Shtolz N, Mishmar D. 2023. The metazoan landscape of mitochondrial DNA gene order and
792 content is shaped by selection and affects mitochondrial transcription. Commun Biol 6:93.

793 Shimada D, Hiruta SF, Takahoshi K, Kajihara H. 2023. Does atp8 exist in the mitochondrial genome
794 of Proseriata (Metazoa: Platyhelminthes)? Anim Gene 30:200161.

795 Slater GS, Birney E. 2005. Automated generation of heuristics for biological sequence comparison.
796 BMC Bioinformatics 6:31.

797 Smith DR. 2016. The past, present and future of mitochondrial genomics: have we sequenced
798 enough mtDNAs? Brief Funct Genomics 15:47–54.

799 Souid A, Gammoudi M, Saponi F, El Cafsi M, Todaro MA. 2025. First investigation of the marine
800 gastrotrich fauna from the waters of North Tunisia, with the description of a new species of
801 *Halichaetonotus* (Gastrotricha, Chaetonotida). Diversity 17:17.

802 Struck TH, Wey-Fabrizius AR, Golombek A, Hering L, Weigert A, Bleidorn C, Klebow S, Iakovenko N,
803 Hausdorf B, Petersen M, et al. 2014. Platyzoan paraphyly based on phylogenomic data supports a
804 noncoelomate ancestry of spiralia. Mol Biol Evol 31:1833–1849.

805 Struck TH, Golombek A, Hoesel C, Dimitrov D, Elgetany AH. 2023. Mitochondrial genome evolution
806 in Annelida—a systematic study on conservative and variable gene orders and the factors
807 influencing its evolution. Syst Biol 72:925–945.

808 The Galaxy Community. 2024. The Galaxy platform for accessible, reproducible, and collaborative
809 data analyses: 2024 update. Nucleic Acids Res gkae410.

810 Todaro MA, Luporini P. 2022. Not too big for its mouth: direct evidence of a macrodasyidan
811 gastrotrich preyed in nature by a dileptid ciliate. Eur Zool J 89:785–790.

812 Todaro MA, Balsamo M, Guidi L, Bernhard JM. 2000. Peculiarità ultrastrutturali di un gastrotrico
813 microaerofilo. In: Atti 61° Congresso UZI. S. Benedetto del Tronto. p. 130. [In Italian]

814 Todaro MA, Littlewood DTJ, Balsamo M, Herniou EA, Cassanelli S, Manicardi G, Wirz A, Tongiorgi P.
815 2003. The interrelationships of the Gastrotricha using nuclear small rRNA subunit sequence data,
816 with an interpretation based on morphology. Zool Anz 242:145–156.

817 Todaro MA, Telford MJ, Lockyer AE, Littlewood DTJ. 2006. Interrelationships of the Gastrotricha
818 and their place among the Metazoa inferred from 18S rRNA genes. Zool Scr 35:251–259.

819 Todaro MA, Dal Zotto M, Jondelius U, Hochberg R, Hummon WD, Kånneby T, et al. 2012.
820 Gastrotricha: a marine sister for a freshwater puzzle. PLoS One 7:e31740.

821 Todaro MA, Leasi F, Hochberg R. 2014. A new species, genus and family of marine Gastrotricha
822 from Jamaica, with a phylogenetic analysis of Macrodasyida based on molecular data. Syst
823 Biodivers 12:473–488.

824 Todaro MA, Cesaretti A, Dal Zotto M. 2017. Marine gastrotrichs from Lanzarote, with a description
825 of a phylogenetically relevant species of *Urodasys* (Gastrotricha, Macrodasyida). Mar Biodivers
826 49:2109–2123.

827 Todaro MA, Sibaja-Cordero JA, Segura-Bermúdez OA, Coto-Delgado G, Goebel-Otárola N, Barquero
828 JD, Cullell-Delgado M, Dal Zotto M. 2019. An introduction to the study of Gastrotricha, with a
829 taxonomic key to families and genera of the group. Diversity 11:117.

830 Todaro MA, Dal Zotto M, Segura-Bermúdez OA, Cambronero-Bolaños R, Vargas JA, Sibaja-Cordero
831 JA. 2025. Biodiversity and distribution of marine gastrotricha along the Pacific coast of Costa Rica.
832 Estuar Coast Shelf Sci 313:109097.

Yahalomi D, Atkinson SD, Neuhof M, Chang ES, Philippe H, Cartwright P, Bartholomew JL, Huchon D. 2020. A cnidarian parasite of salmon (Myxozoa: *Henneguya*) lacks a mitochondrial genome. Proc Natl Acad Sci U S A 117:5358–5363.

Xiao Y, Niu G, Shi H, Wang Z, Du R, Li Y, Wei M. 2025. Enhanced dynamicity: evolutionary insights into amphibian mitogenomes architecture. BMC Genomics 26:261

Yakovchuk P, Protozanova E, Frank-Kamenetskii MD. 2006. Base-stacking and base-pairing contributions into thermal stability of the DNA double helix. Nucleic Acids Res 34:564–574.

Zrzavy J. 2003. Gastrotricha and metazoan phylogeny. Zool Scr 32:61–81.

DATA AVAILABILITY

Results of all analyses are available in the article and in its online supplementary material.

Mitochondrial genome sequences are available in the GenBank Nucleotide Database (https://www.ncbi.nlm.nih.gov/nucleotide/), with accession numbers PX661596-PX661616. Additionally, the alignments used to generate phylogenetic trees, as well as the mitochondrial genome sequences with their annotations, have been uploaded to Figshare (https://figshare.com/) and are available at the following DOIs: 10.6084/m9.figshare.29414720 and 10.6084/m9.figshare.30788585.

Funding

This research is funded under the National Recovery and Resilience Plan (NRRP), Mission 4 Component 2 Investment 1.4—Call for tender No. 3138 of 16 December 2021, rectified by Decree n. 3175 of 18 December 2021 of the Italian Ministry of University and Research funded by the European Union—NextGenerationEU. Project Code CN_00000033, Concession Decree No. 1034 of 17 June 2022 adopted by the Italian Ministry of University and Research, CUP E93C22001090001, Project title “National Biodiversity Future Center—NBFC”.

857 **Tables**

858 **Table 1.** The comparison of mitochondrial genome length, gene number, GC content, repeats and transcriptional order through studied

859 gastrotrich lineages.

Species (Chaetonotida)	Lenght of mt DNA (bp)	Number of PCGs	Number of tRNA	GC %	Number of tandem repeats	Transcriptional direction of the genes
Aspidiophorus tentaculatus	14547	13	22	38	1	unidirectional with exception trnT, trnD, trnP
Chaetonotus sp.	14426	13	22	40	0	unidirectional with exception trnT, trnD, trnP
Chaetonotus neptuni	14585	13	22	37	1	unidirectional with exception trnT, trnD, trnP
Chaetonotus schultzei	14503	13	22	40	1	unidirectional with exception trnT, trnD, trnP
Chaetonotus apolemmus	14597	13	22	40	0	unidirectional with exception trnT, trnD, trnP
Lepidodermella squamata	14558	13	22	40	1	unidirectional with exception trnT, trnD, trnP
Litigonotus ghinii	14384	13	22	42	0	unidirectional with exception trnT, trnD, trnP
Setopus sp.	14495	13	22	42	0	unidirectional with exception trnT, trnD, trnP
Xenotrichula intermedia 1	15095	12	22	31	0	unidirectional with no exception
Xenotrichula intermedia 2	14919	12	22	31	0	unidirectional with no exception
Neodasys sp.	14156	12	22	40	0	unidirectional with no exception
Species (Macrodasyida)						
Anandrodasys agadasys	16207	11	17	29	2	not unidirectional, cox1,cox2, cox3, cob, nad2, nad3, nad5, nad6, rrnL and trnH, S1, Y, R, F, W have opposite direction
Dolichodasys sp.	15893	11	22	26	0	not unidirectional, cox1,cox2, cox3, cob, nad1, nad2, nad4, nad4L nad6, rrnL and trnP,F, S1, S2, E, A, T, I, V, L1, C, M have opposite direction
Macrodasys meristocytalis	14402	11	21	29	9	not unidirectional, cox1, cox2, nad1, nad5, nad4l, rrnS, and trnT, E, Q, L1, P, S1, C have oposite direction
Megadasys sp.	14487	11	21	24	5	not unidirectional, cox1, cox3, nad2, nad6 rrnS, rrnL

						and trnQ, N, L1, D, C, l, S2, K, R, P, F, L2, S1, W have oposite direction
Paradasys sp.	12838	11	17	25	2	not unidirectional, cox1-0, nad4, nad4L, nad5, nad6 and trnV, M, A, P, S2;R, G, Y have opposite direction
Paraturbanella pallida	14981	11	22	20	7	not unidirectional, cox3, cox2, nad1-3, rrnL, rrnS and trnS1, S2, D, F, Y, K, S2; M, G, L2; P have opposite direction
Turbanella ambronensis	14297	11	17	46	1	not unidirectional, but only for tRNAs such as trnQ, N, L2, T, K, H, F have opposite direction
Urodasys bifidostylis	15624	11	19	21	8	not unidirectional, cox3, cox2, nad6, 4L, nad5, rrnL and trnT,W, S2, Y, K, l, M, R, A, Q have opposite direction
Urodasys mirabilis	19009	11	22	31	2	not unidirectional, cox1,cox2-1/0, cox3, nad4L, nad2, nad4, nad5, rrnS, rrnL and trnP,G, Y, D, E, I, M, T, C, W, S1 have opposite direction
Urodasys apuliensis	18723	11	20	22	4	not unidirectional, cob, nad1, nad4-1, nad4-0, nad6, and trnE, L1, G, H, Q, N, V, S2, D, F, R, K have opposite direction
Urodasys acanthostylis	15508	11	19	22	2	not unidirectional, cox1, cox2, nad1, nad3, nad4, nad5, nad6, rrnL and trnP, G, F, H, V, W, S2, T, Y, K, D, I, M, S1 have opposite direction
Urodasys viviparus	13219	11	22	20	8	not unidirectional, cox1, cox2, cox3, cob, nad1, nad3, nad5, nad6, rrnL, rrnS, and trnT, Y, A, I, D, L1, W, R, S1, Q, M, V have opposite direction

863 **Table 2.** Codon usage preferences in gastrotrich species (*when codon usage preference is equal).

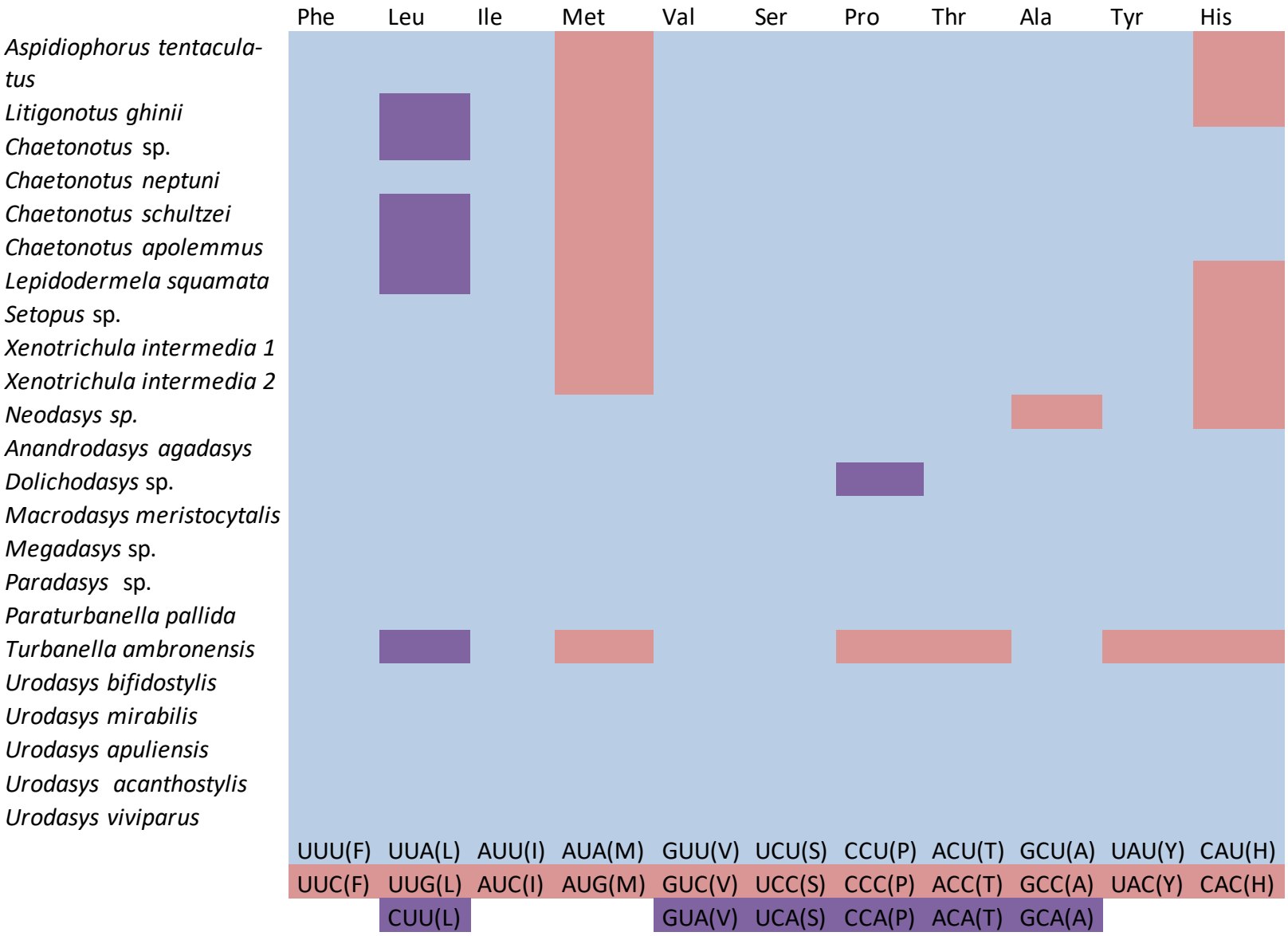

CUC(L) GUG(V) UCG(S) CCG(P) ACG(T) GCG(A)
CUA(L)
CUG(L)

864

865 **Table 2 (continuation).** Codon usage preferences in gastrotrich species (*when codon usage preference is equal).

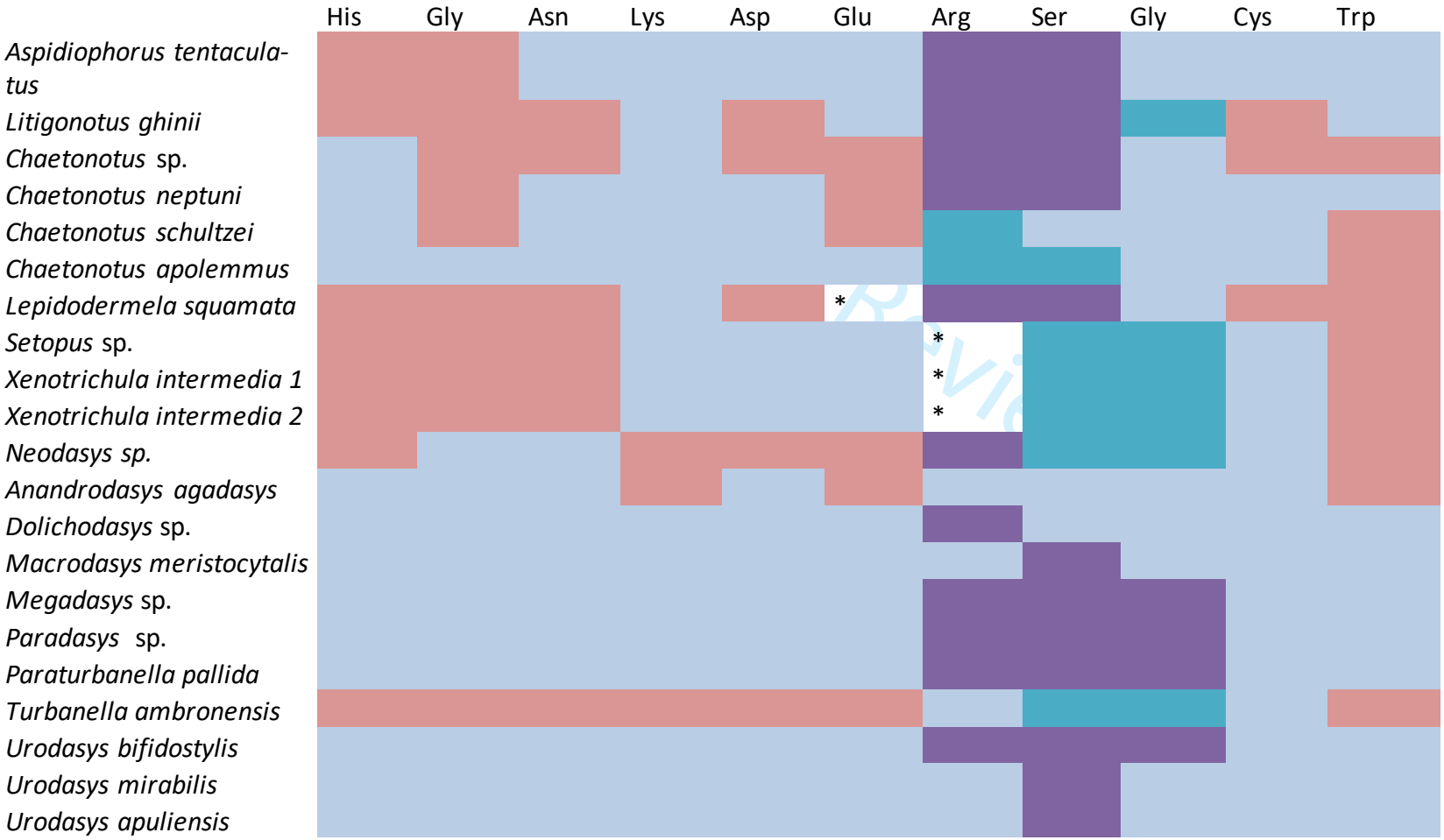

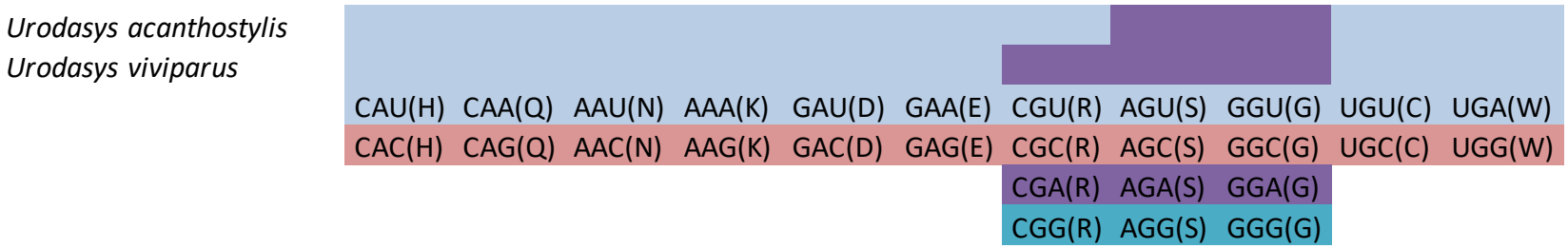

866

867

868 **Table 3.** Specimens used in this study, with notes on classification, sampling locations, ecology, mt DNA GenBank accession codes and references.

Species	Classification	Sampling location	Reproduction/Ecology	GenBank accession/References
Aspidiophorus tentaculatus	Chaetonotidae, Oiorpata, Chaetonotida	Carlotto, IT 41°13'44.56''N, 9°22'31.44''E	parthenogenetic, marine	PX661610
Chaetonotus sp.	Chaetonotidae, Oiorpata, Chaetonotida	Pisa, IT 43°43’16.60”N, 10°23’45.75” E	parthenogenetic, freshwater	PX661611
Chaetonotus neptuni	Chaetonotidae, Oiorpata, Chaetonotida	Asinara, IT 40° 59' 41.28''N, 8° 12' 50.76''E	parthenogenetic, marine	PX661597
Chaetonotus schultzei	Chaetonotidae, Oiorpata, Chaetonotida	San Rossore, IT 43°43'12,33"N, 10°17'6,02" E	parthenogenetic, freshwater	PX661598
Chaetonotus apolemmus	Chaetonotidae, Oiorpata, Chaetonotida	Asinara, IT 41°0'47.959"N, 8°14'56.306"E	parthenogenetic, marine	PX661612
Lepidodermella squamata	Chaetonotidae, Oiorpata, Chaetonotida	N. A. purchased from Carolina Biological Supply	parthenogenetic, freshwater	Golombek et al. 2015
Litigonotus ghinii	Chaetonotidae, Oiorpata, Chaetonotida	Pisa, IT 43°43’16.60”N, 10°23’45.75” E	parthenogenetic, freshwater	Gammuto et al. 2024
Setopus sp.	Chaetonotidae, Oiorpata, Chaetonotida	Pisa, IT 43°43’16.60”N, 10°23’45.75” E	parthenogenetic, freshwater	PX661599
Xenotrichula intermedia 1	Xenotrichulidae, Chaetonotida	Liguria, IT 44°02’57.66”N 9°58’53.51”E	hermaphroditic, marine	PX661603

Xenotrichula intermedia 2	Xenotrichulidae, Chaetonotida	Milano Marittima, IT 44°16’41”N 12°20’53”E	hermaphroditic, marine	PX661602
Neodasys sp.	Neodasyidae, Chaetonotida	SurfBeach, Panama, 7°25'51.6"N, 80°11'45.599"W	hermaphroditic, marine	PX661604
Anandrodasys agadasys	Redudasyidae, Macrodasiyda	St John Island, USA 18°21’50” N; 64°43’47” W	parthenogenetic, marine	PX661600
Dolichodasys sp.	Cephalodasyidae, Macrodasiyda	Sicily, IT 37°25’58” N; 13°14’29” E	hermaphroditic, marine	PX661601
Macrodasys meristocytalis	Macrodasyidae, Macrodasiyda	Duncans, JM 18°29'13” N; 77°32'03" W	hermaphroditic, marine	PX661605
Megadasys sp.	Planodasyidae, Macrodasiyda	Lanzarote, ES 28°55'08” N; 13°40'06” W	hermaphroditic, marine	PX661606
Paradasys sp.	Cephalodasyidae, Macrodasiyda	Sardegna, IT 41°03’9’’N; 8°56’16” E	hermaphroditic, marine	PX661607
Paraturbanella pallida	Turbanellidae, Macrodasiyda	Sardegna, IT 41°16’43” N; 09°21’28” E	hermaphroditic, marine	PX661608
Turbanella ambronensis	Turbanellidae, Macrodasiyda	Sicilia, IT 36°47'18"N; 14°29'34"E	hermaphroditic, marine	PX661609
Urodasys bifidostylis	Macrodasyidae, Macrodasiyda	Sardegna, IT 41°03’9’’N; 8°56’16” E	hermaphroditic, marine	PX661613
Urodasys mirabilis	Macrodasyidae, Macrodasiyda	Willemstad, Curaçao 12°07’19” N; 68°58’09” W	hermaphroditic, marine	PX661614
Urodasys apuliensis	Macrodasyidae, Macrodasiyda	Sardegna, IT 41°16’43” N; 09°21’28” E	hermaphroditic, marine	PX661615
Urodasys acanthostylis	Macrodasyidae, Macrodasiyda	Lanzarote, ES 28°55'08” N; 13°40'06” W	hermaphroditic, marine	PX661596
Urodasys viviparus	Macrodasyidae, Macrodasiyda	Abruzzo, IT 42°40’44” N; 14°01’05” E	parthenogenetic, marine	PX661616

869 **Figures**

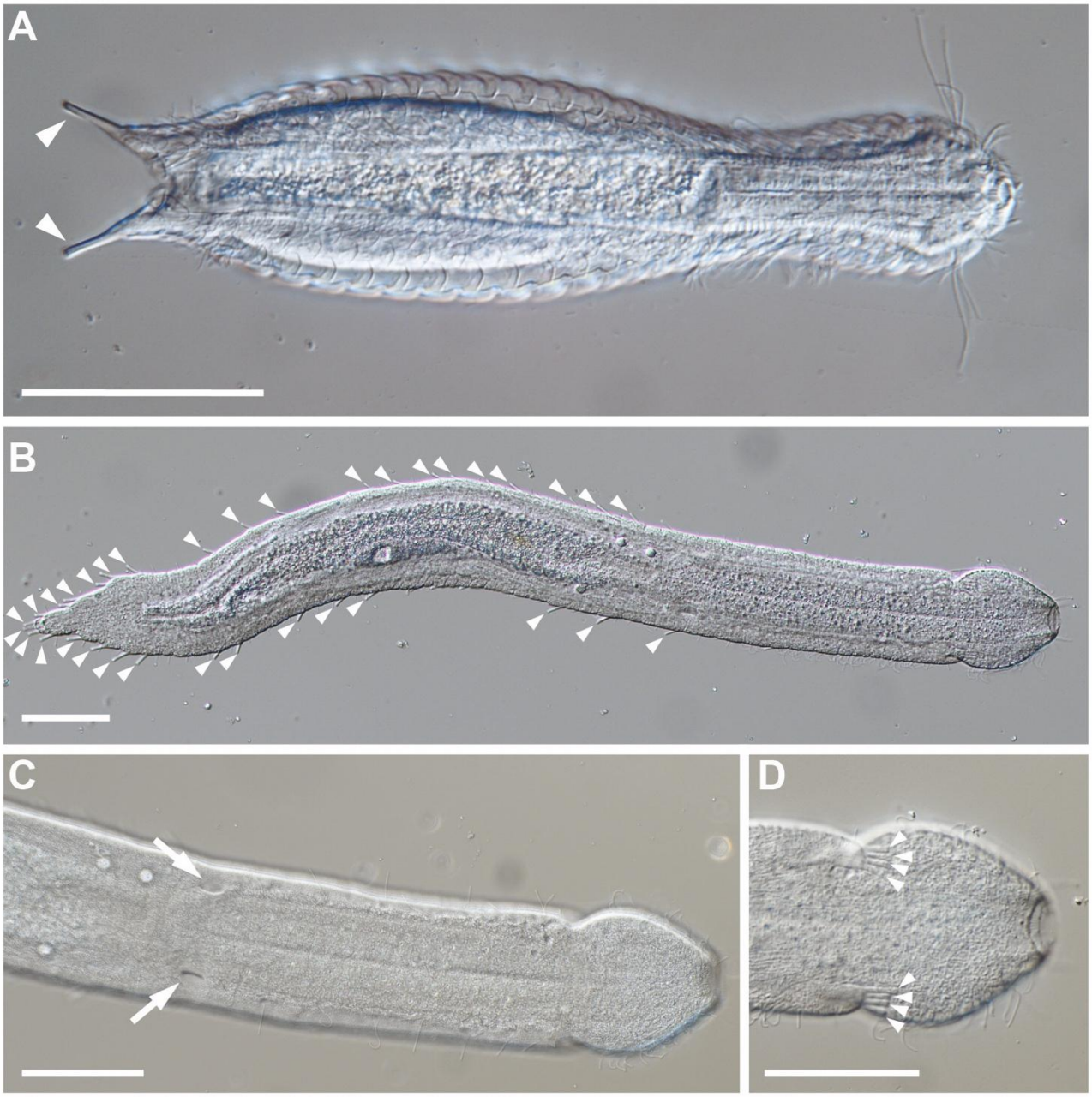

870

871 **Fig. 1.** Differential Interference Contrast microscopy (Nomarski) images of representatives of a
872 chaetonotidan and a macrodasyidan species showing some of the morphological differences
873 between two orders. **A:** *Lepidodermella* sp. (Chaetonotida) with bottle-shaped body and two
874 adhesive tubes situated in posterior part of the body (arrowheads). **B:** *Cephalodasys* sp.
875 (Macrodasyida) with vermiform body and multiple adhesive tubes situated in the posterior part
876 and along the lateral sides of the body (arrowheads). **C&D:** Details of pharyngeal pores (arrows in
877 C) and anterior adhesive tubes (arrowheads in D) in *Cephalodasys* sp. Scale bars = 50 µm.

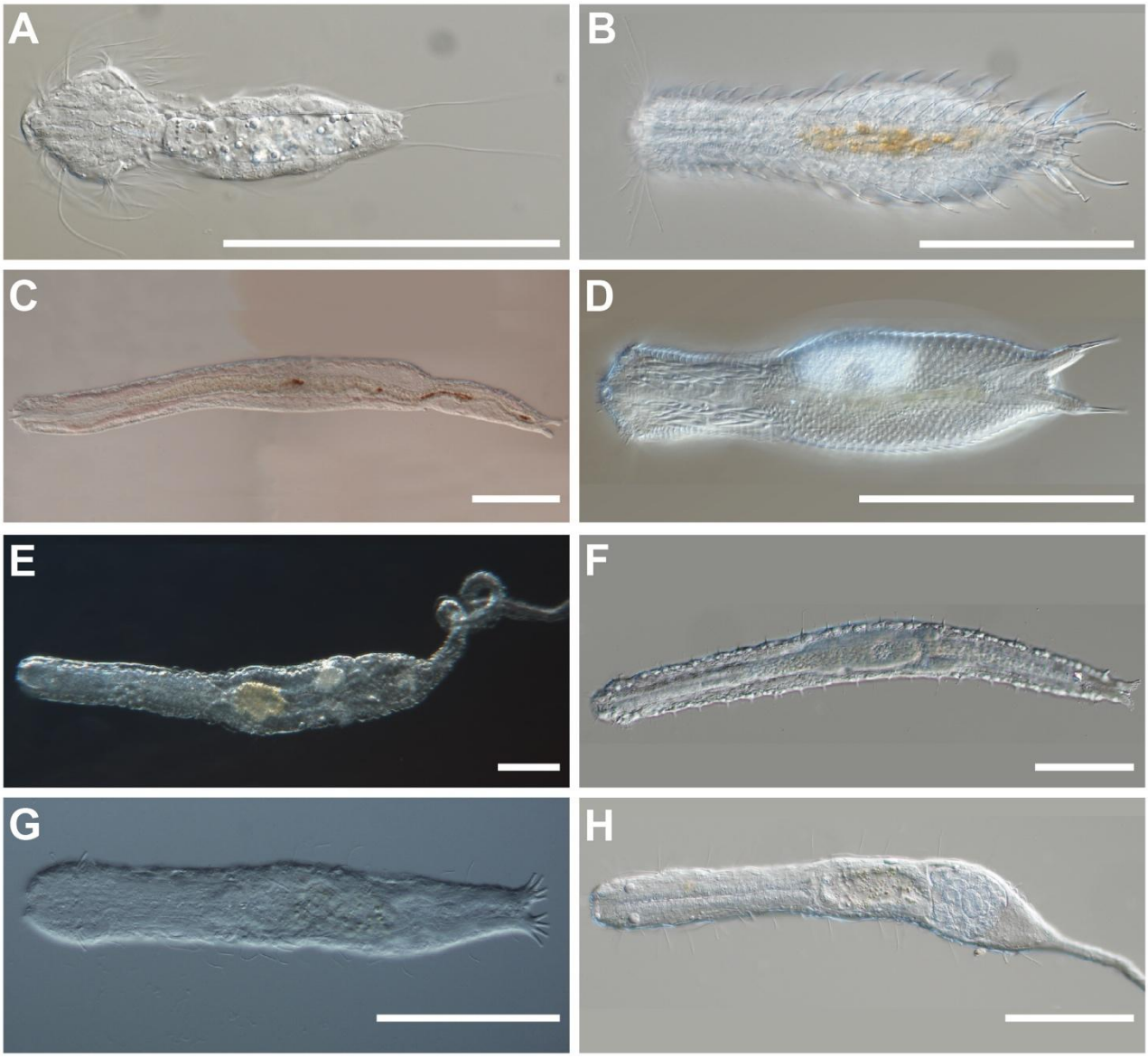

878
879 **Fig. 2.** Differential Interference Contrast microscopy (Nomarski) images of representatives of
880 studied gastrotrich groups. **A-D**: Chaetonotida; **E-H** Macrodasyida. **A&B:** Representatives of the
881 parthenogenetic Oiorpata clade: *Setopus* sp. and *Chaetonotus neptuni* respectively. **C&D:**
882 Representatives of the hermaphroditic marine *Neodasys* sp. and *Xenotrichula intermedia*
883 respectively. **E&F:** Representatives of hermaphroditic species: *Urodasys apuliensis* and *Turbanella*
884 *ambronensis* respectively. **G&H:** Representatives of parthenogenetic species: *Anandrodasys*
885 *agadasys* and *Urodasys viviparus* respectively. Scale bars = 100 µm.

886

887

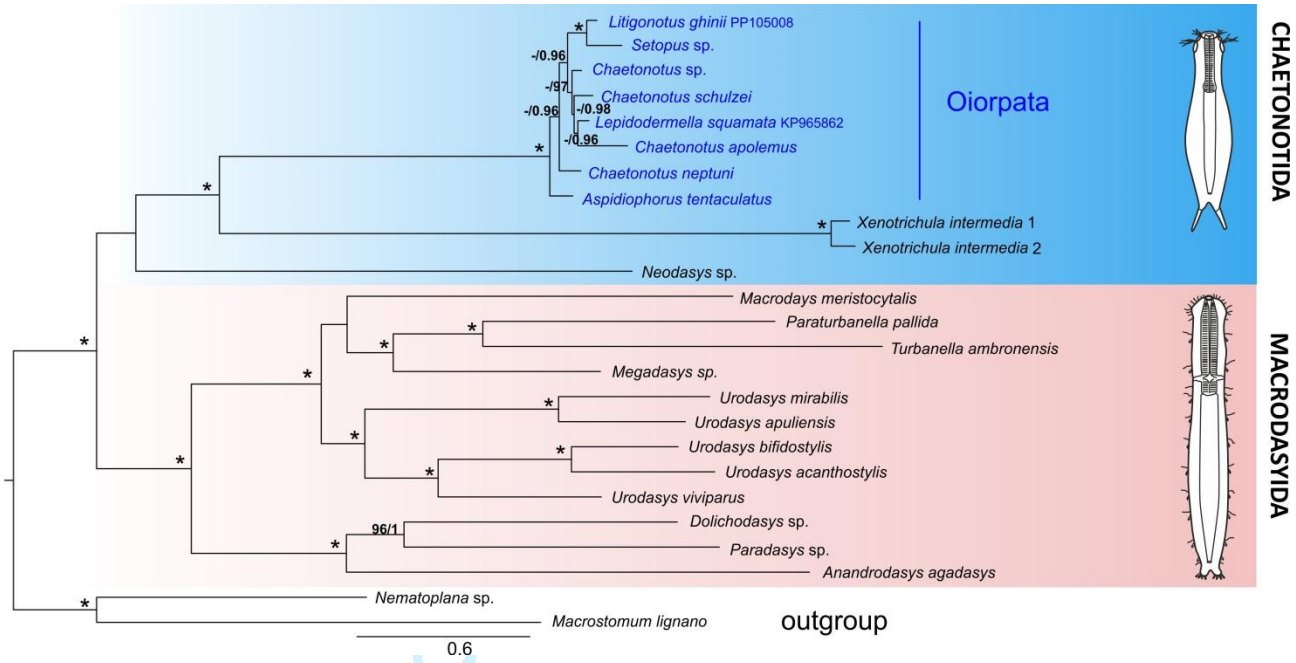

Fig. 3. Phylogenetic tree of 22 gastrotrich species and two flatworm outgroups based on a concatenated alignment of 13 mitochondrial protein-coding genes (*cox1-3, cob, nad1-6, nad4L, atp6, atp8*). The topology is derived from the IQ-TREE maximum likelihood (ML) analysis. Branch support values are shown as Ultrafast Bootstrap (ML) and Posterior Probability (BI). * Asterisks indicate 100% support for both, while values lower than 95% are not shown. The scale bar represents substitutions per site.

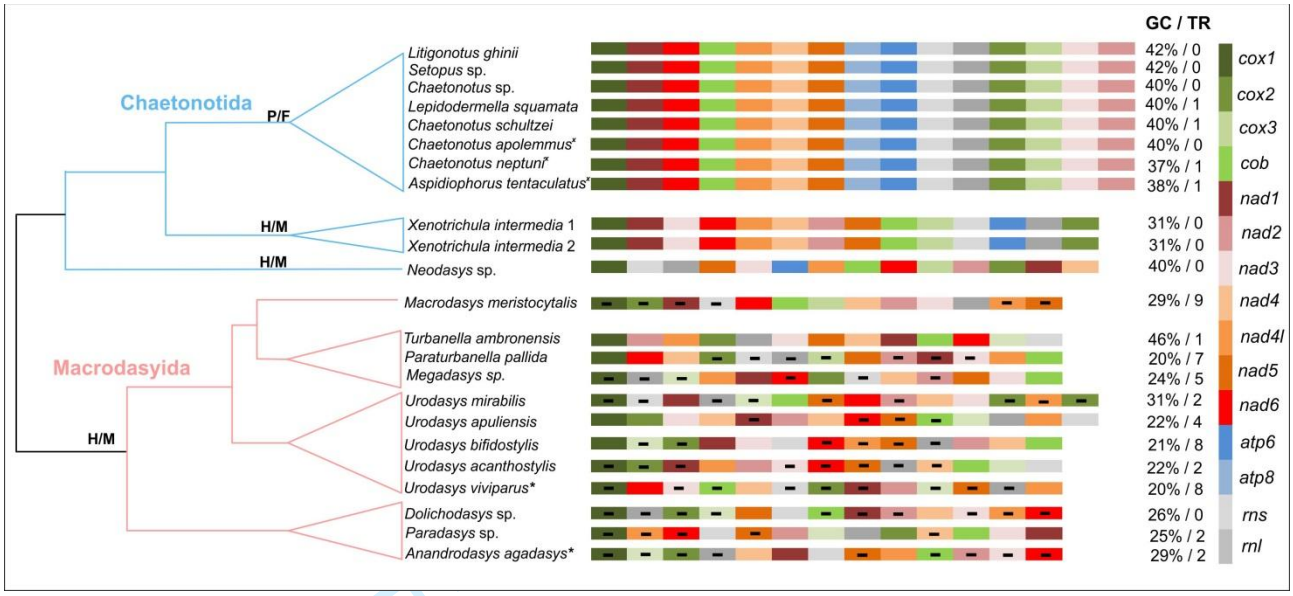

905

906

907 **Fig. 4.** Mitochondrial protein coding and ribosomal gene order mapped to schematic phylogenetic
908 relationships of the studied gastrotrich species. Abbreviations on the nodes indicate: P/F-
909 parthenogenetic freshwater species, H/M-hermaphroditic marine species. * Asterisks indicate
910 exception for *Urodasys viviparous* and *Anandrodasys agadasys* which are parthenogenetic. [X]
911 Crosses indicate exception for *Chaetonotus apolemmus*, *C. neptuni* and *Aspidiophorus tentaculatus*
912 which are marine. Gene boxes are color-coded by gene name. "–" symbol within a box indicates
913 that the gene is located on the minus strand, while empty boxes represent genes on the plus
914 strand. GC/TR values denote the GC content (%) of the mitochondrial genome and the number of
915 tandem repeats identified.

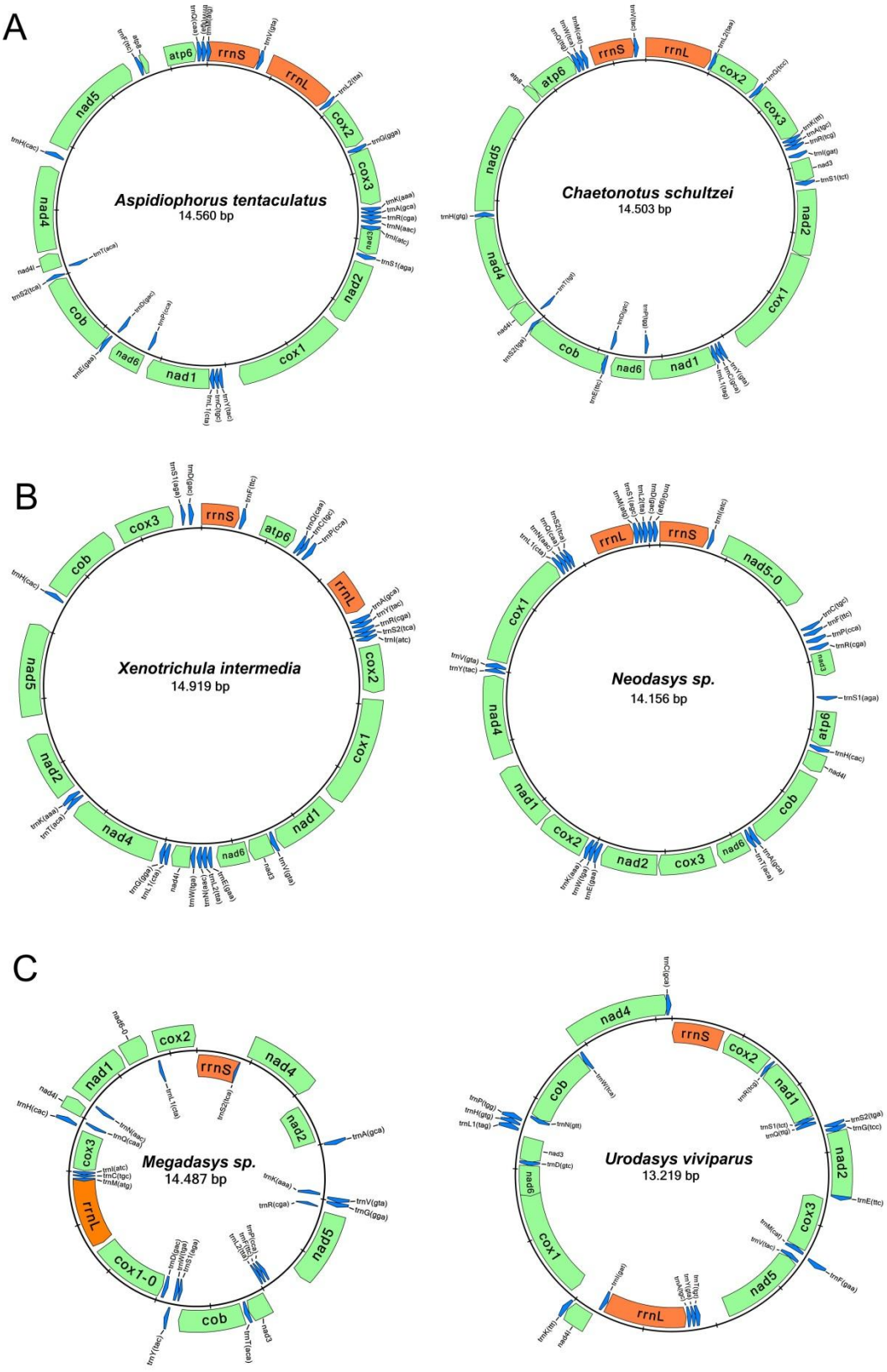

Fig. 5. Comparison of gene transcriptional direction in representatives of the different gastrotrich linages. **A.** Almost unidirectional transcription with exception of trnT, trnD, trNP in the members of Oiorpata clade, **B.** Complete unidirectional transcription in the members of marine hermaphroditic chaetonotidans, and **C.** mixed directional transcription in the macrodasyidans. Protein coding genes are in green, ribosomal genes are in orange, tRNAs are in blue.

3. CONCLUSIONS

The complexity and diversity of microscopic animals can often be surprising at first. We tend to overlook their contributions to our shared world simply because they are invisible to the naked eye. However, they are all around us and are just as important as any other branch of the tree of life. Therefore, it is essential to gain a better understanding of them within the One Health framework.

The results obtained during my PhD significantly advance our understanding of the evolutionary history of the understudied phylum Gastrotricha. The use of multi-gene concatenated datasets consistently produced well-supported phylogenetic trees at the nodes of interest, and brought new insight on the deeper relationships of the involved taxa. Additionally, the exploratory study conducted on the general structure of the gastrotrich mitochondrial genome revealed a new layer of diversity in the taxa of the phylum, a line of research deserving of further investigation in the future.

The WGA + NGS and bioinformatics protocols established during this PhD proved well-suited to the study of gastrotrichs, obtaining a total of 87 new gene sequences and 20 new complete mitogenomes for the projects illustrated in this thesis. Moreover, the material from WGS is available for additional future gene mining. While starting from whole animals generally produced more reliable outcomes, the pipeline also worked on previously extracted and frozen DNA, and the quality of the results was not significantly impacted by the age of the starting samples. The 18S rDNA sequences obtained through NGS and bioinformatics retrieval are highly congruent with those obtained through traditional Sanger sequencing, confirming the accuracy of the Next Gen sequencing Illumina and NanoPore platforms. The methodology shows promise for studying the molecular genetics of other meiofauna-sized organisms and could certainly be used to explore phylogenetic relationships within Gastrotricha not addressed in this thesis.

Although the outcomes of this approach are generally positive, it does have some drawbacks and is not infallible. While the WGA reaction protocol is robust, there is uncertainty regarding the proportion of the input genetic material that is actually amplified and to what extent. As mentioned in the Introduction chapter, the risk of contamination can never be entirely eliminated. Additionally, when using whole organisms, the genetic material of microbes present in the gut or attached to the specimens' exterior may also be amplified. This microbial genetic material can impact the quality of the target DNA and, in some cases, may be the only material that is amplified.

The data analysis step also shows room for improvement. In some cases, the nuclear ribosomal genes were isolated successfully but the mitochondrial genes were not, or were recovered only after considerably more effort was expended in the analysis of the sequencing output.

On a practical level, analysing Next-Generation Sequencing (NGS) data with bioinformatics tools requires specialized training and access to high-performance computing resources. This is especially crucial for assembling the short reads produced by the Illumina sequencing technology. Additionally, it is important to consider data storage, as NGS output files can often reach several gigabytes in size. Lastly, having a reliable reference database of validated sequences is essential for accurately identifying and isolating the target molecular markers from the resulting reads.

Enhancing the taxonomic sampling had a significant positive impact on all analyses, as expected. However, achieving this can be quite challenging. The research conducted during my PhD was made possible by the resources available at the UNIMORE MeioLab BioBank. The species collection, assembled by my supervisor, Professor M. A. Todaro, along with various collaborators, includes thousands of preserved specimens. These specimens were gathered through sampling campaigns that began in 2008. Thanks to these prior efforts, I was able to include the necessary species from multiple regions around the world in my projects at no additional cost (Fig. 3).

Fig. 3. World map illustrating the geographic regions (red dots) from which the species sequenced in this research project have been sampled. Collecting the necessary species to clarify the phylogenetic relationships of gastrotrichs may incur significant costs.

Even so, not all taxa potentially of interest for my lines of research were available for sequencing, or were sequenced successfully. Many species of gastrotrichs that are important for understanding phylogeny are often rare and/or found in remote geographic locations or are associated with sediments that are difficult to access, e.g., due to water depth. Securing the species

essential for elucidating the phylogenetic relationships of gastrotrichs is not only vital for advancing our understanding but can also be a significant financial investment. Additionally, collecting multiple specimens is necessary to increase the likelihood of successful analysis for each taxon, as these delicate specimens can be damaged during deep microscopic examinations and are destroyed during DNA extraction. Therefore, the experimental design, particularly the selection of taxa, is the most critical and challenging step in the entire process. Nevertheless, proper taxonomic sampling is essential to obtain reliable results.

Reconstructing the evolutionary history of these complex animals will likely always involve a degree of inference. However, well-informed inferences can only be made through detailed and accurate observations that enhance our understanding of the biology of the related taxa, particularly when using advanced microscopy techniques. The integration of both morphological and molecular data is essential for deepening our understanding of this microscopic phylum. These two aspects work together: molecular analysis provides insights into the phylogenetic significance of anatomical traits, while anatomical observations help interpret molecular phylogenetic trees.

4. REFERENCES

- Alekseyev, Y. O., Fazeli, R., Yang, S., Basran, R., Maher, T., Miller, N. S., & Remick, D. (2018). A Next-Generation Sequencing primer – How does it work and what can it do? Academic Pathology, 6(5), 2374289518766521. DOI: 10.1177/2374289518766521.
- Araujo T. Q., King-Trudeau S., VanDyke J., & Hochberg, R. (2023). First ultrastructural description of an apomictic opsiblastic egg in freshwater Gastrotricha. Journal of Morphology 285, e21659. DOI: 10.1002/jmor.21659
- Artois, T., Fontaneto, D., Hummon, W. D., McInnes, S. J., Todaro, M. A., Sørensen, M. V. & Zullini, A. (2011). Ubiquity of microscopic animals? Evidence from the morphological approach in species identification. In: Fontaneto, D. (ed.) Biogeography of microscopic organisms. Is everything small everywhere? Systematics Association Special Volume 79 (pp. 244–283). Cambridge University Press, Cambridge.
- Atherton, S., & Hochberg, R. (2014). The evolution of the reproductive system of *Urodasys* (Gastrotricha: Macrodasyida). Invertebrate Biology, 133, 314–23. DOI: 10.1111/ivb.12068
- Balsamo, M., Guidi, L., Pierboni, L., Marotta, R., Todaro, M. A., & Ferraguti, M. (2007). Living without mitochondria: spermatozoa and spermatogenesis in two species of *Urodasys* (Gastrotricha, Macrodasyida) from dysoxic sediments. Invertebrate Biology, 126(1), 1–9. DOI: 10.1111/j.1744-7410.2007.00071.x
- Balsamo, M., Guidi, L., Grilli, P., & d'Hondt, J.-L. (2010). The phylogenetic position and the intraphyletic relationships of Gastrotricha. Bulletin de la Societé Zoologique de France, 135(1–2), 79–91.
- Balsamo, M. & Todaro, M. A. (1987). *Aspidiophorus polystictos*, a new marine species (Gastrotricha, Chaetonotida) and its life cycle. Bollettino di Zoologia 54, 147–153. DOI: 10.1080/11250008709355574
- Balsamo, M., & Todaro, M. A. (1988). Life history traits of two chaetonotids (Gastrotricha) under different experimental conditions. Invertebrate Reproduction & Development, 14(2), 161–176. DOI: 10.1080/01688170.1988.10510375
- Bekkouche, N., & Worsaae, K. (2016). Neuromuscular study of early branching *Diuronotus aspetos* (Paucitubulatina) yields insights into the evolution of organs systems in Gastrotricha. Zoological Letters, 2, 21. DOI: 10.1186/s40851-016-0054-3
- Bentley, D. R., Balasubramanian, S., Swerdlow, H. P., Smith, G. P., Milton, J., Brown, C. G., Hall, K. P., Evers, D. J., Barnes, C. L., Bignell, H. R., Boutell, J. M., Bryant, J., Carter, R. J., Cheetham, R., Cox, A. J., Ellis, D. J., Flatbush, M. R., Gormley, N. A.,

Humphray, … Smith, A. J. (2008). Accurate whole human genome sequencing using reversible terminator chemistry. Nature, 456(7218), 53–59. DOI: 10.1038/nature07517

- Boaden, P. J. S. (1985). Why is a gastrotrich? In S. Conway Morris, J. D. George, R. Gibson, & H. M. Platt (Eds.), The origins and relationships of lower invertebrates. Systematics Association Special Volume 28 (pp. 248–260). Oxford University Press, New York.
- Bogaerts, B., Van den Bossche, A., Verhaegen, B., Delbrassinne, L., Mattheus, W., Nouws, S., Godfroid, M., Hoffman, S., Roosens, N. H. C., De Keersmaecker, S. C. J., & Vanneste, K. (2024). Closing the gap: Oxford Nanopore Technologies R10 sequencing allows comparable results to Illumina sequencing for SNP-based outbreak investigation of bacterial pathogens. Journal of Clinical Microbiology, 62, e01576-23. DOI: 10.1128/jcm.01576-23
- Boore, J. L. (1999). Animal mitochondrial genomes. Nucleic Acids Research, 27, 1767–1780. DOI: 10.1093/nar/27.8.1767
- Butenko, A., Lukeš, J., Speijer, D., & Wideman, J. G. (2024). Mitochondrial genomes revisited: why do different lineages retain different genes? BMC Biology, 22, 15. DOI: 10.1186/s12915-024-01824-1
- Cavalier-Smith, T. (1998). A revised six-kingdom system of life. Biological Reviews, 73, 203–266.
- Dunn, C. W., Hejnol, A., Matus, D. Q., Pang, K., Browne, W. E., Smith, S. A., Seaver, E., Rouse, G. W., Obst, M., Edgecombe, G. D., Sørensen, M. V., Haddock, S. H. D., Schmidt-Rhaesa, A., Okusu, A., Kristensen, R. M., Wheeler, W. C., Martindale, M. Q., & Giribet, G. (2008). Broad phylogenomic sampling improves resolution of the animal tree of life. Nature, 452, 745–750. DOI: 10.1038/nature06614
- Egger, B., Lapraz, F., Tomiczek, B., Müller, S., Dessimoz, C., Girstmair, J., Škunca, N., Rawlinson, K. A., Cameron, C. B., Beli, E., Todaro, M. A., Gammoudi, M., Noreña, C., & Telford, M. J. (2015). A transcriptomic-phylogenomic analysis of the evolutionary relationships of flatworms. Current Biology, 25(10), 1347–53. DOI: 10.1016/j.cub.2015.03.034.
- Fontaneto, D., Flot, J.-F., & Tang, C. Q. (2015). Guidelines for DNA taxonomy, with a focus on the meiofauna. Marine Biodiversity, 45, 433–451. DOI: 10.1007/s12526-015-0319-7
- Fromm, B., Tosar, J. P., Aguilera, F., Friedländer, M. R., Bachmann, L., Hejnol, A. (2019). Evolutionary Implications of the microRNA- and piRNA Complement of *Lepidodermella squamata* (Gastrotricha). Non-coding RNA, 5, 19. DOI: 10.3390/ncrna5010019
- Gammuto, L., Serra, V., Petroni, G., & Todaro, M. A. (2024). Molecular phylogenetic position and description of a new genus and species of freshwater Chaetonotidae

(Gastrotricha: Chaetonotida: Paucitubulatina), and the annotation of its mitochondrial genome. Invertebrate Systematics, 38, IS23059. DOI: 10.1071/IS23059

- Garraffoni A. R. S., Araujo T. Q., Lourenço A. P., Guidi L., & Balsamo M. 2017. A new genus and new species of freshwater Chaetonotidae (Gastrotricha: Chaetonotida) from Brazil with phylogenetic position inferred from nuclear and mitochondrial DNA sequences. Systematics and Biodiversity, 15(1) 49–62. DOI: 10.1080/14772000.2016.1214189
- Giere, O. (2009). Meiobenthology: The microscopic motile fauna of aquatic sediments. Springer. DOI: 10.1007/978-3-540-68661-3
- Giribet, C. (2008). Assembling the lophotrochozoan (=spiralian) tree of life. Philosophical Transactions of the Royal Society B, 363, 1513–1522. DOI: 10.1098/rstb.2007.2241
- Giribet, G., Sorensen, M. V., Funch, P., Kristensen, R. M., & Sterrer, W. (2004). Investigations into the phylogenetic position of Micrognathozoa using four molecular loci. Cladistics, 20, 1–13. DOI: 10.1111/j.1096-0031.2004.00004.x
- Gissi, C., Iannelli, F., & Pesole, G. (2008). Evolution of the mitochondrial genome of Metazoa as exemplified by comparison of congeneric species. Heredity, 101, 301–320. DOI: 10.1038/hdy.2008.62
- Golombek, A., Tobergte, S., & Struck, T. H. (2015). Elucidating the phylogenetic position of Gnathostomulida and first mitochondrial genomes of Gnathostomulida, Gastrotricha and Polycladida (Platyhelminthes). Molecular Phylogenetics and Evolution, 86, 49–63. DOI: 10.1016/j.ympev.2015.02.013
- Guidi, L., Balsamo, M., Grassi, L., Semprucci, F., & Todaro, M. A. (2022). New data on reproductive system and spermatozoa confirm *Macrodasys* as a model in comparative reproductive analysis in Macrodasyida (Gastrotricha). Water, 14, 3085. DOI: 10.3390/w14193085
- Guidi, L., Todaro, M. A., Ferraguti, M., & Balsamo, M. (2014). Reproductive system and spermatozoa ultrastructure support the phylogenetic proximity of *Megadasys* and *Crasiella* (Gastrotricha, Macrodasyida). Contributions to Zoology, 83, 119–131. DOI: 10.1163/18759866-08302003
- Hebert, P. D., Cywinska, A., Ball, S. L., & deWaard, J. R. (2003). Biological identifications through DNA barcodes. Proceedings of the Biological Sciences, 270(1512), 313–321. DOI: 10.1098/rspb.2002.2218
- Higgins, R. P., & Thiel, H. (1988). Introduction to the study of meiofauna. Smithsonian Institution Press.

- Hillis, D. M., & Dixon, M. T. (1991). Ribosomal DNA: molecular evolution and phylogenetic inference. The Quarterly Review of Biology, 66(4), 411–453. DOI: 10.1086/417338
- Hochberg, R. (2005). Musculature of the primitive gastrotrich *Neodasys* (Chaetonotida): functional adaptations to the interstitial environment and phylogenetic significance. Marine Biology, 146, 315–323. DOI: 10.1007/s00227-004-1437-0
- Hochberg, R., & Litvaitis, M. K. (2000). Phylogeny of Gastrotricha: a morphology-based framework of gastrotrich relationships. Biological Bulletin, 198, 299–305. DOI: 10.2307/1542532.
- Hochberg, R., & Litvaitis, M. K. (2001). A muscular double helix in Gastrotricha. Zoologischer Anzeiger, 240, 61–68. DOI: 10.1078/0044-5231-00006
- Hochberg, R., & Litvaitis, M. K. (2003). Organization of muscles in Chaetonotida Paucitubulatina (Gastrotricha). Meiofauna Marina, 12, 47–58.
- Hummon, M. R., & Hummon, W. D. (1992). Gastrotricha. In K. G. Adiyodi & R. G. Adiyodi (Eds.), Reproductive Biology of Invertebrates, Vol. 5: Sexual Differentiation and Behaviour (pp. 137–146). Wiley.
- Hummon, W. D., & Todaro, M. A. (2010). Analytic taxonomy and notes on marine, brackish-water and estuarine Gastrotricha. Zootaxa, 2392, 1–32. DOI: 10.11646/zootaxa.2392.1.1
- Hyman, L. H. (1951). The invertebrates. Vol. 3: Acanthocephala, Aschelminthes, and Entoprocta: the pseudocoelomate Bilateria. McGraw-Hill.
- Kånneby, T., Todaro, M. A., & Jondelius, U. (2012). A phylogenetic approach to species delimitation in freshwater Gastrotricha from Sweden. Hydrobiologia, 683, 185–212. DOI: 10.1007/s10750-011-0956-1
- Kånneby, T., Todaro, M. A., & Jondelius, U. (2013). Phylogeny of Chaetonotidae and other Paucitubulatina (Gastrotricha: Chaetonotida) and the colonization of aquatic ecosystems. Zoologica Scripta, 42(1), 88–105. DOI: 10.1111/j.1463-6409.2012.00558.x
- Kieneke, A., Martinez, A., & Fontaneto, D. (2012). Spatially structured populations with a low level of cryptic diversity in European marine Gastrotricha. Molecular Ecology, 21, 1239–1254. DOI: 10.1111/j.1365-294X.2011.05421.x
- Kieneke, A., Riemann, O., & Ahlrichs, W. H. (2008). Novel implications for the basal internal relationships of Gastrotricha revealed by an analysis of morphological characters. Zoologica Scripta, 37, 429–460. DOI: 10.1111/j.1463-6409.2008.00334.x

- Kieneke, A., & Schmidt-Rhaesa, A. (2014). Gastrotricha. In: Schmidt-Rhaesa, A. (Ed.), Handbook of Zoology. Gastrotricha, Cycloneuralia and Gnathifera. Vol. 3: Gastrotricha and Gnathifera (pp. 1–134). De Gruyter, Berlin.
- Kieneke, A., & Todaro, M. A. (2021). Discovery of two "chimeric" Gastrotricha and their systematic placement based on an integrative approach. Zoological Journal of the Linnean Society, 192, 710–735. DOI: 10.1093/zoolinnean/zlaa117
- Kolicka, M., Dabert, M., Olszanowski, Z., & Dabert, J. (2020). Sweet or salty? The origin of freshwater gastrotrichs (Gastrotricha, Chaetonotida) revealed by molecular phylogenetic analysis. Cladistics, 36, 458–480. DOI: 10.1111/cla.12424
- Lake, N. J., Ma, K., Liu, W., Battle, S. L., Laricchia, K. M., Tiao, G., Puiu, D., Ng, K. K., Cohen, J., Compton, A. G., Cowie, S., Christodoulou, J., Thorburn, D. R., Zhao, H., Arking, D. E., Sunyaev, S. R., & Lek, M. (2024). Quantifying constraint in the human mitochondrial genome. Nature, 635, 390–397. DOI: 10.1038/s41586-024-08048-x
- Laumer, C. E., Bekkouche, N., Kerbl, A., Goetz, F., Neves, R. C., Sørensen, M. V., Kristensen, R. M., Hejnol, A., Dunn, C. W., Giribet, G., & Worsaae, K. (2015). Spiralian phylogeny informs the evolution of microscopic lineages. Current Biology, 25(15), 2000–2006. DOI: 10.1016/j.cub.2015.06.068
- Laumer, C. E., Fernández, R., Lemer, S., Combosch, D., Kocot, K. M., Riesgo, A., Andrade, S. C. S., Sterrer, W., Sørensen, M. V., & Giribet, G. (2019). Revisiting metazoan phylogeny with genomic sampling of all phyla. Proceedings of the Biological Sciences, 286(1906), 20190831. DOI: 10.1098/rspb.2019.0831
- Lavrov, D. V., & Pett, W. (2016). Animal mitochondrial DNA as we do not know it: mt-genome organization and evolution in nonbilaterian lineages. Genome Biology and Evolution, 8, 2896–2913. DOI: 10.1093/gbe/evw195
- Leasi, F., Rothe, B. H., Schmidt-Rhaesa, A. & Todaro, M. A. (2006). The musculature of three species of gastrotrichs surveyed with confocal laser scanning microscopy (CLSM). Acta Zoologica 87, 171-180. DOI: 10.1111/j.1463-6395.2006.00230.x
- Leasi, F., & Todaro, M. A. (2008). The muscular system of *Musellifer delamarei* (RenaudMornant, 1968) and other chaetonotidans with implications for the phylogeny and systematization of the Paucitubulatina (Gastrotricha). Biological Journal of the Linnean Society, 94, 379–398. DOI: 10.1111/j.1095-8312.2008.00974.x
- Lee, Y. C., Ke, H. M., Liu, Y. C., Lee, H. H., Wang, M. C., Tseng, Y. C., Kikuchi, T., & Tsai, I. J. (2023). Single-worm long-read sequencing reveals genome diversity in free-living nematodes. Nucleic Acids Research, 51(15), 8035–8047. DOI: 10.1093/nar/gkad647

- Lin, B., Hui, J., & Mao, H. (2021). Nanopore technology and its applications in gene sequencing. Biosensors, 11(7), 214. DOI: 10.3390/bios11070214
- Manylov, O. G., Vladychenskaya, N. S., Milyutina, I. A., Kedrova, O. S., Korokhov, N. P., Dvoryanchikov, G. A., Aleshin, V. V., & Petrov, N. B. (2004). Analysis of 18S rRNA gene sequences suggests significant molecular differences between Macrodasyida and Chaetonotida (Gastrotricha). Molecular Phylogenetics and Evolution, 30, 850–854. DOI: 10.1016/S1055-7903(03)00251-3.
- Marotta, R., Guidi, L., Pierboni, L., Ferraguti, M., Todaro, M. A., & Balsamo, M. (2005). Sperm ultrastructure of *Macrodasys caudatus* (Gastrotricha: Macrodasyida) and a sperm-based phylogenetic analysis of Gastrotricha. Meiofauna Marina, 14, 9–21.
- Marotta, R., Todaro, M. A., & Ferraguti, M. (2008). The unique gravireceptor organs of *Pleurodasys helgolandicus* (Gastrotricha: Macrodasyida). Zoomorphology, 127, 111–119. DOI: 10.1007/s00435-008-0056-6
- Minowa A. K., Kieneke A., Balsamo M., Guidi L., & Garraffoni A. R. S. (2025a). Addressing taxonomic shortfalls in Neotropical gastrotrichs: a new genus and species of freshwater Gastrotricha (Chaetonotida: Paucitubulatina) from Brazil. Invertebrate Systematics, 39, IS25003. DOI: 10.1071/IS25003
- Minowa, A. K., Kieneke, A., Campos, A., Balsamo, M., Plewka, M., Guidi, L., Araújo, T. Q., & Garraffoni, A. R. S., (2025b). New branch on the tree of life of Gastrotricha: establishment of a new genus for limno-terrestrial species. Zoological Journal of the Linnean Society, 203, zlae166. DOI: 10.1093/zoolinnean/zlae166.
- Montoliu-Nerin, M., Sanchez-Garcia, M., Bergin, C., Grabherr, M., Ellis, B., Kutschera, V. E., Kierczak, M., Johannesson, H., & Rosling, A. (2020). Building de novo reference genome assemblies of complex eukaryotic microorganisms from single nuclei. Scientific Reports, 10, 1303. DOI: 10.1038/s41598-020-58025-3
- Morin, P. A., Archer, F. I., Foote, A. D., Vilstrup, J., Allen, E. E., Wade, P., Durban, J., Parsons, K., Pitman, R., Li, L., Bouffard, P., Abel Nielsen, S. C., Rasmussen M., Willerslev E., Gilbert M. T., & Harkins T. (2010). Complete mitochondrial genome phylogeographic analysis of killer whales (*Orcinus orca*) indicates multiple species. Genome Research, 20, 908–916. DOI: 10.1101/gr.102954.109
- Nielsen, C. (2001). Animal evolution: Interrelationships of the living phyla (2nd ed.). Oxford University Press.
- Paps, J., & Riutort, M. (2012). Molecular phylogeny of the phylum Gastrotricha: new data brings together molecules and morphology. Molecular Phylogenetics and Evolution, 63, 208–212. DOI: 10.1016/j.ympev.2011.12.010

- Petrov, N. B., Pegova, A. N., Manylov, O. G., Vladychenskaya, N. S., Mugue, N. S., & Aleshin, V. V. (2007). Molecular phylogeny of Gastrotricha on the basis of a comparison of the 18S rRNA genes: rejection of the hypothesis of a relationship between Gastrotricha and Nematoda. Molecular Biology, 41, 445–452. DOI: 10.1134/S0026893307030107
- Powell, E. N., Bright, T. J., Woods, A. & Gittings, S. (1983). Meiofauna and the thiobios in the East Flower garden brine seep. Marine Biology, 73, 269–283. DOI: 10.1007/BF00392253
- Rataj Križanová F, & Vďačný P. (2023) A *Heterolepidoderma* and *Halichaetoderma* gen. nov. (Gastrotricha: Chaetonotidae) riddle: integrative taxonomy and phylogeny of six new freshwater species from Central Europe. Zoological Journal of the Linnean Society, 200, 283–335. DOI: 10.1093/zoolinnean/zlad079
- Remane, A. (1936). Gastrotricha. In H. G. Bronn (Ed.), Klassen und Ordnungen des Tierreiches. Gastrotricha und Kinoryncha. Vol. 4: Vermes II. Abteilung Aschelminthes, Trochhelminthes (pp. 1–242). Akademische Verlagsgesellschaft.
- Rieger, R. M., & Mainitz, M. (1977). Comparative fine structure study of the body wall in Gnathostomulida and their phylogenetic position between Platyhelminthes and Aschelminthes. Zeitschrift für Zoologische Systematik und Evolutionsforschung, 15, 9–35. DOI: 10.1111/j.1439-0469.1977.tb00530.x
- Rieger, G. E., & Rieger, R. M. (1977). Comparative fine structure study of the gastrotrich cuticle and aspects of cuticle evolution within the Aschelminthes. Zeitschrift für Zoologische Systematik und Evolutionsforschung, 15, 81–124.
- Rieger, G. E., & Rieger, R. M. (1980). Fine structure and formation of eggshells in marine Gastrotricha. Zoomorphology, 96, 215–229. DOI: 10.1007/BF00310287
- Rundell, R. J., & Leander, B. S. (2010). Masters of miniaturization: convergent evolution among interstitial eukaryotes. BioEssays, 32, 430–437. DOI: 10.1002/bies.200900116
- Ruppert, E. E. (1978). The reproductive system of gastrotrichs. II. Insemination in *Macrodasys*: a unique mode of sperm transfer in Metazoa. Zoomorphologie, 89, 207–228. DOI: 10.1007/BF00993948
- Ruppert, E. E. (1982). Comparative ultrastructure of the gastrotrich pharynx and the evolution of myoepithelial foreguts in Aschelminthes. Zoomorphologie, 99, 181–220.
- Ruppert, E. E. (1991). Gastrotricha. In F. W. Harrison & E. E. Ruppert (Eds.), Microscopic Anatomy of Invertebrates (pp. 41–109). Wiley.
- Saccone, C., De Giorgi, C., Gissi, C., Pesole, G., & Reyes, A. (1999). Evolutionary genomics in Metazoa: the mitochondrial DNA as a model system. Gene, 238, 195–209. DOI: 10.1016/S0378-1119(99)00270-X

- Saponi, F., Kosakyan, A., Cesaretti, A., & Todaro, M. A. (2024). A contribution to the taxonomy and phylogeny of the genus *Chaetonotus* (Gastrotricha, Paucitubulatina, Chaetonotidae), with the description of a new species from Italian inland waters. European Zoological Journal, 91, 1078–1092. DOI: 10.1080/24750263.2024.2397473.
- Schmidt-Rhaesa, A., Bartolomaeus, T., Lemburg, C., Ehlers, U., & Garey, J. R. (1998). The position of the Arthropoda in the phylogenetic system. Journal of Morphology, 238, 263–285. DOI: 10.1002/(SICI)1097-4687(199812)238:3<263::AID-JMOR1>3.0.CO;2-L
- Semprucci, F., & Sandulli, R. (2020). Editorial for Special Issue "Meiofauna Biodiversity and Ecology". Diversity, 12(6), 249. DOI:10.3390/d12060249
- Serra, V., Fokin, S. I., Gammuto, L., Nitla, V., Castelli, M., Basuri, C. K., Satyaveni, A., Sandeep, B. V., Modeo, L., & Petroni, G. (2020). Phylogeny of *Neobursaridium* reshapes the systematics of *Paramecium* (Oligohymenophorea, Ciliophora). Zoologica Scripta, 50, 241–268. DOI: 10.1111/zsc.12464
- Smith, D. R. (2016). The past, present and future of mitochondrial genomics: have we sequenced enough mtDNAs? Briefings in Functional Genomics, 15, 47–54. DOI: 10.1093/bfgp/elv027
- Sterrer, W., Mainitz, M., & Rieger, R. M. (1985). Gnathostomulida: enigmatic as ever. In S. Conway Morris, J. D. George, R. Gibson, & H. M. Platt (Eds.), The origins and relationships of lower invertebrates (pp. 181–191). Clarendon Press.
- Shtolz, N., & Mishmar, D. (2023). The metazoan landscape of mitochondrial DNA gene order and content is shaped by selection and affects mitochondrial transcription. Communications Biology, 6, 93. DOI: 10.1038/s42003-023-04471-4
- Struck, T. H., Golombek, A., Hoesel, C., Dimitrov, D., & Elgetany, A. H. (2023). Mitochondrial genome evolution in Annelida — A systematic study on conservative and variable gene orders and the factors influencing its evolution. Systematic Biology, 72(4), 925–945. DOI: 10.1093/sysbio/syad023
- Struck, T. H., Wey-Fabrizius, A. R., Golombek, A., Hering, L., Weigert, A., Bleidorn, C., Klebow, S., Iakovenko, N., Hausdorf, B., Petersen, M., & Kück, P. (2014). Platyzoan paraphyly based on phylogenomic data supports a noncoelomate ancestry of Spiralia. Molecular Biology and Evolution, 31(7), 1833–1849. DOI: 10.1093/molbev/msu143
- Teuchert, G. (1968). Zur Fortpflanzung und Entwicklung der Macrodasyoidea (Gastrotricha). Zeitschrift für Morphologie der Tiere, 63, 343–418. DOI: 10.1007/BF00391930

- Teuchert, G. (1977). The ultrastructure of the marine gastrotrich *Turbanella cornuta* Remane (Macrodasyoidea) and its functional and phylogenetic importance. Zoomorphologie, 88, 189–246. DOI: 10.1007/BF00995474
- Todaro, M. A., Bernhard, J. M., & Hummon W. D. (2000). A new species of *Urodasys* (Gastrotricha, Macrodasyida) from dysoxic sediments of the Santa Barbara Basin (California, U.S.A.). Bulletin of Marine Science, 66, 467–76.
- Todaro, M. A., Cesaretti, A., & Dal Zotto, M. (2019c). Marine gastrotrichs from Lanzarote, with a description of a phylogenetically relevant species of *Urodasys* (Gastrotricha, Macrodasyida). Marine Biodiversity, 49, 2109–2123. DOI: 10.1007/s12526-017-0747-7
- Todaro, M. A., Dal Zotto, M., Jondelius, U., Hochberg, R., Hummon, W. D., Kånneby, T., & Rocha, C. E. F. (2012). Gastrotricha: a marine sister for a freshwater puzzle. PLoS ONE, 7, e31740. DOI: 10.1371/journal.pone.0031740
- Todaro M. A., Dal Zotto M., Kånneby T., & Hochberg R. (2019b). Integrated data analysis allows the establishment of a new, cosmopolitan genus of marine Macrodasyida (Gastrotricha). Scientific Reports, 9, 7989. DOI: 10.1038/s41598-019-43977-y
- Todaro, M. A., Dal Zotto, M., & Leasi, F. (2015). An integrated morphological and molecular approach to the description and systematisation of a novel genus and species of Macrodasyida (Gastrotricha). PLoS ONE 10(7), e0130278. DOI: 10.1371/journal. pone.0130278
- Todaro, M. A., Kånneby, T., Dal Zotto, M., & Jondelius, U. (2011). Phylogeny of Thaumastodermatidae (Gastrotricha: Macrodasyida) inferred from nuclear and mitochondrial sequence data. PLoS ONE, 6, e17892. DOI: 10.1371/journal.pone.0017892
- Todaro, M. A., Littlewood, D. T. J., Balsamo, M., Herniou, E. A., Casanelli, S., Manicardi, G., Wirz, A., & Tongiorgi, P. (2003). The interrelationships of the Gastrotricha using nuclear small rRNA subunit sequence data, with an interpretation based on morphology. Zoologischer Anzeiger, 242, 145–156. DOI: 10.1078/0044-5231-00093
- Todaro, M. A., & Luporini, P. (2022). Not too big for its mouth: direct evidence of a macrodasyidan gastrotrich preyed in nature by a dileptid ciliate. The European Zoological Journal, 89(1), 785–790. DOI: 10.1080/24750263.2022.2095048
- Todaro, M. A., Sibaja-Cordero, J. A., Segura-Bermúdez, O. A., Coto-Delgado, G., Goebel-Otárola, N., Barquero, J. D., Cullell-Delgado, M., Dal Zotto, M. (2019a). An introduction to the study of Gastrotricha, with a taxonomic key to families and genera of the group. Diversity, 11, 117. DOI: 10.3390/d11070117

- Todaro, M. A., Telford, M. J., Lockyer, A. E., & Littlewood, D. T. J. (2006). Interrelationships of Gastrotricha and their place among the Metazoa inferred from 18S rRNA genes. Zoologica Scripta, 35, 251–259. DOI: 10.1111/j.1463-6409.2006.00228.x
- Toews, D. P., & Brelsford, A. (2012). The biogeography of mitochondrial and nuclear discordance in animals. Molecular Ecology, 21(16), 3907–3930. DOI: 10.1111/j.1365-294X.2012.05664.x
- Travis, P. B. (1983). Ultrastructural study of body wall organization and Y-cell composition in the Gastrotricha. Zeitschrift für Zoologische Systematik und Evolutionsforschung, 21, 52–68. DOI: 10.1111/j.1439-0469.1983.tb00275.x
- Winnepenninckx, B., Backeljau, T., Mackey, L. Y., Brooks, J. M., De Wachter, R., Kumar, S., & Garey, J. R. (1995). 18S rRNA data indicate that Aschelminthes are polyphletic in origin and consist of at least three distinct clades. Molecular Biology and Evolution, 12, 1132-1137. DOI: 10.1093/oxfordjournals.molbev.a040287
- WoRMS Editorial Board (2025). World Register of Marine Species. Available from https://www.marinespecies.org at VLIZ. Accessed 2025-10-07. DOI: 10.14284/170
- Zrzavý, J. (2003). Gastrotricha and metazoan phylogeny. Zoologica Scripta, 32, 61–81. DOI: 10.1046/j.1463-6409.2003.00104.x

5. CONTRIBUTIONS TO MEETINGS ON THESIS TOPICS

- **Cesaretti, A.**, Kosakyan, A., & Todaro, M. A. (2023). Evolutionary trajectories of the reproductive system of the Gastrotrich genus *Urodasys* (Macrodasyida, Gastrotricha) inferred from morphological and molecular data. 82° Congresso Unione Zoologica Italiana, Palermo 19-22/09/23 (Poster).
- **Cesaretti, A.**, Kosakyan, A., & Todaro, M. A. (2024). A fast and accurate pipeline to sequence fresh and preserved soft-bodied meiofaunal specimens. Simposio "Cambiamento della biodiversità nell'Antropocene: priorità per la ricerca", Fano Marine Center 10-11/04/24 (Poster).
- **Cesaretti, A**., Kosakyan, A., Saponi, F., & Todaro, M. A. (2024). Phylogenetic alliances of the Cephalodasyidae (Gastrotricha, Macrodasyida) inferred through a multi-gene approach. 83° Congresso Unione Zoologica Italiana, 11-14/09/24, Pisa, Italia (Poster).
- **Cesaretti, A.**, Kosakyan, A., Saponi, F., & Todaro, M. A. (2025). Exploring the phylogeny of Macrodasyida (Gastrotricha) through multi-gene analysis, with a focus on Cephalodasyidae. Forum Nazionale della Biodiversità, 19-22/05/25, Università Bicocca, Milano, Italia (Poster).
- **Cesaretti, A.**, Kosakyan, A., Saponi, F., & Todaro, M. A. (2025). Phylogenetic insights into Macrodasyida (Gastrotricha) with emphasis on Cephalodasyidae. Willi Hennig Society XLII annual meeting, 22-25/07/25, The Chinese University of Hong Kong, HKSAR, China (Poster).
- **Cesaretti, A.**, Kosakyan, A., Saponi, F., & Todaro, M. A. (2025). A new look at the phylogeny of Macrodasyida (Gastrotricha) through improved taxonomic and molecular sampling. 84° Congresso Unione Zoologica Italiana, 16-19/09/25, Cagliari, Italia (Presentation).

6. ADDITIONAL JOURNAL PUBLICATIONS

- Saponi, F., Rebecchi, C., **Cesaretti, A.**, Souid, A., & Todaro, M. A. (2024). New data on marine gastrotrichs from Sicily. Biologia Marina Mediterranea, 28(1), 133-136.

- Saponi, F., Kosakyan, A., **Cesaretti, A.**, & Todaro, M. A. (2024). A contribution to the taxonomy and phylogeny of the genus *Chaetonotus* (Gastrotricha, Paucitubulatina, Chaetonotidae), with the description of a new species from Italian inland waters. The European Zoological Journal, 91(2), 1078-1092. https://doi.org/10.1080/24750263.2024.2397473

- Clò, E., Braga, L., Brandoli, S., **Cesaretti, A.**, Denami, M., Ricucci, C., Saponi, F., Sommaggio, D., Zappa, J., & Kosakyan, A. (2025). Thoughts on "Multidisciplinarity: tools and approaches for studying Biodiversity". Atti della Società dei Naturalisti e Matematici di Modena, 156.

- Saponi, F., **Cesaretti, A.**, Kosakyan, A., Serra, V., & Todaro, M. A. (2025). Phylogenetic position of *Setopus* (Gastrotricha, Paucitubulatina) among planktonic Gastrotricha, with the description of a new species. Accepted for publication with minor revisions in Zoologischer Anzeiger.

- Souid, A., Gammoudi, M., El Cafsi, M., **Cesaretti, A.,** Kosakyan, A., Saponi, F., & Todaro, M. A. (2025). A new *Tetranchyroderma* species (Gastrotricha, Macrodasyida) from Tunisia, with its phylogenetic position based on molecular markers. Submitted to Zootaxa.

7. APPENDIX: SUPPLEMENTARY MATERIALS

SUPPLEMENTARY MATERIALS – CHAPTER 2

Table S1. Reproductive system and reproductive modality in 17 known species of the genus *Urodasys*.

Species name	Reproductive system	Reproductive modality
U. anorektoxys Todaro, Bernard & Hummon, 2000	Paired ovaries, paired testes, no frontal organ, no caudal organ	Hermaphroditism with cross-fertilization coupled with oviparity
U. apuliensis Fregni, Faienza, Grimaldi *et al.*, 1999	〃	〃
U. elongatus Renaud-Mornant, 1969	〃	〃
U. mirabilis Remane, 1926	〃	〃
U. completus Todaro, Cesaretti & Dal Zotto, 2017	Paired ovaries, paired testes, frontal organ, caudal organ with stylet	〃
U. acanthostylis Fregni, Tongiorgi & Faienza, 1998	Single testis, frontal organ, caudal organ with stylet	〃
U. bifidostylis Cesaretti, Leasi & Todaro, 2023	〃	〃
U. calicostylis Schoepfer-Sterrer, 1974	〃	〃
U. cornustylis Schoepfer-Sterrer, 1974	〃	〃
U. nodostylis Schoepfer-Sterrer, 1974	〃	〃
U. poculostylis Atherton, 2014	〃	〃
U. remostylis Schoepfer-Sterrer, 1974	〃	〃
U. spirostylis Schoepfer-Sterrer, 1974	〃	〃
U. toxostylus Hummon, 2011	〃	〃
U. uncinostylis Fregni, Tongiorgi & Faienza, 1998	〃	〃
U. bucinastylis Fregni, Faienza, Grimaldi *et al.*, 1999	Paired ovaries, no testes, no frontal organ, caudal organ with stylet	Parthenogenesis coupled with oviparity
U. viviparus Wilke, 1954	Paired ovaries, no testes, no frontal organ, no caudal organ	Parthenogenesis coupled with ovoviviparity

Table S2. 18S primers used in the validation step and their respective direction, sequence and usage.

Primer	Direction	Sequence 5' to 3'	Usage	Reference
S30	forward	GCTTGTCTCAAAGATTAAGCC	PCR	Norén and Jondelius 1999
1806R	reverse	CCTTGTTACGACTTTTACTTCCTC	PCR	Norén and Jondelius 1999
PCR regime	3 min at 95 °C, 35 × (30 s at 94 °C, 30 s at 50 °C, 2 min at 72 °C), 7 min at 72 °C			
18S R536	reverse	CTGGAATTACCGCGGCTG	sequencing	Rosati *et al.* 2004
18S R1052	reverse	AACTAAGAACGGCCATGCA	sequencing	Rosati *et al.* 2004
18S F783	forward	GACGATCAGATACCGTC	sequencing	Rosati *et al.* 2004

Table S3. Specimens used in a preliminary phylogenetic analysis based on 18S rDNA sequences with sampling locations, GenBank accession codes and references.

Species	Sampling location	GenBank Accession (18S)	Reference
Urodasys viviparus	Grape Tree Bay (Little Cayman Island)	KM289036	Atherton and Hochberg 2014
″ ″	″ ″	KM289038	″ ″
″ ″	″ ″	KM289039	″ ″
″ ″	Point of Sand (Little Cayman Bay)	KM289042	″ ″
″ ″	Jackson Wall (Little Cayman Bay)	KM289035	″ ″
″ ″	″ ″	KM289037	″ ″
″ ″	Owen Island (Little Cayman Bay)	KM289043	″ ″
″ ″	″ ″	KM289051	″ ″
″ ″	″ ″	KM289055	″ ″
″ ″	Mary's Bay (Little Cayman Bay)	KM289045	″ ″
″ ″	Playa Jeremi (Curaçao)	KM289053	″ ″
″ ″	Playa Parasasa (Curaçao)	KM289050	″ ″
″ ″	Angel Reef (Tobago)	KM289040	″ ″
″ ″	50/50 (Tobago)	KM289048	″ ″
″ ″	″ ″	KM289049	″ ″
″ ″	Highway to Heaven (Tobago)	KM289041	″ ″
″ ″	Pereque, Ilhabela (Brazil)	KM289044	″ ″
″ ″	″ ″	KM289046	″ ″
″ ″	″ ″	KM289047	″ ″
″ ″	″ ″	KM289052	″ ″
″ ″	″ ″	KM289054	″ ″
Urodasys poculostylis	Capron Shoal (USA)	KM289056	″ ″
″ ″	″ ″	KM28957	″ ″
″ ″	″ ″	KM289058	″ ″
Urodasys nodostylis	Carrie Bow Caye (Belize)	KM289059	″ ″
Urodasys sp.	Capron Shoal (USA)	KM289060	″ ″
Urodasys calicostylis	Capron Shoal (USA)	KM289061	″ ″
″ ″	″ ″	KM289062	″ ″
″ ″	″ ″	KM289063	″ ″
Urodasys spirostylis	Capron Shoal (USA)	KM289064	″ ″
Urodasys mirabilis	50/50 (Tobago)	KM289065	″ ″
″ ″	″ ″	KM289066	″ ″
″ ″	″ ″	KM289067	″ ″
Urodasys sp.	Unknown	AY218102	Giribet *et al.* 2004
Urodasys sp.	Unknown	DQ079912	Sørensen *et al.* 2006
Urodasys acanthostylis	Puerto del Carmen, Lanzarote (Canary Islands, Spain)	PQ415490	Present study
Urodasys apuliensis	Sardinia (Italy)	PQ415491	Present study
Urodasys bifidostylis	Costa Paradiso (Italy)	PQ415492	Present study
Urodasys completus	Puerto del Carmen, Lanzarote	PQ415493	Present study

	(Canary Islands, Spain)		
″″ ″″	″″ ″″	PQ415494	″″ ″″
Urodasys mirabilis	Beach of the Marine Biological Station (CARMABI) (Curaçao)	PQ415495	Present study
Urodasys viviparus	Abruzzo (Italy)	PQ415496	Present study
Macrodasys sp1	Torre Civette (Italy)	JF357654	Todaro *et al.* 2011
Macrodasys sp2	Bohuslän (Sweden)	JF357670	Todaro *et al.* 2011

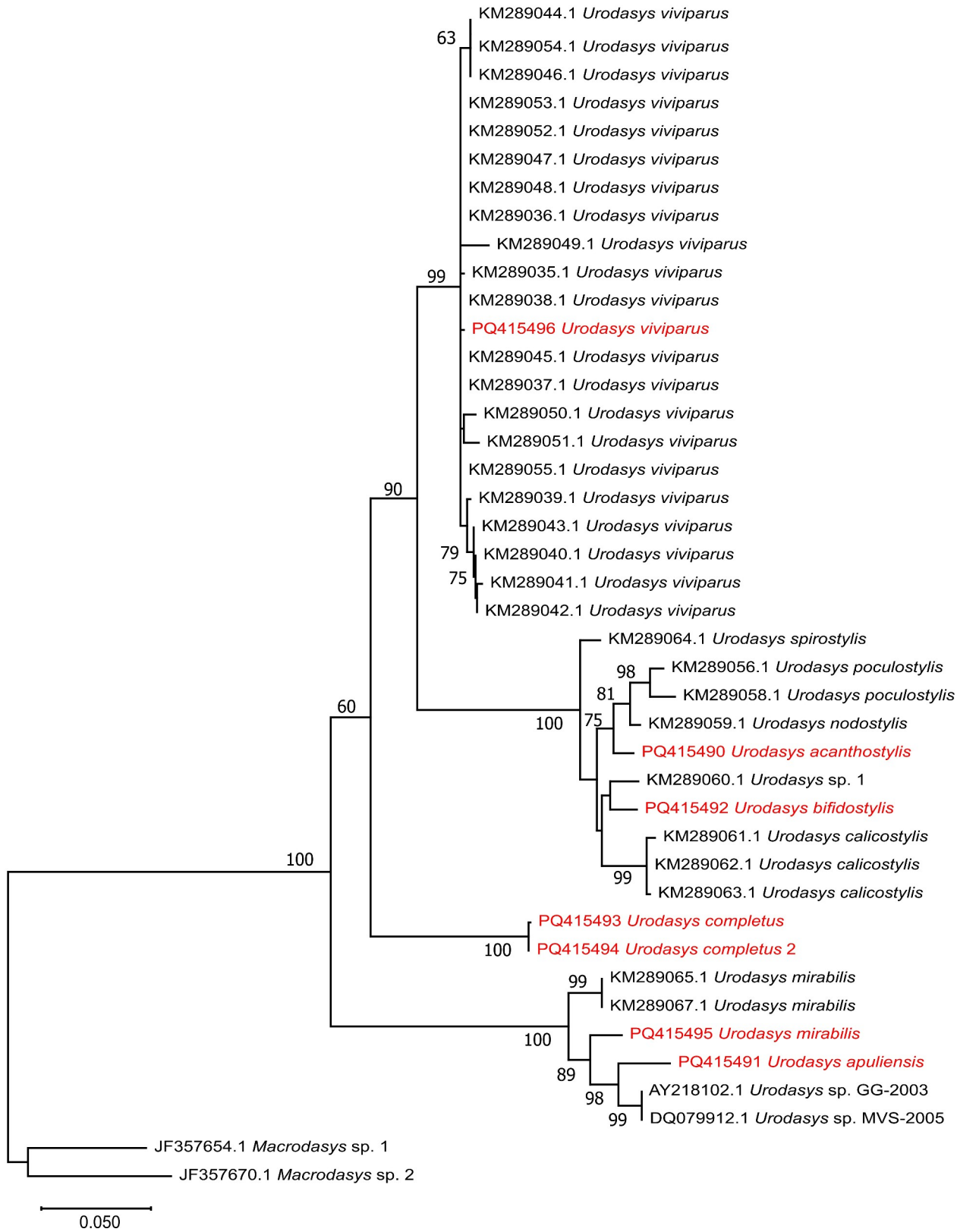

Figure S1. Phylogenetic tree resulting from Maximum Likelihood (ML) analysis conducted on the dataset of 18S rDNA sequences from the present study complemented with the *Urodasys* sequences from Atherton and Hochberg (2014); GTR+I+G was applied as the nucleotide substitution model. The outgroup is represented by two *Macrodasys* species. Numbers at nodes represent bootstrap values (1000 replicates); only values ≥ 60 are reported. Sequences in red were obtained in the present study.

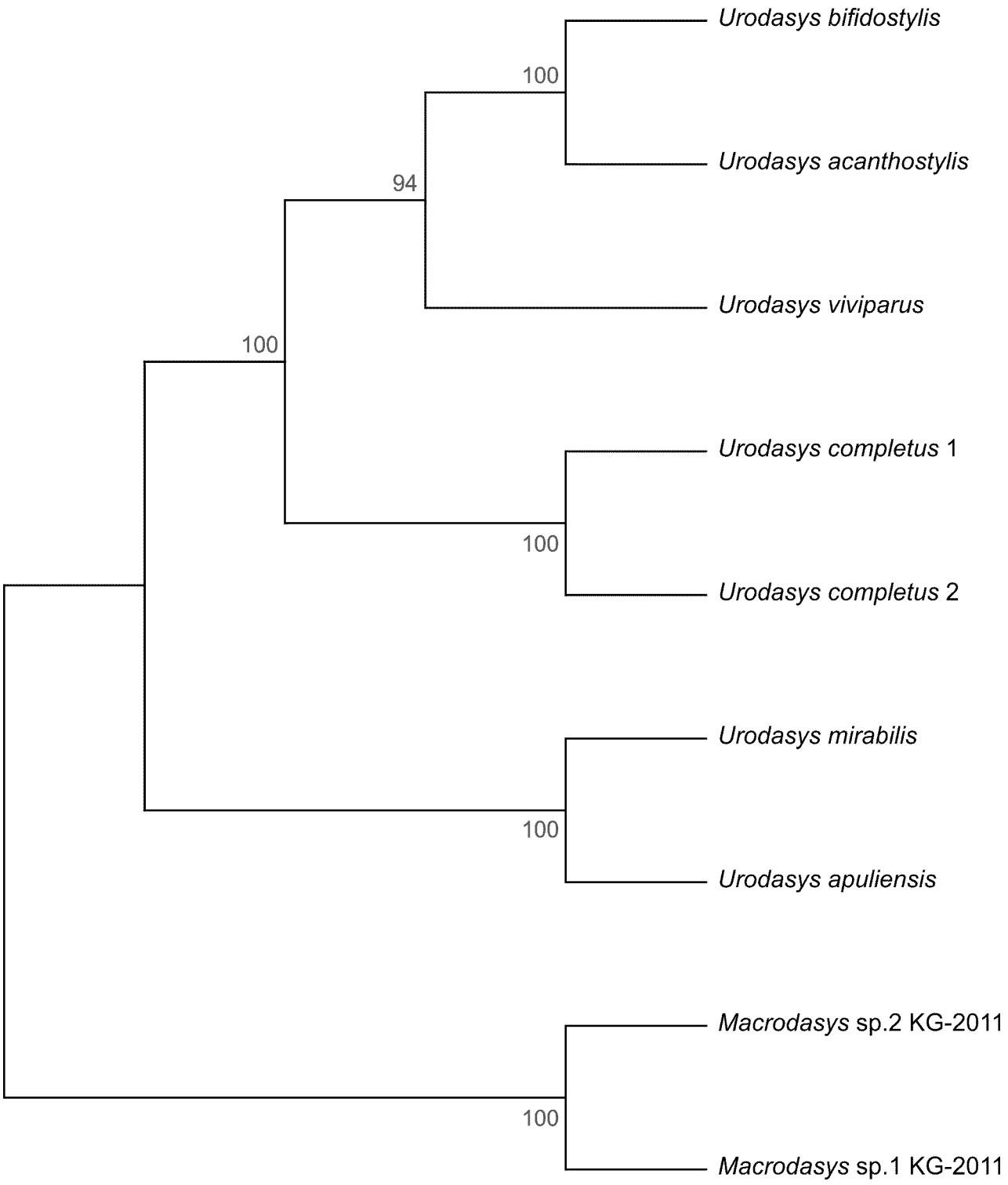

Figure S2. Phylogenetic relationships of the genus *Urodasys* inferred from Maximum Parsimony (MP) analysis conducted on the concatenated dataset of 18S rDNA, 28S rDNA and COI sequences obtained in the present study. The outgroup is represented by two *Macrodasys* species. Numbers at nodes represent bootstrap values (1000 replicates).

SUPPLEMENTARY MATERIALS – CHAPTER 3

File S1. Protocol for the validation step

PCRs were carried out in a T-Personal thermal cycler (Biometra, Goettingen, Germany). High-fidelity Takara Ex Taq PCR reagents (Takara Bio Inc., Otsu, Japan) were employed following the protocol provided by the manufacturer, using the primer combinations and thermal cycler programs presented in Supplementary Table 2. The PCR products were then purified using the Monarch PCR and DNA Cleanup Kit (New England BioLabs Inc., Ipswich, MA, USA). Sanger sequencing was conducted on the purified products by an external sequencing company (Macrogen Europe Laboratory in Milan, Italy), using the sequencing primers indicated in Supplementary Table 2. The resulting reads were assembled using the Staden package v. 2.0 (Staden, 1996) and the obtained *18S* sequences were examined with the GenBank online BLAST tool (https://www.ncbi.nlm.nih.gov/genbank/Blast.cgi).

Table S1. Sequences sourced from GenBank for this study, with sampling area, GenBank accession codes and references.

Taxon	Sampling area	GenBank Accession (18S, 28S, COI)	Reference
Cephalodasyidae			
Cephalodasys mahoae Yamauchi and Kajihara, 2018	Hokkaido, Japan 43°15'42" N; 141°21'43" E	LC018992, LC383934, LC383935	Yamauchi and Kajihara 2018
Mesodasys laticaudatus 2	Tuscany, Italy 42°29'29" N; 11°11'28" E	JF357657, JF357705, JF432043	Todaro *et al.* 2011
Mesodasys littoralis 2	Bou Ficha, Tunisia 36°16'50" N; 10°29'41" E	JF357658, JF357706, JF432044	Todaro *et al.* 2011
Dactylopodolidae			
Dactylopodola mesotyphle Hummon, Todaro, Tongiorgi and Balsamo, 1998	Tuscany, Italy 42°48'42" N; 10°44'46" E	JF357651, JF357699, JF432036	Todaro *et al.* 2011
Dactylopodola typhle 1 (Remane, 1927)	Bou Ficha, Tunisia 36°16'50" N; 10°29'41" E	JF357652, JF357700, JF432037	Todaro *et al.* 2011
Dactylopodola typhle 2	Tuscany, Italy 42°50'42" N; 10°46'31" E	JF357653, JF357701, JF432038	Todaro *et al.* 2011
Macrodasyidae			
Macrodasys sp. 1	Tuscany, Italy 42°50'42" N; 10°46'31" E	JF357654, JF357702, JF432040	Todaro *et al.* 2011
Macrodasys sp. 2	Bohuslän, Sweden 58°52'05" N; 11°04'57" E	JF357670, JF357714, JF432052	Todaro *et al.* 2011
Urodasys acanthostylis Fregni, Tongiorgi and Faienza, 1998	Lanzarote, Spain 28°55'08" N; 13°40'06" W	PQ415490, PQ429034, PQ462511	Cesaretti *et al*. 2024
Urodasys apuliensis Fregni, Faienza, Grimaldi, Tongiorgi and Balsamo, 1999	Sardinia, Italy 41°16'43" N; 09°21'28" E	PQ415491, PQ429035, PQ462513	Cesaretti *et al*. 2024
Urodasys completus Todaro, Cesaretti and Dal Zotto, 2017	Lanzarote, Spain 28°55'08" N; 13°40'06" W	PQ415493, PQ429037, PQ462510	Cesaretti *et al*. 2024
Urodasys mirabilis Remane, 1926	Willemstad, Curaçao 12°07'19" N; 68°58'09" W	PQ415495, PQ429039, PQ462514	Cesaretti *et al*. 2024
Urodasys viviparus Wilke, 1954	Abruzzo, Italy 42°40'44" N; 14°01'05" E	PQ415496, PQ429040, PQ462515	Cesaretti *et al*. 2024
Planodasyidae			
Megadasys sp. 1	Apulia, Italy 39°50'38" N; 18°23'09" E	JF357655, JF357703, JF432041	Todaro *et al.* 2011
Megadasys sp. 2	Apulia, Italy 40°15'33" N; 17°53'53" E	JF357656, JF357704, JF432042	Todaro *et al.* 2011
Redudasyidae			
Redudasys brasiliensis 1 Garraffoni, Araújo, Lourenço, Guidi and Balsamo, 2019	Minas Gerais State, Brazil 18°12′00" S; 43°37′00" W	MH361310, MH361316, MH370134	Garraffoni *et al*. 2019
Redudasys brasiliensis 2	Minas Gerais State, Brazil 18°12′00" S; 43°37′00" W	MH361311, MH361317, MH370135	Garraffoni *et al*. 2019
Redudasys brasiliensis 3	Minas Gerais State, Brazil 18°12′00" S; 43°37′00" W	MH361313, MH361319, MH370137	Garraffoni *et al*. 2019
Redudasys fornerise Kisielewski, 1987	Sao Paulo, Brazil 22°11'9" S; 47°54'1" W	JN203489, MF577024, KJ950122	Kånneby and Kirk, 2017

Thaumatostodermatidae			
Diplodasys meloriae Todaro, Balsamo and Tongiorgi, 1992	Tuscany, Italy 43°33'11" N; 10°13'20" E	JF357640, JF357680, JF432031	Todaro *et al.* 2011
Tetranchyroderma hirtum Luporini, Magagnini and Tongiorgi, 1973	Tuscany, Italy 43°00'53" N; 09°49'24" E	JF357628, JF357676, JF432023	Todaro *et al.* 2011
Oregodasys tentaculatus (Swedmark, 1956)	Tuscany, Italy 43°33'11" N; 10°13'20" E	JF357626, JF357674, JF432021	Todaro *et al.* 2011
Pseudostomella etrusca Hummon, Todaro and Tongiorgi, 1993	Tuscany, Italy 42°29'29" N; 11°11'28" E	JF357633, JF357681, JF432026	Todaro *et al.* 2011
Ptychostomella tyrrhenica Hummon, Todaro and Tongiorgi, 1993	Tuscany, Italy 42°29'29" N; 11°11'28" E	JF357634, JF357682, JF432027	Todaro *et al.* 2011
Turbanellidae			
Paraturbanella pallida Luporini, Magagnini and Tongiorgi, 1973	Tuscany, Italy 43°00'53" N; 09°49'24" E	JF357660, JF357708, JF432045	Todaro *et al.* 2011
Turbanella bocqueti Kaplan, 1958 sensu Boaden, 1974	Waterford, Ireland 52°09'24" N; 07°08'12" W	JF357662, JF357710, JF432046	Todaro *et al.* 2011
Turbanella cornuta Remane, 1925	Veneto, Italy 45°12'57" N; 12°17'57" E	JF357663, JF357711, JF432047	Todaro *et al.* 2011
Muselliferidae			
Diuronotus aspetos Todaro, Balsamo and Kristensen, 2005	Disko Island, Greenland 69°38'63" N; 51°51'13" W	KX531005, KX531006, KX531007	Bekkouche and Worsaae, 2016
Xenotrichulidae			
Xenotrichula intermedia Remane, 1934	Mahdia, Tunisia 35°30'57" N; 11°03'00" E	JF357664, JF357712, JF432948	Todaro *et al.* 2011

Table S2. 18S primers used in the validation step and their respective direction, sequence and usage.

Primer	Direction	Sequence 5' to 3'	Usage	Reference
S30	forward	GCTTGTCTCAAAGATTAAGCC	PCR	Norén and Jondelius, 1999
1806R	reverse	CCTTGTTACGACTTTTACTTCCTC	PCR	Norén and Jondelius, 1999
PCR regime	3 min at 95 °C, 35 × (30 s at 94 °C, 30 s at 50 °C, 2 min at 72 °C), 7 min at 72 °C			
18S R536	reverse	CTGGAATTACCGCGGCTG	sequencing	Rosati et al., 2004
18S R1052	reverse	AACTAAGAACGGCCATGCA	sequencing	Rosati et al., 2004
18S F783	forward	GACGATCAGATACCGTC	sequencing	Rosati et al., 2004

SUPPLEMENTARY MATERIALS – CHAPTER 4

Supplementary Material

From rigid order to radical variation: mitogenome evolution in the main lineages of a lesser-known animal phylum (Gastrotricha)

Anush Kosakyan[1,2*] ✝ , Leandro Gammuto[3] ✝ , Agata Cesaretti[1], Francesco Saponi[1,2,4], Valentina Serra[5], Giulio Petroni[5,6,7], Jan-Niklas Macher[8,9], Oscar Wallnoefer[10], Federico Plazzi[10], M. Antonio Todaro[1,2]

[1]Department of Life Sciences, University of Modena and Reggio Emilia, Modena, Italy
[2]National Biodiversity Future Center (NBFC), Palermo, Italy
[3]Department of Biology and Biotechnology "Lazzaro Spallazani", University of Pavia, Pavia, Italy
[4]Department of Earth and Marine Sciences, University of Palermo, Palermo, Italy
[5]Dipartimento of Biology, University of Pisa, Pisa, Italy
[6] Interdepartmental Center for Electron Microscopy (CIME), University of Pisa, Pisa, Italy
[7] Center for Instrument Sharing of the University of Pisa (CISUP), University of Pisa, Pisa, Italy
[8]Naturalis Biodiversity Center, Leiden, Netherlands
[9]Department of Environmental Biology, Institute of Environmental Sciences (CML), Leiden University, Leiden, The Netherlands
[10]Department of Biological, Geological and Environmental Sciences, University of Bologna, Bologna, Italy

Suppl. Mat. 1. Comparing phylogenetic results based on 13 mt PCGs and 11 mt PCGs (when excluding *atp6* and *atp8* genes from concatenated dataset).

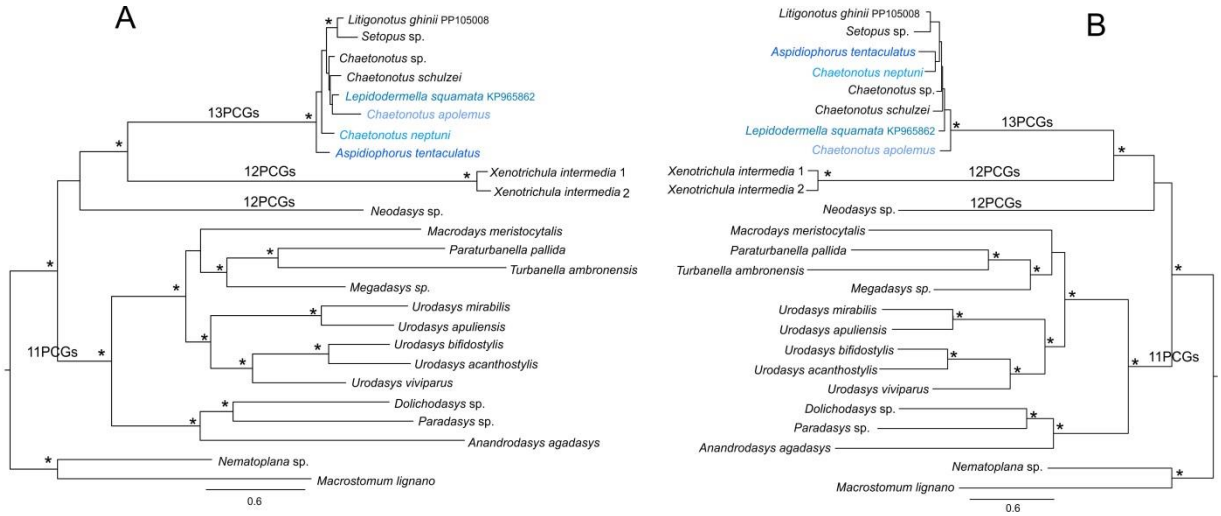

IQ ML tree showing phylogenetic relationships of 22 gastrotrich species and two flatworm species (used as outgroup) based on 13 mitochondrial protein coding gene (*cox1-3*, *cob*, *nad1-6*, *nad4L, atp6, atp8*) concatenated alignment in **A** and IQ tree showing phylogenetic relationships of 22 gastrotrich species and two flatworm species (used as outgroup) based on 11 mitochondrial

protein coding gene (*cox1-3*, *cob*, *nad1-6*, *nad4L*) concatenated alignment in **B**. The terminals with altered positions are indicated in blue. Nodes are indicated with ***** when SHaLRT support is > 85% and when Ultrafast Bootstrap support is > 95%. The scale bar indicates the number of substitutions per site. The information on number of protein coding genes (PCGs) of mtDNA for representatives of each lineage is presented on the branches.

Suppl. Mat. 2. The comparision of mtDNA base calculation across studied species.

Species	**mtDNA base calculation**	**GC %**
Aspidiophorus tentaculatus	Full Length(14560bp) | A(22% 3221) | T(40% 5561) | G(22% 3304) | C(16% 2474)	38
Chaetonotus sp.	Full Length(14488bp) | A(21% 3108) | T(39% 5480) | G(23% 3340) | C(17% 2560)	40
Chaetonotus neptuni	Full Length(14585bp) | A(23% 3407) | T(40% 5646) | G(22% 3239) | C(15% 2293)	37
Chaetonotus schultzei	Full Length(14503bp) | A(20% 3044) | T(40% 5535) | G(23% 3398) | C(17% 2526)	40
Chaetonotus apolemmus	Full Length(14599bp) | A(21% 3118) | T(39% 5431) | G(23% 3481) | C(17% 2569)	40
Lepidodermella squamata	Full Length(14558bp) | A(21% 3113) | T(39% 5454) | G(22% 3338) | C(18% 2653)	40
Litigonotus ghinii	Full Length(14384bp) | A(20% 2945) | T(38% 5271) | G(24% 3529) | C(18% 2639)	42
Setopus sp.	Full Length(14495bp) | A(20% 2952) | T(38% 5298) | G(24% 3604) | C(18% 2641)	42
*Xenotrichula intermedia*1	Full Length(15103bp) | A(26% 4021) | T(38% 5586) | G(19% 2880) | C(17% 2616)	31
*Xenotrichula intermedia*2	Full Length(14919bp) | A(27% 4164) | T(42% 5902) | G(17% 2672) | C(14% 2181)	31
Neodasys sp.	Full Length(14156bp) | A(22% 3155) | T(38% 5303) | G(22% 3124) | C(18% 2574)	40
Anandrodasys agadasys	Full Length(16272bp) | A(45% 7326) | T(26% 4071) | G(10% 1682) | C(19% 3193)	29
Dolichodasys sp.	Full Length(15893bp) | A(38% 6066) | T(36% 5564) | G(12% 1989) | C(14% 2274)	26
Macrodasys meristocytalis	Full Length(14402bp) | A(40% 5767) | T(31% 4346) | G(10% 1510) | C(19% 2779)	29
Megadasys sp.	Full Length(14487bp) | A(35% 5160) | T(41% 5725) | G(11% 1631) | C(13% 1971)	24
Paradasys sp.	Full Length(12838bp) | A(37% 4823) | T(38% 4683) | G(13% 1719) | C(12% 1613)	25
Paraturbanella pallida	Full Length(14981bp) | A(38% 5796) | T(42% 6149) | G(10% 1505) | C(10% 1531)	20
Turbanella	Full Length(14297bp) | A(21% 3104) | T(33% 4522) | G(24% 3515) |	**46**

ambronensis	C(22% 3156)	
Urodasys bifidostylis	Full Length(15624bp) | A(39% 6195) | T(40% 6031) | G(8% 1334) | C(13% 2064)	21
Urodasys mirabilis	Full Length(19009bp) | A(38% 7224) | T(31% 5685) | G(10% 1956) | C(21% 4144)	31
Urodasys apuliensis	Full Length(18723bp) | A(36% 6867) | T(42% 7599) | G(12% 2323) | C(10% 1934)	22
Urodasys acanthostylis	Full Length(15504bp) | A(39% 6070) | T(39% 5939) | G(13% 2084) | C(9% 1411)	22
Urodasys viviparus	Full Length(13340bp) | A(41% 5504) | T(39% 5012) | G(9% 1303) | C(11% 1521)	20

Suppl. Mat. 3. Detailed information on tandem repeats identified in studied mtDNA by TandemRepeatsFinder. The table contains the following information: Indices of the repeat relative to the region of the sequence, Period size of the repeat, Number of copies aligned with the consensus pattern, Size of consensus pattern (may differ slightly from the period size), Percent of matches between adjacent copies overall, Percent of indels between adjacent copies overall, Alignment score, Percent composition for each of the four nucleotides, Entropy measure based on percent composition.

Aspidiophorus tentaculatus

Indices	Period Size	Copy Number	Consensus Size	Percent Matches	Percent Indels	Score	A	C	G	T	Entropy (0-2)
13842--13869	14	2.0	14	100	0	56	28	7	35	28	1.84

Chaetonotus neptuni

Indices	Period Size	Copy Number	Consensus Size	Percent Matches	Percent Indels	Score	A	C	G	T	Entropy (0-2)
8052--8105	27	2.0	27	100	0	108	29	29	22	18	1.97

Chaetonotus schultzei

Indices	Period Size	Copy Number	Consensus Size	Percent Matches	Percent Indels	Score	A	C	G	T	Entropy (0-2)
66--98	9	3.7	9	95	0	57	60	0	6	33	1.21

Lepidodermella squamata

Indices	Period Size	Copy Number	Consensus Size	Percent Matches	Percent Indels	Score	A	C	G	T	Entropy (0-2)
52--94	2	21.5	2	100	0	86	51	0	48	0	1.00

Anandrodasys agadasys

Indices	Period Size	Copy Number	Consensus Size	Percent Matches	Percent Indels	Score	A	C	G	T	Entropy (0-2)
116--140	13	1.9	13	100	0	50	8	88	4	0	0.64
5608--5656	26	1.9	26	87	4	73	71	12	10	6	1.30

Macrodasys meristocytalis

Indices	Period Size	Copy Number	Consensus Size	Percent Matches	Percent Indels	Score	A	C	G	T	Entropy (0-2)
2088--2126	18	2.2	18	95	0	69	64	17	0	17	1.30
2690--2897	43	4.8	43	98	0	398	41	1	7	49	1.41
2807--2967	69	2.3	70	87	5	229	42	1	7	48	1.42
2868--2967	25	4.2	25	70	17	104	43	1	9	47	1.41
2982--3035	17	3.2	17	100	0	108	29	0	11	59	1.32
2892--3001	45	2.4	46	95	4	197	40	1	7	50	1.41
3017--3095	25	3.2	25	72	3	88	41	1	7	49	1.39
2982--3047	34	1.9	34	87	0	96	34	0	10	54	1.35
2936--	83	2.0	80	87	6	234	39	1	8	51	1.39

3096											

Megadasys sp.

Indices	Period Size	Copy Number	Consensus Size	Percent Matches	Percent Indels	Score	A	C	G	T	Entropy (0-2)
918--1012	49	1.9	49	100	0	190	41	4	0	54	1.20
944--1014	15	4.5	15	68	13	52	39	2	0	57	1.13
5935--5964	16	1.9	16	93	6	53	23	0	0	76	0.78
8006--8053	21	2.3	21	89	7	71	77	4	0	18	0.93
12979--13020	21	1.9	23	90	9	70	45	0	2	52	1.13

Paradasys sp.

Indices	Period Size	Copy Number	Consensus Size	Percent Matches	Percent Indels	Score	A	C	G	T	Entropy (0-2)
1190--1226	18	2.0	19	94	5	67	40	21	21	16	1.91
5885--5951	30	2.2	29	80	17	75	34	8	0	56	1.31

Paraturbanella pallida

Indices	Period Size	Copy Number	Consensus Size	Percent Matches	Percent Indels	Score	A	C	G	T	Entropy (0-2)
2485--2726	121	2.0	121	100	0	484	33	7	15	42	1.75
2838--2890	24	2.2	24	93	0	88	39	0	1	58	1.09
2831--	15	3.8	15	69	28	51	41	0	0	58	0.98

2881											
5350--5382	15	2.2	15	100	0	66	39	0	0	60	0.97
6605--6642	20	1.9	20	84	10	51	21	5	2	71	1.19
10383--10435	22	2.3	23	80	3	63	52	1	0	45	1.11
13213--13241	15	1.9	15	100	0	58	68	6	0	24	1.13

Turbanella ambronensis

Indices	Period Size	Copy Number	Consensus Size	Percent Matches	Percent Indels	Score	A	C	G	T	Entropy (0-2)
13653--14297	239	2.7	239	89	3	1035	27	26	21	24	1.99

Urodasys bifidostylis

Indices	Period Size	Copy Number	Consensus Size	Percent Matches	Percent Indels	Score	A	C	G	T	Entropy (0-2)
1--1278	237	5.8	215	81	10	1350	39	11	8	40	1.72
160--1276	444	2.5	445	88	3	1634	38	11	8	40	1.72
621--1035	207	2.0	207	89	1	636	37	13	8	40	1.75
828--1409	237	2.5	237	89	3	861	40	11	7	41	1.68
6869--6895	14	1.9	14	100	0	54	74	3	0	22	0.98
8132--8175	14	3.1	14	80	0	61	79	11	2	6	1.01
1469	240	3.9	239	90	3	147	3	1	7	4	1.71

4--15624						8	8	1		1	
14678--15624	480	2.0	479	98	0	1815	38	11	7	41	1.70

Urodasys mirabilis

Indices	Period Size	Copy Number	Consensus Size	Percent Matches	Percent Indels	Score	A	C	G	T	Entropy (0-2)
11463--11500	14	2.5	15	79	12	51	71	21	2	5	1.19
13232--13288	24	2.5	22	78	16	53	70	5	3	21	1.22

Urodasys apuliensis

Indices	Period Size	Copy Number	Consensus Size	Percent Matches	Percent Indels	Score	A	C	G	T	Entropy (0-2)
1--2590	164	16.0	161	88	3	3552	39	6	10	43	1.65
1--2956	485	6.2	485	87	5	3981	39	6	10	43	1.65
2392--2957	142	4.0	143	82	6	688	39	7	10	43	1.66
2392--2957	283	2.0	281	83	7	709	39	7	10	43	1.66

Urodasys acanthostylis

Indices	Period Size	Copy Number	Consensus Size	Percent Matches	Percent Indels	Score	A	C	G	T	Entropy (0-2)
10316--10348	16	2.0	17	88	5	50	42	6	9	42	1.61
10704--1073	13	2.1	14	93	6	51	51	0	0	48	1.00

2											

Urodasys viviparus

Indices	Period Size	Copy Number	Consensus Size	Percent Matches	Percent Indels	Score	A	C	G	T	Entropy (0-2)
423--474	25	2.1	25	100	0	104	69	0	7	23	1.14
434--486	25	2.2	24	83	6	63	73	0	9	16	1.08
1841--1875	11	3.1	11	91	4	52	37	0	0	62	0.95
1840--1899	12	4.6	12	75	17	57	33	0	1	65	1.03
1847--1911	29	2.3	28	76	7	69	44	0	1	53	1.09
2060--2099	19	2.2	18	86	13	55	32	2	5	60	1.32
4792--4818	7	3.9	7	100	0	54	44	0	0	55	0.99
6228--6257	9	3.3	9	95	0	51	13	0	0	86	0.57

Suppl. Mat. 4. *atp6* presence/absence matrix in macrodasyidan draft assemblies (nuclear contigs) using Blast and Exonerate search with chaetonotodan atp6 sequences as queries. Dark blue color suggests stronger hit (highest homology) of chaetonotidan atp6 quiery sequences in studied macrodasyidan nuclear contigs. White color indicates no hit. *atp6* was found in two different *T. ambronensis* nuclear contigs reported here as *T. ambronensis* 1 and 2.

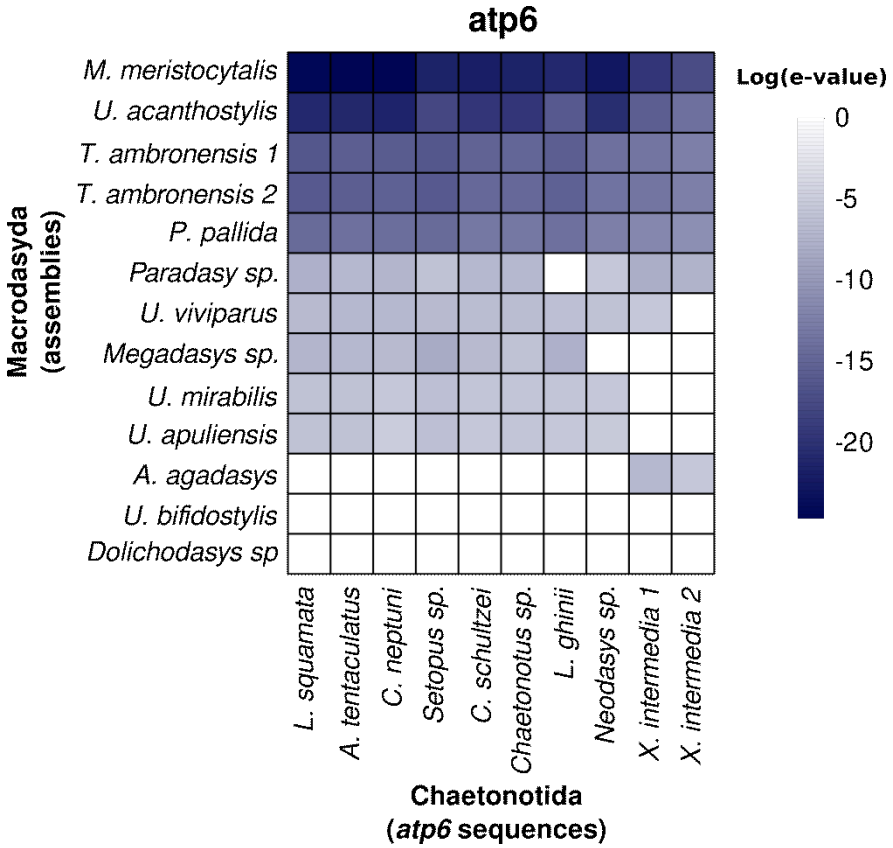

Suppl. Mat. 5 Details on primers and PCR programs used for amplification and sequencing of the 18S rDNA gene in the validation step.

Primer	Direction	Sequence 5' to 3'	Usage	Reference
S30	forward	GCTTGTCTCAAAGATTAAGCC	PCR	Norén and Jondelius 1999
1806R	reverse	CCTTGTTACGACTTTTACTTCCTC	PCR	Norén and Jondelius 1999
18S R536	reverse	CTGGAATTACCGCGGCTG	sequencing	Rosati *et al.* 2004
18S R1052	reverse	AACTAAGAACGGCCATGCA	sequencing	Rosati *et al.* 2004
18S F783	forward	GACGATCAGATACCGTC	sequencing	Rosati *et al.* 2004

Details of PCR protocol: 3 min at 95 °C, 35 × (30 s at 94 °C, 30 s at 50 °C, 2 min at 72 °C), 7 min at 72 °C

Suppl. Mat. 6 Details of primers and schematic representation of the PCR design that was used to close the mitochondrial DNA of *Urodasys mirabilis* and Anandrodasys agadasys. For each species, we designed two pairs of primers that allowed three different products: one pair of primers amplified a known region in the extreme "A", while another pair amplified the extreme "B". Additionally, the forward primer from extreme A also worked with the reverse primer from extreme B, ensuring the functionality of each primer. As a control, we included *Chaetonotus schultzei*, a species previously confirmed to have circular mtDNA through bioinformatic analysis.

Primer Code	Primer Sequence (5'-3')
Umir_Fwd_A	TATAGATGCCAACCCCCACC
Umir_Rvs_B	AGAAGTCACCACAAAGCCGA
Umir_Rvs_A	GGTGGAGTGCTGATAGACGA
Umir_Fwd_B	CCGAAATTACAGGAGAGGGTT
Csch_Fwd_A	ATGCCCCGACGATATAGGGA
Csch_Rvs_B	GGACAACAACACCTAGCCCA
Csch_Rvs_A	AAAGGCAGCACGTCTTCTCA
Csch_Fwd_B	AAATGGCTGAAGTTAGGCGGA
Aaga_Fwd_A	TCTCTAACCGCTGTGCAAGAA
Aaga_Rvs_B	ACCCTAGCCAATTAGTGGTGAT
Aaga_Rvs_A	GGGTTCCCTATGGGCCTTGT
Aaga_Fwd_B	AGCTACCGAGAACGTAGGGT

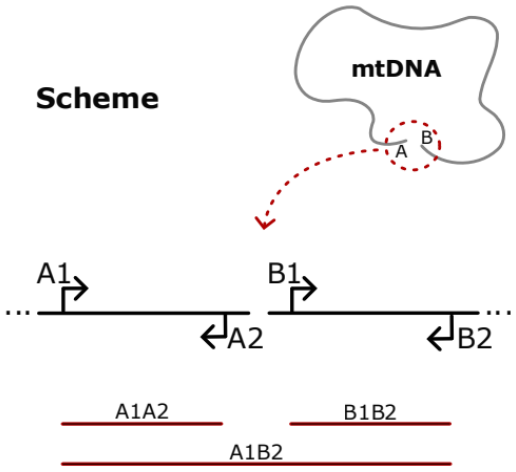

Amplified region

	A1A2	A1B2	B1B2
U. mirabilis	269	499	193
C. schultzei	194	694	207
A. agadasys	208	736	215

Suppl. Mat. 7. Partition models used for phylogenetic analyses

The concatenated amino acid alignment was partitioned as following

charset part1=1-550; for *cox1*
charset part2=551-817; for *cox2*
charset part3=818-1100; for *cox3*
charset part4=1101-1497; for *cob*
charset part5=1498-1825; for *nad1*
charset part6=1826-2272; for *nad2*
charset part7=2273-2413; for *nad3*
charset part8=2414-2937; for *nad4*
charset part9=2938-3062; for *nad4l*
charset part10=3063-3667; for *nad5*
charset part11=3668-3856; for *nad6*
charset part12=3857-4095; for *atp6*
charset part13=4096-4150; for *atp8*

ModelFinder integrated in IQ platform suggested the following model combination

Best-fit model according to BIC:
mtZOA+G4:part1,mtZOA+F+I+G4:part2,mtZOA+I+G4:part3,mtZOA+I+G4:part4,mtART+I+G4:part5,
mtInv+I+G4:part6,mtART+I+G4:part7,mtInv+I+G4:part8,mtInv+G4:part9,mtInv+I+G4:part10,mtInv
+G4:part11,mtZOA+G4:part12,mtInv+G4:part13

List of best-fit models per partition:

ID	Model	LogL	AIC	w-AIC	AICc	w-AICc	BIC	w-BIC
1	mtZOA+G4	-11797.7492	23691.4984	+ 0.0000	23700.8877	+ 0.0000	23898.3745	+ 0.0000
2	mtZOA+F+I+G4	-7403.0891	14942.1781	+ 0.0000	14989.5721	+ 0.0000	15186.1111	+ 0.0000
3	mtZOA+I+G4	-8049.4672	16196.9343	+ 0.0000	16217.9644	+ 0.0000	16375.5612	+ 0.0000
4	mtZOA+I+G4	-11402.7812	22903.5623	+ 0.0000	22917.6834	+ 0.0000	23098.7752	+ 0.0000
5	mtART+I+G4	-9298.9242	18695.8484	+ 0.0000	18713.4743	+ 0.0000	18881.7061	+ 0.0000
6	mtInv+I+G4	-12095.4359	24288.8717	+ 0.0000	24301.2143	+ 0.0000	24489.8971	+ 0.0000
7	mtART+I+G4	-4055.3547	8208.7095	+ 0.0000	8262.5556	+ 0.0000	8353.1987	+ 0.0000
8	mtInv+I+G4	-15363.7711	30825.5422	+ 0.0000	30835.8798	+ 0.0000	31034.3553	+ 0.0000
9	mtInv+G4	-3642.9138	7381.8275	+ 0.0000	7443.7223	+ 0.0000	7517.5866	+ 0.0000
10	mtInv+I+G4	-17579.1137	35256.2274	+ 0.0000	35265.0562	+ 0.0000	35472.0836	+ 0.0000
11	mtInv+G4	-6212.1887	12520.3774	+ 0.0000	12553.9774	+ 0.0000	12675.9813	+ 0.0000
12	mtZOA+G4	-3462.9865	6973.9730	+ 0.0000	6979.5804	+ 0.0000	7057.4081	+ 0.0000
13	mtInv+G4	-373.8154	779.6308	+ 0.0000	793.9466	+ 0.0000	811.7482	+ 0.0000

AIC, w-AIC: Akaike information criterion scores and weights.
AICc, w-AICc: Corrected AIC scores and weights.
BIC, w-BIC: Bayesian information criterion scores and weights.

Plus signs denote the 95% confidence sets.
Minus signs denote significant exclusion.